DTIC FILE COPY

SECURITY CLASSIFICATION OF THIS PAGE

1

REPORT DOCUMENTATION PAGE

Form Approved
OMB No 0704-0188

1a

AD-A217 376

1b. RESTRICTIVE MARKINGS
NONE

2

3. DISTRIBUTION/AVAILABILITY OF REPORT
APPROVED FOR PUBLIC RELEASE;
DISTRIBUTION UNLIMITED.

4. PERFORMING ORGANIZATION REPORT NUMBER(S)

5. MONITORING ORGANIZATION REPORT NUMBER(S)
AFIT/CI/CIA-88-225

6a. NAME OF PERFORMING ORGANIZATION
AFIT STUDENT AT
MEMPHIS STATE UNIVERSITY

6b. OFFICE SYMBOL (If applicable)

7a. NAME OF MONITORING ORGANIZATION
AFIT/CIA

6c. ADDRESS (City, State, and ZIP Code)

7b. ADDRESS (City, State, and ZIP Code)
Wright-Patterson AFB OH 45433-6583

8a. NAME OF FUNDING/SPONSORING ORGANIZATION

8b. OFFICE SYMBOL (If applicable)

9. PROCUREMENT INSTRUMENT IDENTIFICATION NUMBER

8c. ADDRESS (City, State, and ZIP Code)

10. SOURCE OF FUNDING NUMBERS

PROGRAM ELEMENT NO.	PROJECT NO.	TASK NO	WORK UNIT ACCESSION NO.

11. TITLE (Include Security Classification) (UNCLASSIFIED)
THE STYRENE PROBE APPLIED TO ^{15}N and ^{77}Se NMR

12. PERSONAL AUTHOR(S)
ALAN A. SHAFFER

13a. TYPE OF REPORT
~~THESIS~~/DISSERTATION

13b. TIME COVERED
FROM ________ TO ______

14. DATE OF REPORT (Year, Month, Day)
1988

15. PAGE COUNT
346

16. SUPPLEMENTARY NOTATION
APPROVED FOR PUBLIC RELEASE IAW AFR 190-1
ERNEST A. HAYGOOD, 1st Lt, USAF
Executive Officer, Civilian Institution Programs

17. COSATI CODES

FIELD	GROUP	SUB-GROUP

18. SUBJECT TERMS (Continue on reverse if necessary and identify by block number)

19. ABSTRACT (Continue on reverse if necessary and identify by block number)

DTIC
ELECTE
FEB 01 1990
S D
D

90 02 01 009

20. DISTRIBUTION/AVAILABILITY OF ABSTRACT
☒ UNCLASSIFIED/UNLIMITED ☐ SAME AS RPT. ☐ DTIC USERS

21. ABSTRACT SECURITY CLASSIFICATION
UNCLASSIFIED

22a. NAME OF RESPONSIBLE INDIVIDUAL
ERNEST A. HAYGOOD, 1st Lt, USAF

22b. TELEPHONE (Include Area Code)
(513) 255-2259

22c. OFFICE SYMBOL
AFIT/CI

DD Form 1473, JUN 86

Previous editions are obsolete.

SECURITY CLASSIFICATION OF THIS PAGE

AFIT/CI "OVERPRINT"

THE STYRENE PROBE APPLIED TO ^{15}N and ^{77}Se NMR

A DISSERTATION

PRESENTED TO

THE FACULTY OF THE GRADUATE SCHOOL

MEMPHIS STATE UNIVERSITY

Accesion For
NTIS CRA&I ☑
DTIC TAB ☐
Unannounced ☐
Justification
By
Distribution
Availability Codes
Dist | Avail and/or Special
A-1

DTIC COPY INSPECTED 5

IN PARTIAL FULFILLMENT

OF

THE REQUIREMENTS FOR THE DEGREE

DOCTOR OF PHILOSOPHY

BY

ALAN A. SHAFFER

AUGUST 1988

ABSTRACT

Previous work had shown that the ^{19}F NMR chemical shift (δ)/Hammett Substituent Constant (σ) correlation of ethyl α-fluorocinnamates gave a positive slope (greater deshielding with increasing sigma value), opposite to that predicted by the π-polarization mechanism. To ascertain if this was a general phenomenon in α-substituted cinnamate esters for atoms having unshared pairs of electrons, ^{15}N chemical shift correlations were obtained for the Z and E isomers of ethyl α-diethylaminocinnamates. A positive slope was found for both isomers, with the σ^- scale giving the best single substituent parameter result compared to σ, σ^+, and σ^{13}, indicating through-resonance to be predominant in these compounds.

This correlation study was extended to a series of benzylidene azlactones and ethyl α-cyanocinnamates. Here, the orthogonality of nitrogen's unshared electron pair to the styryl system prevents through-resonance , with the result that the ^{15}N/δ correlation slopes predicted by the π-polarization mechanism (negative and positive, respectively) were observed.

^{77}Se NMR of the E and Z isomers of ethyl α-(phenylseleno)cinnamates also revealed a positive slope, although there was a large isomer disparity in correlative behavior. The E isomer correlation displayed a wide chemical shift range (40 ppm), and good overall correlations, with σ^{13}/σ^+ collectively superior to σ/σ^-. The Z isomer series gave a much narrower chemical shift range (13 ppm), a good correlation only with σ^- and greater deshielding (100 ppm). These Z/E isomer differences may be related to variations in n-π overlap due to steric encumbrance of the SePh moiety with the styryl probe.

KEY REFERENCES (out of 87 total cited in dissertation)

1. W.F. Reynolds, Prog. Phys. Org. Chem, 14, 165 (1983).

2. D.J. Craik and R.T.C. Brownlee, Prog. Phys. Org. Chem., 14, 1 (1983).

3. G.J. Martin, M.L.Martin, and S.P. Gouesnard, ^{15}N NMR Spectroscopy, Berlin, Springer-Verlag, 1981.

4. D.G.Craik, in Annual Reports on NMR Spectroscopy, 15, (G.A. Webb, ed), Academic Press, London, 1983.

5. N.P. Luthra and J.D. Odom, in The Chemistry of Organic Selenium and Tellurium Compounds, Volume I, (S. Patai and Z. Rappoport, eds.), John Wiley and Sons, Chichester, England, 1986.

6. G.P. Mullen, N.P. Luthra, R.B. Dunlap, and J.D. Odom, J. Org. Chem,, 50, 811 (1985).

7. C.N. Robinson, C.D. Slater, J.S. Covington III, C.R. Chang, L.S. Dewey, J.M. Franceschini, J.L. Fritzsche, J.E. Hamilton, C.C. Irving, Jr., J.M. Morris,D.W. Norris, L.E. Rodman, V.I. Smith, G.E. Stablein, and F.C. Ward, J. Magn. Reson., 41, 293 (1980).

8. W. Schwotzer and W. von Phillipsborn, Helv. Chim Acta,60, 1501 (1977).

9. G.C. Levy and R.L. Lichter, Nitrogen-15 Nuclear Magnetic Resonance Spectroscopy, John Wiley and Sons, New York, 1979.

DISSERTATION ABSTRACT INFORMATION

AUTHOR: Alan A. Shaffer

TITLE: The Styrene Probe Applied to ^{15}N and ^{77}Se NMR

MILITARY RANK: Major

SERVICE BRANCH: Air Force

DATE: 1988

NUMBER OF PAGES: 326

DEGREE AWARDED: Doctor of Philosophy

INSTITUTION: Memphis State University

MICROFILM VERSION/MSU

ABSTRACT

Fluor 14

Previous work had shown that the ^{19}F NMR chemical shift (δ)/Hammett Substituent Constant (σ) correlation of ethyl α-fluorocinnamates gave a positive slope (greater deshielding with increasing sigma value), opposite to that predicted by the π-polarization mechanism. To ascertain if this was a general phenomenon in α-substituted cinnamate esters for atoms having unshared pairs of electrons, ^{15}N chemical shift correlations were obtained for the Z and E isomers of ethyl α-diethylaminocinnamates (Series A, 13 compounds). A positive slope was found for both isomers, with the σ^- scale giving the best single substituent parameter result compared to σ, σ^+, and σ^{13}, indicating through-resonance to be predominant in these compounds.

This correlation study was extended to a series of benzylidene azlactones (Series B, 10 compounds) and ethyl α-cyanocinnamates (Series C, 7 compounds). Here the orthogonality of nitrogen's unshared electron pair to the styryl system prevents through-resonance, with the result that the ^{15}N δ/σ correlation slopes predicted by the π-polarization mechanism were observed; (negative/Series B, positive/Series C). The correlation for Series C was far superior implying that phenyl ring anisotropy may be adversely affecting the spatially proximate unshared electron pair in Series B.

^{77}Se NMR of the E and Z isomers of ethyl α-(phenylseleno)-cinnamates (Series D) also revealed a positive slope, although there was a large isomer disparity in correlative behavior. The E isomer correlation (17 compounds) displayed a wide chemical shift range ($\approx$ 40 ppm), and good overall correlations, with σ^{13}/σ^{+} collectively superior to σ/σ^{-}. The Z isomer series (10 compounds) gave a much narrower chemical shift range ($\approx$ 13 ppm), a good correlation only with σ^{-} and greater deshielding ($\approx$ 100 ppm). These Z/E isomer differences may be related to variations in n-π overlap due to steric encumbrance of the SePh moiety with the styryl probe.

Dual Substituent Parameter (DSP) analysis of the ^{15}N and ^{77}Se δ's from Series A, B, and D was performed to augment the single substituent parameter treatment. Also, ^{13}C correlations of selected nuclei from Series A, B and D were examined to evaluate the interplay of the π-polarization and through-resonance mechanisms.

MICROFILM VERSION/MSU

ABSTRACT

Previous work had shown that the ^{19}F NMR chemical shift (δ)/Hammett Substituent Constant (σ) correlation of ethyl α-fluorocinnamates gave a positive slope (greater deshielding with increasing sigma value), opposite to that predicted by the π-polarization mechanism. To ascertain if this was a general phenomenon in α-substituted cinnamate esters for atoms having unshared pairs of electrons, ^{15}N chemical shift correlations were obtained for the Z and E isomers of ethyl α-diethylaminocinnamates (Series A, 13 compounds). A positive slope was found for both isomers, with the σ^- scale giving the best single substituent parameter result compared to σ, σ^+, and σ^{13}, indicating through-resonance to be predominant in these compounds.

This correlation study was extended to a series of benzylidene azlactones (Series B, 10 compounds) and ethyl α-cyanocinnamates (Series C, 7 compounds). Here the orthogonality of nitrogen's unshared electron pair to the styryl system prevents through-resonance, with the result that the ^{15}N δ/σ correlation slopes predicted by the π-polarization mechanism were observed; (negative/Series B, positive/ Series C). The correlation for Series C was far superior implying that phenyl ring anisotropy may be adversely affecting the spatially proximate unshared electron pair in Series B.

^{77}Se NMR of the E and Z isomers of ethyl α-(phenylseleno)-cinnamates (Series D) also revealed a positive slope, although there

was a large isomer disparity in correlative behavior. The E isomer correlation (17 compounds) displayed a wide chemical shift range (≈ 40 ppm), and good overall correlations, with σ^{13}/σ^{+} collectively superior to σ/σ^{-}. The Z isomer series (10 compounds) gave a much narrower chemical shift range (≈ 13 ppm), a good correlation only with σ^{-} and greater deshielding (≈ 100 ppm). These Z/E isomer differences may be related to variations in n-π overlap due to steric encumbrance of the SePh moiety with the styryl probe.

Dual Substituent Parameter (DSP) analysis of the ^{15}N and ^{77}Se δ's from Series A, B, and D was performed to augment the single substituent parameter treatment. Also, ^{13}C correlations of selected nuclei from Series A, B and D were examined to evaluate the interplay of the π-polarization and through-resonance mechanisms.

To The Graduate Council:

I am submitting herewith a dissertation written by Alan A. Shaffer, entitled, "The Styrene Probe Applied to ^{15}N and ^{77}Se NMR." I recommend that it be accepted for thirty hours of credit in partial fulfillment of the requirements for the degree of Doctor of Philosophy, with a major in Organic Chemistry.

Charles N. Robinson

Dr. Charles N. Robinson,
Major Professor

We have read this dissertation
and recommend its acceptance:

Peter K. Bridson

Dr. Peter K. Bridson

Richard Williams

Dr. Richard V. Williams

Ted Burkey

Dr. Theodore J. Burkey

J C Williams

Dr. James C. Williams

Accepted for the Graduate Council:

Dorothy Arata

Dorothy Arata, Dean
Graduate School

DEDICATION

To Dad, who served the Great Chemist, and who also minored in Chemistry at Otterbein College.

TABLE OF CONTENTS

Page

LIST OF TABLES viii
LIST OF FIGURES x
ACKNOWLEDGEMENTS xii
ABSTRACT xiii

CHAPTER

I. HISTORICAL PERSPECTIVE 1
A. Introduction 1
B. ^{15}N NMR 2
C. ^{77}Se NMR 10
D. The Styrene System 19
E. NMR Studies of Compounds Containing Nitrogen and the Styrene System 24
1. Correlative Studies of Enamines and Enaminones (^{15}N) 24
2. Correlative Studies of Z-5-Aryl-methylenehydantoins (^{13}C/^{1}H) 28

II. STATEMENT OF THE PROBLEM 32
A. Ethyl α-fluorocinnamates 32
B. Approach/Predictions 37
1. Series A) (E+Z) Ethyl 2-diethylamino-3-phenyl-2-propenoates 37
2. Series B) (Z) 4-benzylidene-2-methyl-2-oxazolin-5-ones 38
3. Series C) (Z) Ethyl 2-cyano-3-phenyl-2-propenoates 39
4. Series D) (E+Z) Ethyl 3-phenyl-2-phenylseleno-2-propenoates. 40
C. Geometrical Isomerism 40
D. Cross-Conjugative Competition 42

III. EXPERIMENTAL 45
A. Synthesis 45
1. Nitrogen Compounds (Series A-C)/General Comments 45
2. Series A/Example Procedure 46
a. Synthesis Summary 48
b. Starting Compounds 52
1) Ethyl diethylaminoacetate 52
2) Methyl diethylaminoacetate 53
3. Series B/General Comments 53
a. Example Procedure 54

TABLE OF CONTENTS

CHAPTER Page

III. EXPERIMENTAL (Continued)

4. Series C/General Comments 55
5. Selenium Compounds (Series D)/General Comments/ Mechanistic Considerations 55
  a. Example Procedure (liquid products). 58
  b. Example Procedure (solid products) 60
  c. Starting Compounds 67
    1) Ethyl phenylselenoacetate 67
B. NMR 68
1. Series A 68
  a. ^{15}N NMR 68
    1) Sample Preparation 68
    2) ^{15}N NMR Standard Parameters 72
  b. ^{13}C/^{1}H NMR Standard Parameters 73
  c. Selective Decoupling 74
2. Series B 76
  a. ^{15}N NMR 76
  b. ^{1}H NMR 77
3. Series C 77
  a. ^{15}N NMR 77
  b. ^{13}C/^{1}H NMR 77
4. Series D 78
  a. ^{77}Se NMR 78
  b. ^{13}C/^{1}H NMR 79

IV. DISCUSSION OF RESULTS 80
A. Hammett Single Substituent Parameter Constants (σ, σ^+, σ^- and σ^{13}). 80
1. Sigma (σ) scale. 80
2. Sigma plus (σ^+) and Sigma minus (σ^-) scales . . 81
  a. Sigma plus (σ^+) 81
  b. Sigma minus (σ^-) 82
3. Sigma thirteen (σ^{13}) scale 83
B. Single Substituent Parameter Correlations 86
1. Series A: General Comments/Isomer Assignments . 86
  a. E vs Z Isomers 91
    1) Summary of the Data 101
    2) Interpretation of the Results 106
      a) Positive Slope 106
      b) Superiority of σ^- Correlations . . . 106
  b. The E/Z Isomer Correlations/A Closer Look . 109
  c. The E Correlation 110
  d. The Z Correlation 117
  e. Secondary Effects/Proximity of the N(Et)$_2$ to the Phenyl Substituent. 120

TABLE OF CONTENTS

CHAPTER Page

IV. DISCUSSION OF RESULTS (Continued)

2. Series B 122
  a. Summary of the Data 122
  b. Interpretation of the Results 127
    1) Negative slope 127
    2) Narrow ^{15}N SCS Range/Poor Correlations . 128
    3) Worst Fit by σ^{-}. 129
3. Series C 130
  a. Summary of the Data 130
  b. Interpretation of Results 135
    1) Positive Slope 135
    2) ^{15}N SCS Range/Correlation Excellence . . 136
4. Series D 137
  a. Isomer Assignments 137
  b. E Isomers 138
    1) *Summary of the Data* 138
    2) Interpretation of the Results 138
      a) Large Positive Slope 138
      b) Superiority of σ^{13}/σ^{+} Correlations Over σ/σ^{-} 143
  c. Z Isomers/Discussion of the Data in Contrast with the E Isomers 148
    1) Negative Hyperconjugation 157
    2) d-orbital Involvement in Divalent Se Compounds/Evidence From the Literature . 161
    3) d-Orbital Participation of Se in Series D 164
      a) Model 1 164
      b) Model 2 166
C. Dual Substituent Parameter Analysis 167
1. General Comments 167
2. ^{77}Se DSP Analysis/ Series D (E Isomers) 171
3. ^{15}N DSP Analysis/Series A and B 179
  a. Series A 179
  b. Series B 182
D. ^{13}C Correlations 186
1. Series A/General Comments 186
  a. General Interpretation of the Data 186
  b. Specific Aspects of the Data 191
    1) #6 Carbon Correlations 191
    2) #5 Carbon Correlations 191
    3) #4 Carbon Correlations 192
    4) The #5 and #6 Carbon Shieldings 193
2. Series D (E isomers) 193
3. Series B 196

TABLE OF CONTENTS

Chapter Page

V. CONCLUSION 200

REFERENCES 204

APPENDICES 210

A. General Experimental Methods 211
B. ^{1}H NMR 212
C. ^{13}C NMR 250
D. Mass Spectra/Gas Chromatography 283
E. Infrared Spectra 294

LIST OF TABLES

Table Page

1. Substituent Effects on NMR Chemical Shifts in Sidechain Systems 3
2. Series A: (E+Z) Ethyl 2-diethylamino-3-phenyl-2-propenoates/Synthesis and Physical Data 49-50
3. Series D: (E+Z) Ethyl 2-phenylseleno-3-phenyl-2-propenoates/Synthesis and Physical Data 62-63
4. ^{15}N Standard Parameters (Series A) 72
5. ^{13}C Standard Parameters (Series A) 73
6. ^{1}H Standard Parameters (Series A). 74
7. ^{13}C Fully Coupled Parameters (Series A). 75
8. ^{13}C Selective Decoupling Parameters (Series A) 76
9. ^{15}N Standard Parameters (Series B) 77
10. ^{77}Se Standard Parameters (Series D). 78
11. ^{77}Se Selective Decoupling Parameters (Series D). 79
12. Hammett Single-Substituent Values 85
13. ^{15}N Chemical Shifts/Series A 87
14. Series A Correlations From Figures 9 and 8 101
15. ^{15}N Chemical Shifts/Series B 122
16. Series B Correlations From Figure 11 122
17. ^{15}N Chemical Shifts/Series C 130
18. Series C Correlations From Figure 12 130
19. ^{77}Se Chemical Shifts/Series D 137
20. Series D Correlations From Figure 13 143
21. Series D (Z Isomer) Correlations From Figure 14 149

LIST OF TABLES

TABLE Page

22. Taft Resonance Models 169-170

23. DSP Parameters 172

24. Taft Resonance Scale Values 176

25. Correlation Results for Selected ^{13}C Nuclei/Series A . 187

26. ^{13}C Assignments: (Z) Ethyl 2-diethylamino-3-phenyl-2-propenoates 188

27. ^{13}C Assignments: (E) Ethyl 2-diethylamino-3-phenyl-2-propenoates 189

28. Correlation Results for Selected ^{13}C Nuclei/Series D (E isomers) 194

29. ^{13}C Assignments: (E) Ethyl 2-phenylseleno-3-phenyl-2-propenoates 195

30. Correlation Results for Selected ^{13}C Nuclei/Series B . 197

31. ^{1}H NMR Chemical Shifts/Series A 213

32. ^{1}H NMR Chemical Shifts/Series D 216

LIST OF FIGURES

FIGURE Page

1. ^{13}C Shieldings from Styrene π-Polarization 21

2. a. $^{19}F\delta/\sigma^{13}$ Correlation of Ethyl α-fluorocinnamates . . 34
   b. $J_{F-C(\beta)}/\sigma^{13}$ Correlation of Ethyl α-fluorocinnamates. 35

3. $CDCl_3$ vs CD_3NO_2 N-15 Chemical Shifts
   a. E-Ethyl α-diethylaminocinnamates 70
   b. Z-Ethyl α-diethylaminocinnamates 71

4. Fully Coupled Carbonyl Spectrum/p-Me Derivative (Series A) 90

5. Selectively Decoupled Carbonyl Spectrum/pMe Derivative (Series A) 90

6. $^{15}N/^{13}C/^{1}H$ Chemical Shift Intensity Patterns; Z and E Isomers (Series A) 92

7. E-Ethyl α-diethylaminocinnamates; N-15 Chemical Shift vs:
   a. Sigma Minus 93
   b. Sigma 94
   c. Sigma 13 95
   d. Sigma Plus 96

8. Z-Ethyl α-diethylaminocinnamates; N-15 Chemical Shift vs:
   a. Sigma Minus 97
   b. Sigma 13 98
   c. Sigma 99
   d. Sigma Plus 100

9. E-Ethyl α-diethylaminocinnamates (without p-NO_2); N-15 Chemical Shift vs:
   a. Sigma Minus 102
   b. Sigma 13 103
   c. Sigma 104
   d. Sigma Plus 105

LIST OF FIGURES

FIGURE Page

10. Two-Line Linear Regression Analysis: E-Ethyl α-diethylaminocinnamates (without p-NO_2); N-15 Chemical shift vs:
    a. Sigma Minus 112
    b. Sigma 13 113
    c. Sigma 114
    d. Sigma Plus 115

11. Benzylidene Azlactones; N-15 Chemical Shift vs:
    a. Sigma 123
    b. Sigma 13 124
    c. Sigma Plus 125
    d. Sigma Minus 126

12. Z-Ethyl α-cyanocinnamates; N-15 Chemical Shift vs:
    a. Sigma 13 131
    b. Sigma 132
    c. Sigma Plus 133
    d. Sigma Minus 134

13. E-Ethyl α-(phenylseleno)cinnamates; Se-77 Chemical Shift vs:
    a. Sigma 13 139
    b. Sigma Plus 140
    c. Sigma 141
    d. Sigma Minus 142

14. Z-Ethyl α-(phenylseleno)cinnamates; Se-77 Chemical Shift vs:
    a. Sigma Minus 150
    b. Sigma 151
    c. Sigma 13 152
    d. Sigma Plus 153

ACKNOWLEDGEMENTS

First and foremost my thanks go to Dr. Charles N. Robinson, my research advisor. His help, guidance, and patience have been crucial in my completion of this program within the strict time constraints of the Air Force. I wish to also express my gratitude to the Frank J. Seiler Research Laboratory (Air Force Systems Command) for sponsoring me in this school assignment.

I also thank Dr. Richard Williams for his valuable technical guidance with the department's new VXR-300. Before this instrument was operational, Dr. Leslie Gelbaum of the Georgia Institute of Technology, Atlanta, Georgia, performed the ^{77}Se, ^{1}H, and ^{13}C NMR's for the selenium compounds. This was vital for timely completion of this research effort.

I also wish to thank several other individuals for their assistance: Dr. James Williams for his help with the GRAPHPAD® plotting procedure; Dr. Randy Johnston and Dr. Larry Houk for their insight regarding Se d-orbital participation; Dr. Carl Slater, Northern Kentucky University, for performing the DSP calculations and providing us a very valuable critique of the DSP discussion; Marius Toldi for his assistance in preparing the ^{15}N-labeled benzylidene azlactones; and Jeanne Tutor for typing the manuscript.

A final very special thanks goes to all my family members, but especially to my wife, Patsy, for all her understanding, patience, and generous moral support over the last three years!

ABSTRACT

Previous work had shown that the ^{19}F NMR chemical shift (δ)/Hammett Substituent Constant (σ) correlation of ethyl α-fluorocinnamates gave a positive slope (greater deshielding with increasing sigma value), opposite to that predicted by the π-polarization mechanism. To ascertain if this was a general phenomenon in α-substituted cinnamate esters for atoms having unshared pairs of electrons, ^{15}N chemical shift correlations were obtained for the Z and E isomers of ethyl α-diethylaminocinnamates (Series A, 13 compounds). A positive slope was found for both isomers, with the σ^- scale giving the best single substituent parameter result (Z $R^2 = 0.9604$; E $R^2 = 0.9166$; R^2 = (correlation coefficient)^2) compared to σ, σ^+, and σ^{13}, indicating the through-resonance mechanism to be predominant in these compounds. (The E isomer correlations displayed a concave upward determinate error, implying a substantial change of the substituent effect transmission mechanism, probably due to the ethyl carboxylate group.)

This ^{15}N δ correlation study was extended to a series of benzylidene azlactones (Series B, 10 compounds) and ethyl α-cyano-cinnamates (Series C, 7 compounds) with sp^2 and sp hybridized nitrogens, respectively. In both series, the nitrogen's unshared electron pairs are rigidly held orthogonally to the π-electrons in the styryl system, preventing the through-resonance phenomenon observed in Series A. The π-polarization mechanism predicts a negative ^{15}N δ/σ

correlation slope for Series B and a positive slope for Series C. In both cases, these predicted slopes were observed; however, the correlation for Series C was far superior (vs σ^{13}, $R^2 = 0.9897$) to that of Series B (vs σ, $R^2 = 0.8016$). The most likely explanation for this difference is that the phenyl ring anisotropy may be affecting the spatially proximate unshared electron pair in Series B, while the nitrile triple bond displays a well-defined variable polarizability, consistent with the sp character of the nitrile carbon.

^{77}Se NMR of the E and Z isomers of ethyl α-(phenylseleno)-cinnamates (Series D) also revealed a positive slope, although there was a large isomer disparity in correlative behavior. The E isomer correlation (17 compounds) displayed a wide chemical shift range (≈ 40 ppm), and good overall correlations, with R^2 values for σ^{13}/σ^+ (0.9525/0.9386), greater than those for σ/σ^- (0.9093/0.9050). The Z isomer series (10 compounds) gave a much narrower chemical shift range (≈ 13 ppm), a good correlation only with σ^- ($R^2 = 0.9467$) and greater deshielding (≈ 100 ppm). These differences in the Z versus E isomer may be related to variations in n-π overlap due to steric encumbrance of the SePh moiety with the styryl probe.

Dual Substituent Parameter (DSP) analysis of the ^{15}N and ^{77}Se δ's from Series A, B, and D was performed to augment the single substituent parameter treatment. Also, ^{13}C correlations of selected nuclei from Series A, B and D were examined to evaluate the interplay of the π-polarization and through-resonance mechanisms.

CHAPTER I

HISTORICAL PERSPECTIVE

A. Introduction

Recent improvements of NMR technology have allowed an increased number of nuclei to be studied. Among the most promising of these are ^{15}N and ^{77}Se. The important roles of both of these elements in biochemistry and, respectively for N and Se, in chemical energetics and organic synthesis increase the value of learning more of their bonding properties through NMR.

In the last 10-15 years, NMR spectroscopy (particularly ^{13}C) has provided a thorough, accurate data base for correlation analyses of substituent effects. The general goal has been to use relationships between chemical shifts and substituent parameters (Hammett σ constants most notably) to obtain one or more "transmission coefficients" (termed ρ, the slope of the above correlation), which can then be used to quantify the ways in which substituent effects are transmitted. Any molecular structure that allows a useful measurement of substituent effects is called a probe.[1]

The relative importance of varying transmission modes of substituent effects depends on the specific physical probe being studied. For ^{13}C NMR chemical shifts, the relevant mechanisms are sensitive to π-electron densities, and are different from those involved in reactivity studies. In Table 1, taken verbatim from reference 2, the important transmission modes affecting NMR chemical shifts are listed. Included is an indication of how these effects contribute to the polar and resonance components of the Dual Substituent Parameter (DSP) equation,

$$\Delta Q = \rho_I\sigma_I + \rho_R\sigma_R$$

where ΔQ = substituent effect on any measured quantity
(i.e., NMR chemical shift)

which has come to be one of the most common correlative techniques used.[2]

Resonance effects relate to the ability of a substituent to delocalize or transfer charge, while polar effects refer to a substituent's ability to polarize the electron distribution of a probe site. Resonance effects are more clearly understood and are commonly represented by the familiar canonical structures. In contrast, polar effects involve no formal π charge transfer between the substituent and the probe site; a substituent's polar effect can be transmitted by one or more mechanisms and is, generally, a more complex phenomenon.

B. ^{15}N NMR

^{15}N chemical shifts have been shown to be particularly sensitive to the molecular environment of the nitrogen atom [3], largely due to nitrogen's lone pair of electrons. In those series of compounds in which substituents can interact directly with this lone pair, generally large ^{15}N substituent chemical shifts (SCS) values have been observed. (SCS) is defined as the change in chemical shift that occurs when a hydrogen atom in one part of the molecule is

Table 1 [2]

Substituent Effects on NMR Chemical Shifts in Sidechain Systems[a]

Mechanism	Contribution[b]	Explanation
1. Resonance Effect (R_π) 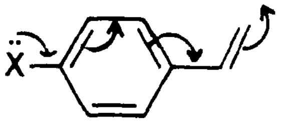	ρ_R	The substituent transfers π-electrons to C-β. A classical valence bond type approach is often used to represent this effect. This mechanism also contributes to ^{13}C para chemical shifts.
2. π-Polarization (F_π) 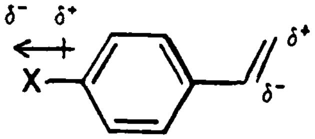	ρ_I	The substituent dipole polarizes the π-system in the sidechain. The effect is transmitted through-space (but may be modified by the dielectric properties of the intermediate molecular cavity). In the example shown π electron density is increased at C-α and decreased at C-β. This is the most important polar effect on ^{13}C chemical shifts in unsaturated sidechains.
3. Direct through-space field effect (F_D) 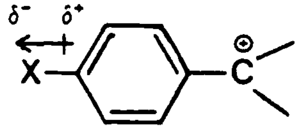	ρ_I	This is most important in charged sidechains and arises from a direct (through-space) electrostatic interaction between the charge at the probe site and the substituent dipole.

[a] These are not the only mechanisms that affect NMR chemical shifts, but are the most important.

[b] This column indicates which term (ρ_I, or ρ_R) of a DSP correlation is affected by the indicated mechanism.

replaced with a substituent group. The accepted sign convention is that positive values imply deshielding associated with the shift of a resonance to a lower magnetic field (higher frequency) and vice versa. For example, the *para* carbon SCS for the NH_2 substituent in benzene is given as -9.8 ppm): [4]

$\delta = 118.51$ ppm

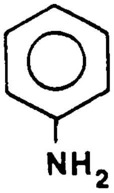

I

$\delta = 128.31$ ppm

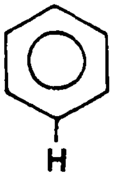

II

$$SCS_{(NH_2)} \text{ of } p\text{-carbon} = 118.51-128.31 = -9.8 \text{ ppm}$$

In the aniline series III, where X represents the standard set of substituents for e^-(electron) withdrawers through e^- donors: NO_2, CN, CF_3, H, CH_3, Cl, OMe, and $N(Me)_2$, the range of shifts for the ^{15}N is about 20 ppm.[5]

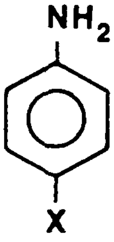

III

Factors reducing lone pair interaction with the substituent lessen the range of the observed ^{15}N shifts. A clear example of this is a direct comparison of the aniline series noted above with the anilinium ion series; a much reduced interaction between the substituent and the sidechain is evident in the anilinium ion series.[6] This is easily understood in terms of the loss of strong conjugative interaction of the unprotonated amine with acceptor substituents, i.e. p-NO_2:

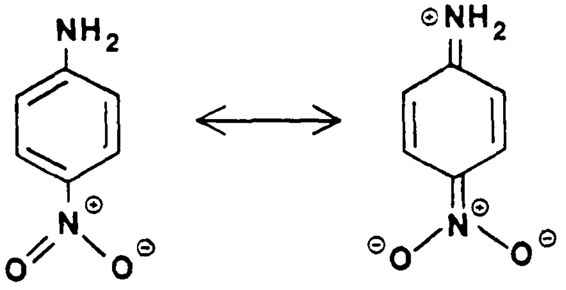

IV

Here, electron donation from the lone pair causes a downfield shift of 14.9 ppm. For the anilinium ions, this kind of interaction is not possible and a para-NO_2 group causes a downfield shift of only 1.1 ppm.

Another example illustrating the importance of the nitrogen lone pair in determining SCS values is the small range of ^{15}N shifts noted in the quinoline series V, where the nitrogen is at a similar distance from X but its lone pair is restricted to the ring plane and thus can not interact via resonance with the substituent. The ^{15}N SCS values for CH_3 and NO_2 groups were -1.3 ppm and +2.2 ppm respectively. [5] In contrast, in 5-substituted indoles (VI) where the substituent can interact more strongly with the nitrogen lone pair, SCS values of -0.7 ppm and +6.9 ppm were found.

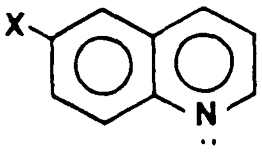

V

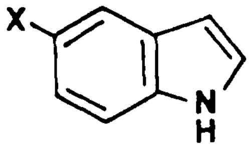

VI

Compound series having the structure VII have also illustrated the importance of the lone pair in effecting ^{15}N SCS values. Dual substituent parameter analysis of the ^{15}N SCS values decrease in the order for Z: H > CH=C(Ph)CH_3 > SO_2Ph > $COCH_3$.[7] The largest shifts (as reflected in the greater ρ values) for the anilines (Z=H) can be assumed to reflect the greater ability of the X group to interact with the nitrogen lone pair in this series. In the other members, the nitrogen lone pair is delocalized to some extent with the Z group (VIII). An increased π electron-withdrawing tendency of the Z group produces increasing delocalization of the nitrogen lone pair. This reduces its interaction with the X substituent (which is farther away) and is reflected in the reduced ^{15}N SCS values.

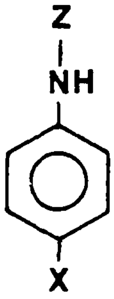

VII

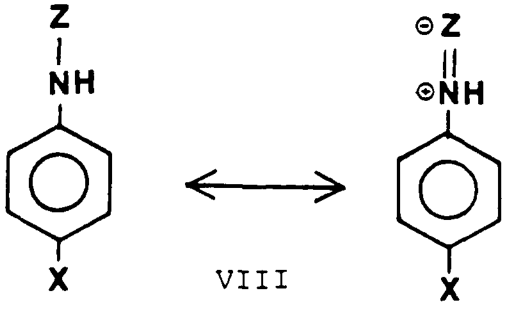

VIII

An interesting contrast to the type of compounds discussed so far is provided by the imine series IX. Again, ρ_I and ρ_R values decrease with increasing π-withdrawal mesomeric effect of Z but to a lesser extent. This implies that the geometry of the molecule, maintaining full mesomeric interaction of C=N and Ph precludes as significant an interaction of the nitrogen lone pair with X (the lone pair is orthogonal to the resonance plane).

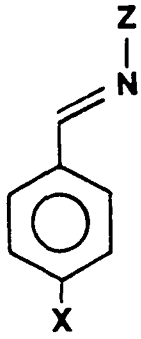

IX

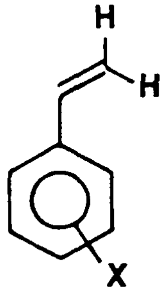

X

However, in spite of the lone pair not interacting with the Z group or with the π system containing the X substituent, significant substituent effects in the ^{15}N chemical shifts can still be observed. For the oximes (Z=OH) the range of shifts is about 25 ppm as X is varied from $N(Me)_2$ to NO_2 reflecting a considerable shielding range inherent in the π framework. A plot of these shifts versus the corresponding ^{13}C shifts for the β carbon in styrenes (X) has a slope of 2.3 showing that the ^{15}N shifts are more than twice as sensitive to substituent effects as are ^{13}C shifts.[8]

As a further example, DSP analysis of the ^{15}N shifts in N-(arylmethylidene) cyclohexanamine derivatives (XI) gave ρ_I and ρ_R values of 16.6 and 30.1 respectively. When the lone pair becomes protonated (XII) the ρ values were not significantly affected

($\rho_I=13.8$, $\rho_R=31.5$), although the absolute chemical shift values were, of course, markedly changed.[9] This similarity obtained in transmission coefficient values would help substantiate the premise that in neither structure (XI or XII) could the unshared electron pair be markedly affected by X due to its orthogonality to the π system. This latest example helps to illustrate the versatility of ^{15}N NMR: the lone pair on nitrogen is not an essential requirement for large ^{15}N SCS values to be obtained.

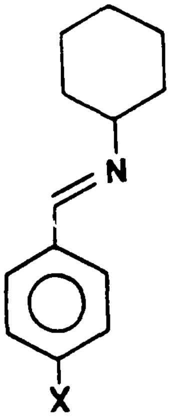

XI

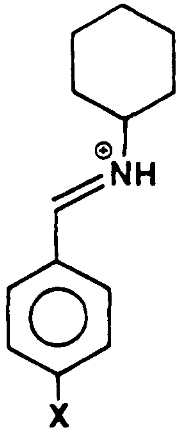

XII

^{15}N NMR has also been used more recently to evaluate in detail the bonding structure of compounds with cumulated nitrogen atoms, in particular the benzenediazonium salts (XIII) [10] and 1-phenyl-3, 3-pentamethylenetriazenes (XIV).[11]

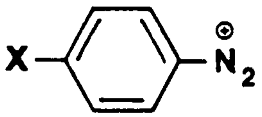

XIII

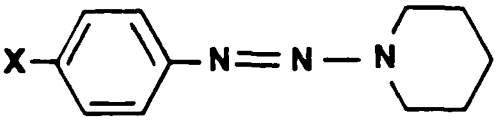

XIV

From studies of the ^{1}J (^{13}C-^{15}N) values for a series of aryldiazoniumtetrafluoroborates and comparable anilinium fluorosulfonates, it was concluded that contributions from resonance structures involving double-bond character of the C-N bond (XV C) are relatively unimportant in the ground state structure of aryldiazonium ions, consistent with x-ray and IR spectroscopic findings. The ipso C-N α bond was found to have ordinary single bond length and the N_α - N_β bond length and stretching frequencies were those of a normal triple bond.[10]

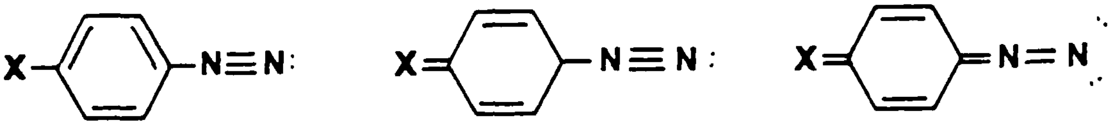

A B C

XV

By careful analysis of SCS data for nitrogens 1,2, and 3 in XVI, Patrick and Willaredt were able to conclude that of the three presumably major contributing resonance forms of this compound, (XVIA-C) structure XVI B is minor relative to A and C. The relatively small sensitivity of N2 chemical shifts (over the usual substituent range) of 4.2 ppm in contrast to 20 ppm for N1 and 14.2 ppm for N3 led to this conclusion.[11]

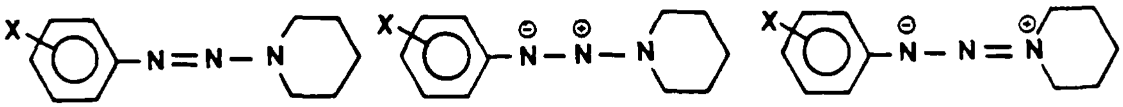

A B C

XVI

The consistent success of these correlative studies coupled with the advent of high sensitivity NMR has led to a promulgation of correlation analysis between $\delta\ ^{15}N$ and a wide variety of physical constants, including the Hammett substituent parameters. Specific quantitative correlation equations have been developed for the following N-containing compounds: anilines, benzenesulfonamides, acetanilides, enamines, benzamides, imines, oximes, hydrazones, porphyrins, aminophosphines and silatranes.[12]

C. ^{77}Se NMR

The ^{77}Se nucleus is particularly well suited for evaluating electronic effects. Its wide chemical shift range ($\approx$ 3000 ppm), due to the greater polarizability of this larger atom, and its high sensitivity should provide a useful contrast to that obtained from the ^{15}N nucleus. Also, selenium is important in many biochemical processes [13] and its wide use in organic synthesis [14] further merit its investigation, as evidenced by the increasing number of ^{77}Se NMR studies in the last few years; these have included many correlative studies for a variety of organic structures. These investigations have illustrated the versatility of this element in its chemical bonding nature. Selenium's polarizability has been a dominant theme in accounting for these observations. Several examples serve to illustrate this inherent versatility/flexibility in Se's NMR behavior.[15]

Symmetrically substituted diphenyl diselenides (XVII) were studied through the typical range of X substituents. As X became increasingly e^- withdrawing, positive slopes were observed for the circled carbons (as shown below), whereas the selenium atoms displayed negative slopes (this directly parallels the π-polarization mechanism described in the introduction, page 3).[16]

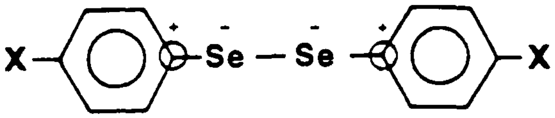

XVII

An interesting variation on this theme was observed in comparing diphenyldiselenide (XVIII) to the mono-substituted p-CH_3O analogue (XIX), where very different NMR shifts of the adjacent selenium atoms were observed. [16] A high sensitivity to adjacent charge buildup is shown here.

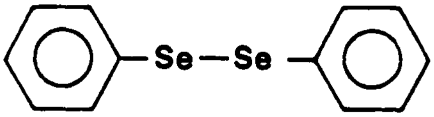

XVIII

VS

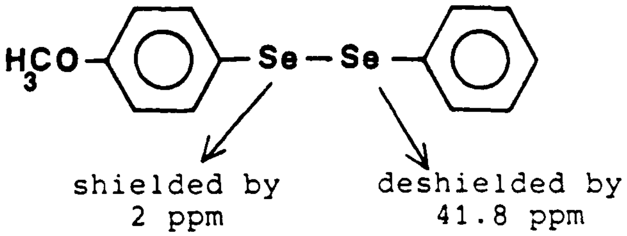
H3CO
Se
Se
shielded by
2 ppm
deshielded by
41.8 ppm

XIX

The polarizability concept for Se has also been used to account for the considerable solvent induced shifts (up to 40-50 ppm in some cases) observed in ^{77}Se NMR, as well as the large effect in Se shielding from successive α site methyl substitution in dialkylselenides. The greater deshielding of Se in the series

$$CF_3SeCF_3 \rightarrow CF_3SeCF_2Cl \rightarrow CF_3SeCFCl_2 \rightarrow CF_3SeCCl_3$$

is consistent with the fact that the more polarizable Cl (versus F) can polarize electron density of the adjacent Se more effectively.[17]

Selenium's versatility in charge stabilization has been shown by its ability to stabilize both anionic and cationic α sites. Generally, the electron withdrawing inductive effect of Se(-I) and its electron-donating resonance effect (+M) are invoked to account for these observations, respectively. Consistent with this is the observation that the SeMe group shows a -I and a +M effect, as does the TeMe group (many comparisons have been made between Se and Te). ^{13}C-NMR work has shown the weak electron donating character of SeR groups and that the level of p-π interaction decreases as the size of R increases.[18] A variety of investigative techniques has shown the increase in the +M effect in the order:[19]

$$TeMe < SeMe < SMe < OMe$$

^{13}C-NMR studies of chalcogenoanisoles, including Se, have shown that the +M effect outweighs the -I effect.[20]

As a specific detailed example, Kalabin investigated selenoanisoles (XX). The ^{77}Se chemical shifts in the para series correlated well and covered a 50 ppm range as X was varied from

$N(CH_3)_2$ to NO_2 (181.2 to 225.6 ppm downfield from $Se(CH_3)_2$). This range was much larger than had been observed for ^{13}C chemical shifts in any sidechain system and attested to its potential usefulness. In these compounds, the direction of shifts for the ^{77}Se was "normal" based on direct field-inductive effects (e^- donors caused upfield ^{77}Se shifts and e^- withdrawers downfield ones).[21]

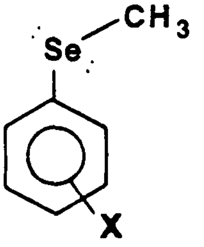

XX

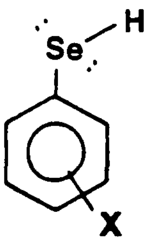

XXI

This good correlative behavior was in contrast to that obtained for meta and para substituted phenylselenols (XXI) where the poor correlation observed was argued to be due to H-bond formation in these selenols (up to a 20 ppm effect according to the investigators).[22] This is intriguing in light of the fact that the total chemical shift range observed was about 45 ppm, and, as of this publication, no additional definitive studies showing significant H-bonding to Se had appeared.

Selenium's transmissivity of electronic substituent effects has been studied through a range of molecular structure. The first studies of this nature examined the reactivity ratios at 25°C of the selenides (XXII) in their reactions forming the quaternary amine salt with picryl chloride and p-nitrobenzyl chloride.[23] At 25°C, the $k(H)/k(NO_2)$ for these two reactions were 22.2 and 17, respectively, which were higher than those for oxygen as the bridging atom (16 and 12.1) and lower than those found for the S compounds (30.6 and 23.8). Other subsequent work has shown the following decreasing order of transmissivity:[24] (NMe > NH > S > Se > O > CH_2).

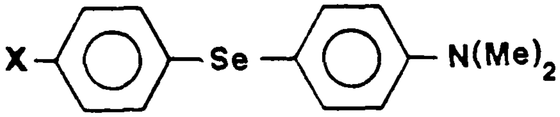

(X = p-NO_2, H)

XXII

Studies involving the hydrolysis of aryl chalcogenesters (XXIII) [25] and ionization of aryl chalcogenacetic acids (XXIV) [26] generally indicate a high similarity of electronic transmissivity among these chalcogen atoms. This has been rationalized as a consequence of the interplay (as one goes down the chalcogen family) between the increase in polarizability of the heteroatom and the increased distance of the substituent from the reaction center. These studies also showed that, as expected, the methylene unit has a greater insulating effect than any of the chalcogen atoms.

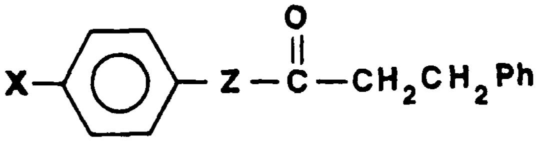

Z = O,S,Se

XXIII

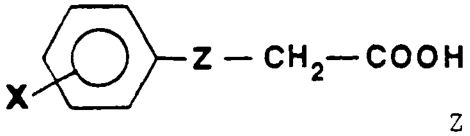

Z = O,S,Se

XXIV

Another particularly interesting ^{77}Se NMR correlative study reflecting the transmissivity of this nucleus appeared in 1985 with the investigation of eleven _para_-substituted phenylselenobenzoates (XXV):[27]

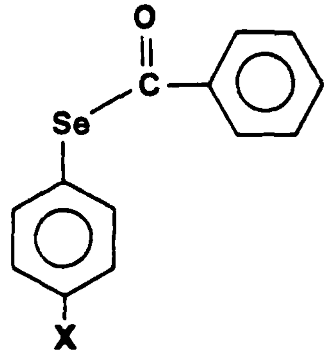

XXV

Selenium-77 chemical shifts ranged from 622.9 ppm (for X = NMe_2) to 650.4 ppm (X=CN). Single and dual substituent parameter analyses of the SCS for ^{77}Se, C-1 of the selenophenyl ring, and the carbonyl carbon were performed. It was found that the predominant contribution to both the ^{77}Se and _ipso_ (C1) ^{13}C chemical shift data was a resonance effect with a smaller contribution from the effect of substituent induced polarization of the ring π electrons. DSP analysis of the ^{13}C

SCS data for the carbonyl carbon (using σ_R^{BA}, that Taft resonance scale based on benzoic acid ionization), however, showed a reverse substituent effect. Presumably this arose from the interaction of the substituent dipole with the SeC(O)Ph sidechain system:

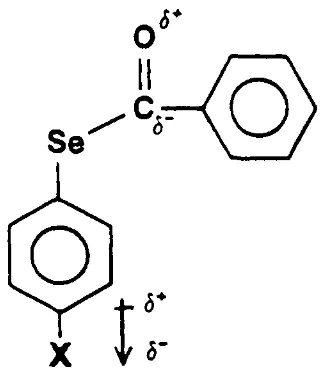

XXV

A comparison of structures where methylene, oxygen or selenium was the moiety attached to the ipso carbon showed that selenium strongly enhanced transmission of the polar field effect (π polarization) over carbon or oxygen.

The authors also observed that e^- donating substituents affected the infrared stretching frequencies of the carbonyl more than e^- withdrawing groups. For instance, the carbonyl stretching frequency observed with p-N(Me)$_2$ was 10 cm^{-1} less than the parent compound, whereas that observed with p-NO$_2$ was only 4 cm^{-1} greater than the parent compound. This led them to conclude that mesomeric donating substituents were interacting through the aromatic ring into the relatively electron deficient SeC(O)Ph moiety. In their opinion, electron withdrawing substituents do not interact effectively with non-bonding selenium electrons and DSP analyses imply the prime importance of the $n_{se} - \pi_{co}$ interaction, (XXV A-D) at the expense of any significant $n_{se} - \pi$ phenyl interaction:

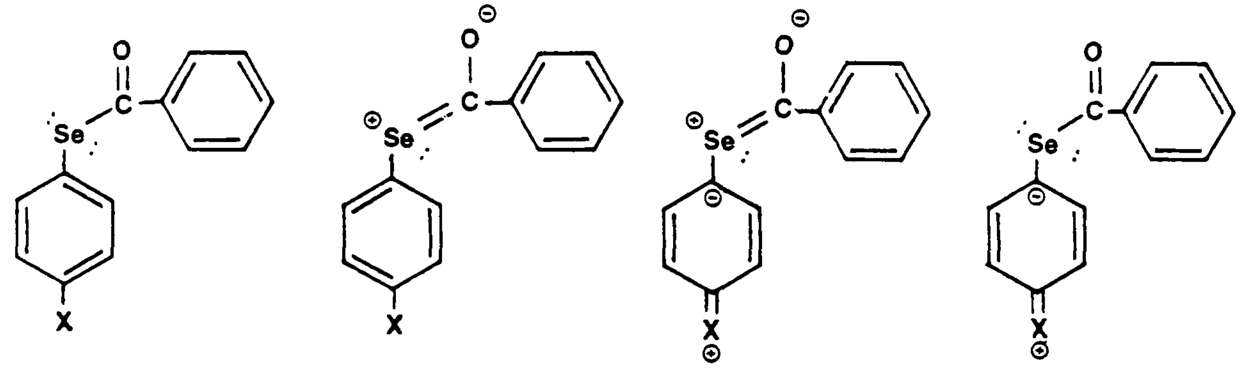

A B C D

XXV

These investigators, however, were not able to get good fits of the ^{77}Se SCS data to a DSP equation, regardless of the method used. The fact that excellent ^{13}C SCS fits were obtained for these same compounds illustrates the need for further studies of correlations of "heavy nuclei." The authors state:[27]

> At first glance, it would appear that these resonance scales are incapable of treating ^{77}Se NMR data with the same precision as NMR data of light nuclei (e.g. ^{13}C, ^{15}N, ^{17}N, ^{17}O, ^{19}F). However, that conclusion would be rather hasty. Chemical shifts of these heavier nuclei are not well understood and, clearly, with many more electrons and a much more polarizable electron cloud, subtle effects may be observed in their chemical shifts that have not been dealt with in nuclei of the second row of the periodic table.

Studies of the specific electronic nature of the SePh group show that it, like the Ph group, exhibits an electron-withdrawing inductive effect (-I) and a push-pull resonance effect (+M/-M) meaning it can be e^- donating (+M) or e^- withdrawing (-M) depending on electron demand in the overall structure. Only the polarizability concept has generally been employed to explain the observed stabilization of an incipient carbanionic site α to S and Se[28], but the lower value of σ_p^- of the SePh group versus that of the SPh group does not agree with this explanation. (A larger effect would be predicted for the larger and more polarizable Se atom). Consequently, a conjugative interaction where the higher energy, less accessible empty d orbitals of the Se atom are less able than those of S to overlap with the filled p orbitals of carbon must be asserted.

The PhZ structure (Z=O,S,Se) also stabilizes an adjacent carbocationic center, but the type of electron donation is generally recognized as being related to the heteroatom involved: electron donation via the π system is best for oxygen since its valence 2p electrons can best overlap with the empty 2p orbital on carbon. Alternatively, electron donation within the sigma framework can be expected to be highest for the most polarizable heteroatom, selenium. Consequently, the conjugative stabilizing order is O > S > Se whereas the inductive order is Se > S > O with the effects somewhat cancelling. The overall predominance, however, of the mesomeric effect is shown in the observed results.

For example, McClelland and Leung studied the rate determining step in acid-catalyzed hydrolysis of aryl vinyl chalcogenides,[29]

$$\mathrm{(X)ArZCH{=}CH_2} \xrightarrow[\text{slow}]{\mathrm{H+}} \mathrm{(X)ArZ\overset{+}{C}HMe} \longrightarrow \mathrm{ArZH + MeCHO}$$

Z = Se,S,O

and found that the Hammett ρ constant of the selenides (-1.55) was smaller in magnitude than that of the sulfides (-1.84) and ethers (-2.00). This argues for the overall importance of the resonance effect in α-site carbocation stabilization, since that atom capable of strongest resonance interaction, oxygen, gives the greatest rate increase through the substituent series. Measurements of dipole moments have shown that for strongly electron donating or withdrawing groups para to the SePh moiety, the push-pull resonance effect is particularly exaggerated.[30]

An application of ^{77}Se and ^{15}N NMR to an important diagnostic conjugative π system could further enhance an understanding of the transmission of electronic effects through the C-Se and C-N moieties while evaluating an extension of the limit of Se and N lone pair interaction with a carbon-skeleton π system. Such a system is provided by the styrene structure.

D. The Styrene System

Ring substituted styrene systems have probably been studied in terms of sidechain chemical shifts more than any other single class of compounds. This reflects the attractive structural and electronic characteristics of this moiety making it such a useful probe: the sidechain carbons are far enough removed from the substituents to minimize anisotropic effects while structural/electronic effects can still be transmitted to them via the extended conjugation.[2] In these series, the chemical shifts of the α-carbon atoms (XXVI)

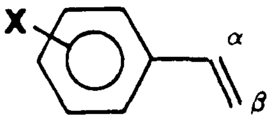

XXVI

show a narrow range and a "reverse correlation" that has come to be understood as a normal manifestation of the π-polarization mechanism of substituent effects on sidechain systems. To review, this can be illustrated as in XXVII,

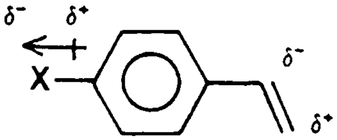

XXVII

where the substituent dipole acting through the σ electron framework of the molecule polarizes the π system in the sidechain, in this case increasing electron density of C_α rather than reducing it as one would expect from simple electrostatic effects (thus the term "reverse"), and decreasing electron density at C_β.[31] In ^{13}C NMR this is manifested as increased shielding for the α carbon atom versus increased deshielding for the para and β-sidechain carbons as X becomes more electron withdrawing (increasing Hammett constant value). (See Figure 1, page 21).

However, the first study to observe this "reverse" effect was by J. Bromilow and R.T.C. Brownlee on the ^{13}C NMR shifts of substituted benzonitriles. They found that the direction of change of the substituent chemical shift of the cyanide carbon and the adjacent ring carbon to be reversed from each other: as X became more e^- withdrawing, the ring carbon became more deshielded (+ slope) and the cyanide carbon became more shielded (- slope), shown in XXVIII(A): [32] NOTE: Within this text, uncircled +/- signs will illustrate correlation slopes and circled ⊕/⊖ signs will indicate formal charges.

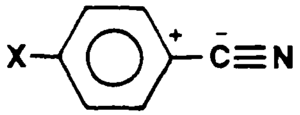

XXVIII(A)

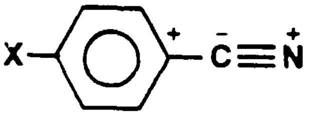

XXVIII(B)

Earlier work by Pregosin, Randall, and White had already demonstrated a "normal" (+ slope) for the N atom correlation, completing the π-polarization picture (XXVIIIB) for this simple but important sidechain system.[33]

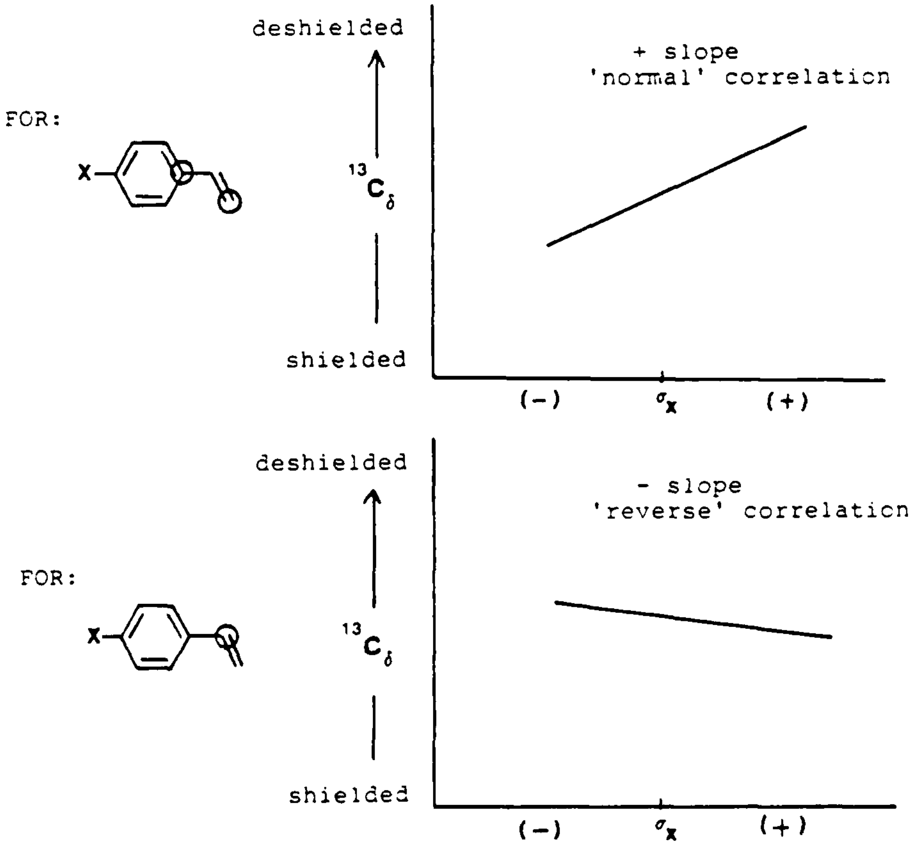

*qualitative representation only.

Figure 1. ^{13}C Shieldings From Styrene π-Polarization

As a further example, in XXIX the ^{15}N ρ_I value was positive, but in XXX with the N at the other end of the polarized C=N π system, the ρ_I was negative.[8] This is consistent with the regular alternation in slope predicted by the π-polarization mechanism as represented above.

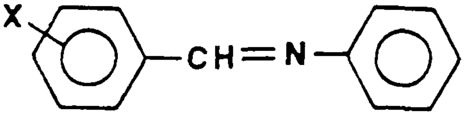

XXIX

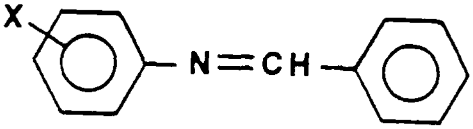

XXX

These studies have borne out the conclusion reached (1972) in the pioneering work of Pregosin, Randall, and White on substituted benzamides and benzonitriles; that ^{15}N SCS values reflect, in general and from whatever influence, π-density changes of the nitrogen atom.[33]

Extensive ^{13}C NMR studies of 12 series of meta and para-substituted styrenes (XXXI) has clearly demonstrated this π-polarization mechanism to be an inherent property of molecular bonding in these compounds.[34]

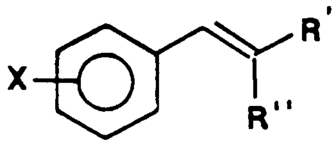

XXXI

X = $N(Me)_2$, OMe, Me, F, H, Cl,
Br, CN, NO_2
R' + R" = H, CN, Ph, CO_2Et,
PhCO, COMe, PO_3Et_3

Further work by Robinson and Slater indicated that the phenomenon of charge alternation generated by this π-polarization mechanism does indeed occur in more extensively conjugated styryl systems, such as 1, 1-dicyano-3-methyl-4-aryl-1,3-butadienes (XXXII):[34]

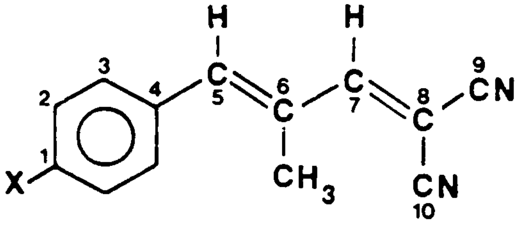

XXXII

A regular alternation of slope (σ^+ versus ^{13}C δ) for the carbon atoms numbered 5-10 (positive slopes at C6 and C8 and negative slopes at C5,7,9, and 10) were found. This provided dramatic support of Pople, Gordon,[35], and Fliszar's [36] provocative assertion based on CNDO/2 calculations that if a substituent causes that atom attached to it to become depleted in electron density, the adjacent attached atom will become somewhat electron rich. Instead of the classical picture:

$$\overset{\delta-}{F} \leftarrow \overset{\delta+}{C} \leftarrow \overset{\delta\delta+}{C} \leftarrow \overset{\delta\delta\delta+}{C} \ldots$$

we have: $$\overset{\delta-}{F} \leftarrow \overset{\delta+}{C} \leftarrow \overset{\delta\delta-}{C} \leftarrow \overset{\delta\delta+}{C} \ldots$$

It must be stressed that polarization of the sigma framework by the substituent generates the π-polarization response.

E. NMR Studies of Compounds Containing Nitrogen and the Styrene System

1. Correlative Studies of Enamines and Enaminones (^{15}N)

One of the most significant areas of research directly relating ^{15}N NMR with unsaturated systems (i.e. styryl) was that of Schwotzer and von Phillipsborn on n-π interaction in enamines and enaminoketones.[37] Their very thorough evaluation of the ^{15}N NMR of these compounds underlined the valuable diagnostic tool of this nucleus in understanding n-π delocalization in nitrogen-containing conjugated systems. In their study of ^{15}N NMR, three general classifications were employed: cyclic and simple open-chain amines, enamines with extended conjugation and enaminoketones. As generally expected from applying the resonance formalism to these structural classifications, a decrease in the shielding constant of the ^{15}N nucleus (i.e., a low-field shift) with increasing electron delocalization was observed in going from amines to enamines and finally to enaminoketones (verifying the greater importance of resonance structure XXXIV over resonance structure XXXIII.

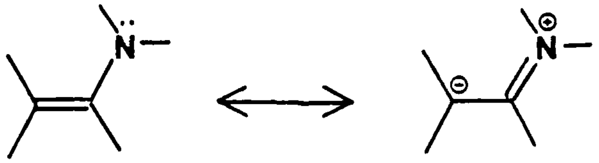

XXXIII

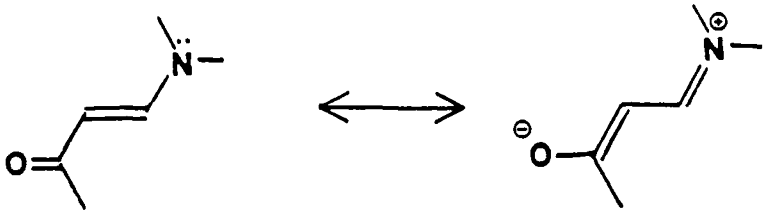

XXXIV

The considerable deshielding of nitrogen in enaminoketones (or esters, nitriles, etc.) is further substantiated by its chemical shift range (-295 to -260 ppm referenced to NO_3^- as an external standard) which extends into the range of amide resonances (-280 to -235 ppm).

Schwotzer and von Phillipsborn went one important step further in their data treatment: in an attempt to isolate the influence of π-electron delocalization in enamines from all other structural effects, the chemical shift of the enamine was considered relative to the shift of the corresponding tertiary amine obtained by hydrogenation of the carbon-carbon double bond. Termed $\Delta\ \delta(N)$ values, and derived from the following equation,

$$\Delta\delta(N) = \delta_N \text{ (amine)} - \delta_N \text{ (enamine) (negative value)}$$

inductive and steric influences due to different N substitution could be cancelled. With this frame of reference, a comparison of enamines obtained from various bases or carbonyl compounds in terms of lone pair delocalization could be done more clearly. Calculated (taking advantage of the additivity of substituent effects) and observed Δδ(N) values obtained from this treatment provided a useful measure of the relative importance of the iminium resonance structure for a wide variety of enamine structures (the larger the Δδ(N) the greater the delocalization). To determine to what extent this Δδ(N) treatment was a quantitative measure of π-electron delocalization in enamines (and to get independent support of this concept), barriers to internal rotation about the N-C(α) bond in conjugated systems were determined. Free energies of activation ($\Delta G^{\neq}_{rot}$) were obtained from the temperature dependence of the C (α) carbon signals in the amine moiety of the following enamines and enaminoketones:

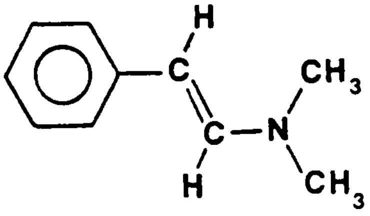
XXXV

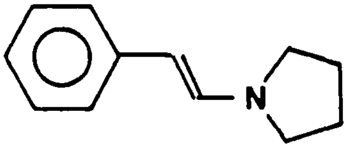
XXXVI

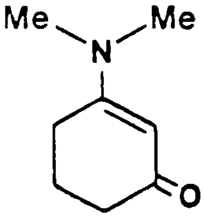
XXXVII

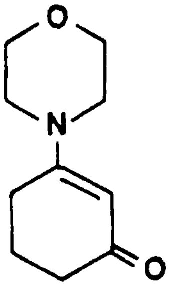
XXXVIII

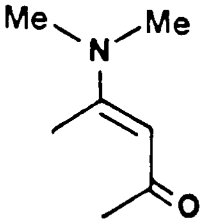
XXXIX

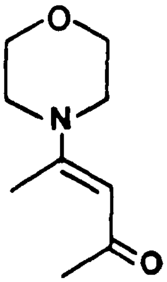
XL

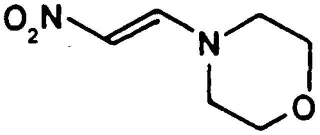
XLI

A satisfactory linear correlation between the $\Delta G^{\neq}_{rot}$ and $\Delta\delta(N)$ data was obtained. Regression analysis (correlation coefficient 0.94) gave

$$\Delta G^{\neq}_{rot}(\text{Kcal/mol}) = -0.19(\Delta\delta(N)[\text{ppm}] + 2.91$$

consistent with and verifying the quantitative relationship between increased conjugative resonance and increased hindrance to C-N rotation. .he authors state:[37]

> since the height of the barrier to rotation will be largely determined by the C(α)-Nπ bond order, this correlation supports the significance of $\Delta\delta(N)$ values as a measure for n,π interaction, provided that the entropy term in $\Delta G^{\neq}$ is small over the whole range of coalescence temperatures.

Further, and very relevant substantiation that relative ^{15}N chemical shifts are a reliable means to evaluate π-electron delocalization was provided by a study of a series of substituted anilinostyrenes (XLII):[37]

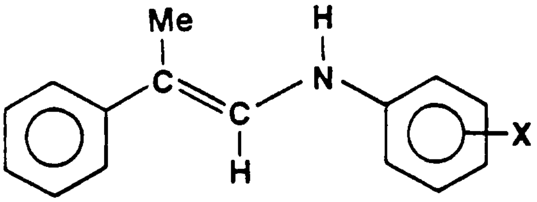

XLII

Here, with the nitrogen lone pair involved in the mesomeric system of the aniline structure, it was expected that the nature of substituents would affect the degree of enamine polarization; that is, there should be a Hammett-type relationship between substituent constants and $\Delta\delta(N)$ values. Also, the ^{13}C shift of the C(β) should be affected by approximately the same steric and inductive factors through the series as long as only _para_ or _meta_ located substituents are considered.

Therefore, the C(β) chemical shift should also be a useful probe for enamine polarization.

As anticipated, the Δδ(N) values displayed a linear correlation with Hammett constants and with the ^{13}C shifts of the C(β) atom.[37] The authors provided a specific correlation equation between $\Delta\delta^{15}N$ and the $\delta^{13}C_{\beta}$: (where R=NO_2, Cl, OCH_3, H, and CH_3)

$$\Delta\delta^{15}N = -161.1 + 1.11\delta^{13}C_{\beta}\ (DMSO\text{-}d_6)\ R=0.96\ s.d.=0.5$$

The one-bond N,H coupling constant reflected values typical for sp^2 hybridized nitrogen and showed only a very small and non-systematic variation with changes in X, in contrast to the large effects seen in substituted anilines. This showed that hybridization of the nitrogen was mainly determined by the enamine character of these compounds and that the X substituents only influenced the degree of enamine polarization.

This work was important in that it showed that nitrogen chemical shifts can be related fairly precisely to n-π interaction in enamines and that they can be correlated with parameters that are sensitive to the same phenomenon. The superior results obtained with ^{15}N NMR are consistent with this nucleus exhibiting a much larger chemical shift range (400 ppm) than ^{13}C (100 ppm).[3]

2. Correlative Studies of Z-5-Arylmethylenehydantoins ($^{13}C/^{1}H$)

More recently, a very important correlative study was reported for the Z-5-arylmethylenehydantoins:[38]

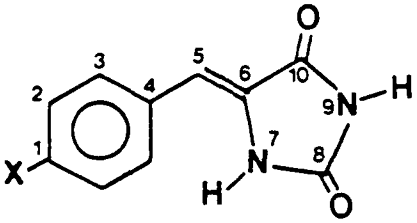

XLIII

X = $N(Me)_2$,OH,OMe,Me,H,Cl,CN,NO_2

In addition to the expected correlations for the H chemical shift of the vinylic proton and the ^{13}C chemical shift of the β carbon atom (C-6), good linear correlations were also found for the N-7 and N-9 proton chemical shifts.

For the N-7 proton the use of σ and σ^- gave better correlations than with σ^+, consistent with the anticipated through-resonance interaction between the unshared electron pair on N-7 and electron withdrawing aryl substituents. The N-9 proton correlation showed little preference for a specific σ scale, but the good correlations of the N-9 proton chemical shifts were meaningful in light of their relatively long distance from the aryl substituents.

Alternating slopes of the chemical shift/substituent constant correlations for C6(+), C5(-), and C4(+) confirm the π-polarization mechanism, as discussed earlier, with C5 showing a much better correlation with σ and σ^- values than generally found in styrene derivatives. The C-8 carbonyl showed no substituent effect whatever. Also, the C-10 carbonyl did not correlate well with any set of substituent constants which seems surprising in comparison to excellent correlations found by Robinson et al. in indanediones and barbituric acids.[39]

These investigators also found evidence of the opposing conjugative interactions of the carbonyl and amino groups with the benzylidene structure. The carbonyl group is known to lessen electron density of the C=C bond (XLIV),

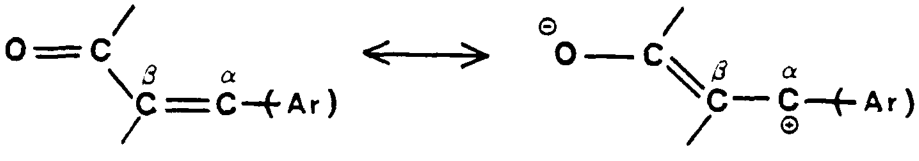

XLIV

giving rise to strong resonance interaction of this bond with _para_ e$^-$ donating aryl substituents. The usual effect observed with styrene derivatives is that the resulting electron density changes are more significant at the β carbon (C6) meaning a greater transmission of substituent effects to this site than the α carbon (C5). This usually results in a poor correlation for this carbon, presumably due to some extent to the fact that the same degree of error applied to a narrower range will give a poorer correlation. In these compounds, however, the opposing influence of the N-7 increased electron density of the C=C, particularly at the α carbon (C-5) because of the resonance effect (XLV):

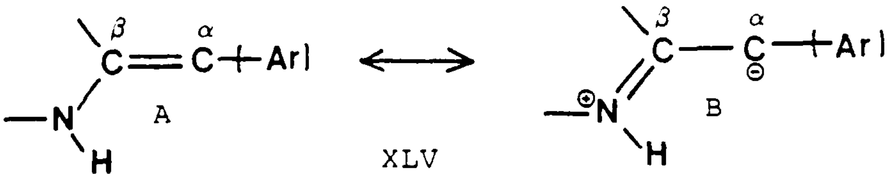

XLV

With this influence, the ^{13}C shifts of the α-carbon were observed to correlate _well_ with σ or σ$^-$ constants, consistent with the through-resonance phenomenon shown in XLV (A/B). The amine group was thus causing a reversal of the C=C bond polarization, due to greater contribution (importance) of resonance interaction XLV A/B over that of XLIV A/B. As a result the α carbon at C-5 was more shielded than the β carbon at C-6, a trend contrary to what had been observed in previous styrene derivatives studied up to this publication.

The excellent correlations of the N-7 proton chemical shifts in XLIII coupled with the very small range and poor correlative behavior of the carbonyl carbons in this series argues that in the competitive resonance interactions of the amino and carbonyl groups, the amino group provides the dominant interaction.

CHAPTER II

STATEMENT OF THE PROBLEM

A. Ethyl α-fluorocinnamates

The π-polarization mechanism pr vided a well-documented accounting for the distribution of electron density in substituted styryl systems where R' and R" are generally electron withdrawing groups and do not possess any lone electron pairs (XXXI):

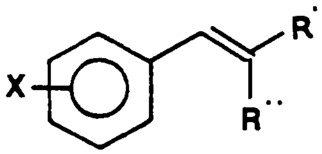

XXXI (see page 22)

At this stage it was felt useful to examine a simple contrasting structure (XLVI);

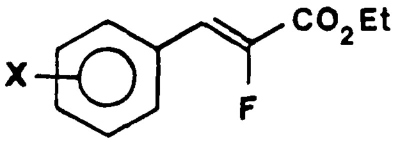

XLVI

Here, the fluorine atom, though strongly electron withdrawing inductively, does possess three unshared electron pairs.

A correlation study of these ethyl α-fluorocinnamates gave surprising results: instead of the expected negative slope of the ^{19}F chemical shift vs σ[13] correlation, based on the π-polarization mechanism and viability of negative charge concentration on fluorine due to its high electronegativity (XLVl A),

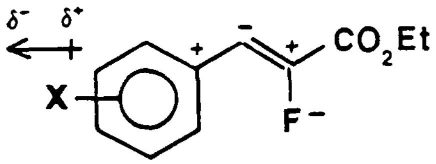

XLVI

a positive slope was obtained.[40] See Figure 2a, page 34. (Negative slopes had been consistently observed for P and C atoms in this position). An explanation for this may be that the fluorine atom, like the PO_3Et_2, CN, CO_2Et, and keto groups can act as an electron withdrawing group by the inductive effect (XLVII). However, it can also behave as an electron donating group via resonance interaction of its unshared electron pairs which the other groups lack (XLVIII). This is consistent with the well-known fact that F is e^- withdrawing in the σ-bond framework, while e^- donating in the π-bond framework. To provide the positive slope, this resonance interaction must be the dominant factor here.

$^{19}F\ \delta/\sigma^{13}$ CORRELATION OF ETHYL α-FLUOROCINNAMATES

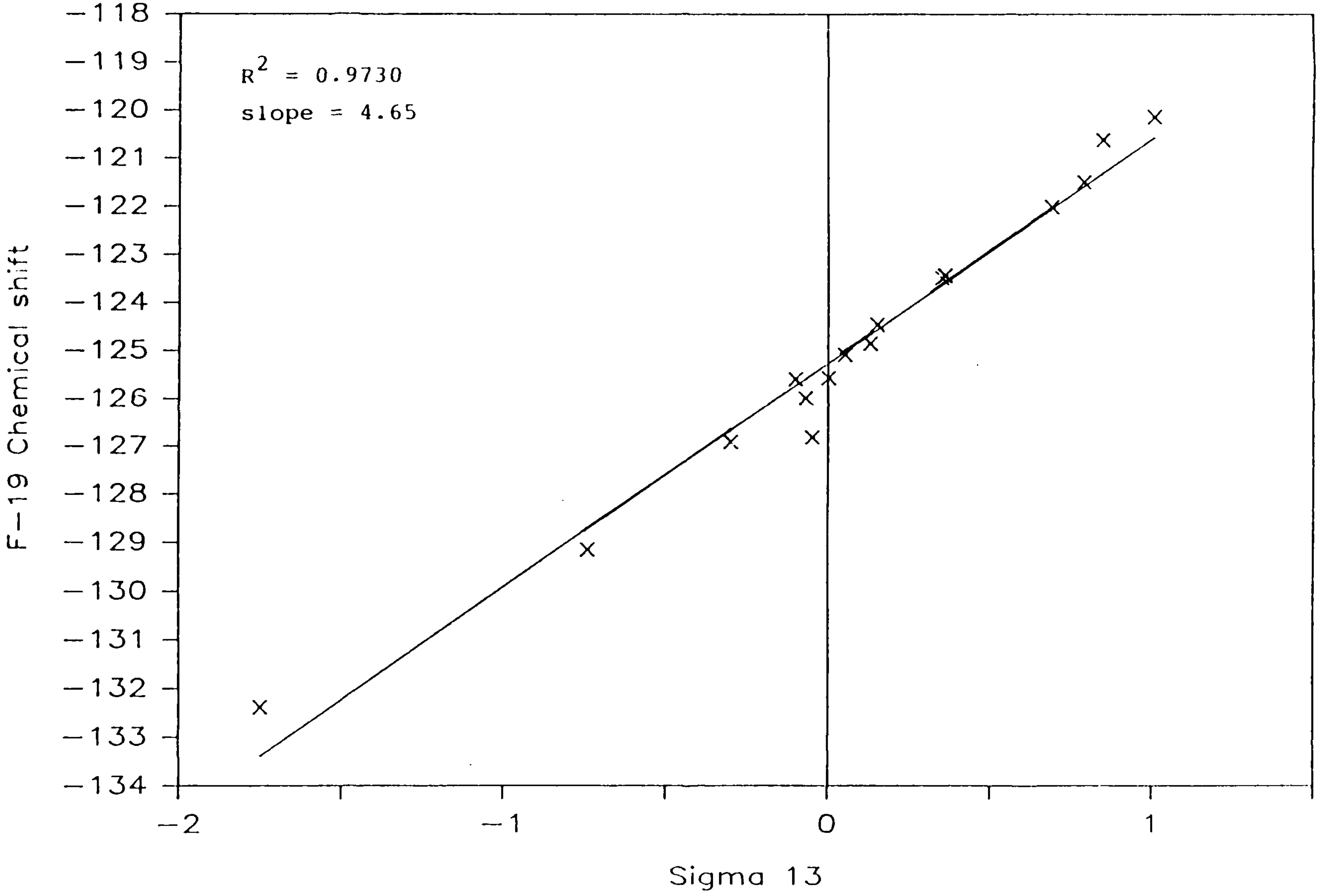

FIGURE 2a

$J_{F-C(Hz)}$ / σ^{13} CORRELATION OF ETHYL α -FLUOROCINNAMATES

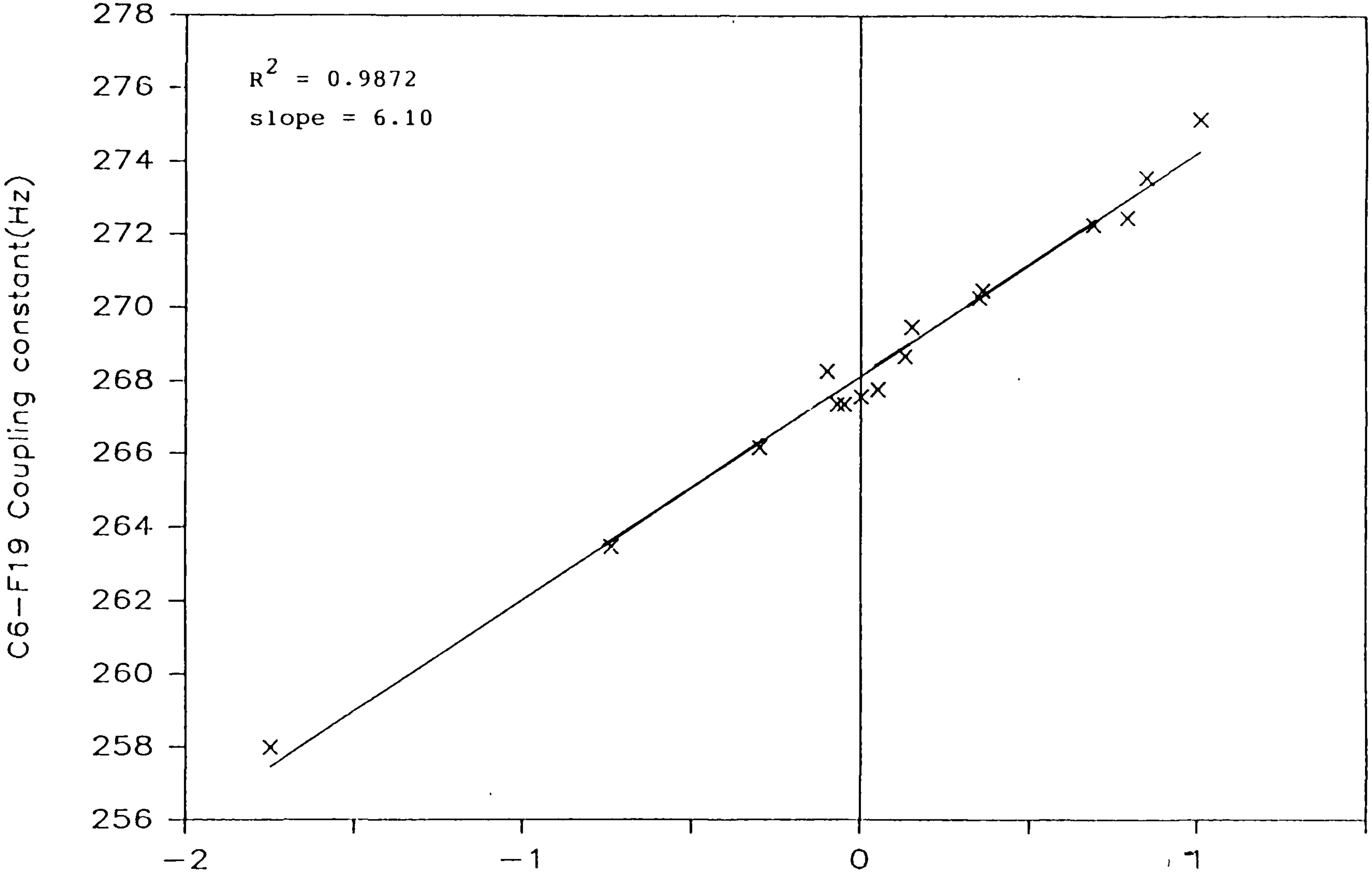

FIGURE 2b

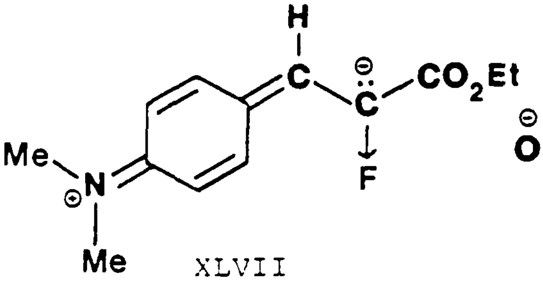

XLVII

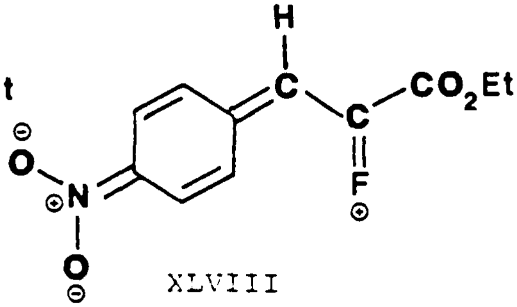

XLVIII

It should also be pointed out that much evidence in the literature indicates that the p-NO_2 group acts only as a very powerful σ electron withdrawer, and that the resonance form invoked in XLVIII is probably not accurate. However, the overall effect of the p-NO_2 group on the π framework can be viewed conveniently in this fashion.

In addition, a plot of $J_{F\text{-}C(\beta)}$ versus σ^{13} (Figure 2b, page 35) gave an excellent positive correlation which would be expected if increased π-character of the F-$C_{(\beta)}$ bond occurs with increasing electron withdrawal of X. This model is provocative in that it argues, in the α-fluorocinnamate case, for resonance interaction to significantly outweigh the π-polarization mechanism. Otherwise, a small or negative slope would be observed due to the influence of the π-polarization process.

This unexpected behavior of the α-fluorocinnamates may indeed have been due to this mesomeric interaction of the unshared electron pairs. But to clarify this matter, a general method was needed to evaluate the behavior of nuclei possessing unshared electron pair(s) when attached to the β carbon of the styrene system. It was felt the most viable approach would involve the element nitrogen, due to the relative accessiblity (using modern NMR instrumentation) of the spin

1/2 ^{15}N isotope. Also, the greater versatility of nitrogen's molecular bonding (over that of F) would provide an excellent probe nucleus for examining this question in detail. In fact, from this perspective the major tenet of this research effort was developed--to combine the sensitivity of ^{15}N chemical shift phenomena (due largely to nitrogen's unshared electron pair) with the usefulness of the styrene probe in evaluating substituent effects through an extended π system.

B. Approach/Predictions

To parallel initially the fluorostyrene system for comparison, but also to evaluate nitrogen's interactive nature with the styrene system based on its formal hybridization, the following compounds were prepared and examined:

1. Series A) (E+Z) Ethyl 2-diethylamino-3-phenyl-2-propenoates (ethyl α-diethylaminocinnamates)

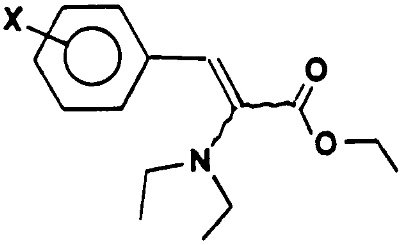

XLIX

Here, formal sp^3 hybridization of nitrogen provided a system parallel to the α-fluorocinnamates. Thus, a positive slope for σ versus δ ^{15}N was anticipated. In addition, instead of evaluating the N lone pair delocalization from a position directly in-line for mesomeric interaction with X as examined in reference 37 for XLII (see page 27),

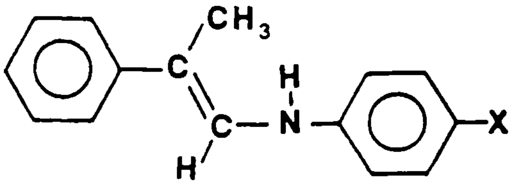

XLII

this system evaluated nitrogen's ability to interact over a significantly larger π system, and in terms of Z and E isomers from very different molecular orientations. (More detail in this regard will be covered later.)

2. Series B) (Z) 4-benzylidene-2-methyl-2-oxazolin-5-ones (benzylidene azlactones)

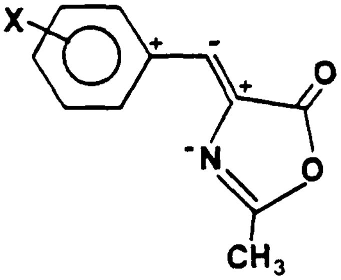

L

Formal sp^2 hybridization of nitrogen requiring orthogonality of its unshared electron pair to the π system should significantly inhibit (or prevent) its mesomeric interaction, providing a useful contrast to series A, and a parallel to the imine studies of reference 8, page 7. Also, the imine bond structure provided extended conjugation analogous to the butadiene system previously cited (reference 34, page 22). The resultant π-polarization scheme would be expected to cause a negative ^{15}N δ/σ correlation slope (as shown), in contrast to the positive slope predicted in the enamine series A.

3. Series C) (Z) Ethyl 2-cyano-3-phenyl-2-propenoates (ethyl α-cyanocinnamates)

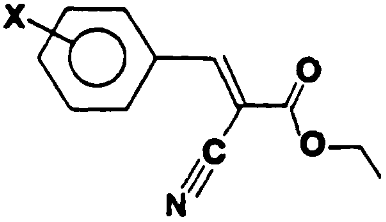

LI

Formal sp hybridization completed the scheme in terms of nitrogen's immediate bonding, although here the following π-polarization scheme was expected,

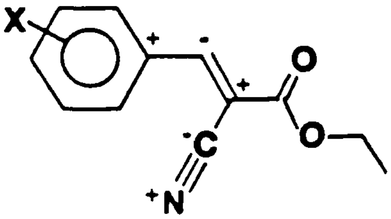

LI

since nitrogen was not in the same position as in Series A or B. However, based on the known resonance behavior of the nitrile system, a positive slope was still expected. (The unshared electron pair on the nitrile nitrogen is unavailable for resonance donation into the styryl system.) It was also of interest to evaluate this ^{15}N δ correlation with that of the benzonitriles (reference 33, page 21).

To extend this investigation to the ^{77}Se nucleus, the following compound series was prepared:

4. Series D) (E+Z) Ethyl 3-phenyl-2-phenylseleno-2-propenoates (ethyl α-(phenylseleno)cinnamates)

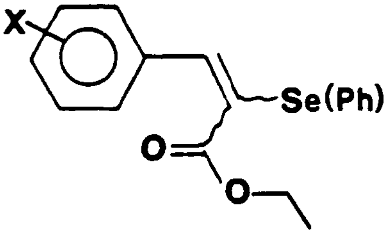

LII

This system illustrated selenium's relative tendency to interact with its unshared electron pairs with an extended π system, in contrast to the more direct interactive system in the selenoanisoles (reference 21, page 13). Also, the lone pairs on Se would not be under the direct influence of the C=O group (as they were in the selenobenzoates, reference 27, page 15), and thus were expected to be more freely available to interact directly with the styryl system.

C. Geometrical Isomerism

Series A and D above have been represented as Z/E isomer mixtures. In the preparation of these compounds, both isomers were formed in most cases. This normally considered synthetic drawback could be used to advantage in this NMR study: the presence of both isomers offered an opportunity to compare the ^{15}N and ^{77}Se correlative behavior in terms of geometrical isomerism.

For Series A, the E and Z isomers provided very contrasting geometrical arrangements of the amine and carboxylate functionalities.

For the ^{15}N "target" nucleus, the E isomer represented a kind of transoid configuration with the styryl system, while the Z isomer displayed a cisoid arrangement:

E

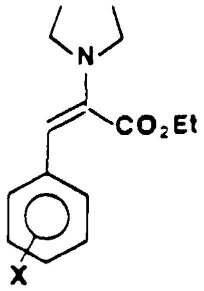

XLIXA

transoid

Z

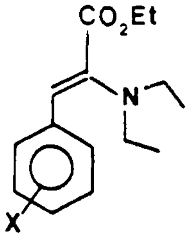

XLIXB

cisoid

Here a quantitative comparison could be made concerning the effect of this cis/trans isomerism on the transmission coefficients of the ^{15}N SCS values.

Similarly, for the selenide series D, the same scenario presented itself; here, steric factors would be expected to be particularly pronounced, due to the large volume requirement of the SePh moiety (C-Se-Ph bond angle of ≈ 99°).

E

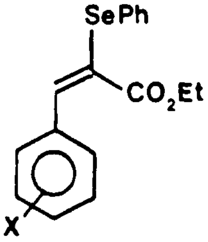

LIIA

transoid

Z

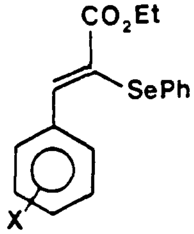

LIIB

cisoid

Stereochemical assignments for Series A and D were made based on the determination of ^{3}J vinylic $^{1}H/C=O$ and ^{3}J vinylic $^{1}H/Se$ values, respectively. See pages 74 and 78.

These investigations would complement that of a study of differently oriented π systems, notably the following:[41]

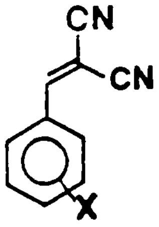

LIII

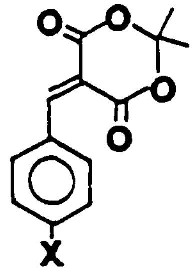

LIV

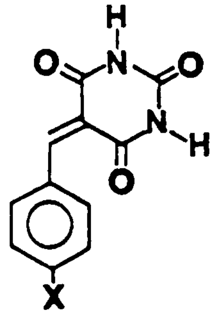

LV

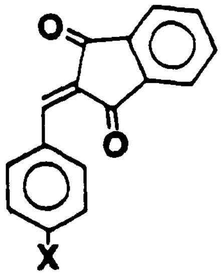

LVI

where, in spite of an orientation difference of 120° for each nitrile group in LIII, as for the carbonyl groups in LIV through LVI, very similar ρ_I values were obtained in each case.

D. Cross-Conjugative Competition

These same two series of compounds provided interesting examples of a push/pull mesomeric system arranged in a cross-conjugative sense. (The term "cross-conjugative" as applied to these structures is meant to contrast with the term "through-conjugation," where these groups can act synergistically rather than competitively, as in XXXIV, page 25).

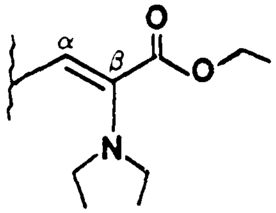

XLIXB

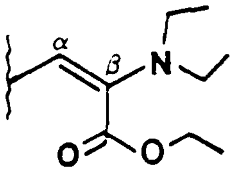

XLIXA

For Series A, an enaminocarbonyl structure is present (XLIX A/B). Here for XLIXB the positions of the (push) amine and (pull) carbonyl groups are similar to those in the arylmethylenehydantoins (reference 38, page 28, (XLIII)):

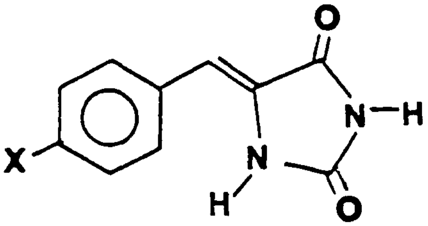

XLIII

For Series D, the phenylseleno moiety took the place of $N(Et)_2$, and provided an interesting extension of this push-pull cross-conjugative resonance system to a much heavier element (LII A/B). The more complex mesomeric behavior (+M/-M) of the SePh group (reference 28, page 17) added another interesting dimension to this study. Finally, in both of these series there was the opportunity to examine this cross conjugative competition from the perspective of both isomers.

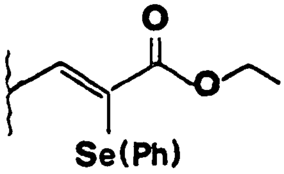

LIIB

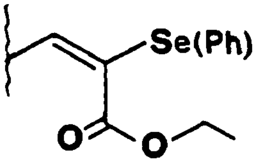

LIIA

CHAPTER III

EXPERIMENTAL

A. Synthesis

1. Nitrogen Compounds (Series A-C)/(General Comments)

Literature methods were followed for all three series of nitrogen compounds (Series A through C).[42,43,44] All of the enamines (Series A) were collected from vacuum distillation as liquids with varying shades of yellow-green, with the exception of the red p-NO_2 derivative. After long-term storage in the freezer room, these compounds became discolored. Consequently, whenever practicable, these compounds were redistilled prior to performing the NMR experiments. The benzylidene azlactones and α-cyanocinnamates were obtained by precipitation from the reaction medium followed by recrystallization. The α-cyanocinnamates were air stable and could be stored indefinitely at ambient temperature, but the benzylidene azlactones tended to slowly hydrolyze to the ring-opened product, LVII.

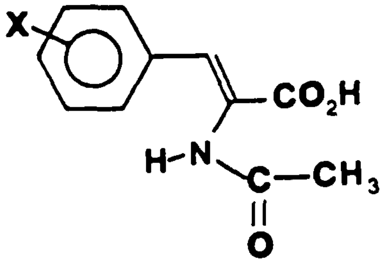

LVII

The azlactones were also much less soluble than the other compound series in the NMR solvents used (CD_3NO_2 and $CDCl_3$), reducing the chance of obtaining meaningful ^{15}N data after a reasonable acquisition time. With the availability of ^{15}N-labeled glycine starting material, these factors led us to remake ten azlactones with the ^{15}N label present in about 10% concentration by mass.

Much of the preparative detail for each compound in a given series was highly repetitive. Rather than giving a detailed accounting of every preparation, a single representative example from each series will be discussed in detail. Following this, a table will be presented that will list the physical and experimental data for each compound as well as footnote any further unusual detail that merits attention. Due to the large number of compounds involved in this NMR study, microanalyses were, for the most part, restricted to the "target nuclei" (N and Se) for the minimum basis set for the two new series of compounds prepared (Series A and D).

2. Series A/Example Procedure [42]

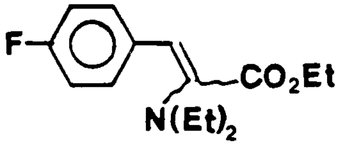

XLIX (p-F)

(Z+E)ethyl 2-diethylamino-3-(4-fluorophenyl)-2-propenoate

To a dry 250-mL three-necked round-bottomed flask equipped with nitrogen inlet and thermometer adapter was added 50 mL anhydrous ether. Sodium hydride (2.4g/0.10 mole), which had previously been washed free of its oil disperson by positive nitrogen pressure filtration, was added to the flask under nitrogen purge. Absolute ethanol (10 drops from a Pasteur pipette) was added, the flask was placed under nitrogen blanket and the contents were cooled with an ice bath to an internal temperature of 2-3°C.

At this point, 4-fluorobenzaldehyde (6.21 g/0.050 mole) and ethyl diethylaminoacetate (23.85g/0.150 mole) which had been mixed together and placed in an addition funnel, were added dropwise over a 45 minute period. The internal temperature was maintained at 2-5°C during the addition. After about 3 minutes of substrate addition, a green coloration became evident in the gray NaH/ether slurry.

After the addition period, the reaction mixture was kept cold for an additional two hours after which it was allowed to gradually warm to room temperature. Stirring under N_2 blanket was continued overnight.

The next morning, the red-brown translucent mixture was added in portions with stirring to 50 mL water to destroy excess NaH. The ethereal and aqueous phases were separated. The aqueous phase was extracted with ether (3 x 50 mL), and the combined ethereal phase was extracted twice with saturated $NaHSO_3$ solution to remove unreacted aldehyde and washed with water. Drying over $MgSO_4$ and removal of solvent gave a yellow-brown liquid residue.

Simple vacuum distillation was used to remove excess amine starting material. Subsequent fractional vacuum distillation through a 6 inch Vigreaux column gave the following boiling point ranges and yields, in grams (.30 torr); Fraction 1, 47-95°C (0.42g); Fraction 2, 97-108°C (2.11 g); Fraction 3, 109-111°C (1.37g); GC/MS analysis indicated fraction 3 to be the product isomers in the Z/E ion abundance ratio of ≈ 2.67/1. Fraction 3 represented a 10.3% yield.

a. Synthesis Summary

Larger scale reactions (.1 - .2 molar) were often carried out with the less expensive benzaldehydes (i.e. H, p-Me, p-OMe). These reactions were allowed to run 3-5 days. Simple distillation under vacuum to remove excess amine starting compound was followed by fractional vacuum distillation to obtain product. Yields generally ranged from 10-20%. These low yields were largely due to product loss during vacuum distillation.

In other cases, scarcity of starting aldehyde or very high boiling points of enamine product necessitated using short path vacuum distillation for product isolation. Yields were generally comparable, although redistillation was sometimes required to provide sufficient product purity for NMR analysis.

The following table summarizes the synthetic and physical data for the Series A compounds.

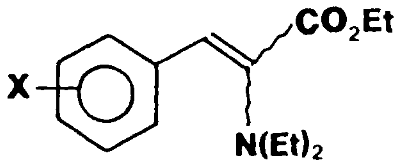

Table 2

Series A

(E+Z) Ethyl 2-diethylamino-3-phenyl-2-propenoates
Synthesis and Physical Data*

X	vacuum distillation method	b.p(°C)/mmHg	yield (%) (isolated)	elemental analysis found	elemental analysis (theory)	Z/E Ratio# (GC/MS)
H	fractional	102-103.5/.30	8.5	known compound[45]		100/3.0
p-N(Me)$_2$ [1]	simple	172-175/.35	8.9	--	--	100/15.9
p-OMe	fractional	122-124/.09	10.4	C=69.32 H= 8.72 N= 5.05	(69.29) (8.36) (5.05)	100/38.3
p-Me	fractional	120-123/.15	19.9	C=73.81 H= 9.00 N= 5.37	(73.53) (8.87) (5.36)	only 1 isomer appears
p-Ph [2]	simple	175/.20	1.5	--	--	
p-F	fractional	109-111/.30	10.3	C=67.35 H= 7.55 N= 5.27	(67.90) (7.60) (5.28)	100/37.4
p-Cl	simple	137-141/.20	11.7	N= 4.37	(4.97)	100/23.8
m-F	simple	114-115/.60	8.1	--	--	100/38.5
m-Cl	simple	138-142/.20	37.0	--	--	100/98.5
p-CO$_2$Me [3]	simple	143-145/.10	11.3	C=66.47 H= 7.55 N= 4.60	(65.96) (7.27) (4.81)	100/12.7

Table 2 (Continued)

X	vacuum distillation method	b.p(°C)/mmHg	yield (%) (isolated)	elemental analysis found	elemental analysis (theory)	Z/E Ratio# (GC/MS)
m-CN	simple	135-140/.13	17.4	--	--	36.5/100
p-CF_3	simple	113-116/.16	19.0	--	--	11.9/100
p-CN [2]	simple	147-149/.15	1.8	C=70.41 H= 7.25 N=10.06	(70.56) (7.40) (10.29)	23.3/100
p-NO_2 [4]	simple	167-176/.14	9.1	--	--	

* numbered footnotes indicate unusual detail discussed subsequent to table.

Z/E relative total ion abundance ratio.

Footnotes.

[1] The 4-dimethylaminobenzaldehyde proved to be quite difficult to remove by $NaHSO_3$ extraction. Thus, the combined ether phases were first reduced in volume (about 50%) before extraction with $NaHSO_3$ solution. The product was a low melting solid (m.p.<25°C) indicated by its solidification after long standing in the freezer room. However, it quickly melted when brought out on the bench. This compound failed to give satisfactory elemental analysis presumably due to its greater hydrolytic instability. However, the ^{13}C and ^{1}H NMR's were consistent with the structure shown.

[2] Several distillations were required to affect isolation of sufficiently pure product, resulting in the even lower than usual yield.

[3] The NaH/EtOH system routinely used for enamine synthesis caused transesterification of the CO_2Me moiety resulting in a complex mixture of ethyl/methyl diesters. To avoid this problem, methyl diethylaminoacetate starting compound was employed with this aldehyde, using NaH/MeOH catalyst. Physical data thus pertain to the dimethyl ester product (LVIII):

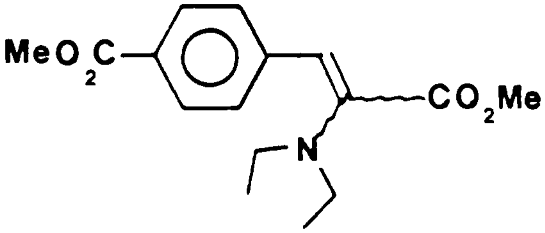

LVIII

Also, in working up this reaction, a large quantity of solid separated from the dark orange-yellow oil upon evaporation of solvent. This byproduct could be washed free of the oil (containing desired product) by trituration with hexanes, giving a white solid, which was not further characterized.

[4]This compound was prepared using a dry benzene/ether (100 mL each) co-solvent system for addition of the organic substrates to the NaH/ether slurry (0.037 mole of aldehyde scale). All other details of the procedure were identical to the general method, although here, the reaction was allowed to continue four days.

Vacuum distillation gave the product as a deep red oil which was contaminated with a less dense yellow-green oil which had coated the distillation pathway prior to collection of this product fraction. This lighter oil remained as a separate non-miscible layer, and was not further characterized.

This product was also a low-melting solid (m.p.<25°C), showing behavior similar to that of the p-$N(Me)_2$ derivative.

b. Starting Compounds

All aldehydes were commercially available from Aldrich. Benzaldehyde, anisaldehyde, and tolualdehyde were distilled prior to use. All other aldehydes were used directly. The amine starting compounds were prepared as follows:

1) Ethyl diethylaminoacetate

Diethylamine (95.26 g/1.30 moles) was placed in a nitrogen purged one-liter flask equipped with a stir bar, nitrogen inlet, addition funnel, and 150 mL benzene. After purging several minutes with nitrogen, ethyl chloroacetate (122.5g/.65 mole) mixed with 50 mL benzene was added dropwise with stirring over a 30 minute period. Stirring was continued overnight at ambient temperature under nitrogen atmosphere.

The next morning, the $Et_2NH.HCl$ salts were filtered from the solution and washed with 100 mL fresh benzene. The combined benzene phase was reduced in volume and distilled through a 6" Vigreaux column to give the product as a constant boiling fraction (40°C/.35 torr) weighing 68.3g (66% yield).

2) Methyl diethylaminoacetate

This compound was made in entirely analogous fashion to that above using a 0.25 molar scale for the methyl chloroacetate starting compound (150 mL total benzene used).

Fractional vacuum distillation gave the product (14.6g, 40.0% yield) at 31°C/.40 torr. Cooling of the collection vessel was helpful to lessen loss of product due to volatilization.

3. Series B/General Comments

These known compounds were prepared following the procedure from Organic Synthesis [43]. ^{15}N-labeled glycine (99.0% MSD Isotopes) was acylated using standard methodology. This label was then employed in ≈ 10% by mass concentration for this series of compounds. Crude product usually separated from the reaction mixture after standing at room temperature overnight (for polar X) or in the cold room overnight (for nonpolar X). Suction filtration, washing first with cold acetic anhydride, then hexanes, and recrystallization (usually from chloroform, carbon tetrachloride, or chloroform/hexanes cosolvent) gave product as a yellow crystalline solid. Generally, polar and/or protic solvents were avoided due to the proclivity of formation of the open-chain hydrolysis product.

a. Example Procedure

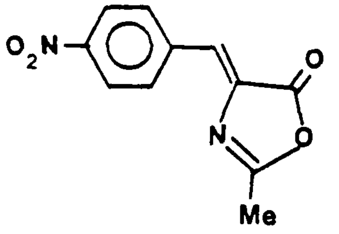

L (p-NO_2)

4-p-nitrobenzylidene-2-methyl-2-oxazolin-5-one

N-acetylglycine (.507g/4.30x10^{-3} mole) incorporating the ^{15}N label in approximately a 10% by mass concentration was combined with p-nitrobenzaldehyde (.649g/4.29x10^{-3} mole) and potassium bicarbonate (0.30g/2.99x10^{-3} mole) in a 5 mL flask. One mL of acetic anhydride was added and the mixture under nitrogen blanket was heated to 90-100°C for one hour. The mixture was allowed to cool to ambient temperature and stand several days under nitrogen atmosphere. Suction filtration gave a dark orange solid.

The crude solid was taken up in hot chloroform and filtered immediately to remove the insoluble hydrolyis product. The filtrate upon evaporation provided 0.228g crude product (22.8% crude yield), m.p. 162-172°C. Recrystallization of a small portion of this crude product from chloroform gave bright yellow needles, m.p. 182-185°C.

4. Series C/General Comments

These known compounds had been previously prepared using standard Knoevenagel condensation reaction conditions. Any further detail can be obtained from reference 44.

5. Selenium compounds (Series D)/General Comments/ Mechanistic Considerations

The only synthetic method found to be generally useful for this series of compounds was a new application, on our part, of a method first described by W. Lehnert using $TiCl_4$ [46]:

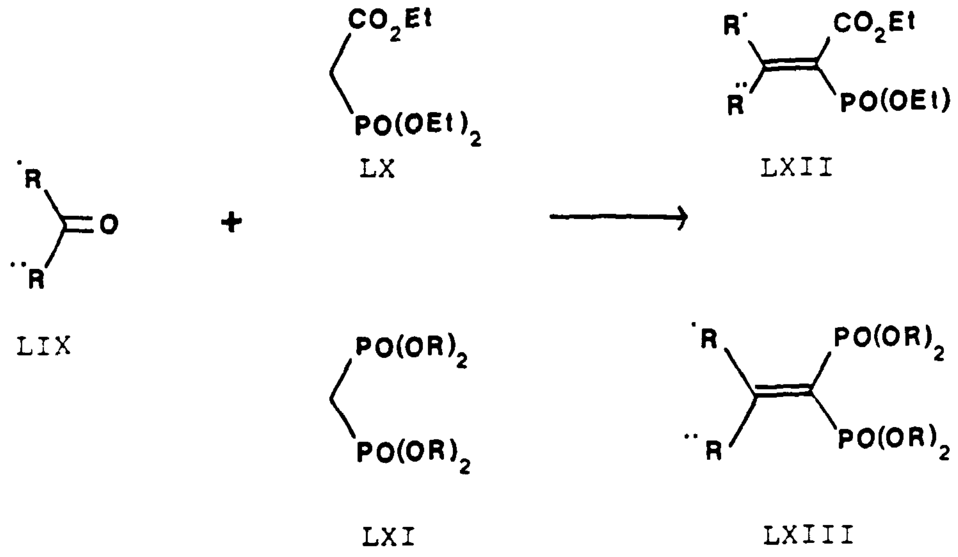

CO2Et
PO(OEt)2
LX
R'
CO2Et
R''
PO(OEt)
LXII
'R
O
''R
+
LIX
PO(OR)2
PO(OR)2
LXI
'R
PO(OR)2
''R
PO(OR)2
LXIII

Lehnert proposed a mechanism involving a cyclic intermediate subsequently opened by action of base:

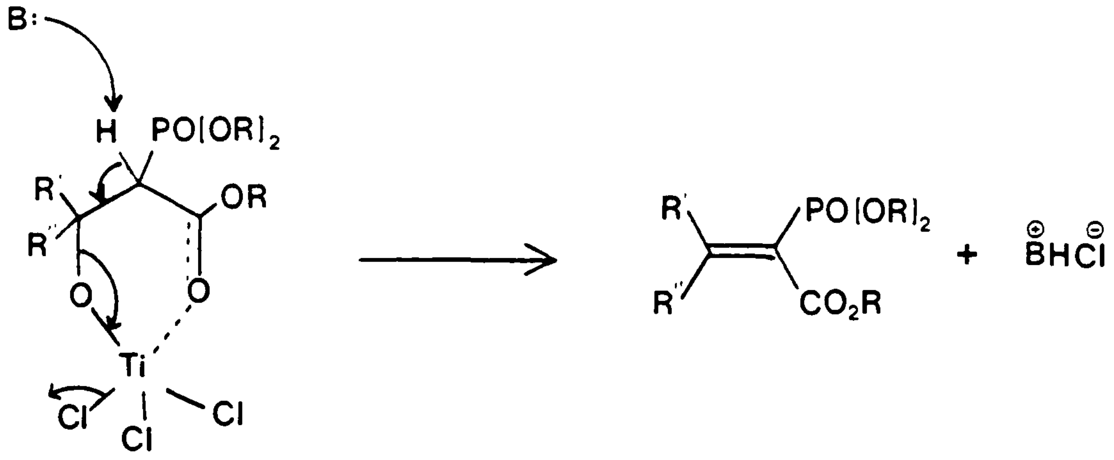

LXIV LXV LXVI

The one-pot, three-step reaction process, following the general method of this above reference, was as follows:

1. Slow addition of $TiCl_4/CCl_4$ solution to cold (0-5°C) dry THF (formation of THF-$TiCl_4$ yellow solid complex).

2. Addition of organic substrates.

3. Slow addition of N-methylmorpholine base.

Addition of this organic base was very exothermic and generated a dark brown-black, but clear solution (up to this point the reaction had maintained a yellow-orange opaque appearance). After about one hour, the hydrochloride salt precipitate was observed.

After overnight reaction at room temperature under nitrogen, water was added with stirring to the thick slurry which dissolved the salts and gave an exotherm up to 35°C. Due to the "salting out" effect, a very convenient separation between the aqueous phase and the organic THF phase was obtained. The more dense aqueous phase was extracted with ether and the combined organic phase was washed with

$NaHSO_3$ solution to remove aldehyde, then water, and finally dried over $MgSO_4$. Removal of solvent gave a yellow-gold oil. (The comments below are in reference to the compilation table for these compounds, Table 3, pages 62,63).

For some of the selenide products having polar substituents on the phenyl ring (p-CO_2CH_3, p-CN, m-CN and m-NO_2), spontaneous crystallization of product occurred after solvent removal after standing for various periods of time either on the bench or in the freezer room. Suction filtration, washing with cold hexanes (to remove excess ethyl phenylselenoacetate) and recrystallization (usually from petroleum ether or petroleum ether/CH_2Cl_2) gave purified product exclusively as the E isomer in low overall yield (7-17%). In other cases, crystalline product separated after solvent removal from certain collected fractions from chromatography (p-Cl, m-Cl, p-CF_3, m-CF_3 and p-Ph). In some of these cases, both E/Z isomers were present according to GC/MS (p-Cl, m-CF_3, p-CF_3).

Most compounds with less polar substituents did not crystallize out spontaneously at any time (H, p-CH_3, p-OCH_3, N-$(CH_3)_2$, p-F and m-F). Vacuum distillation removal of excess ethyl phenylselenoacetate followed by silica gel chromatography provided the product as an E/Z isomer mixture (the isomerization presumably occurring during distillation thermolysis and/or to some extent on the column.) Early fractions in the product band were relatively enriched in the less abundant Z isomer, followed rapidly in successive fractions with the E isomer becoming predominant. However, from chromatography, a quantitative isomer separation (according to GC/MS analysis of the collected fractions) was never obtained in spite of very gradual polarity increase in the eluant. However, because these isomers could be easily differentiated based on the coupling experiments (^{3}J Se/vinylic ^{1}H (E/Z)) described elsewhere, (pages 78 and 137), this matter was not pursued further.

a. Example Procedure (liquid products)

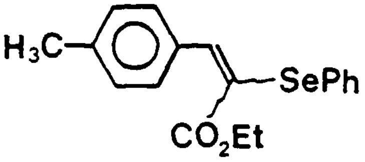
LII (p-Me)

(E+Z) Ethyl-3-(4-methylphenyl)
2-phenylseleno-2-propenoate

Dry tetrahydrofuran (Aldrich/Gold Label, 80 mL), obtained by distillation from the blue sodium ketyl of benzophenone, was placed under N_2 purge in a 250 mL 3-necked flask equipped with magnetic stir bar, N_2 inlet and thermometer adapter. Under nitrogen blanket, the internal temperature was lowered to 0°C using an ice salt bath. At this point, a solution of $TiCl_4$ (5 mL/ACS purified grade) and spectral grade carbon tetrachloride (10 mL) was added slowly dropwise over a 30-minute period. (This solution had been previously prepared in a glovebag (N_2 atmosphere) by injecting these respective volumes via disposable syringes into the addition funnel fitted with a rubber septum.) During addition, the internal temperature was not allowed to go above 5°C. The bright yellow solid THF-$TiCl_4$ complex readily grew from the tip of the addition funnel during the addition period.

Then a solution of ethyl phenylselenoacetate (9.86g/0.020 mole) and p-tolualdehyde (2.4g/0.020 mole) codissolved with 20 mL dry THF was added in one portion through the addition funnel to the THF/$TiCl_4$ suspension. (This helped to break off the THF-$TiCl_4$

"stalactite" that had formed from the addition funnel tip). No change in appearance was observed at this point.

Finally, 9.0 mL of dry N-methylmorpholine (distilled under N_2 from CaH_2) was added slowly dropwise over a 10 minute period to the reaction mixture maintained at 5°C. The reaction mixture darkened considerably to a brown-black but clear appearance. The mixture was allowed to continue stirring at 0-5°C for an additional 3 hours. (After one hour, the hydrochloride salt precipitate was observed which increased in quantity with time.)

The reaction was allowed to stir under N_2 atmosphere and gradually warm to ambient temperature overnight. The next morning, 20 mL water was added with stirring to dissolve the hydrochloride salts. A temperature increase up to 30-35°C was observed.

The aqueous and organic phases were separated. The aqueous phase was extracted with ether (3x50 mL) and the combined organic phase was washed with saturated $NaHSO_3$ solution, and dried over $MgSO_4$. Removal of solvent gave a yellow-green oil.

Vacuum distillation (short path) was used to remove unreacted ethyl phenylselenoacetate. In the process, the foul-smelling pot residue became black with organic-insoluble solids suspended in it (possibly elemental selenium). GC/MS analysis of the pot residue indicated the product isomers in 100.0/0.9% relative ion abundance, diphenyldiselenide at ≈2% relative abundance, and no remaining ethyl phenylselenoacetate.

The pot residue (4.32g) was taken up in methylene chloride which left behind on the sides of the flask the insoluble black solids noted above. Preadsorption of this sample was carried out with 20g 60-mesh silica gel. Chromatography was performed on a 200g silica gel column (70 to 230 mesh) which had been slurry packed with hexanes. Eluant was hexanes (1000 mL) followed by gradual increase in polarity provided by ethyl acetate in 1% increments (per 500 mL eluant volume) up to 6% ethyl acetate concentration.

During the 100% hexanes early elution, two distinct yellow bands developed. The first, which eluted very quickly (almost with the solvent front) was diphenyldiselenide. The second, which was the product band, eluted slowly with gradual polarity increase. With 6% ethyl acetate elution, the product band was collected in 9 separate 50 mL fractions. GC/MS analysis of these fractions indicated trace impurities (4% or less) in the early and late fractions of this band, with center fractions free of impurities, and indicating an E/Z isomer ratio of ≈100/1.

Solvent removal from these center fractions followed by drying under vacuum (0.7 torr) for four days at 60°C gave a yellow oil. $C_{18}H_{18}SeO_4$ requires Se = 22.87%, C = 62.61%, and H = 5.25%; found Se = 22.62%, C = 63.16%, H = 5.29%.

b. Example Procedure (solid products)

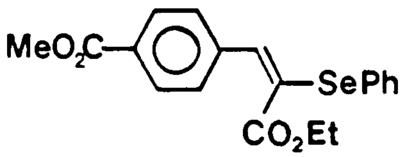

LII (p-CO_2Me)

(E) Ethyl 2-phenylseleno-3-(4-carbomethoxyphenyl)-2-propenoate

Reaction conditions employed were identical to those described above except for using a 0.010 molar scale (half of all quantities) (2.43g ethyl phenylselenoacetate and 1.64g methyl 4-formylbenzoate).

Work-up was also identical up to and including $MgSO_4$ drying. However, at this point, after solvent removal, the residue (which had been placed in a capped sample vial) was allowed to stand at 0°C for four days. (All crude products at this point in the procedure were allowed in similar fashion to stand several days in the freezer room, to provide an opportunity for product crystallization.) Suction filtration, washing with cold hexanes and recrystallization from hexanes gave 0.30g crude product (7.7% yield), m.p. 45-50°C. A small portion of this product was recrystallized two more times from hexanes and dried at ambient temperature at 0.7 torr for 4 days. The final purifed product gave a m.p. 55-56°C. $C_{19}H_{18}SeO_4$ requires Se=20.28%; found Se=20.47%. Further characterization by ^{13}C and ^{77}Se NMR showed this product to be exclusively the E isomer. Furthermore, all other solid products obtained in this fashion were shown to be exclusively E isomer, whereas all product oils consisted in varying degrees of both isomers.

Table 3

Series D

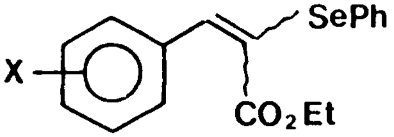

(E+Z) Ethyl-2-phenylseleno-3-phenyl-2-propenoates
Synthesis and Physical Data*

X	Method of isolation/purification RX≡recrystallization	Physical Data‡	Isolated Yield	Elemental Analysis		E/Z Ratio# (GC/MS)
				Found	(Theory)	
H	chromatography	yellow oil	28.8	known compound[47] E isomer m.p. 37.5-40.0°C		100/16.3
p-N(Me)$_2$^{1}	chromatography	yellow-green oil	3.9	Se=20.61	(21.09)	100/91.2
p-OMe	chromatography	yellow oil	25.8	Se=21.03	(21.85)	98.8/100.0
p-Me	chromatography	yellow oil	58.3	Se=22.62 C=63.16 H= 5.29	(22.87) (62.61) (5.25)	100/24.5
p-Ph	chromatography	amorphous waxy solid m.p. 39-45°C	27.7	--	--	100/5.9
p-F^2	chromatography	yellow oil b.p.=157-159°C/.20 torr	36.0	Se=22.79	(22.60)	100/14.3
p-Cl	chromatography/RX (pet ether)	light yellow solid m.p. 32-36°C	20.5	Se=21.36	(21.59)	100/31.9
m-OMe	chromatography	yellow oil	25.3	--	--	100/31.9
m-F	chromatography	yellow oil	19.5	--	--	100/0.4

Table 3 (continued)

X	Method of isolation/purification RX≡recrystallization	Physical Data‡	Isolated Yield	Elemental Analysis		E/Z Ratio# (GC/MS)
				Found	(Theory)	
m-Cl	chromatography/RX (pet ether)	light yellow solid m.p. 56-58°C	34.5	--	--	only E
p-CO_2Me[3]	spontaneous crystalization/RX (hexanes)	bright yellow solid m.p. 55-56°C	7.7 (purified)	Se=20.47	(20.28)	only E
m-CN[3]	spontaneous crystallization/RX (hexanes)	yellow-green solid m.p. 106-107°C	13.3	--	--	only E
m-CF_3[4]	chromatography/RX (hexanes)	light yellow solid m.p. 53-54.5°C	17.5	Se=20.13 C=54.35 H= 3.64 F=13.93	(19.78) (54.15) (3.79) (14.27)	100/28.8
p-CF_3	chromatography/RX (pet ether)	light yellow solid m.p. 33-35°C	6.1 (purified)	--	--	100/16.9
p-CN[3]	spontaneous crystallization/RX (pet ether/ $MeCl_2$)	yellow-green solid m.p. 110-111°C	17.8	Se=21.46 C=60.51 H= 4.16	(22.16) (60.68) (4.24)	only E
m-NO_2	spontaneous crystallization/RX (pet ether/ $MeCl_2$)	light yellow solid m.p. 80-81°C	17.0	Se=20.55	(20.98)	only E
p-NO_2[5]	chromatography	yellow-orange oil	3.18	--	--	14.8/100

*Numbered footnotes indicate unusual detail discussed subsequent to table

‡product oils dried at 60°C overnight at .7 torr
product solids (all crystalline except for p-Ph derivative) dried at ambient temp. 4 days at .7 torr.

#E/Z relative total ion abundance ratio

Footnotes

[1] Altered reaction conditions were required to achieve useful product yield: after formation of the $TiCl_4$-THF complex using the regular reaction procedure, the ice-bath cooling vessel was replaced with one containing dry ice/acetone. Once an internal temperature of -78°C was obtained, the organic substrates (0.040 moles of p-dimethylaminobenzaldehyde and 0.020 moles of ethyl phenylselenoacetate) codissolved in 20 mL dry THF were added slowly over a 45-minute period. A very deep purple-black color quickly developed after several drops had been added. The reaction was kept at -78°C for 4 hours, then allowed to warm to room temperature under nitrogen overnight.

Work up was carried out in normal fashion but including a more concentrated $NaHSO_3$ wash (0.12 moles, 2x150 mL) to remove unreacted aldehyde. GC/MS analysis of the crude reaction product revealed, in order of increasing retention times (percent relative total ion abundance), starting aldehyde (32.0%), diphenyldiselenide (6.4%), p-dimethylaminocinnamate (17.9%), competing Michael or Claisen condensation side-product (100.0%) and desired product (12.4%).

The deleterious side reaction was still, apparently, the predominant reaction pathway, but this approach maximized relative product yield. The side reaction product displayed an isotopic mass cluster around mw 400 consistent with the presence of two Se's, but this molecular weight did not coincide with the molecular ion of either the Claisen product from starting ester (mw 440) or the Michael (mw 617) addition products, (LXVII and LXVIII) respectively:

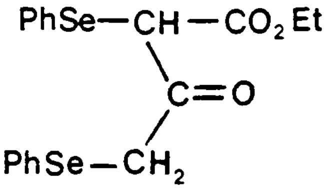
PhSe—CH—CO_2Et
C=O
PhSe—CH_2

LXVII

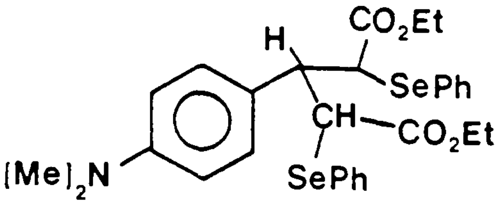
H
CO_2Et
SePh
CH
CO_2Et
SePh
$(Me)_2$N

LXVIII

Possibly, only a fragmentation pattern of this side product could be discerned due to thermal lability of the highly branched structure.

The crude product was taken up in methylene chloride and extracted again with $NaHSO_3$ to remove as much aldehyde as possible prior to chromatography. The crude sample (6.5g) was then preadsorbed onto fine mesh silica gel (15.0g) and subjected to column chromatography using 300g of 70-230 mesh silica gel.

Elution was carried out in like fashion to typical chromatographic separations. After collection of diphenyldiselenide (first eluting band, as usual), the column (at 4% EtOAc elution) revealed its most detailed appearance as shown below.

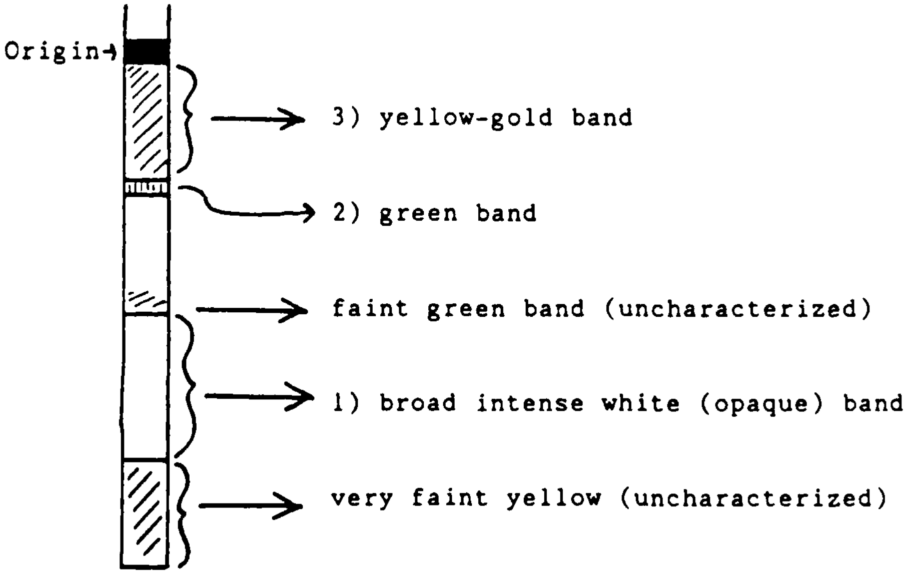
Origin
3) yellow-gold band
2) green band
faint green band (uncharacterized)
1) broad intense white (opaque) band
very faint yellow (uncharacterized)

GC/MS analysis indicated the following:

1) high molecular weight product from competing side reaction (400 m/e cluster); a bright yellow crystalline solid separated from these collected fractions
2) ethyl p-dimethylaminocinnamate
3) two components which separated by the time they came off the column at 7-8% EtOAc elution. The first eluting band was desired product. The second was starting aldehyde. About 12 hours eluting time was required to collect these last two components.

Removal of solvent gave a bright green-yellow oil for the product fractions. Overall yield was very low (3.87%).

[2] This compound was vacuum distilled through a short path to give product for elemental analysis.

[3] Spontaneous crystallization occurred for these compounds within several minutes at ambient temperature, with the exception of the p-CO_2Me derivative, which required 4 days at 0°C.

[4] During distillation removal of excess ethyl phenylselenoacetate, a small portion of this product inadvertently was distilled as a separate component, b.p. 155-160°C/.60 torr (yellow-gold oil). However, due to contamination with ethyl phenylselenoacetate this material was not recovered.

[5] This product was formed in much lower yield than any other derivative in this series. From relative peak intensities in the ^{77}Se NMR, this was the only compound that indicated predominant Z isomer formation. Optimum reaction conditions were found to be use of dry ice/acetone temperatures (-78°C) throughout the entire synthetic

sequence including a 1 hour period after addition of base, followed by gradual warming to ambient temperature overnight under nitrogen. Regular workup, including $NaHSO_3$ washing gave a dark orange oil which revealed two product isomers according to thin layer chromatography (SiO_2/EtOAc, hexanes 20/80), but only one isomer according to GC/MS, and in very small relative abundance (only 3.4% compared to 100.0% for ethyl phenylselenoacetate starting compound).

Using a 25 mL buret, a small scale chromatographic separation (0.15g sample preadsorbed on ≈ 1g fine mesh SiO_2 with ≈ 20 cm^3 of fine mesh (60) SiO_2 packing) was successfully carried out using the same solvent system employed for the other selenide compounds. Here, a 1% increase in EtOAc concentration for every 100 mL hexanes was used (up to 3%).

c. Starting Compounds

All benzaldehyde starting compounds were employed as described for Series A.

1) ethyl phenylselenoacetate[48]

To a solution of diphenyldiselenide (24.0g/0.080 mole) in 400 mL absolute ethanol was added sodium borohydride (6.14g/0.162 mole) in small portions while stirring under nitrogen. The bright yellow solution became nearly colorless after adding a stoichiometric amount. This reaction was very exothermic and evolved hydrogen gas.

The solution was allowed to cool to ambient temperature (30 minutes) and ethyl chloroacetate (19.85g/0.162 mole) was added in one portion. Salt formation was immediately apparent. The mixture was refluxed overnight under N_2, cooled to ambient temperature, and diluted with 500 mL water. To facilitate layer separation, the mixture was initially extracted with 150 mL ether. The subsequently more dense aqueous phase was removed and extracted twice with 200 mL portions of ether. The ether extracts were combined with the original organic phase and washed with sodium carbonate solution (5%) (2x100mL), and dried over $MgSO_4$. Removal of solvent gave a yellow oil which was vacuum distilled fractionally to give the product as a colorless liquid (b.p. 102-104°C/.50 torr), in a yield of 31.4g (80.8%).

B. NMR

1. Series A

a. ^{15}N NMR

1) Sample Preparation

To ensure reliable data acquisition, ^{15}N spectra were originally obtained using CD_3NO_2 solvent. Because of the low natural abundance of the spin=½ ^{15}N isotope (0.36%), fairly concentrated samples (50-55 weight %) were used, (5 mm diameter NMR tubes). CD_3NO_2 was a very useful solvent for initial ^{15}N acquisition, since it provided a convenient reference signal, well downfield from the range of aliphatic amine ^{15}N resonances, had excellent miscibility with these compounds, and provided an internal lock signal.

The importance of solvent effects is known to be greater in ^{15}N than ^{13}C NMR.[49] To large measure, the unshared electron pair on the nitrogen atom, in this case of the $N(Et)_2$ moiety, provides a greater susceptibility to the influence of a polar versus nonpolar solvent. The highly polar CD_3NO_2 solvent was felt to present a risk of differential interaction with the individual compounds in this series diminishing the correlation results.

To avoid the possibility of this solvent effect, another series of ^{15}N NMR's was performed using the less polar $CDCl_3$ solvent. Sample concentrations ranged from 43-47 weight %. Theoretical referencing to CH_3NO_2 was accomplished by using the automatic referencing program available on the VXR-300 system (SETREF®). To calibrate this reference value, a run was performed with CH_3NO_2 in $CDCl_3$ solvent. The chemical shift obtained for CH_3NO_2 ^{15}N signal using the SETREF® program was 3.040 ppm. This value was thus subtracted from all ^{15}N chemical shifts obtained using this technique to bring these values in line with those using internal CD_3NO_2 as the reference signal (δ of CD_3NO_2 $^{15}N = 0.00$ ppm).

To ascertain if this automatic referencing technique was valid, a plot of the ^{15}N chemical shifts obtained for each enamine isomer in CD_3NO_2 versus $CDCl_3$ solvent (calibrated as explained above) was prepared. The plots (shown in Figure 3a and 3b; pages 70 and 71) show an excellent agreement between the two solvents, and verifies the usefulness of this approach. At the same time, these tight correlations indicate the probable absence of any significant $CD_3NO_2/CDCl_3$ solvent effect.

By the time this second series of ^{15}N experiments was being conducted, optimized parameters for use in conjunction with the Waltz Decoupler were employed, greatly reducing the time necessary for data acquisition (from overnight to 4-6 hours). Also, no residual peak splitting (which had occurred in the internal CD_3NO_2 series) was observed. Due to this enhanced sensitivity, chemical shifts for both

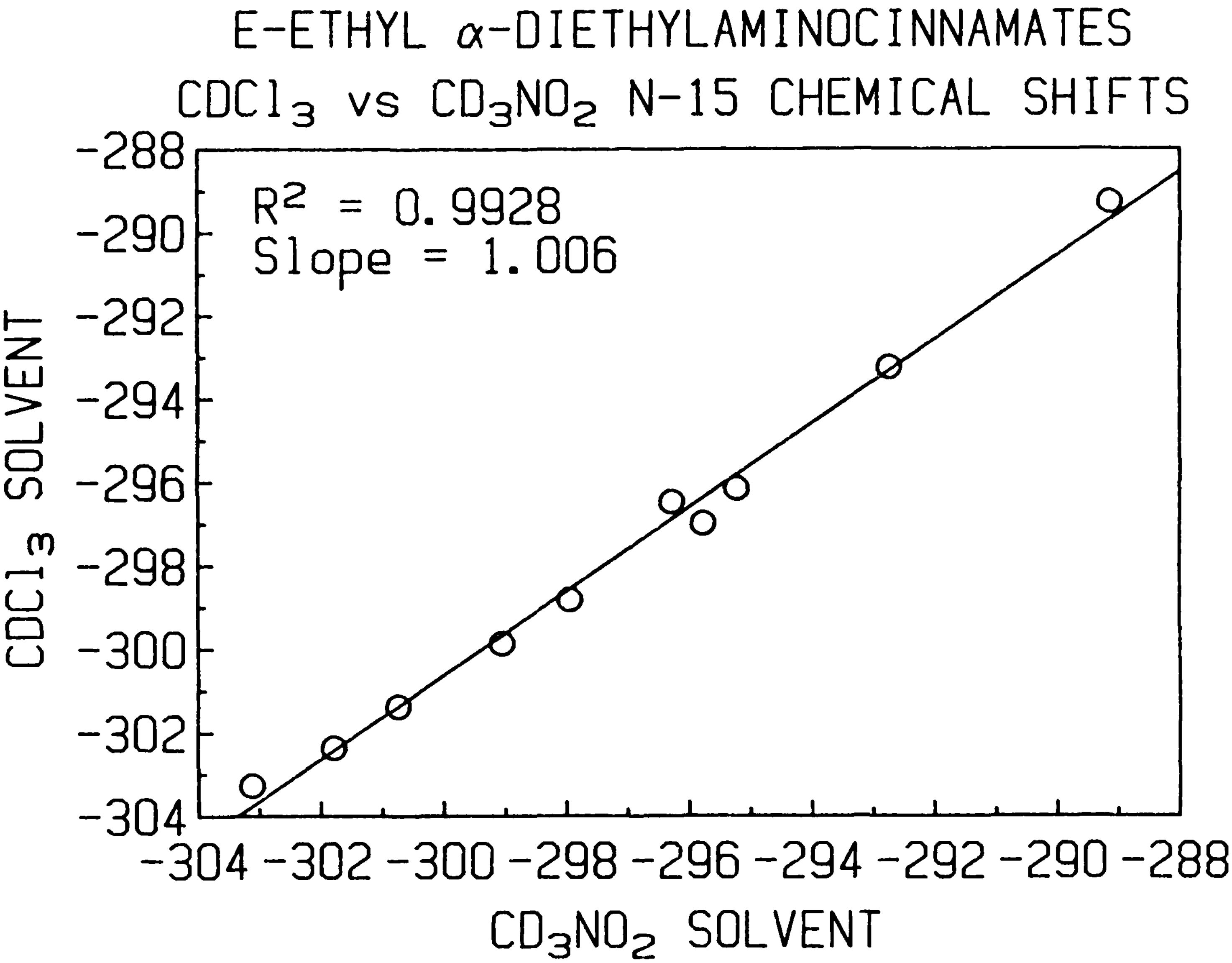
E-ETHYL α-DIETHYLAMINOCINNAMATES
$CDCl_3$ vs CD_3NO_2 N-15 CHEMICAL SHIFTS
R^2 = 0.9928
Slope = 1.006
-288
-290
-292
-294
-296
-298
-300
-302
-304
$CDCl_3$ SOLVENT
-304 -302 -300 -298 -296 -294 -292 -290 -288
CD_3NO_2 SOLVENT

FIGURE 3a

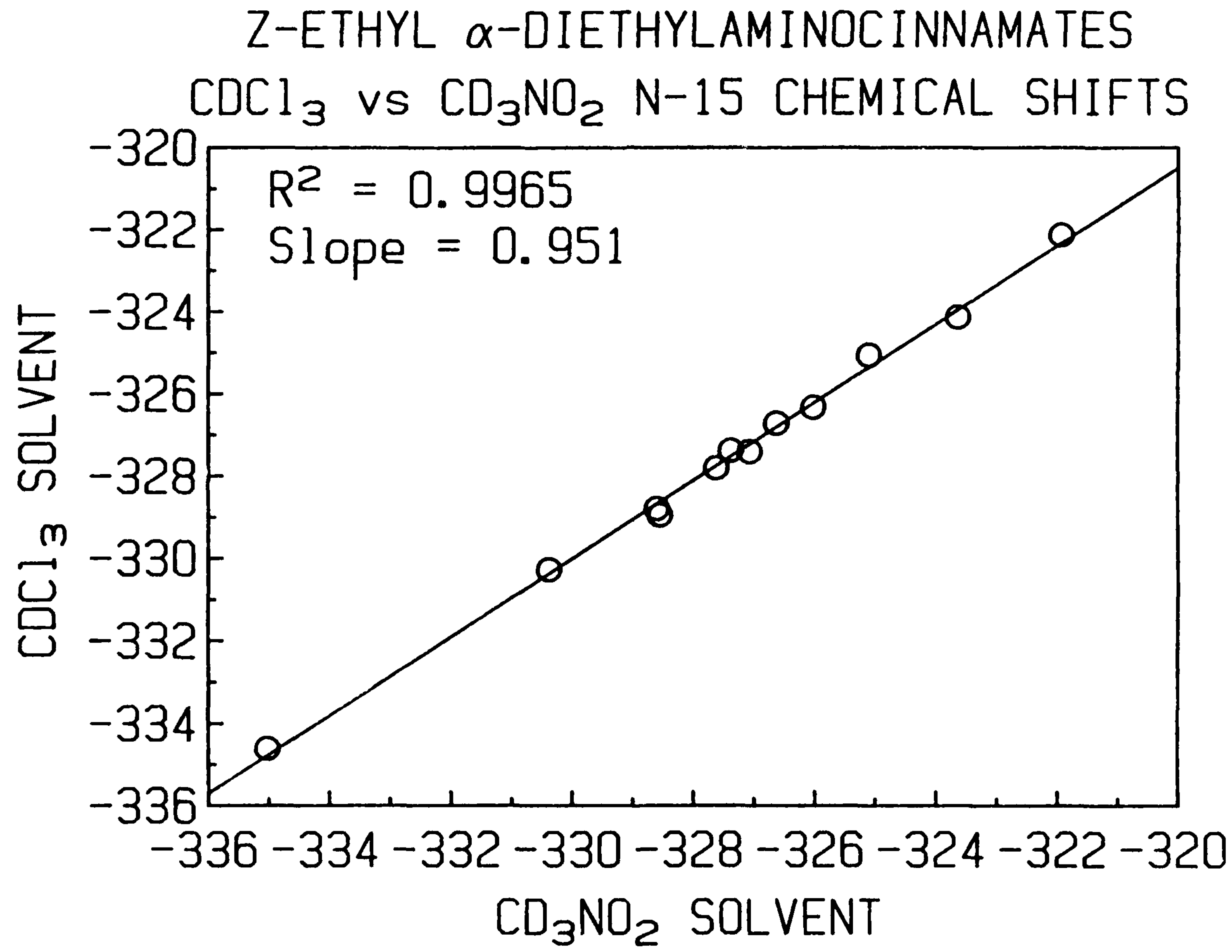
Z-ETHYL α-DIETHYLAMINOCINNAMATES
CDCl3 vs CD3NO2 N-15 CHEMICAL SHIFTS
R2 = 0.9965
Slope = 0.951
CDCl3 SOLVENT
CD3NO2 SOLVENT
-320
-322
-324
-326
-328
-330
-332
-334
-336

FIGURE 3b

the E and Z isomers in the entire series were obtained. Prior to these optimizations, compounds containing a small relative percentage of the less abundant isomer did not give a detectable peak for that isomer; the E isomer for p-N(Me)$_2$, p-F, m-F, and p-Ph did not appear as well as the Z isomer for p-CF$_3$. Consequently, only the calibrated CDCl$_3$ data will be subsequently reported and discussed.

2) ^{15}N NMR Standard Parameters

^{15}N NMR's for the ethyl α-diethylaminocinnamates were run at 30.405 MHz. Waltz Decoupling® was employed. A typical parameter menu* for these runs follows:

Table 4

^{15}N Standard Parameters
(Series A)

```
  ACQUISITION                                          PROCESSING
SFRQ    30.405          DATE  01-20-88          SE          1.061
TN      15.000          SOLVNT CDCL3            LB          0.300
SW     14992.5          FILE   NDMAE2           RE     NOT USED
AT       1.001                                  CD     NOT USED
NP       30016            DECOUPLING            CCD    NOT USED
FB        8300          ON          1.500       AF     NOT USED
BS          25          DO         1499.7       FN     NOT USED
SS           0          DM           YYY        MATH      I
PW        15.8          DMM          S          WERR
P1           0          DMF         6600        WEXP
D1       5.000          DHP    NOT USED         WBS         WFT
D2           0          DLP            5        WNT
TO       -6500          HOMO     N
NT       30000                                    SPECIAL
CT                        FLAGS                 TEMP   NOT USED
                        IL       N              PW90        25.0
                        IN       N
                        DP       Y
                        ALOCK    N
```

*VXR-300 NMR Instrument

b. ^{13}C and ^{1}H Standard Parameters

These NMR's were run at 75.426 and 299.930 MHz, respectively, using CD_3NO_2 solvent, and TMS internal reference. The standard parameters for each are listed below:

Table 5
^{13}C Standard Parameters
(Series A)

ACQUISITION				PROCESSING	
SFRQ	75.426			SE	0.318
TN	13.750	SOLVNT	CD3NO2	LB	1.000
SW	16501.7	FILE	CPPHEN	RE	NOT USED
AT	0.909			CD	NOT USED
NP	30016	DECOUPLING		CCD	NOT USED
BS	16	DN	1.750	AF	NOT USED
SS	0	DO	0	FN	NOT USED
PW	4.2	DM	YYY	MATH	I
P1	0	DMM	S	WERR	
D1	0	DMF	6600	WEXP	
D2	0	DHP	NOT USED	WBS	WFT
TO	0	DLP	5	WNT	
NT	2000	HOMO	N		
CT	0			SPECIAL	
		FLAGS		TEMP	NOT USED
		IL	N	PW90	13.0
		IN	N		
		DP	Y		
		HS	NN		

Table 6

^{1}H Standard Parameters
(Series A)

ACQUISITION				PROCESSING	
SFRQ	299.930	DATE	02-17-88	SE	NOT USED
TN	1.750	SOLVNT	CD_3NO_2	LB	NOT USED
SW	4100.0	FILE	HPPHEN	RE	NOT USED
AT	1.998			CD	NOT USED
NP	16384	DECOUPLING		CCD	NOT USED
BS	NOT USED	DN	1.750	AF	NOT USED
SS	0	DO	350.3	FN	16384
PW	6.2	DM	NNN	MATH	I
P1	0	DHP	NOT USED	WERR	REACT
D1	0	DLP	20	WEXP	
D2	0	HOMO	N	WBS	WFT
TO	700			WNT	
NT	64	FLAGS			
CT	0	IL	N	SPECIAL	
		IN	N	TEMP	NOT USED
		DP	Y	PW90	17.5
		HS	NN		
		ALOCK	S		

c. Selective Decoupling

The p-Me derivative in Series A was subjected to selective decoupling experiments to determine the ^{3}J vinylic $^{1}H/C=O$ values for each of the carbonyls in the ^{13}C spectrum. The fully coupled spectrum was first obtained employing the following parameter group:

Table 7

^{13}C Fully Coupled Parameters
(Series A)

```
   ACQUISITION                                        PROCESSING
SFRQ     75.426        DATE  10-15-87           SE          0.318
TN       13.750        SOLVNT  CDCL3            LB          1.000
SW      16501.7        FILE    MECOU2           RE      NOT USED
AT        0.909                                 CD      NOT USED
NP        30016          DECOUPLING             CCD     NOT USED
BS           64        DN        1.750          AF      NOT USED
SS            0        DO            0          FN      NOT USED
PW          4.2        DM      NNN              MATH       I
P1            0        DMM     S                WERR
D1            0        DMF        7000          WEXP
D2            0        DHP  NOT USED            WBS         WFT
TO            0        DLP           5          WNT
NT            0        HOMO    N
CT        50000                                    SPECIAL
              0           FLAGS                 TEMP    NOT USED
                       IL      N                PW90        13.0
                       IN      N
                       DP      Y
                       HS      NN
                       ALOCK   S
```

Selective decoupling of the methylene protons in the ethyl carboxylate group was obtained by the following parameter group:

Table 8

^{13}C Selective Decoupling Parameters
(Series A)

ACQUISITION				PROCESSING	
SFRQ	75.426			SE	0.318
TN	13.750	SOLVNT	CDCL3	LB	1.000
SW	16501.7	FILE	MESCO2	RE	NOT USED
AT	0.909			CD	NOT USED
NP	30016	DECOUPLING		CCD	NOT USED
BS	64	DN	1.750	AF	NOT USED
SS	0	DO	99.9	FN	NOT USED
PW	4.2	DM	YYY	MATH	I
P1	0	DMM	C	WERR	
D1	0	DMF	7000	WEXP	
D2	0	DHP	NOT USED	WBS	WFT
TO	0	DLP	20	WNT	
NT	50000	HOMO	N		
CT	0			SPECIAL	
		FLAGS		TEMP	NOT USED
		IL	N	PW90	13.0
		IN	N		
		DP	Y		
		HS	NN		
		ALOCK	S		

This caused collapse of the doublet of triplets pattern obtained from the fully coupled run to the clear doublet patterns needed for E/Z isomer assignments. (This is covered in more detail in the Discussion of Results, page 89).

2. Series B

a. ^{15}N NMR

Saturated CD_3NO_2 solutions of the azlactones (≈ 50 mg/mL solvent) were used for these runs, and the CD_3NO_2 was used as an internal reference signal. Due to the presence of the ^{15}N label in approximately 10% concentration, only 4-5 hours was generally required to obtain data, in spite of the much lower solubility of these compounds versus the other series. A typical parameter menu for these runs follows:

Table 9

^{15}N Standard Parameters
(Series B)

ACQUISITION				PROCESSING	
SFRQ	30.405	DATE	01-20-88	SE	1.061
TN	15.000	SOLVNT	CD_3NO_2	LB	0.300
SW	14992.5	FILE	NPFAZ	RE	NOT USED
AT	1.001			CD	NOT USED
NP	30016	DECOUPLING		CCD	NOT USED
FB	8300	DN	1.500	AF	NOT USED
BS	25	DO	1499.7	FN	NOT USED
SS	0	DM	YYY	MATH	I
PW	15.8	DMM	S	WERR	
P1	0	DMF	5000	WEXP	
D1	5.000	DHP	NOT USED	WBS	WFT
D2	0	DLP	20	WNT	
TO	-6500	HOMO	N		
NT	30000			SPECIAL	
CT	0	FLAGS		TEMP	NOT USED
		IL	N	PW90	25.0
		IN	N		
		DP	Y		
		ALOCK	N		

b. ^1H NMR

Table 6 parameters were used to confirm product structure.

3. Series C

a. ^{15}N NMR

These samples were prepared as saturated or near saturated $CDCl_3$ solutions. The solubility of these compounds varied widely, however, from 0.25g/0.5 mL for the p-Me compound to less than 0.10g/1.0mL for the p-CN analogue. As with Series A, the automatic referencing program to CH_3NO_2 was employed for this series, using the same parameter menu shown in Table 4.

b. $^{13}C/^1H$ NMR

These have been obtained elsewhere,[44] and were not examined any further in this study.

4. Series D

Note: All NMR's for this series were obtained by Dr. Leslie Gelbaum, Georgia Institute of Technology, using a VXR-400 instrument.

a. ^{77}Se NMR[50]

All samples (approximately 0.3g each) were dissolved in 2.5 mL $CDCl_3$. Chemical shifts were measured relative to external dimethyl selenide which was placed in a 3 mm diameter capillary inside a 10mm diameter NMR tube. The ^{77}Se NMR spectra were acquired at 76.295 MHz using broadband proton decoupling to ensure accurate chemical shift measurement. The samples were also run without decoupling to determine the Se/vinylic ^{1}H coupling constants. Here, selective proton decoupling of the interfering aromatic protons was required. A typical parameter menu for the broadband proton decoupling ^{77}Se runs follows: NOTE: Parameters adjusted for VXR-300 instrument.

Table 10

^{77}Se Standard Parameters
(Series D)

ACQUISITION				PROCESSING	
SFRQ	57.217	DATE	07-27-87	SE	0.106
TN	77.000	SOLVNT	CDCL3	LB	3.000
SW	59880.2	FILE	CR7277	RE	NOT USED
AT	0.320			CD	NOT USED
NP	38336	DECOUPLING		CCD	NOT USED
BS	16	DN	1.750	AF	0.150
SS	0	DO	0	FN	65536
PW	30.0	DM	YYY	MATH	I
P1	0	DMM	S	WERR	
D1	1.000	DMF	5500	WEXP	
D2	0	DHP	20.0	WBS	
TO	0	DLP	0	WNT	
NT	256	HOMO	N		
CT	0			SPECIAL	
		FLAGS		TEMP	NOT USED
		IL	N	PW90	23.5
		IN	N		
		DP	Y		
		HS	NN		
		ALOCK	N		

The parameter menu used for selective aromatic proton decoupling (to evaluate the Se/vinylic H^1 coupling constants) follows:

Table 11

^{77}Se Selective Decoupling Parameters
(Series D)

ACQUISITION				PROCESSING	
SFRQ	57.217	DATE	07-27-87	SE	NOT USED
TN	77.000	SOLVNT	CDCL3	LB	NOT USED
SW	15822.8	FILE	CR7273	RE	NOT USED
AT	0.320			CD	NOT USED
NP	10112	DECOUPLING		CCD	NOT USED
BS	16	DN	1.750	AF	0.150
SS	0	DO	989.2	FN	65536
PW	30.0	DM	YYY	MATH	I
P1	0	DMM	C	WERR	
D1	1.000	DMF	200	WEXP	
D2	0	DHP	NOT USED	WBS	
TO	11300	DLP	25	WNT	
NT	256	HOMO	N		
CT	0			SPECIAL	
		FLAGS		TEMP	NOT USED
		IL	N	PW90	23.5
		IN	N		
		DP	Y		
		HS	NN		
		ALOCK	N		

b. ^{13}C and ^{1}H NMR[50]

^{13}C and ^{1}H NMR's were run on the same samples as above at 100.573 MHz and 399.928 MHz, respectively. The ^{1}H chemical shifts were reported relative to internal TMS and the ^{13}C chemical shifts are relative to the middle $CDCl_3$ peak at 77 ppm.

CHAPTER IV

DISCUSSION OF RESULTS

A. Hammett Single Substituent Parameter Constants (σ, σ^+, σ^-, and σ^{13})

Four single-substituent Hammett scales were used to evaluate the correlation results: σ, σ^+, σ^-, and σ^{13}. With about 40 σ scales described in the literature, an explanation for why only these four were used is in order.

1. Sigma (σ) scale

This is the originally defined Hammett substituent value and is based on the aqueous ionization of benzoic acids: [51]

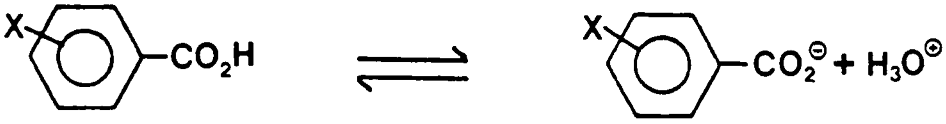

LXIX LXX

$$\log \frac{K_X}{K_H} = \rho\sigma_X$$

$\rho = 1.00$ (reaction constant)

This substituent scale was used in this study for two reasons: 1) its historical significance and 2) it entails no additional correcting terms in its derivation. As the original scale, it provided the standard for comparison.

The magnitude of the reaction constant, ρ, reflects, as the slope of a Hammett correlation, a given reaction's sensitivity to substituent effects relative to this standard reaction (where it is assigned a value of 1.00). The sign of ρ indicates the nature of charge development in the transition state; a positive value corresponding to negative charge buildup while a negative value corresponds to positive charge buildup. When applied to ^{13}C δ/σ correlations, ρ is termed the transmission coefficient and reflects the dependency of δ on substituent effects.

2. Sigma plus (σ^+) and Sigma minus (σ^-) scales

These are the two most important of the 40 or so refinement scales historically developed since the inception of the Hammett correlation; they take into account a major factor not included in the historical derivation--through conjugation (or through-resonance):

a. Sigma plus (σ^+) [52]

In the measurement of the relative rates of hydrolysis of tertiary cumyl chlorides (LXXI),

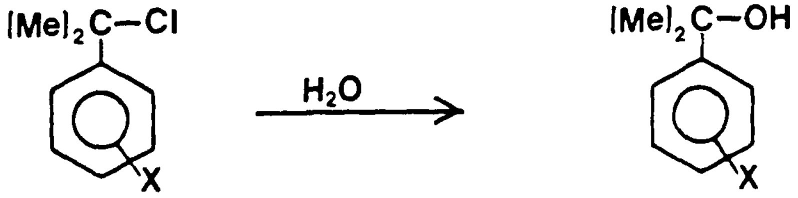

LXXI LXXII

it was found that for strongly electron donating substituents by resonance, the observed rate of reaction far exceeded that predicted by the standard σ value. An additional factor contributing to the ease of the above reaction was rationalized to be through-resonance interaction of the substituent with the SN1 intermediate of the reaction mechanism: (shown below for p-OCH_3, LXXIII)

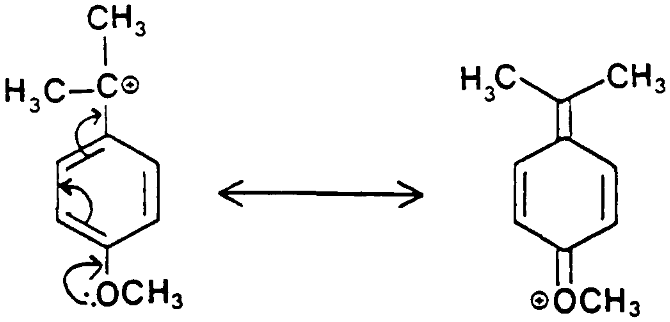

LXXIII

This resonance stabilization of the intermediate lowers the activation energy barrier leading to faster overall reaction. The "through-resonance term" is employed to emphasize that there is a direct effect between the probe site (the reaction center) and the substituent). σ^+ values thus display an enhanced negative value for strongly electron donating (by resonance) substituents.

b. Sigma minus (σ^-) [53]

In the measurement of ionization equilibria for substituted phenols (LXXIV),

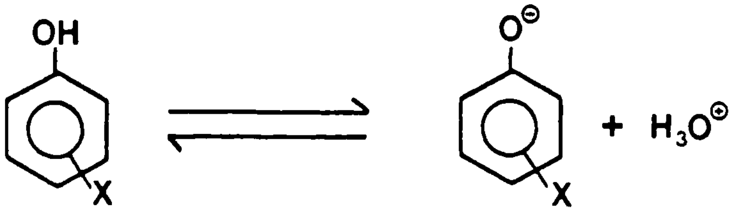

LXXIV LXXV

it was observed that for X = para, strongly electron withdrawing by resonance, the phenoxide anion equilibrium concentration (LXXV) far exceeded that predicted by the sigma value. Here, it was argued that direct through-resonance stabilization of the incipient phenoxide anion led to its markedly greater stability and thus ease of formation (shown for X = p-CN, LXXVI),

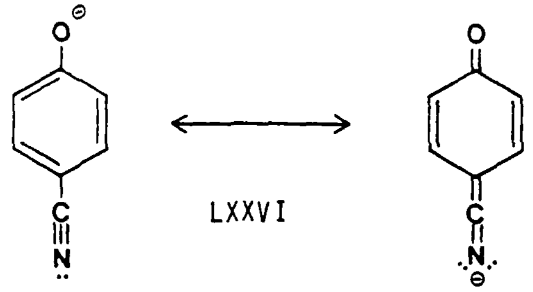

LXXVI

Again, a direct resonance stabilization is provided to the probe site by the substituent. σ^- values thus display an enhanced positive value for strongly electron withdrawing (by resonance) substituents.

The inclusion of the σ^+/σ^- substituent scales in the present correlation analysis stemmed from the fact that the probe site nuclei (N and Se) were in a position to possibly interact in such a through-conjugative fashion. In conjunction with using the σ scale for contrast, the participation of this effect could be more easily discerned.

3. Sigma thirteen (σ^{13}) scale [34]

This is the most recently developed of the four substituent scales and is the result of extensive ^{13}C NMR studies of the effect of substituents on the nuclear shielding of the β carbon atom in the styrene sidechain.

More specifically, the σ^{13} value, derived from the following equation

$$\sigma^{13} = a(\delta_X - \delta_H)$$

evaluates the chemical shift of the β carbon atom in the substituted compound versus that in the unsubstituted styrene molecule:

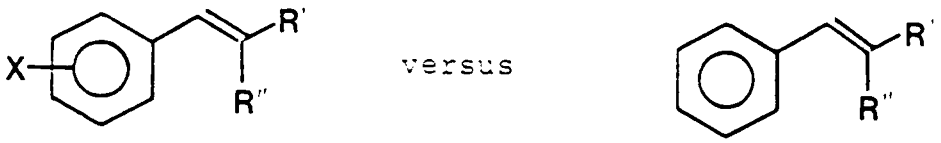

XXXI

(see page 22)

The term a, is simply a scaling factor to bring these values in line with most scales used (p-N(Me)$_2$ = -1.75).

The σ^{13} scale is useful for several reasons: 1) it represents a culmination of substituent-effect analyses for a very large number of compounds. It thus represents a very thorough comprehensive data set and a rigorous basis for individual substituent constant assignments; 2) it is derived solely from the same structure-type used in the present study (styrene probe); and 3) its use provides an important contrast to the other three scales. σ^+/σ^- represent an incorporation of a single important factor (through-resonance) into the Hammett σ scale, whereas σ^{13} represents a statistically averaged effect over 300 substituted styryl compounds.

It was thus felt that the use of these four single substituent scales comprised an effective but practical means of evaluating the correlation data. The scales employed encompass a mix of the widest range commonly encountered (σ^+ to σ^-) and those derived from thorough data sets (σ and σ^{13}).

Table 12 displays the σ, σ^+, σ^-, and σ^{13} values for the substituents used in this research effort, listed according to compound series. This substituent range represents a satisfactory breadth and spacing of the various Hammett constant values. The "minimum basis set" requirement (that substituent set recommended in the literature for valid correlation analysis) [54] is shown by the asterisks in Table 12. This set comprises a mix of substituent electronic properties so that the resultant data reflects a proper range and diversity of effects. As can be seen, in all series, except C (α-cyanocinnamates), this requirement was more than met.

Table 12

Hammett Single-Substituent Values

X	σ	σ^+	σ^-	σ^{13}	Compound Series
p-N(Me)$_2$*	-0.83	-1.7	-0.83	-1.75	A,B,C,D.
p-OMe*	-0.27	-0.78	-0.27	-0.74	A,B,C,D
p-Me*	-0.17	-0.31	-0.17	-0.30	A,B,C,D
p-Ph	-0.01	-0.18	-0.01	-0.10	A,D
p-F*	0.06	-0.07	0.06	-0.05	A,B,C,D
H*	0.00	0.00	0.00	0.00	A,B,C,D
p-Cl*	0.23	0.11	0.23	0.13	A,B,D
m-OMe	0.12	0.12	0.12	0.05	D
m-F	0.34	0.34	0.34	0.35	A,B,C,D
m-Cl	0.37	0.37	0.37	0.36	A,D
p-CO$_2$Me*	0.44	0.48	0.68	0.53	A,B,D
m-CN	0.56	0.56	0.56	0.69	A,D
m-CF$_3$	0.46	0.57	0.49	0.52	D
p-CF$_3$	0.53	0.61	0.65	0.66	A,D
p-CN*	0.66	0.66	0.90	0.85	A,B,C,D
m-NO$_2$	0.71	0.71	0.71	0.79	D
p-NO$_2$	0.78	0.78	1.24	1.01	A,B,D

B. Single Substituent Parameter Correlations

1. Series A/General Comments/Isomer Assignments

A very fortunate aspect of the ^{15}N chemical shift behavior of the E and Z enamine isomers, which allowed a clear interisomer demarcation and correlation comparison, was that a difference of 26-30 ppm between them was consistently observed for the 13 common substituents used in this series. The E isomer had the more deshielded ^{15}N δ range (-304.56 to -289.27 ppm) relative to CH_3NO_2 automatic referencing (see experimental section); the Z isomer's ^{15}N δ was more shielded (-334.61 to -322.13 ppm). Table 13 (page 87) lists the ^{15}N δ's for the E and Z isomers.

A simple accounting for this considerable chemical shift difference centered on the more favorable conditions for deshielding resonance donation of nitrogen's unshared electron pair in the E isomer, (page 89) XLIXA (in-line styryl orientation and relative lack of steric encumbrance), versus the Z isomer (XLIXB), where the combination of increased steric encumbrance to optimal overlap and out-of-line orientation could partially account for N's greater shielding. However, the fact that the Z isomer gave significantly better correlations appeared to contradict this simplistic model, since greater resonance interaction of N's lone pair implies a stronger dependence on the substituent effect and thus a better correlation.

Another factor possibly contributing more substantially to the greater shielding of the Z nitrogen atom became evident from conformational energy studies using the Alchemy® program [55]. Here, for both the E and Z isomers, a substantial twist out of the styryl plane of the phenyl ring was indicated presumably in response to the

Table 13

^{15}N Chemical Shifts*/Series A

X	^{15}N δ E Isomer	Z Isomer
p-N(Me)$_2$	-304.56	-334.61
p-OMe	-303.27	-330.27
p-Me	-302.36	-328.79
p-Ph	-300.10	-327.38
p-F	-301.61	-328.95
H	-301.37	-327.80
p-Cl	-299.86	-327.40
m-F	-299.23	-326.71
m-Cl	-298.81	-326.32
p-CO$_2$Me	-296.15	-324.13
m-CN	-296.47	-325.06
p-CF$_3$	-296.99	-324.70
p-CN	-293.24	-322.13
p-NO$_2$	-289.27	-336.38#

*Upfield from CH_3NO_2; automatic referencing/VXR-300

#not plotted

steric demand of the N(Et)$_2$ group (for Z) and CO$_2$Et (for E). As a consequence, the N atom of the Z isomer could be further shielded by phenyl ring anisotropy, since this phenyl twist could orient the N above the ring plane.

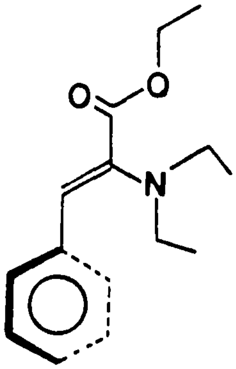

XLIXB

For the most part, whenever the further upfield (shielded) ^{15}N peak was of greater intensity, the carbonyl peaks displayed the following pattern:

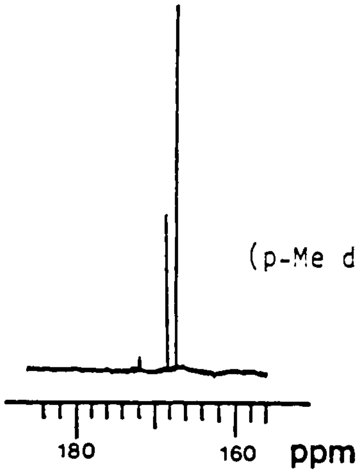

(For some unknown reason, the p-N(Me)$_2$ and m-Cl compounds, which were both predominantly Z isomers, displayed in the ^{15}N NMR a greater intensity of the more deshielded peak). Interestingly, from a synthetic perspective, electron donating and middle range substituents gave predominantly Z isomer, whereas the more strongly electron withdrawing groups gave greater E isomer formation, in some cases predominantly; see Table 2. In these latter cases, a shift in the peak relative intensities described above was observed.

Precise isomer assignments were made on the basis of evaluation of the ^{3}J vinylic $^{1}H/C=O$ values of each of the carbonyls in a typical ^{13}C spectrum (p-Me derivative); see Figure 4, page 90. The fully coupled carbonyl spectrum revealed a clear doublet of triplets pattern for the more deshielded carbonyl versus what appeared to be a similar but overlapping pattern (giving an apparent quartet) for the more shielded carbonyl. Selective proton decoupling of the ethyl carboxylate methylene protons rationalized the splitting pattern described above and allowed clear measurement of these respective J values, see Figure 5, page 90. The further downfield carbonyl displayed the larger J value, consistent with trans geometry of the ^1H vinylic/C=O in the enamine E isomer:[56]

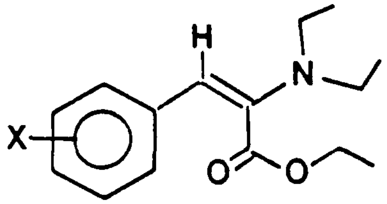

XLIXA

Likewise, the further upfield carbonyl (more shielded) displayed a smaller J value, indicative of the cis vinylic ^1H/C=O arrangement of the Z isomer:[56]

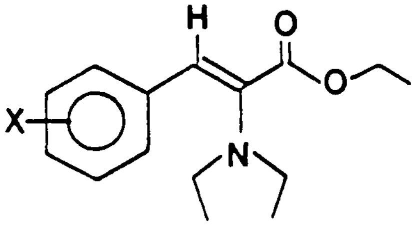

XLIXB

Further corroborative information for these assignments was revealed in the ^1H NMR where a significant difference was consistently observed between the chemical shifts of the vinylic protons of the E and Z isomers. The downfield proton, the result of increased deshielding by the paramagnetic anisotropy of the carbonyl group (/////) was the more intense vinylic absorption when ^{15}N and ^{13}C NMR collectively indicated the Z enamine isomer to be predominant (XLIXB):

FULLY COUPLED CARBONYL SPECTRUM/p-ME DERIVATIVE
(SERIES A)

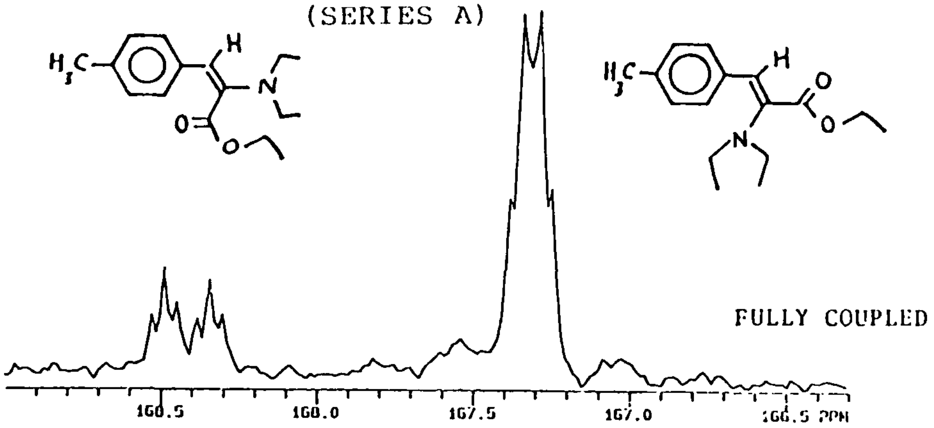

FIGURE 4

SELECTIVELY DECOUPLED CARBONYL SPECTRUM/p-ME
DERIVATIVE (SERIES A)

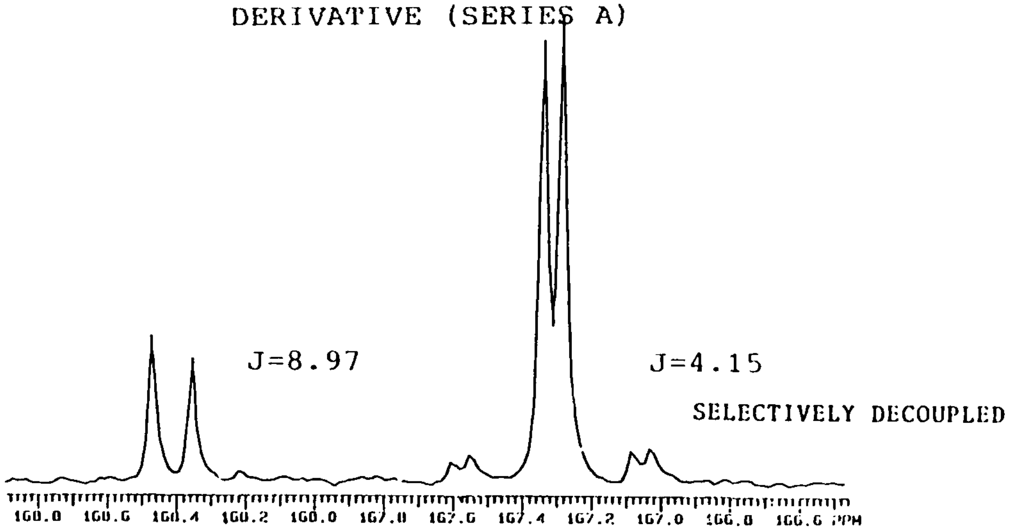

FIGURE 5

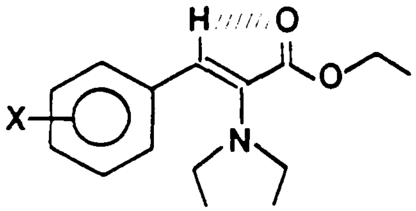

XLIXB

Whereas the more shielded vinylic ^1H resonance was more intense for the p-NO_2, p-CF_3, and p-CN compounds, where the E isomer was predominant (XLIXA),

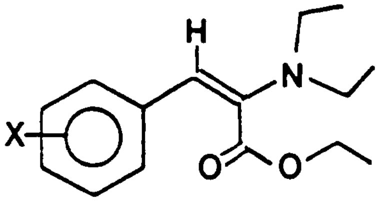

XLIXA

and such a deshielding interaction could not occur. (For some unknown reason, however, the predominantly E m-CN compound did not show this pattern.) A summary of the $^{15}N/^{13}C/^{1}H$ absorption patterns just described is shown in Figure 6, page 92.

a. E vs Z Isomers

The ^{15}N chemical shifts for the E and Z isomers were plotted against the σ^-, σ^{13}, σ, and σ^+ single substituent constant values. The plots and regression analyses are shown in Figures 7a-d (pages 93-96) and 8a-d (pages 97-100), respectively. The -336.38 ppm ^{15}N δ obtained with the p-NO_2 compound (see Table 13) probably corresponded to an impurity. This data point was thus not included in the correlation analysis.

$^{15}N/^{13}C/^{1}H$ CHEMICAL SHIFT INTENSITY PATTERNS
Z AND E ISOMERS (SERIES A)

Z PREDOMINANT (p-Cl EXAMPLE)

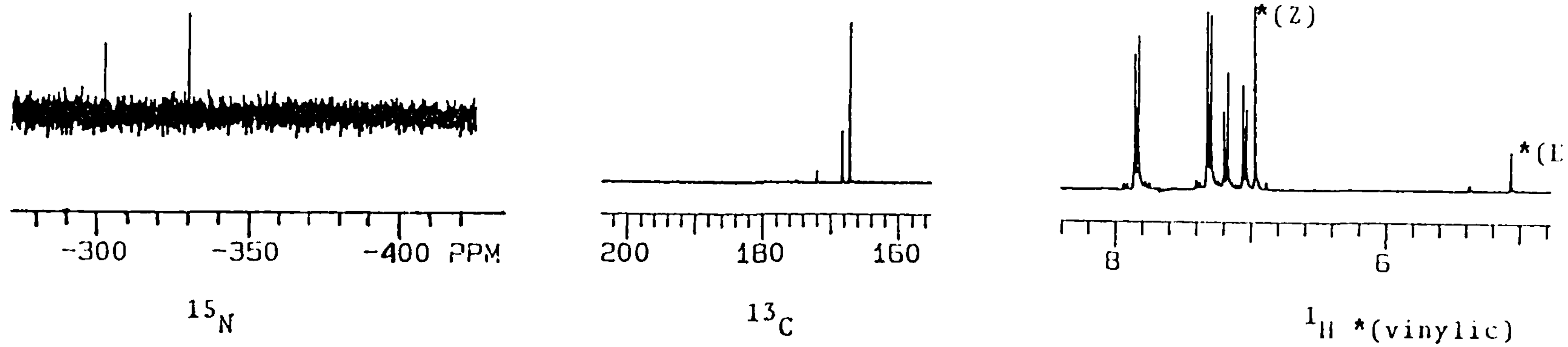

E PREDOMINANT (p-CF_3 EXAMPLE)

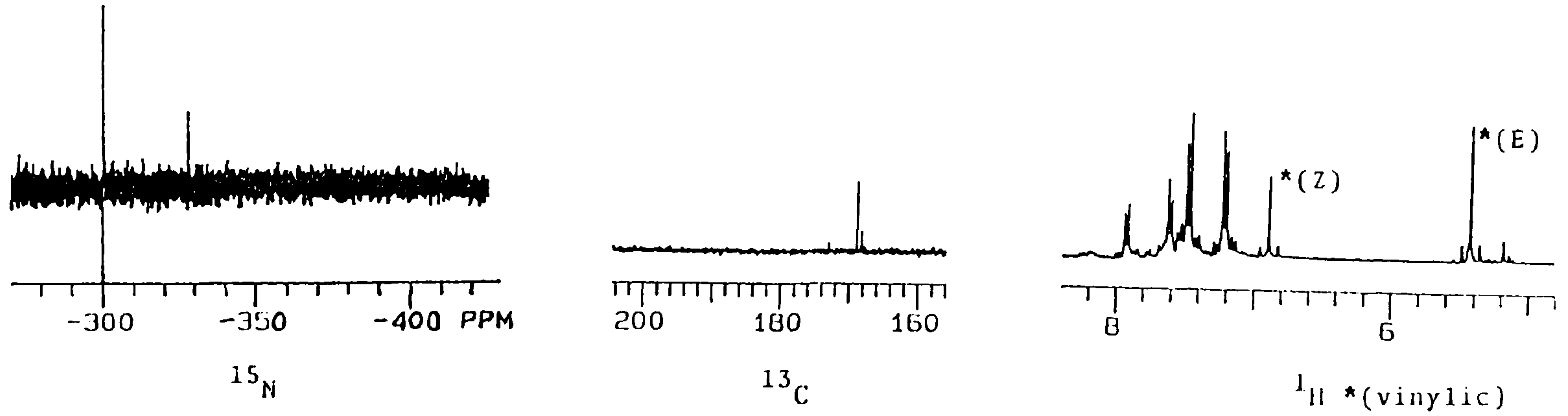

FIGURE 6

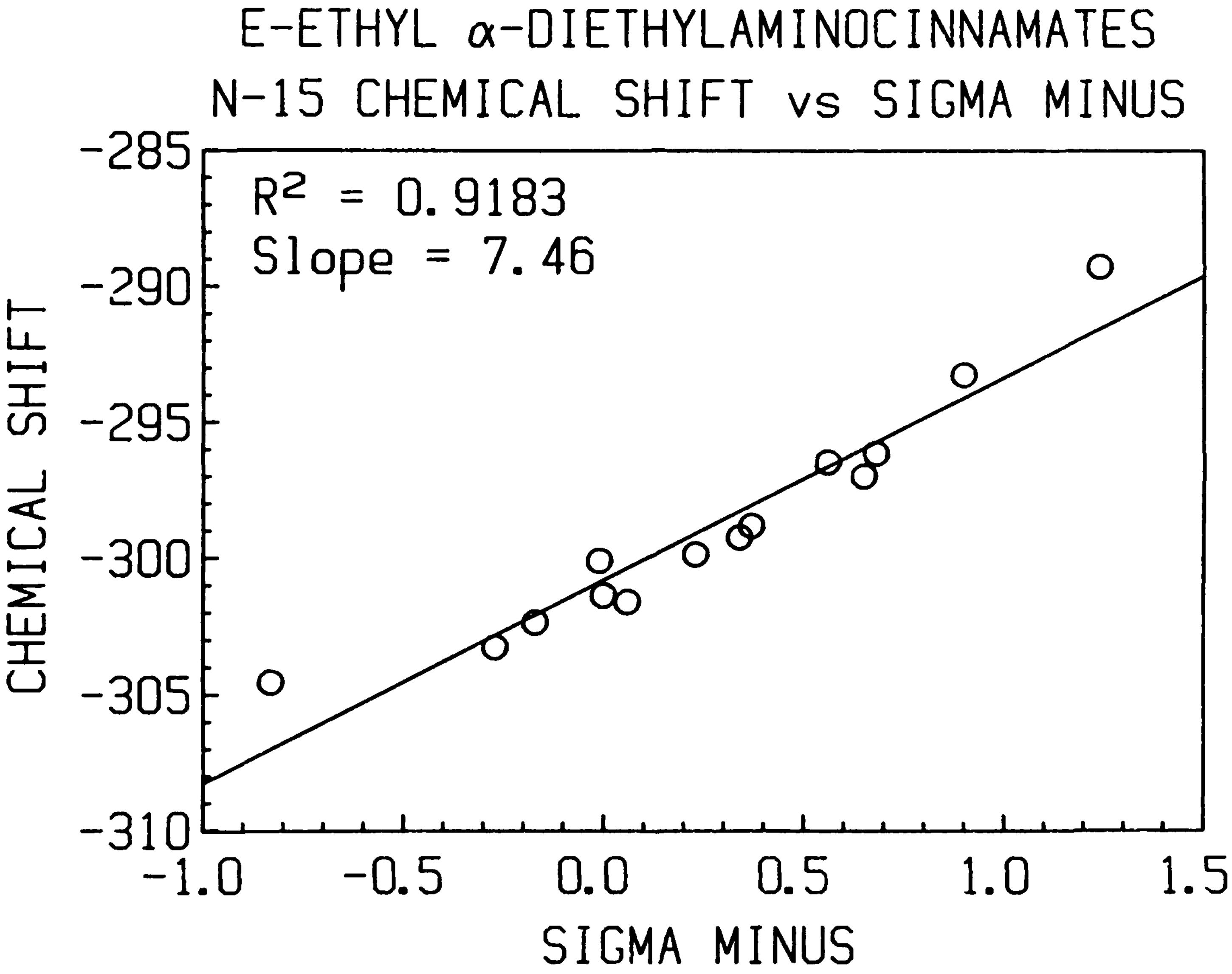
E-ETHYL α-DIETHYLAMINOCINNAMATES
N-15 CHEMICAL SHIFT vs SIGMA MINUS
R² = 0.9183
Slope = 7.46
-285
-290
-295
-300
-305
-310
CHEMICAL SHIFT
-1.0
-0.5
0.0
0.5
1.0
1.5
SIGMA MINUS

FIGURE 7a

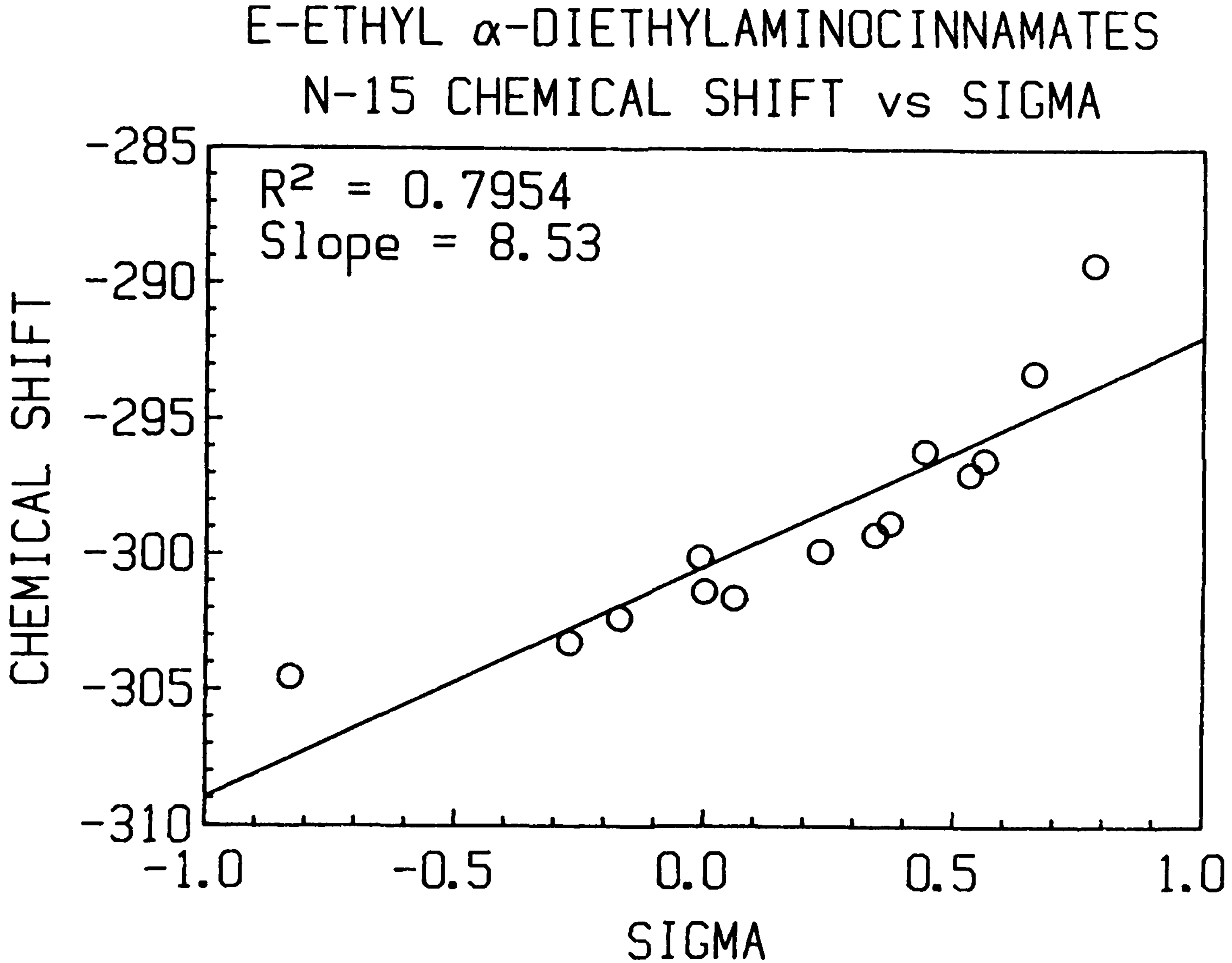
E-ETHYL α-DIETHYLAMINOCINNAMATES
N-15 CHEMICAL SHIFT vs SIGMA
R^2 = 0.7954
Slope = 8.53
CHEMICAL SHIFT
-285
-290
-295
-300
-305
-310
-1.0
-0.5
0.0
0.5
1.0
SIGMA

FIGURE 7b

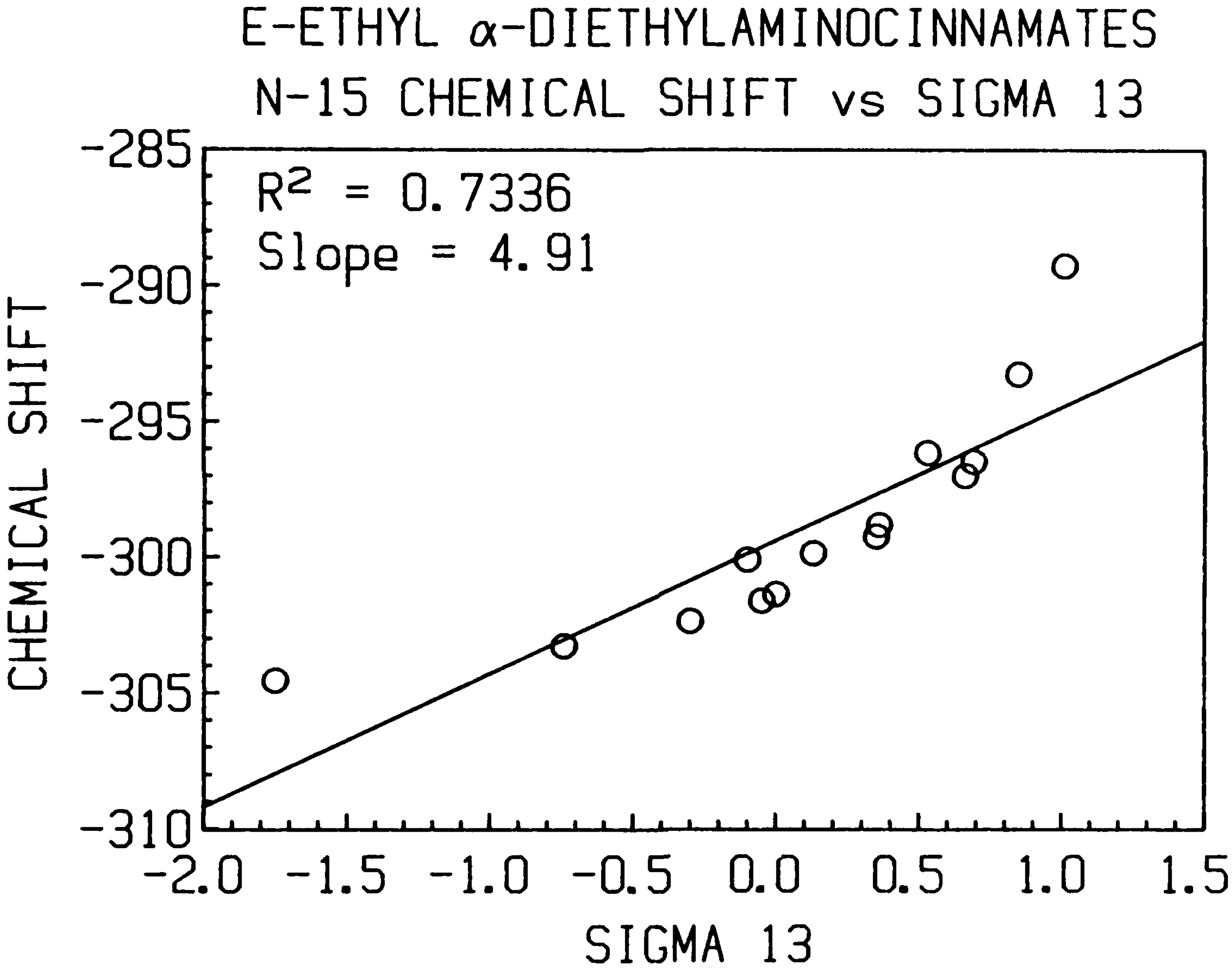
E-ETHYL α-DIETHYLAMINOCINNAMATES
N-15 CHEMICAL SHIFT vs SIGMA 13
R² = 0.7336
Slope = 4.91
CHEMICAL SHIFT
-285
-290
-295
-300
-305
-310
-2.0
-1.5
-1.0
-0.5
0.0
0.5
1.0
1.5
SIGMA 13

FIGURE 7c

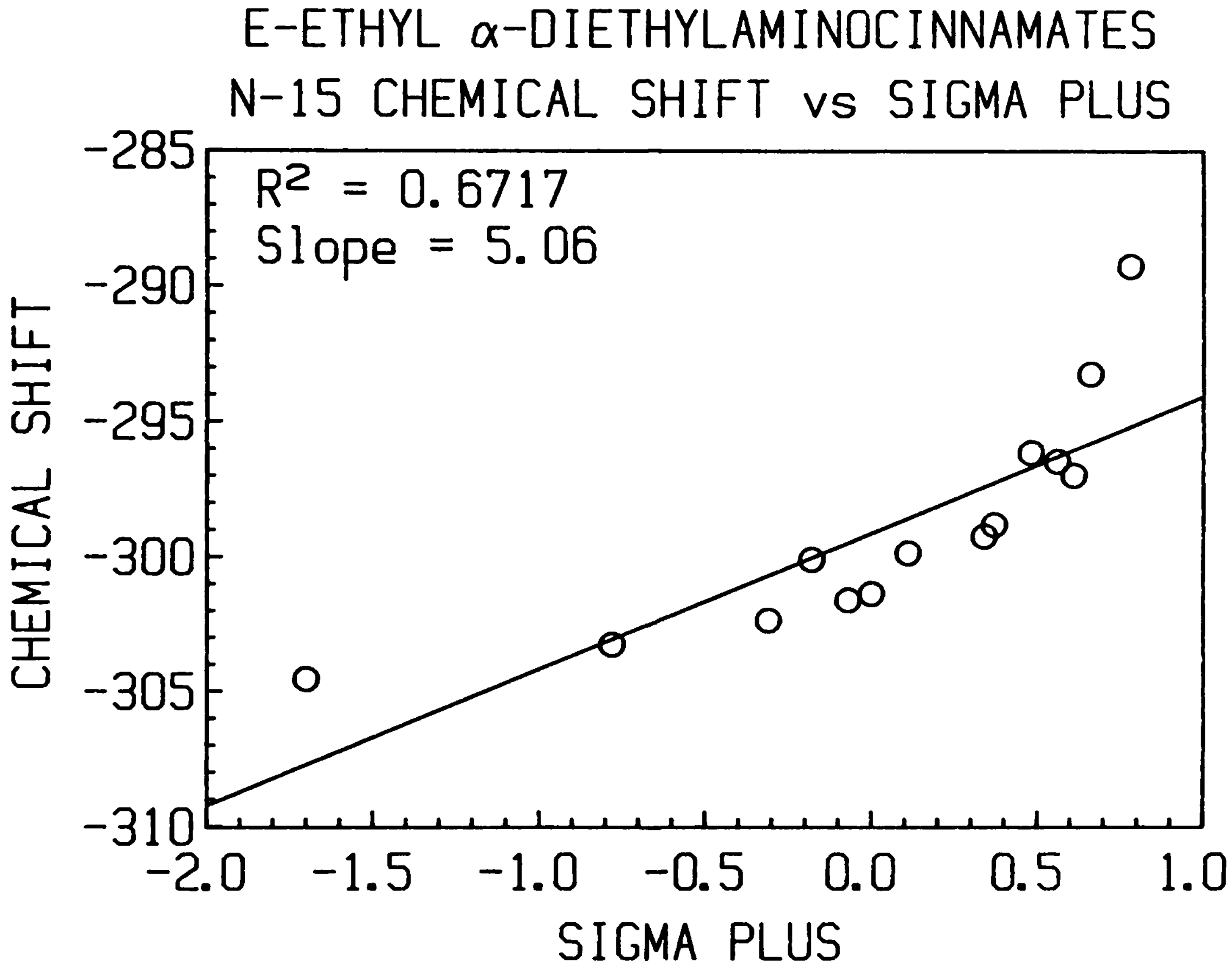
E-ETHYL α-DIETHYLAMINOCINNAMATES
N-15 CHEMICAL SHIFT vs SIGMA PLUS
R² = 0.6717
Slope = 5.06
CHEMICAL SHIFT
-285
-290
-295
-300
-305
-310
-2.0
-1.5
-1.0
-0.5
0.0
0.5
1.0
SIGMA PLUS

FIGURE 7d

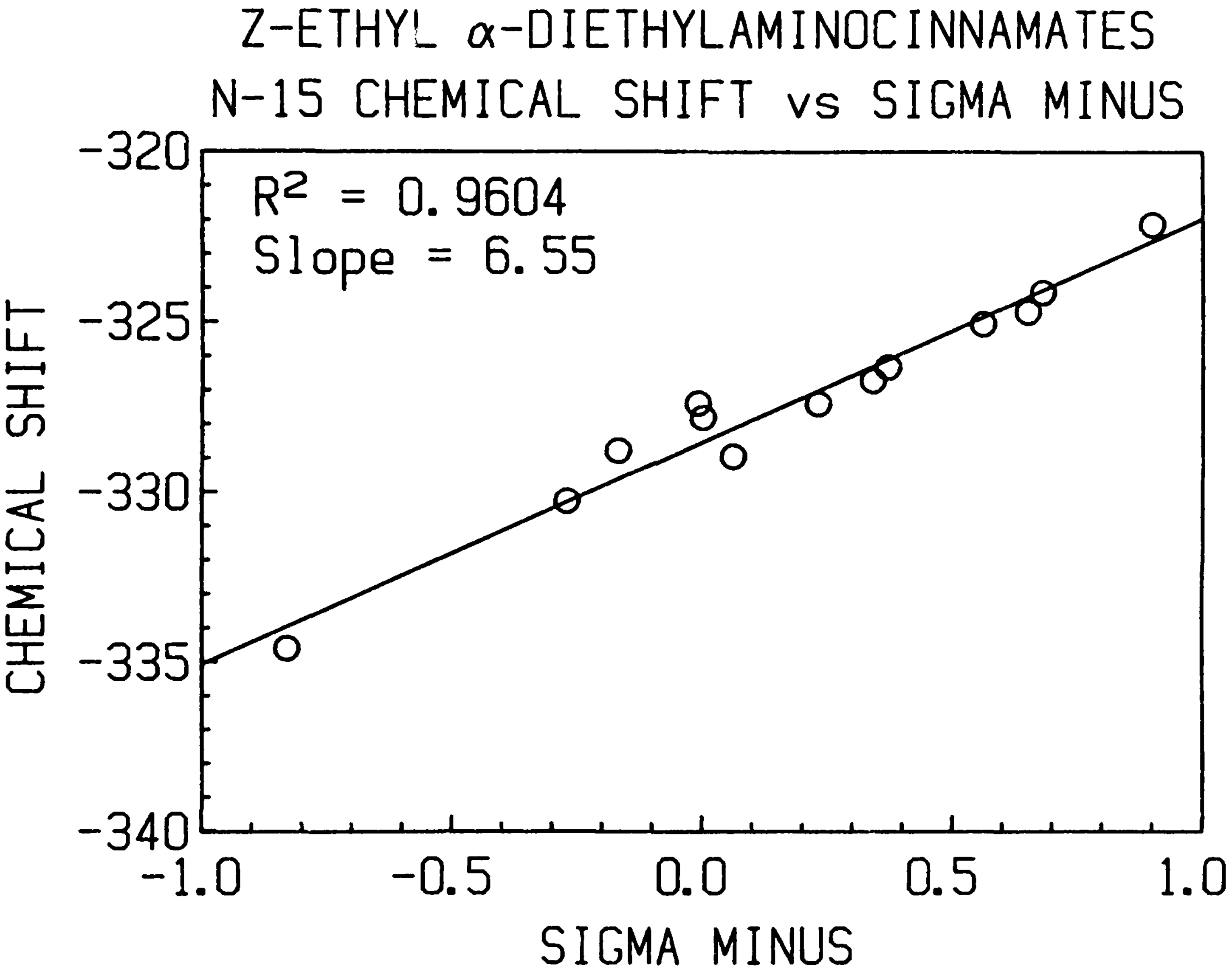
Z-ETHYL α-DIETHYLAMINOCINNAMATES
N-15 CHEMICAL SHIFT vs SIGMA MINUS
R² = 0.9604
Slope = 6.55
CHEMICAL SHIFT
-320
-325
-330
-335
-340
SIGMA MINUS
-1.0
-0.5
0.0
0.5
1.0

FIGURE 8a

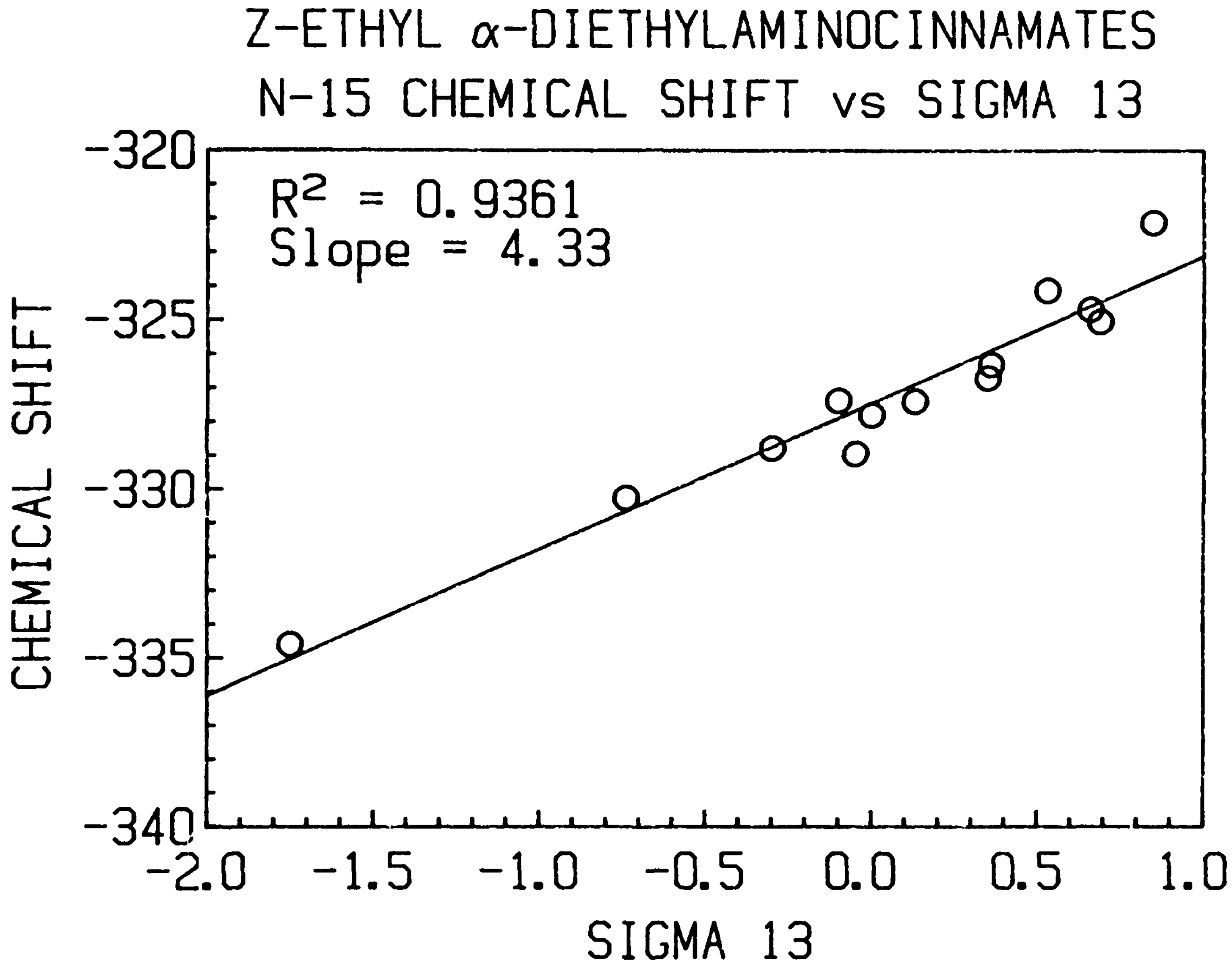
Z-ETHYL α-DIETHYLAMINOCINNAMATES
N-15 CHEMICAL SHIFT vs SIGMA 13
R² = 0.9361
Slope = 4.33
CHEMICAL SHIFT
-320
-325
-330
-335
-340
-2.0
-1.5
-1.0
-0.5
0.0
0.5
1.0
SIGMA 13

FIGURE 8b

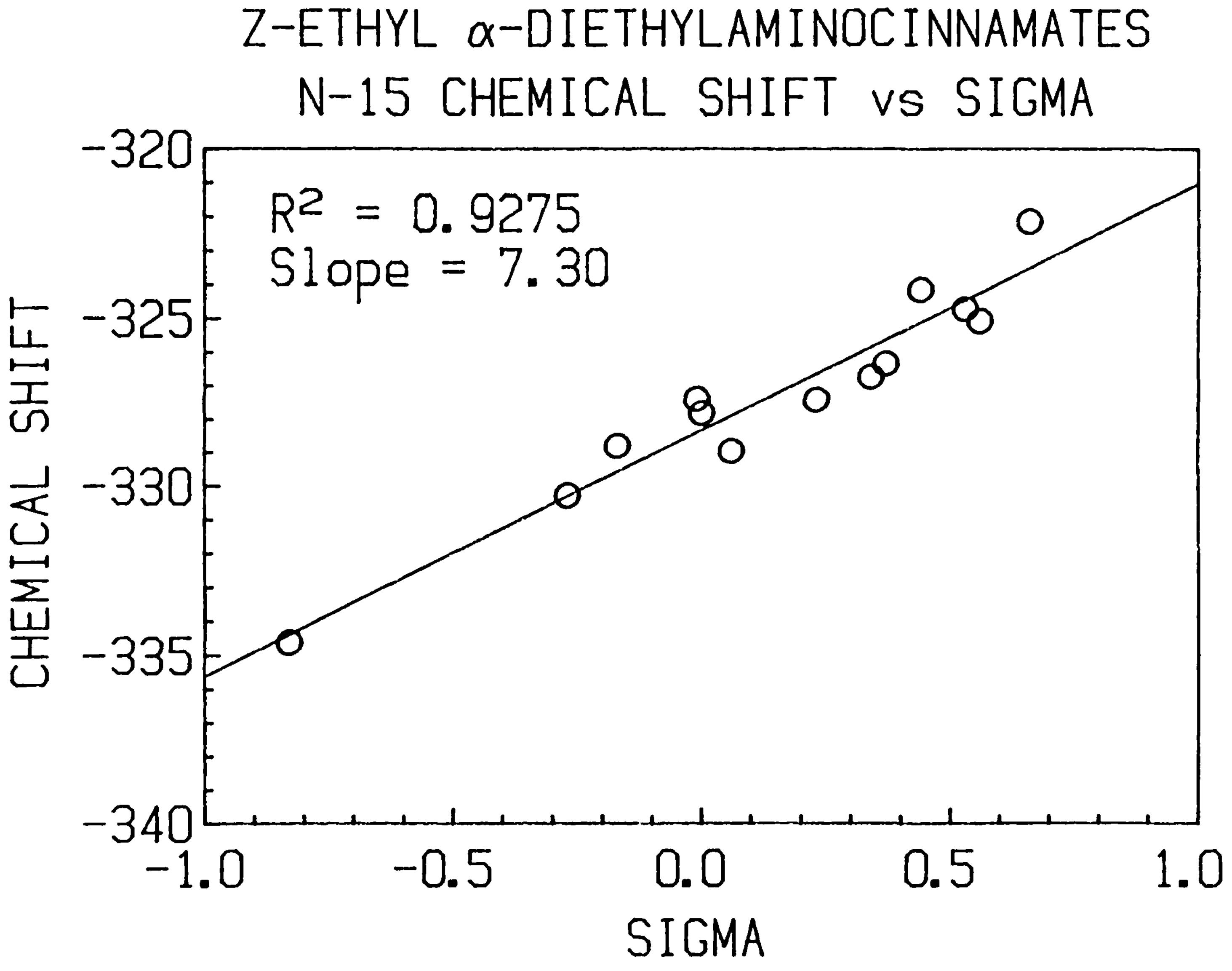
Z-ETHYL α-DIETHYLAMINOCINNAMATES
N-15 CHEMICAL SHIFT vs SIGMA
R2 = 0.9275
Slope = 7.30
CHEMICAL SHIFT
-320
-325
-330
-335
-340
-1.0
-0.5
0.0
0.5
1.0
SIGMA

FIGURE 8c

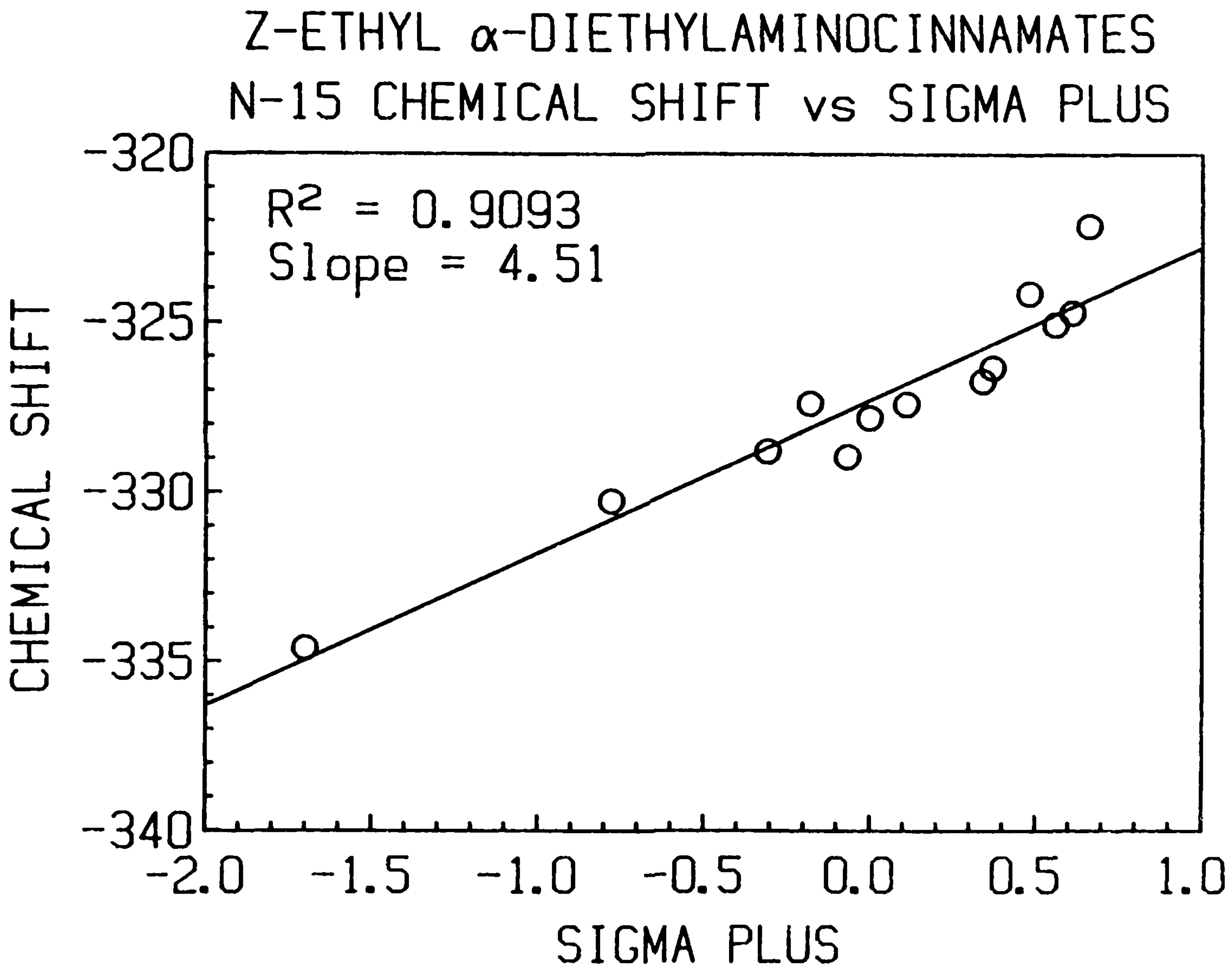
Z-ETHYL α-DIETHYLAMINOCINNAMATES
N-15 CHEMICAL SHIFT vs SIGMA PLUS
R² = 0.9093
Slope = 4.51
CHEMICAL SHIFT
-320
-325
-330
-335
-340
SIGMA PLUS
-2.0
-1.5
-1.0
-0.5
0.0
0.5
1.0

FIGURE 8d

To compare as precisely as possible the correlative behavior of the E and Z isomers, the E isomer was also plotted without its p-NO_2 data point (Figure 9a-d, pages 102-105). In this fashion, plots of 13 common substituents could be compared directly. The results for both isomers are shown in Table 14.

Table 14

Series A Correlations From Figures 9 and 8

E Isomer Hammett Scale	E Isomer R^2	E Isomer Slope	E Isomer Relative Fit	Z Isomer Hammett Scale	Z Isomer R^2	Z Isomer Slope	Z Isomer Relative Fit
σ^-	.9166	6.55	100%*	σ^-	.9604	6.55	100%*
σ^{13}	.8874	4.07	96.81%	σ^{13}	.9361	4.33	97.46%
σ	.8443	7.13	92 [illegible]	σ	.9275	7.30	96.57%
σ^+	.7483	4.19	81.64%	σ^+	.9093	4.51	94.68%

*Relative fits of substituent scales compared to best fit (100%) (listed in descending order)

1) Summary of the Data

General conclusions based on the above compilations were:

1. The σ^- scale gave the best correlation for both isomers. In the E isomer, it made more of an improvement relative to the other scales.

2. The Z isomer gave by far the better correlation behavior; all four scales are at least above 0.9 for R^2. For the E isomer, the correlative behavior is inferior.

3. The σ^+ scale gave the worst correlation in both isomers.

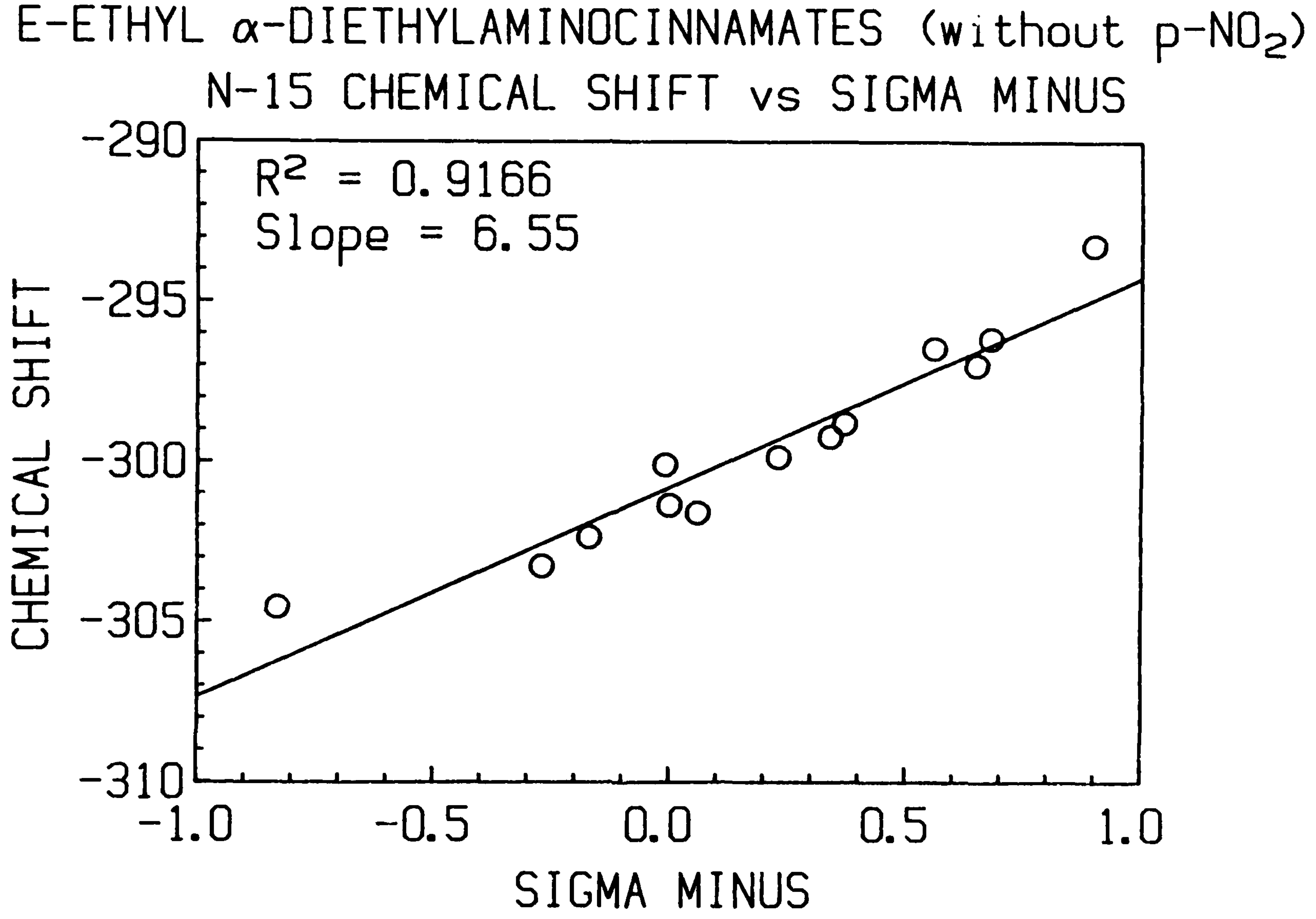
E-ETHYL α-DIETHYLAMINOCINNAMATES (without p-NO₂)
N-15 CHEMICAL SHIFT vs SIGMA MINUS
R² = 0.9166
Slope = 6.55
CHEMICAL SHIFT
-290
-295
-300
-305
-310
-1.0
-0.5
0.0
0.5
1.0
SIGMA MINUS

FIGURE 9a

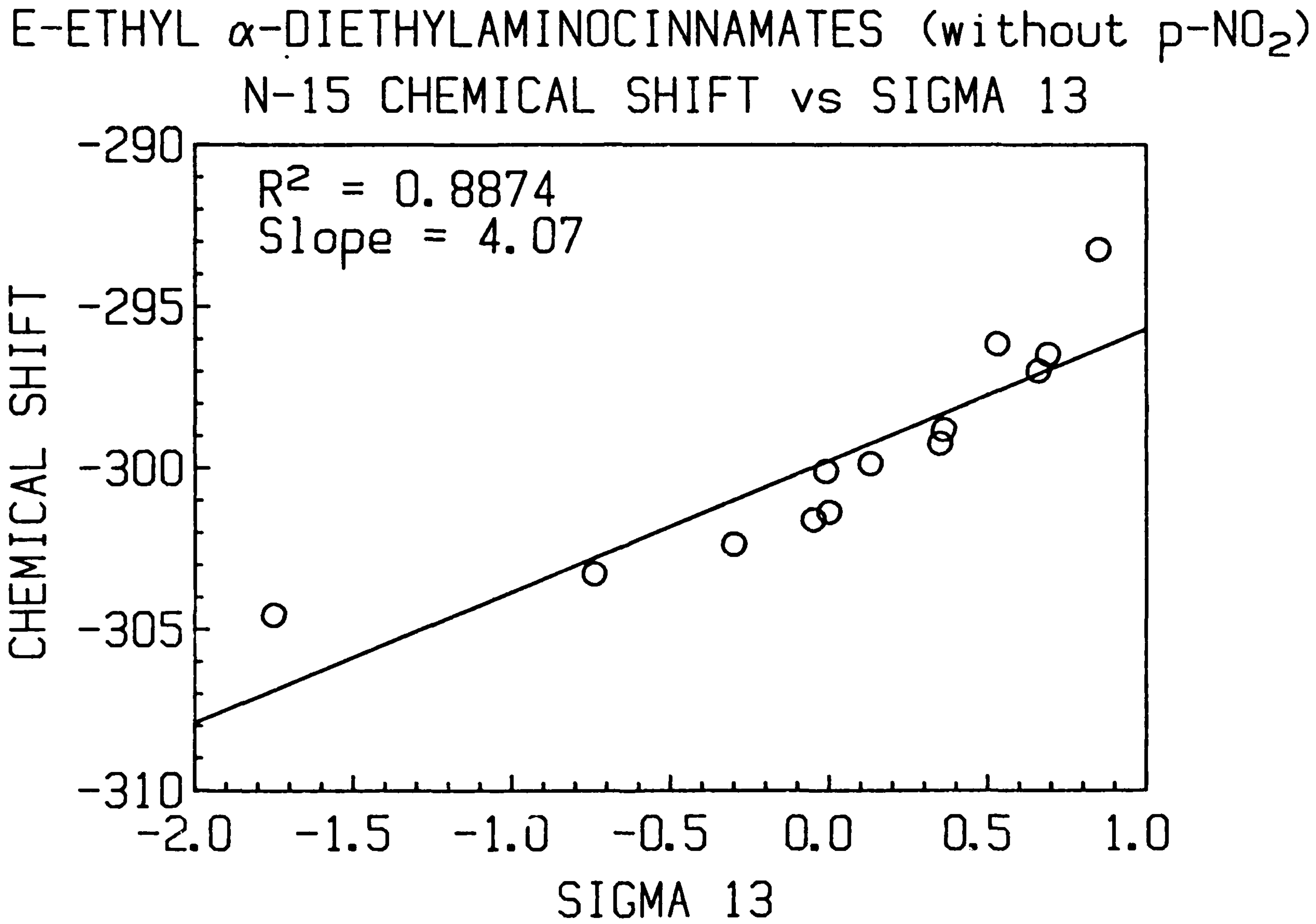
E-ETHYL α-DIETHYLAMINOCINNAMATES (without p-NO_2)
N-15 CHEMICAL SHIFT vs SIGMA 13
R^2 = 0.8874
Slope = 4.07
CHEMICAL SHIFT
-290
-295
-300
-305
-310
-2.0
-1.5
-1.0
-0.5
0.0
0.5
1.0
SIGMA 13

FIGURE 9b

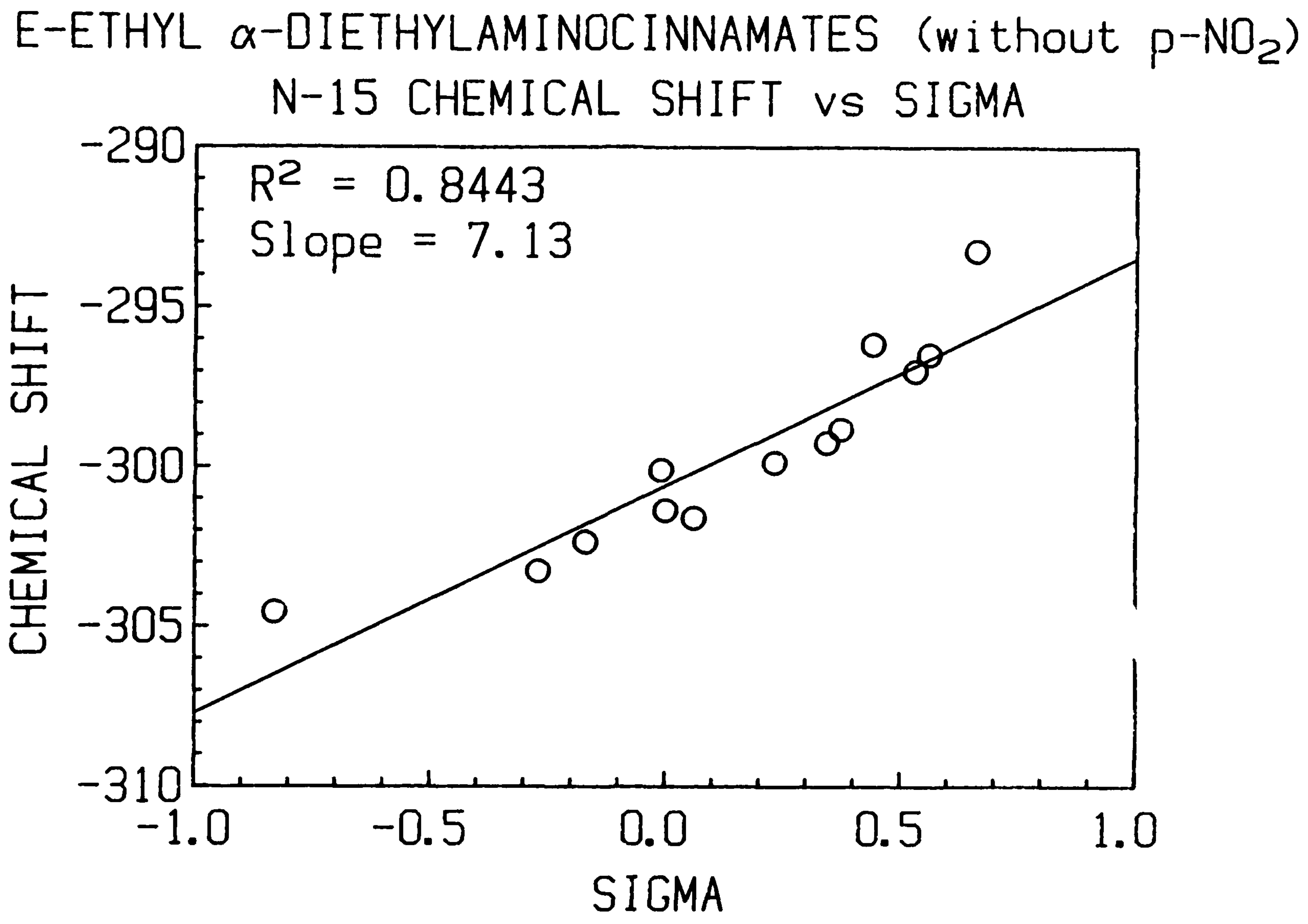
E-ETHYL α-DIETHYLAMINOCINNAMATES (without p-NO₂)
N-15 CHEMICAL SHIFT vs SIGMA
R² = 0.8443
Slope = 7.13
CHEMICAL SHIFT
-290
-295
-300
-305
-310
SIGMA
-1.0
-0.5
0.0
0.5
1.0

FIGURE 9c

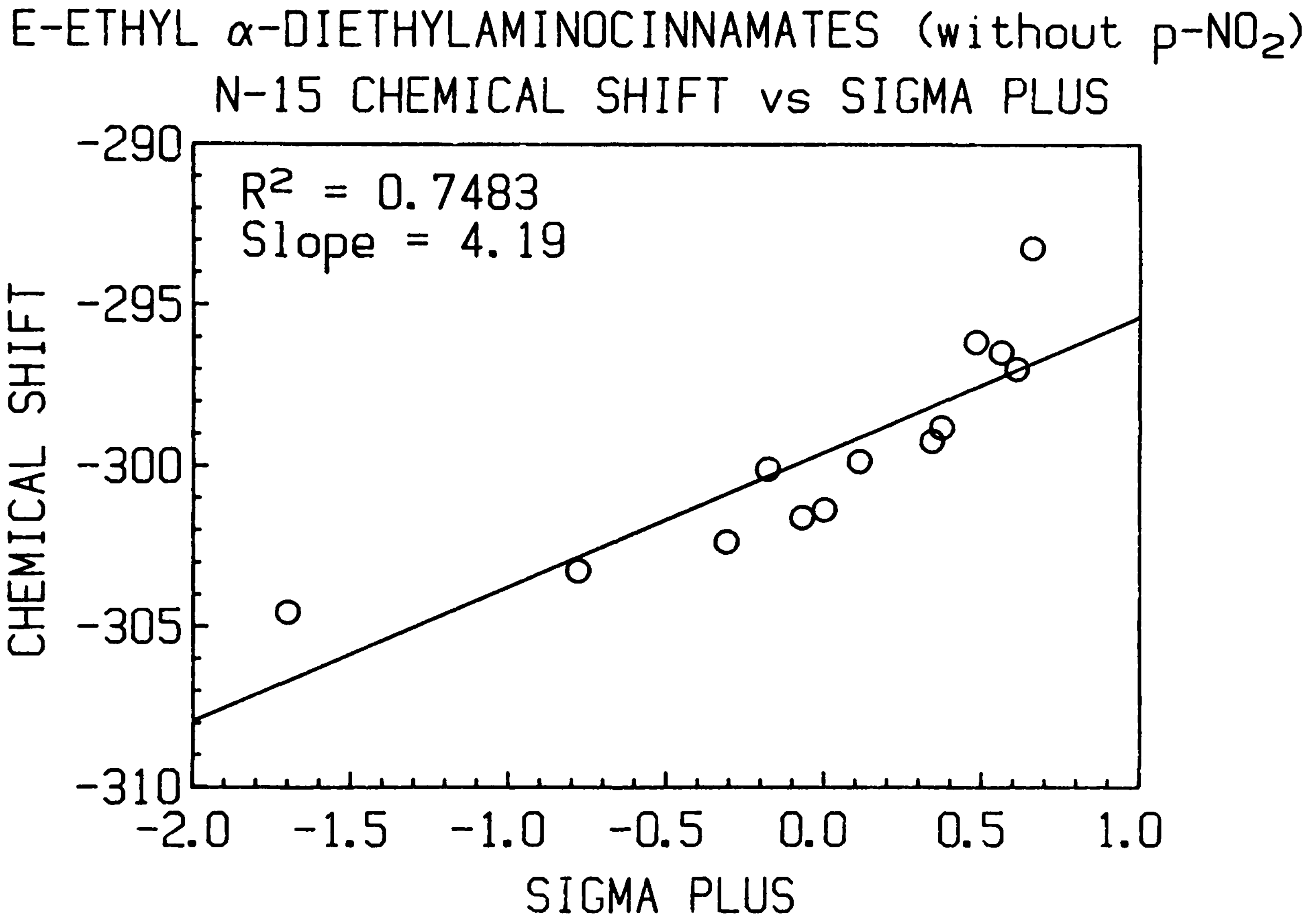
E-ETHYL α-DIETHYLAMINOCINNAMATES (without p-NO2)
N-15 CHEMICAL SHIFT vs SIGMA PLUS
R2 = 0.7483
Slope = 4.19
CHEMICAL SHIFT
-290
-295
-300
-305
-310
-2.0
-1.5
-1.0
-0.5
0.0
0.5
1.0
SIGMA PLUS

FIGURE 9d

4. Positive slopes were observed (greater deshielding with increase in Hammett constant).

2) Interpretation of the Results

a) Positive Slope

The positive slopes observed for the ^{15}N δ's in the E and Z enamine isomers indicated that N, like F, interacts with the styryl system such that the through-resonance effect observably takes precedence over the π-polarization mechanism. (Otherwise, a negative slope would be expected.) Interestingly, the ^{19}F SCS range in the ethyl α-fluorocinnamates (page 33) was equivalent to the ^{15}N SCS range observed in Series A. (≈ 12 ppm).

b) Superiority of σ^- Correlations

The clearly superior fits using the σ^- substituent scale indicated the importance of the through-resonance phenomenon in accounting for ^{15}N chemical shift behavior for strongly electron withdrawing X:

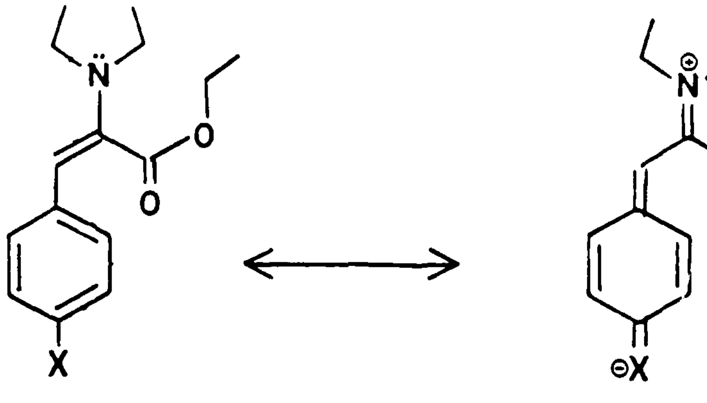

XLIXA

particularly
important
resonance
forms

X = strongly e^- withdrawing by resonance

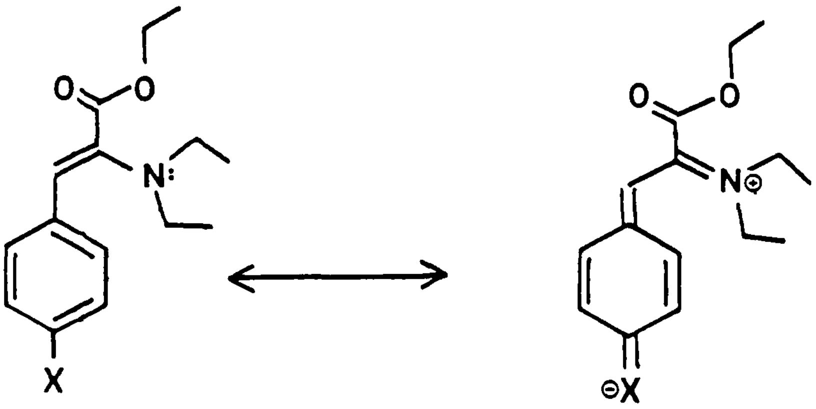

particularly
important
resonance
forms

XLIXB

X = strongly e^- withdrawing by resonance

akin to the through-resonance effect invoked in the classical derivation of the σ^- scale:[53]

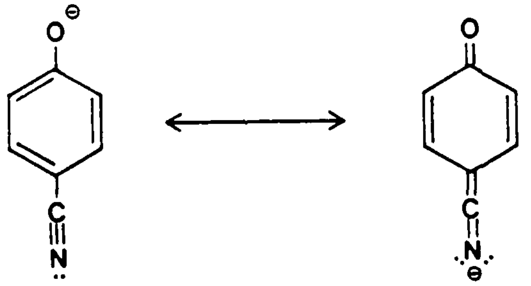

This is also consistent with the results of Krabbenhoft with β, β-dichlorostyrenes (LXXVII) [57],

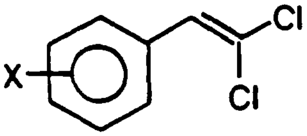

LXXVII

where the σ^- scale was argued to give superior correlations compared to σ and σ^+ due to through-resonance from the unshared electron pairs on Cl (LXXVIII):

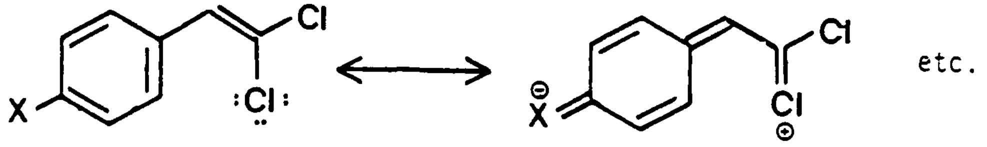

LXXVIII

In addition, Taft et al. have, more recently, included the σ^- and σ_R^- single and dual substituent resonance scales in their evaluation of substituent solvation assisted resonance (SSAR) effects in para substituted anilines (LXXIX):[58]

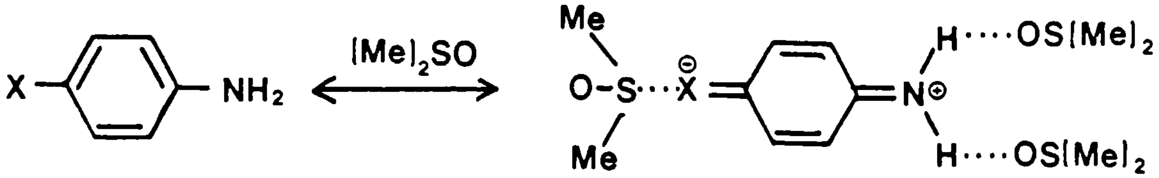

III

LXXIX

In the same vein, it is logical that σ^+ would give the worst-case correlation—the $N(Et)_2$ probe site being, conversely, a poor (and, in fact, unqualified, being a second period element) candidate for electron acceptance by through-conjugation (LXXX):

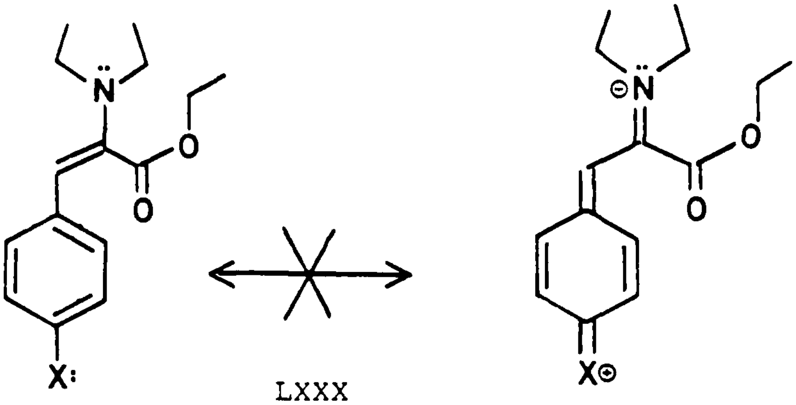

LXXX

b. The E/Z Isomer Correlations/A Closer Look

A classic and ironic attribute of Hammett substituent plots was asserted with a closer inspection of these enamine isomer correlations: their greatest value can sometimes be derived from obvious deviations from linearity. It became apparent that the nature of correlation errors was very different in the two isomers in going from the best to the worst fit. For the Z isomer, the general error appeared to be a random one; basically a greater +/- scatter about the least squares line (shotgun resemblance). For the E isomer, the error appeared to be more determinate, resulting in a more accentuated concave upwards deviation in going from σ^- through to σ^+. (A determinate error will, statistically, have more of a deleterious effect.) This kind of plot implied a change within this substituent range in the way electronic effects were being transmitted, as reflected in the relative shieldings of the nitrogen atom.

The markedly greater deshielding of the ^{15}N δ for the E isomer, however, appeared inconsistent with the poorer correlations obtained with this isomer compared to its Z counterpart. The fact that such a greater deshielding existed inferred a greater interaction between the substituent and the diethylamino moiety. An answer to this seeming contradiction would be any factor that could cause a considerable but unbalanced interference within the substituent series. Two structural variables that could have factored in this E/Z correlation contrast were the relative steric encumbrance of the $N(Et)_2$ moiety and the directionality of the enone resonance form (stemming from the ethyl carboxylate function.) This can be more carefully scrutinized by a closer examination of the E correlations.

c. The E Correlation

An inspection of these correlations (Figure 10a-d, pages 112-115) implied the increasing contribution (from σ^- to σ^{13} to σ to σ^+) of two separate lines of quite different slopes: a steep slope (solid line) and a gradual slope (dashed line). The strong in-line through resonance of the N in the E isomer nicely accounts for this accentuated positive slope of the solid line:

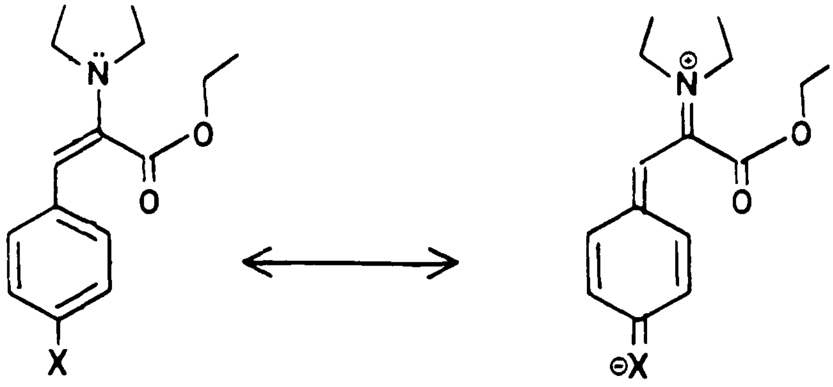

XLIXA

In addition, the $N(Et)_2$ is subject to the full electron withdrawing inductive effect of the CO_2Et group.

For electron-donating substituents, however, something changes (the dashed lines, Figure 10a-d); as X becomes more electron donating (going from right to left), the N atom does not take on electron density as one would expect based on the earlier slope of the correlation. Some factor is preventing the "predicted" greater shielding of the nitrogen atom.

This factor could be related to the considerable difference between the E and Z isomers of the steric encumbrance of the $N(Et)_2$ moiety. Molecular models suggest that the E isomer $N(Et)_2$ is more capable of optimal coplanar deshielding alignment of the methylene carbons attached to the nitrogen atom due to greater conformational freedom. In contrast, the Z isomer $N(Et)_2$ group experiences greater steric hindrance to such an alignment. These postulations were borne out by the ^{13}C correlation data for the $N(Et)_2$ methylene carbons of each isomer, where only those for the E isomer displayed any detectable deshielding trend through the substituent series (see page 187).

This greater conformational freedom of the $N(Et)_2$ moiety of the E isomer provides a means of causing a discernable differential effect of the N shieldings within this substituent series. For X = e^- withdrawers, optimal deshielding alignment is possible. (Note also the deshielding influence of the enone structure.) This corresponds to the steep-sloped solid lines:

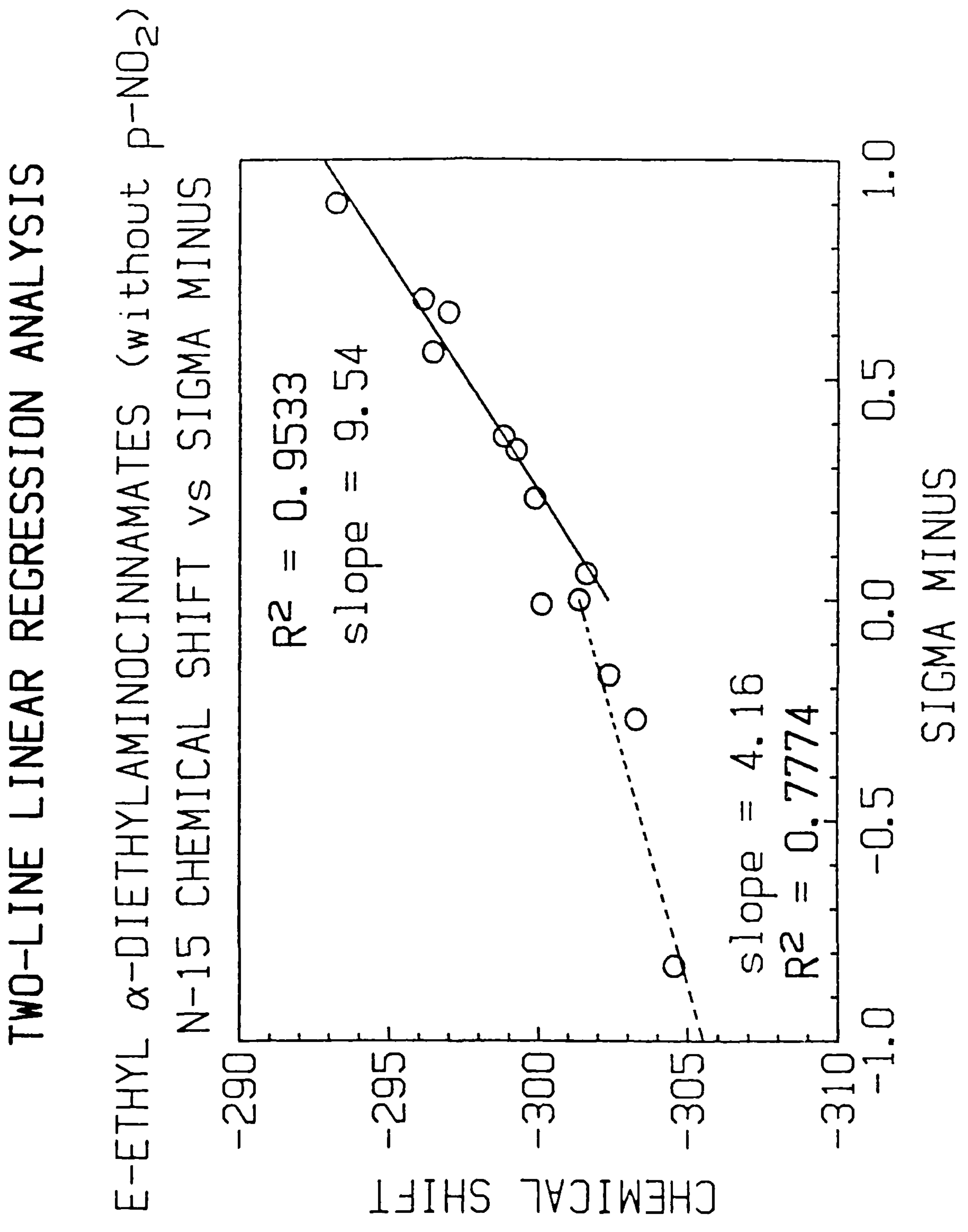
TWO-LINE LINEAR REGRESSION ANALYSIS
E-ETHYL α-DIETHYLAMINOCINNAMATES (without p-NO$_2$)
N-15 CHEMICAL SHIFT vs SIGMA MINUS
R^2 = 0.9533
slope = 9.54
slope = 4.16
R^2 = 0.7774
CHEMICAL SHIFT
-290
-295
-300
-305
-310
SIGMA MINUS
-1.0
-0.5
0.0
0.5
1.0

FIGURE 10a

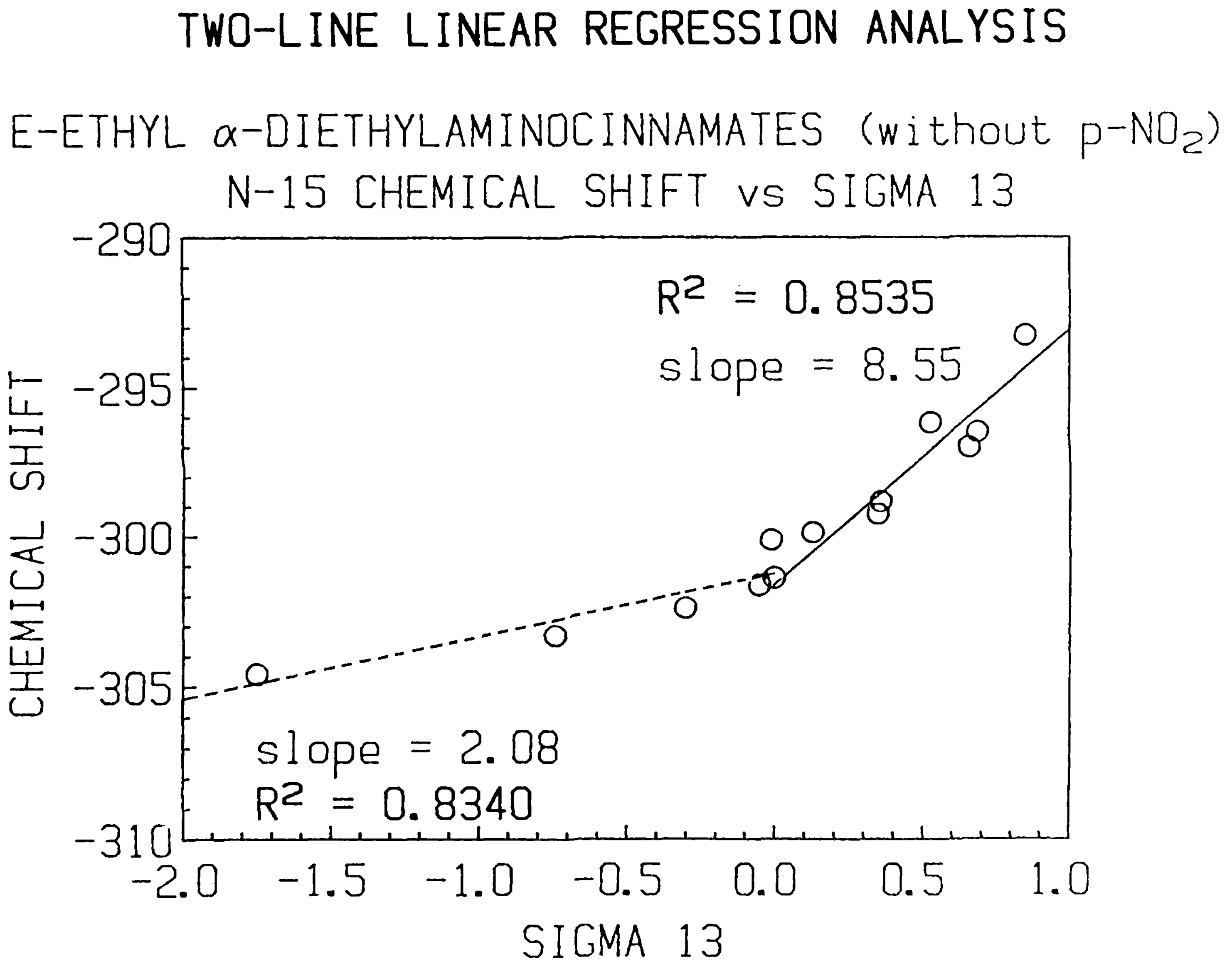
TWO-LINE LINEAR REGRESSION ANALYSIS
E-ETHYL α-DIETHYLAMINOCINNAMATES (without p-NO_2)
N-15 CHEMICAL SHIFT vs SIGMA 13
R^2 = 0.8535
slope = 8.55
slope = 2.08
R^2 = 0.8340
CHEMICAL SHIFT
-290
-295
-300
-305
-310
-2.0
-1.5
-1.0
-0.5
0.0
0.5
1.0
SIGMA 13

FIGURE 10b

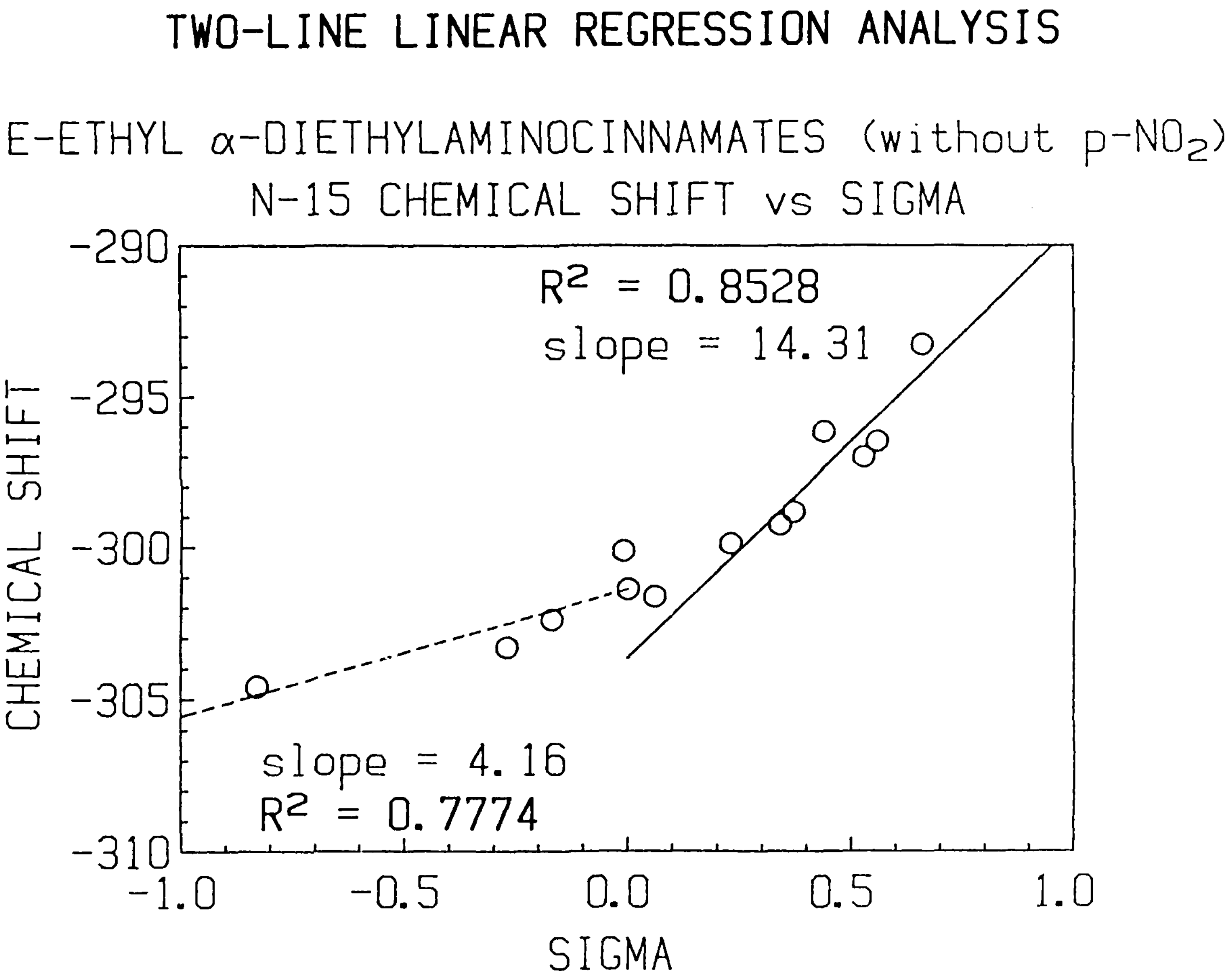

TWO-LINE LINEAR REGRESSION ANALYSIS

E-ETHYL α-DIETHYLAMINOCINNAMATES (without p-NO_2)

N-15 CHEMICAL SHIFT vs SIGMA

FIGURE 10c

TWO-LINE LINEAR REGRESSION ANALYSIS

E-ETHYL α-DIETHYLAMINOCINNAMATES (without p-NO_2)

N-15 CHEMICAL SHIFT vs SIGMA PLUS

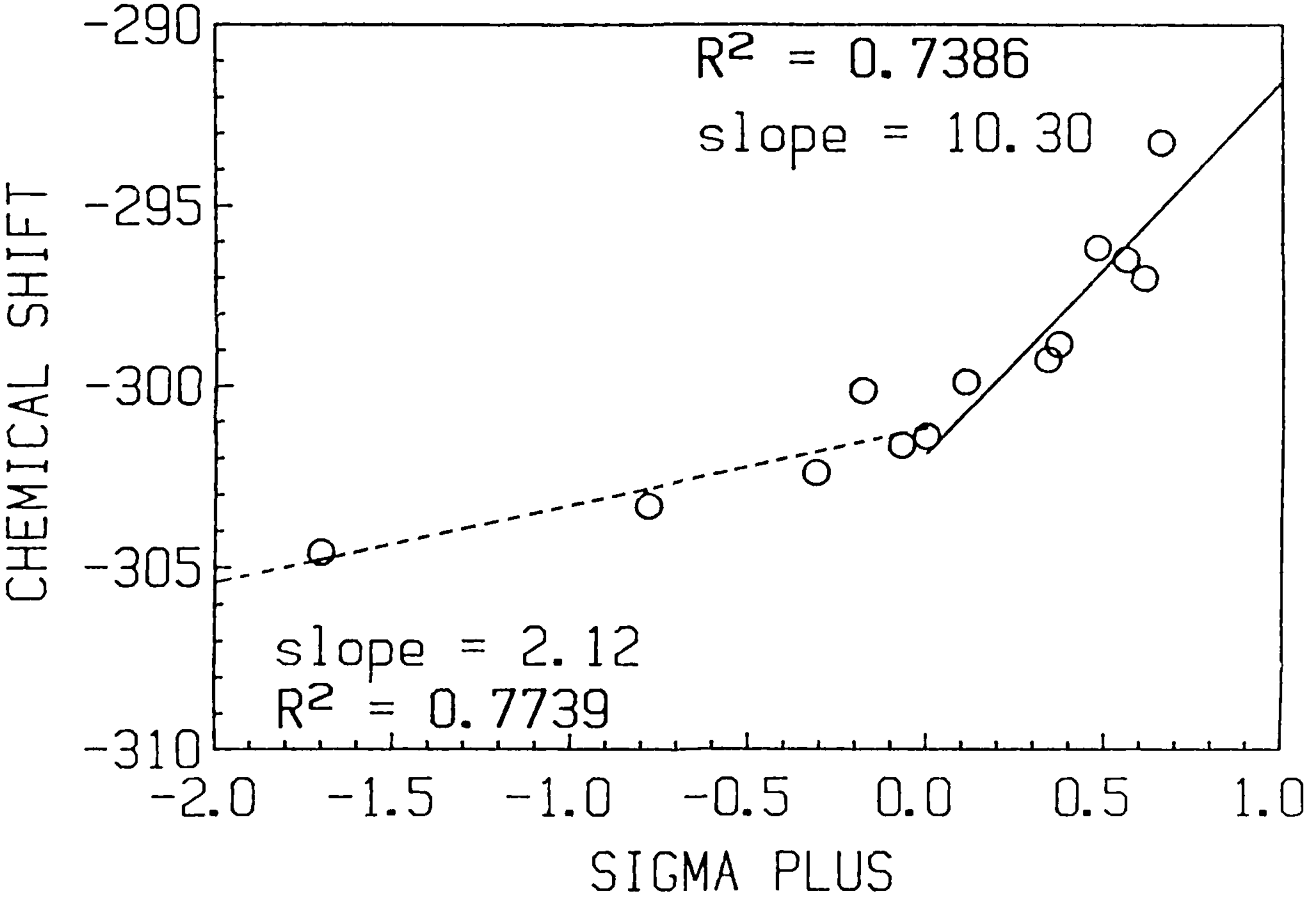

FIGURE 10d

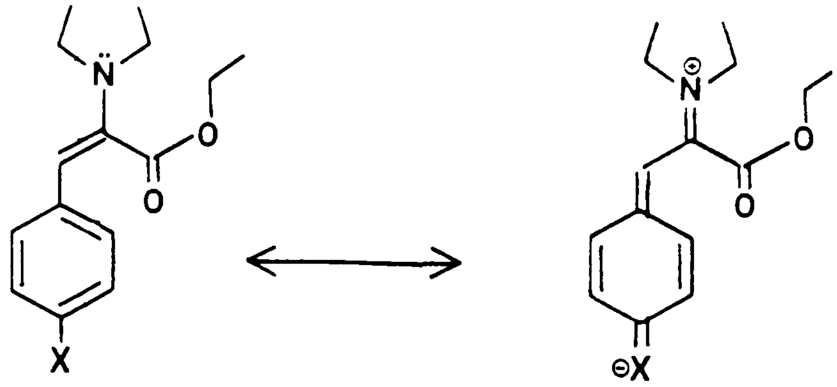

XLIXA

However, when considering the resonance structures derived from $X = e^-$ donors (particularly that with the negative charge on the enolate carbon),

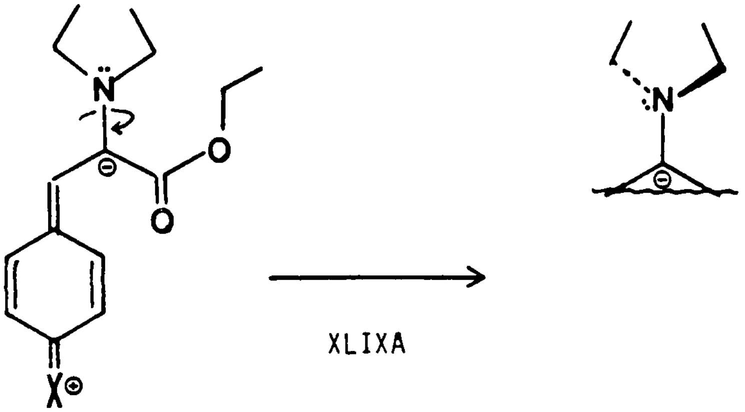

XLIXA

this same conformational freedom of the $N(Et)_2$ allows an out-of-styryl -plane twist to minimize electronic repulsion with the unshared electron pair. This conversion of the $N(Et)_2$ unshared electron pair to a more orthogonal conformation relative to the styryl system could measureably reduce the relative shielding of the N atom, as observed corresponding to the lower-sloped (dashed) lines. The key here is a substantial change in conformational alignment of the $N(Et)_2$ group within this substituent series, resulting in the concave upward determinate error.

d. The Z Correlation

It is more difficult to account for the Z isomer's better correlative behavior. The error is more random in nature, indicating no (dramatic) change in mechanism of transmittance of electronic effects through the series. The chemical shift range for electron withdrawing groups is somewhat greater for the E isomer (8.13 ppm between H and p-CN for E versus 5.67 ppm for the same range in the Z) consistent with somewhat reduced through conjugation for the nitrogen in the out-of-line Z orientation:

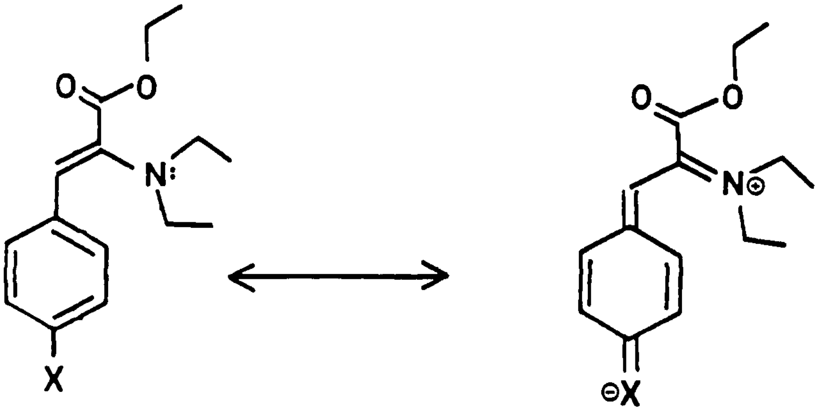

XLIXB

Somewhat reduced over E isomer

However, for the Z isomer correlation, no sudden levelling out of the line occurs with electron donating groups, indicating that in this configuration, the N is better able to take on electron density from the styryl system for electron donors. The increased shielding more closely matches that predicted by the electron withdrawing data points.

Molecular models suggest an out-of-styryl-plane twist of the $N(Et)_2$ moiety in the Z configuration even for e^- withdrawers due to the greater steric encumbrance experienced by this group than in the E configuration. Recall that the Alchemy® conformational energy program called for the phenyl ring to twist out of plane. In either case, the steric impact of the $N(Et)_2$ is evident. The lower SCS range observed for electron withdrawers, as discussed above, is also consistent with this concept. However, this would also cause less of a discernable effect on the relative shieldings of the $\underline{N}(Et)_2$ nitrogen atom as a result of the enolate resonance forms stemming from X = e⁻ donors:

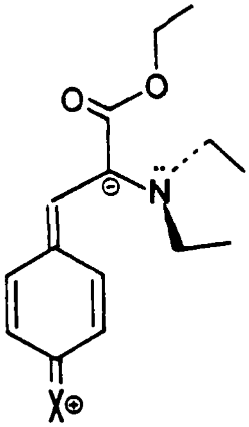

XLIXB

With the N already twisted out of plane, the impact of the adjacent negative charge center could be lessened to the point where a clear determinate error (as seen in the E isomer correlation) could not be observed. This point of view argues for the relative steric effects of the $N(Et)_2$ moiety in the E and Z isomers to be the primary influence on their correlative behavior, rather than molecular "in-line" or "out-of-line" styryl orientation, as suggested earlier.

The carboxylate function may play a secondary role in the E/Z correlation contrast for Series A. In the E configuration, the deshielding effect of the enone carbonyl

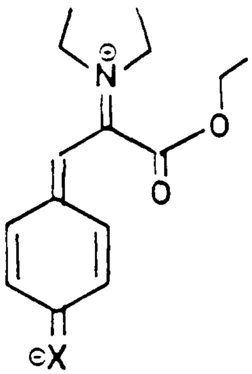

XLIXA

augments that of the styryl system since they are aligned in parallel fashion. This enhanced deshielding of the $N(Et)_2$ nitrogen could further accentuate the determinant error.

For the Z isomer, the analogous enone structure

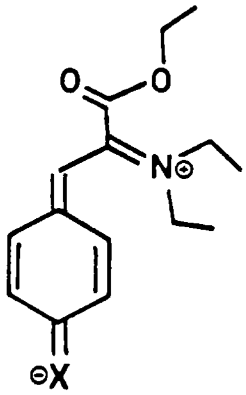

XLIXB

acts in a direction nonaligned with the styryl system, probably reducing its deshielding influence *relative to that in the E isomer*. Additionally, the presence of the *cis* vinylic H could have had a slight attenuating effect on the e^- withdrawing power of the CO_2Et group. This reduced deshielding effect of the CO_2Et, which also by default would allow a more *direct* influence of the substituent on the N shieldings, could have been another factor leading to the better Z correlation.

Several follow-on studies could help clarify the roles of the CO_2Et (electronic) and $N(Et)_2$ (steric) functional groups on the E/Z correlation contrast. β-diethylaminostyrenes could be studied, which would be independent of the influence of the CO_2Et group. Also, ethyl aminocinnamates could be examined which would be free of the steric factors exaggerated in the $N(Et)_2$ moiety.

e. Secondary Effects/Proximity of the $N(Et)_2$ to the Phenyl Substituent

An additional factor that may have played some role in the E/Z isomer contrast was the relative proximity of the $N(Et)_2$ nitrogen to the phenyl substituent in each isomer. Molecular models indicate that the distance from the nitrogen atom to the substituent is about 13% longer in the E versus Z isomer. This would render the nitrogen atom in the Z isomer more susceptible to X's effect by a direct through-space pathway, and thus could also partially account for Z's better correlation; X is exerting more influence on the nitrogen by virtue of nitrogen's position, which is a constant factor in the isomer series.

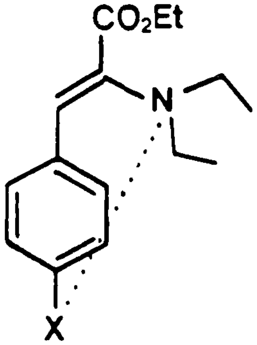

XLIXB

direct through-space pathway

As a corollary to this argument, the CO_2Et group is more out of the way spatially in the Z isomer between $N(Et)_2$ and X:

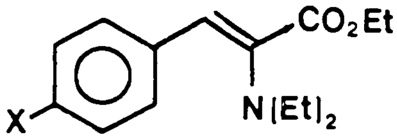

XLIXB

while in the E isomer, it is in more of an intruding position sterically, as well as electronically:

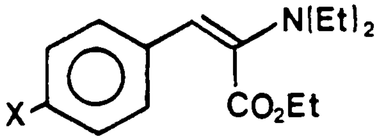

XLIXA

It needs to be stressed that these are strictly secondary effects, of a much weaker/tenuous nature, and may not be factors at all in accounting for the isomer correlation contrast. However, these arguments are consistent with what is observed and were felt worthy of at least cursory mention.

2. Series B

Table 15 lists the ^{15}N δ's for this series of compounds.

Table 15

^{15}N Chemical Shifts*/Series B

X	$^{15}N\delta$
p-N(Me)$_2$	-140.523
p-OMe	-141.770
p-Me	-141.416
p-F	-142.238
H	-141.700
p-Cl	-142.259
m-F	-142.261
p-CO$_2$Me	-141.823
p-CN	-142.429
p-NO$_2$	-142.570

*Upfield from internal CD_3NO_2

a. Summary of the Data

The overall correlative behavior was in obvious contrast to that obtained for Series A: (Figure 11, pages 123-126).

Table 16

Series B Correlations From Figure 11

Hammett Scale	R^2	Slope	Relative Fit*
σ	.8016	-1.14	100.00%
σ^{13}	.7840	-0.66	97.80%
σ^{+}	.7749	-0.72	96.67%
σ^{-}	.6923	-0.83	86.36%

*relative fits of substituents scales compared to best fit (100%).
(listed in descending order)

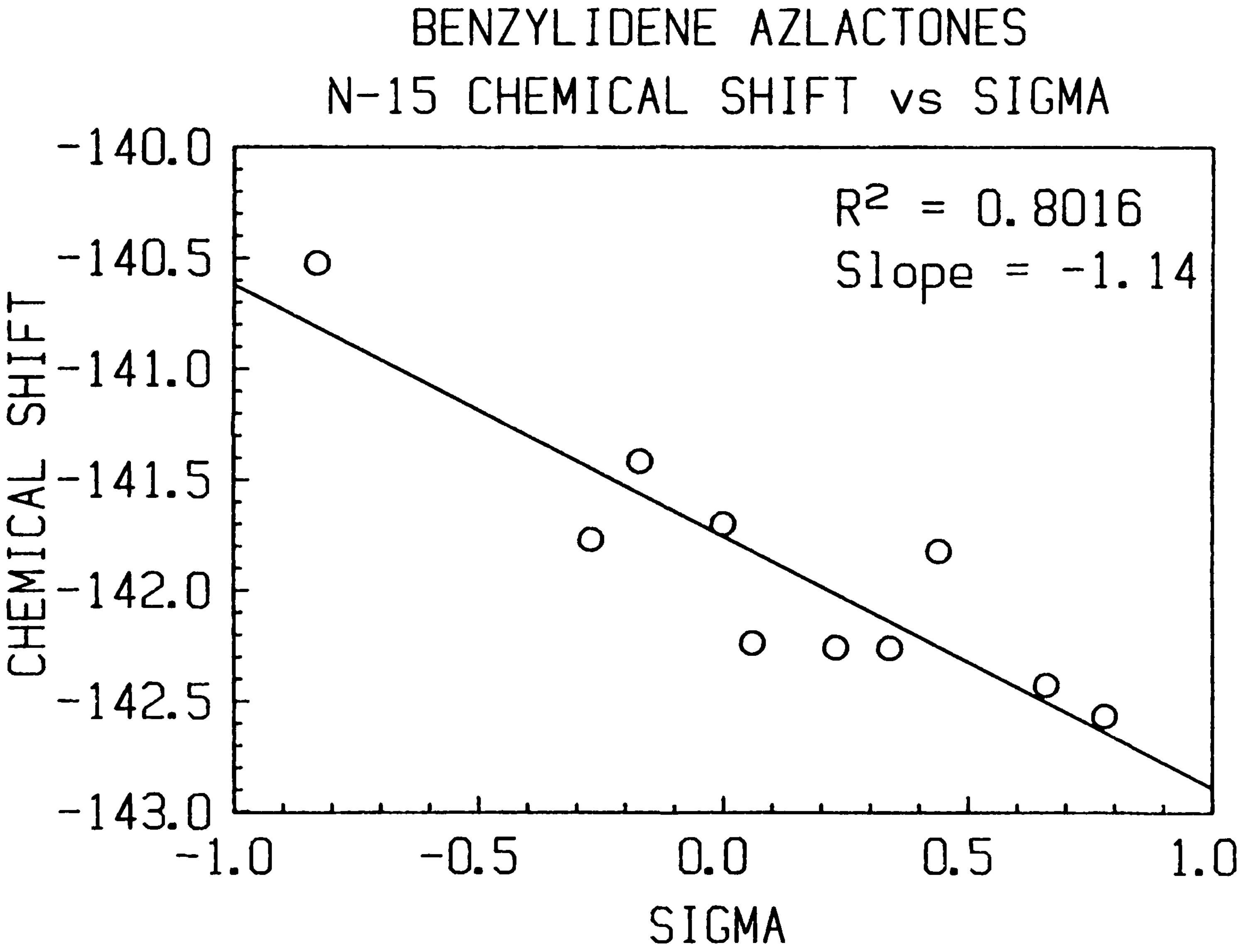
BENZYLIDENE AZLACTONES
N-15 CHEMICAL SHIFT vs SIGMA
R² = 0.8016
Slope = -1.14
CHEMICAL SHIFT
-140.0
-140.5
-141.0
-141.5
-142.0
-142.5
-143.0
-1.0
-0.5
0.0
0.5
1.0
SIGMA

FIGURE 11a

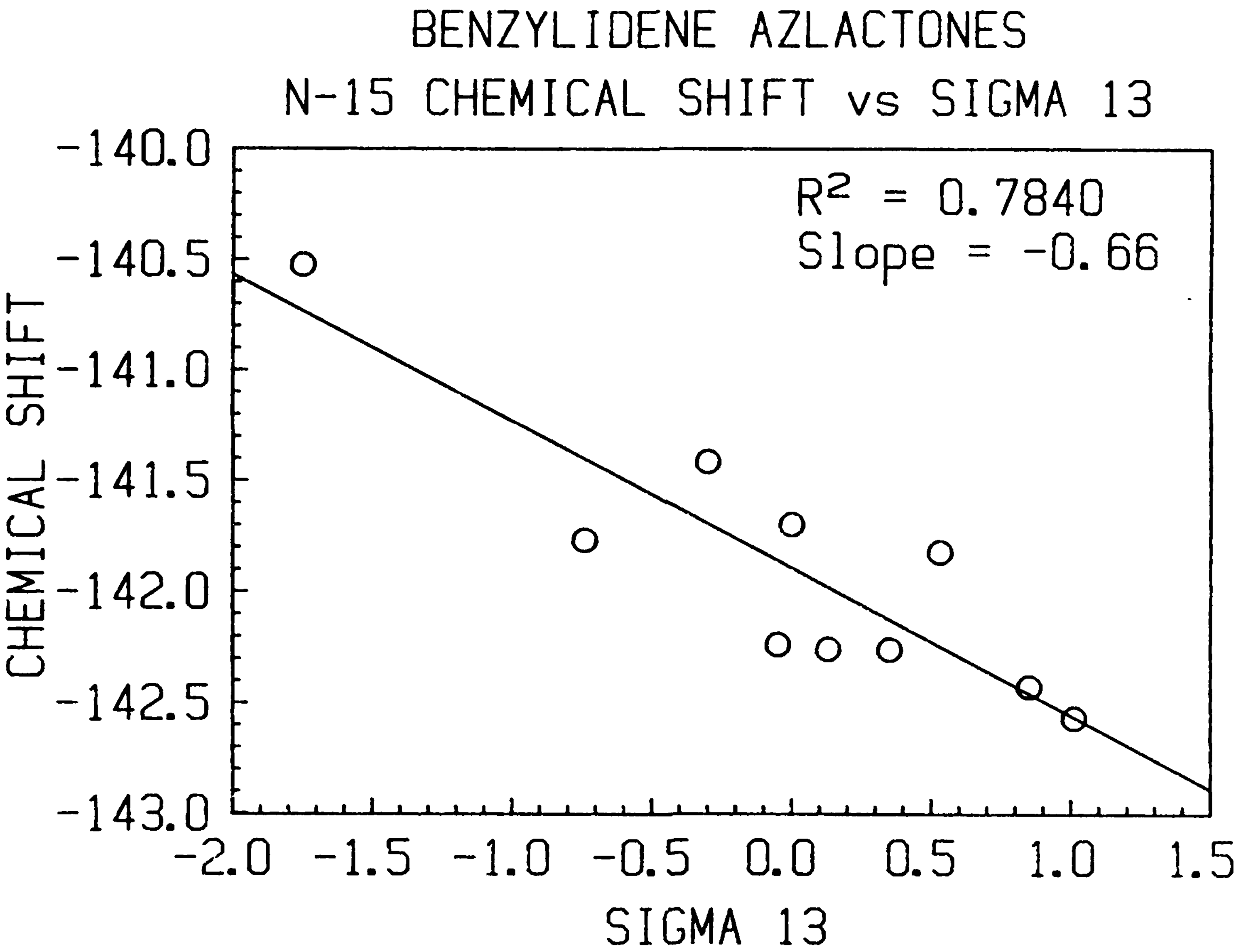
BENZYLIDENE AZLACTONES
N-15 CHEMICAL SHIFT vs SIGMA 13
R^2 = 0.7840
Slope = -0.66
CHEMICAL SHIFT
-140.0
-140.5
-141.0
-141.5
-142.0
-142.5
-143.0
-2.0
-1.5
-1.0
-0.5
0.0
0.5
1.0
1.5
SIGMA 13

FIGURE 11b

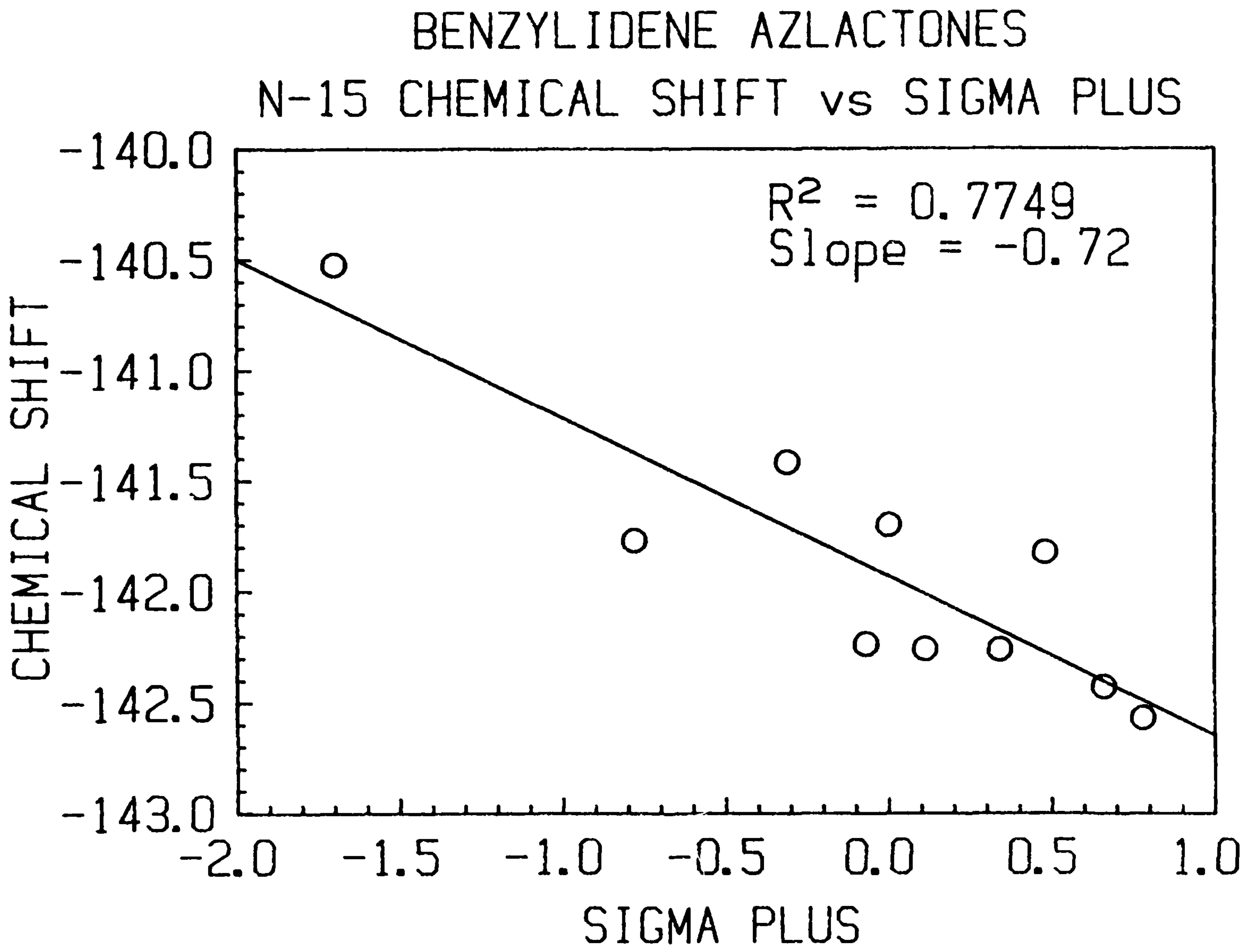
BENZYLIDENE AZLACTONES
N-15 CHEMICAL SHIFT vs SIGMA PLUS
R² = 0.7749
Slope = -0.72
CHEMICAL SHIFT
-140.0
-140.5
-141.0
-141.5
-142.0
-142.5
-143.0
-2.0
-1.5
-1.0
-0.5
0.0
0.5
1.0
SIGMA PLUS

FIGURE 11c

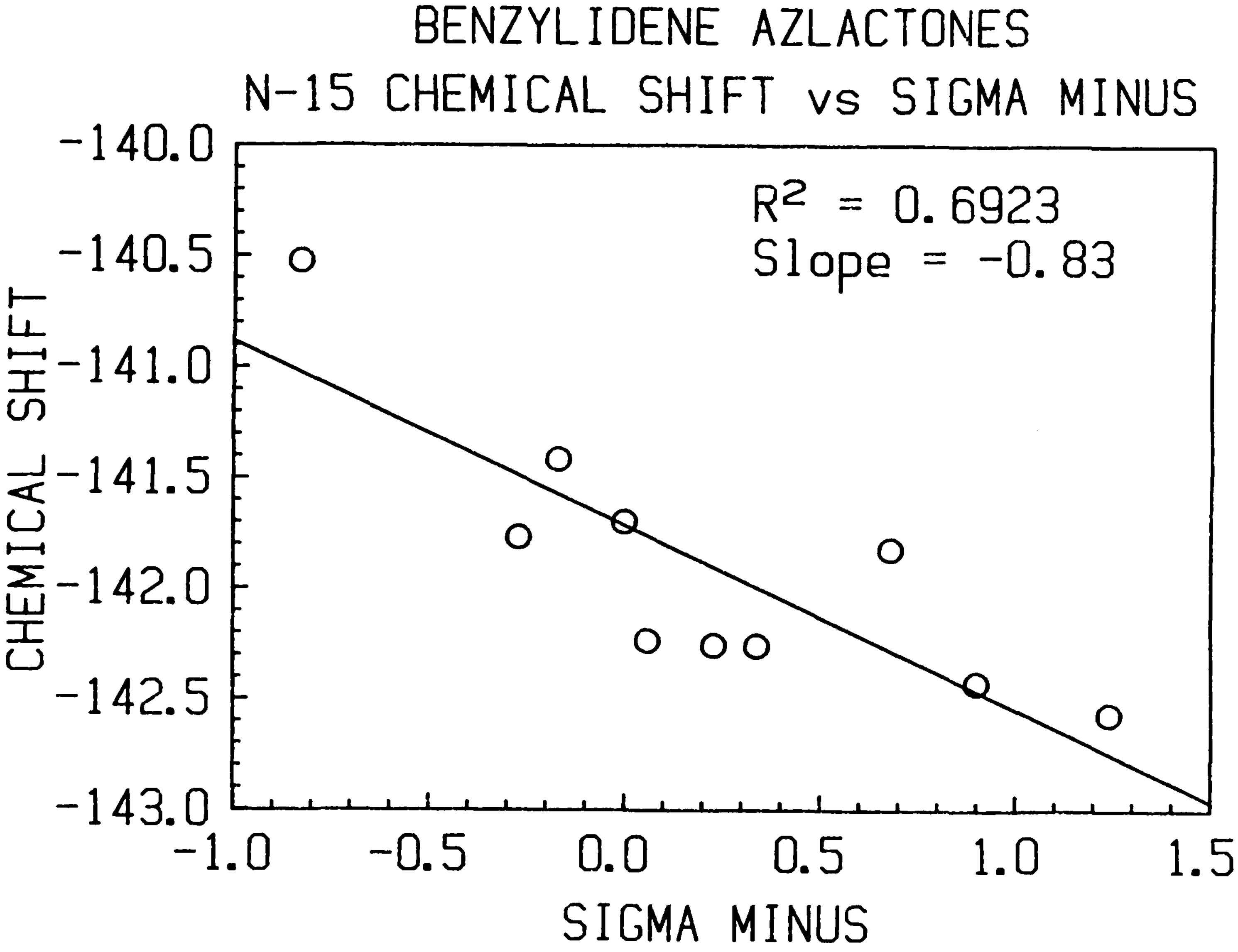
BENZYLIDENE AZLACTONES
N-15 CHEMICAL SHIFT vs SIGMA MINUS
R² = 0.6923
Slope = -0.83
CHEMICAL SHIFT
-140.0
-140.5
-141.0
-141.5
-142.0
-142.5
-143.0
-1.0
-0.5
0.0
0.5
1.0
1.5
SIGMA MINUS

FIGURE 11d

General conclusions reached based on this compilation were:

1. A negative slope was observed throughout (greater shielding with increasing electron withdrawal by X).

2. A much narrower ^{15}N SCS range was observed (≈2 ppm vs 10-12 ppm for Series A).

3. Consistently poorer correlations were obtained. All four substituent scales display a wide scatter of points (made more noticeable by the expanded ppm scale), and do not reveal any clear source of determinant error.

4. The σ^- scale gave definitively the worst correlation, while the other three scales were very comparable.

b. Interpretation of the Results

1) Negative Slope

The observed negative slope supports the contention that the nitrogen of the benzylidene azlactone structure,

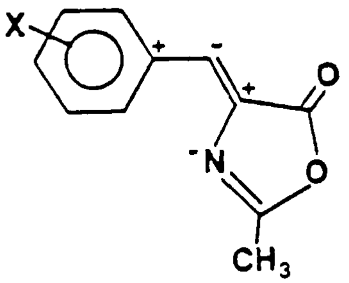

L

as part of an extended conjugated system, follows the same alternating-slope π-polarization pattern (illustrated above) observed for the styryl butadienes [34] and the imines of reference 8, page 7. The confinement of N's unshared electron pair in the molecular plane of the oxazolone ring (and thus orthogonal to the styryl π-system) prevents resonance donation into the styryl system observed in Series A.

2) Narrow ^{15}N SCS Range/Poor Correlations

The very small ^{15}N SCS range was probably due to two factors: 1) the unshared electron pair is not capable of interacting via the styryl system with the X substituent (noted above) and 2) the nitrogen is in a highly unsaturated system.

The random scatter of the data is difficult to explain and prevents a clear assessment of any detrimental factors. A unique aspect of these compounds that could contribute to this poor correlation lies in the spatial orientation of the unshared electron pair of the nitrogen:

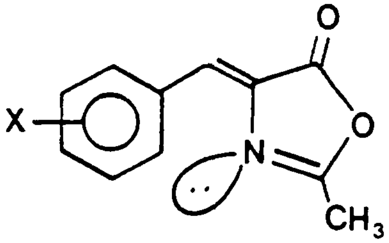

L

Molecular models show that the orbital of the unshared electron pair projects fairly close to the benzene ring plane, and that it may thus be subject to any anisotropic effects of the phenyl system.[59]

However, it should be kept in mind that in the case of the styryl butadienes studied in reference 34 (XXXII), the C-7 gave an R value of only -0.771 using σ^{13} ($R^2 = 0.594$). This carbon is in a position within the conjugated structure analogous to that of nitrogen in the azlactones, and implies that the location of the nitrogen atom may, in itself, have been largely responsible for the poor correlation.

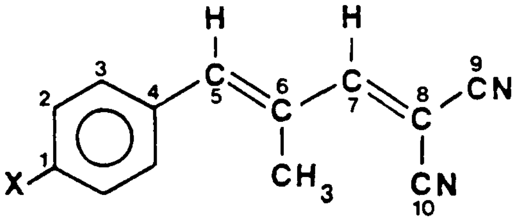

XXXII

In the azlactone system (L) the correlations of the C-7 (R = 0.966, R^2 = 0.934) and C-8 (R = 0.985, R^2 = 0.971) using σ^+ were quite good considering their remote locations. The aromaticity of the iminoenolate resonance structure generated by through resonance e^- donation from X could have accounted for this and the ^{15}N correlation superiority over that of C-7 in the styryl butadienes:[60]

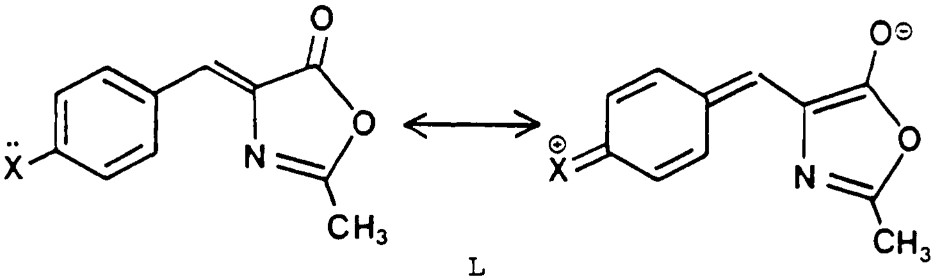

L

3) Worst Fit by σ^-

The decided lack of resonance donation of the N atom in this structure helps account for the σ^- scale giving the worst fit. The other three scales are quite comparable, and, in the context of the data scatter, can not be differentiated to any further extent.

3. Series C

Table 17 lists the ^{15}N δ's for this series of compounds.

Table 17

^{15}N Chemical Shifts*/Series C

X	$^{15}N\delta$
p-N(Me)$_2$	-110.401
p-OMe	-107.722
p-Me	-106.853
p-F	-106.130
H	-106.435
m-F	-104.879
p-CN	-103.839

*Upfield from CH_3NO_2; automatic referencing/VXR-300

a. Summary of the Data

Correlative behavior is more like that observed for Series A (Figure 12a-d, pages 131-134).

Table 18

Series C Correlations From Figure 12

Hammett Scale	R^2	Slope	Relative Fit*
σ^{13}	.9897	2.51	100.00%
σ	.9886	4.43	99.89%
$\sigma+$	.9821	2.67	99.23%
σ^-	.9519	3.84	96.18%

*Relative fits of substituent scales compared to best fit (100.0%)
(Listed in descending order)

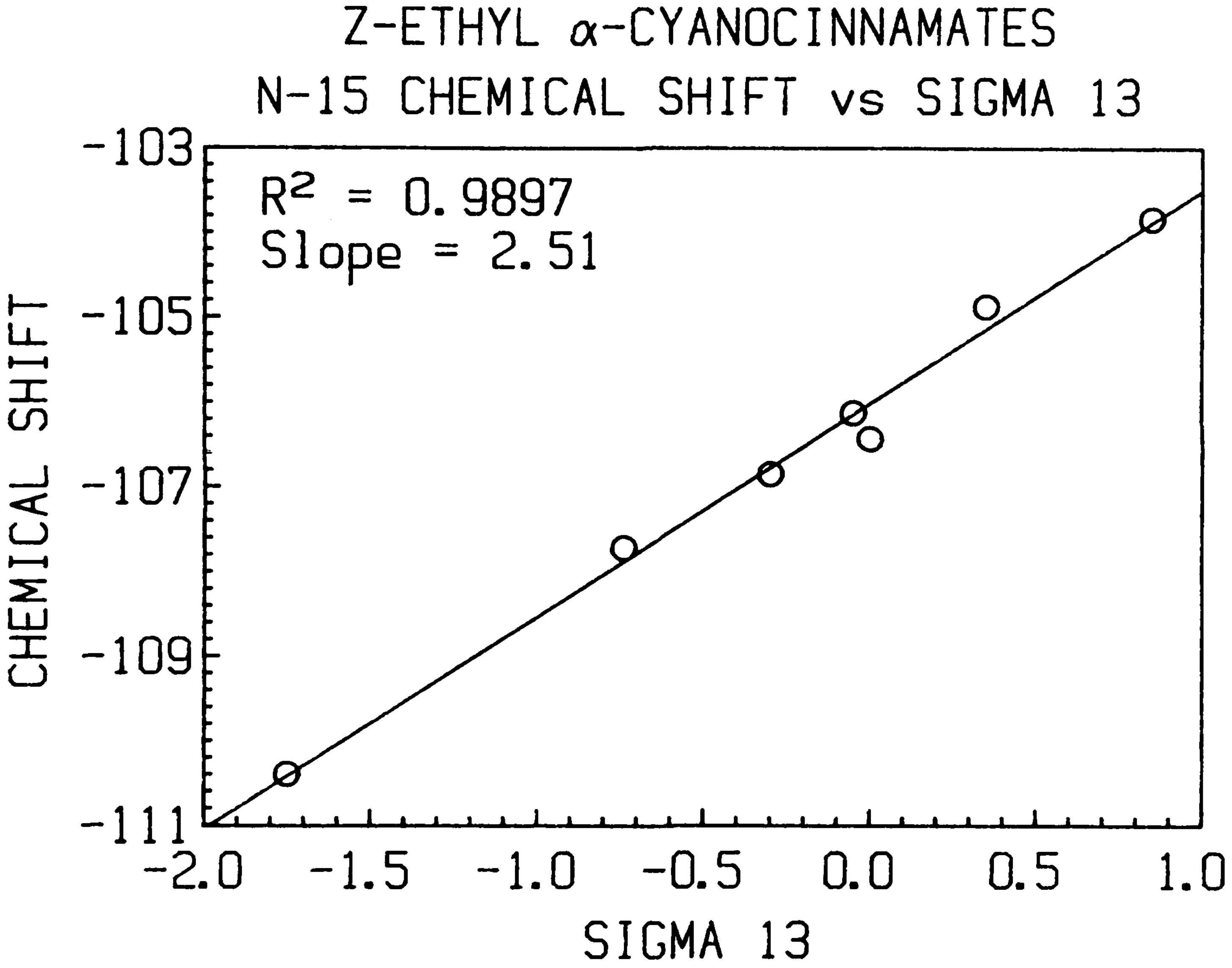
Z-ETHYL α-CYANOCINNAMATES
N-15 CHEMICAL SHIFT vs SIGMA 13
R² = 0.9897
Slope = 2.51
CHEMICAL SHIFT
-103
-105
-107
-109
-111
-2.0
-1.5
-1.0
-0.5
0.0
0.5
1.0
SIGMA 13

FIGURE 12a

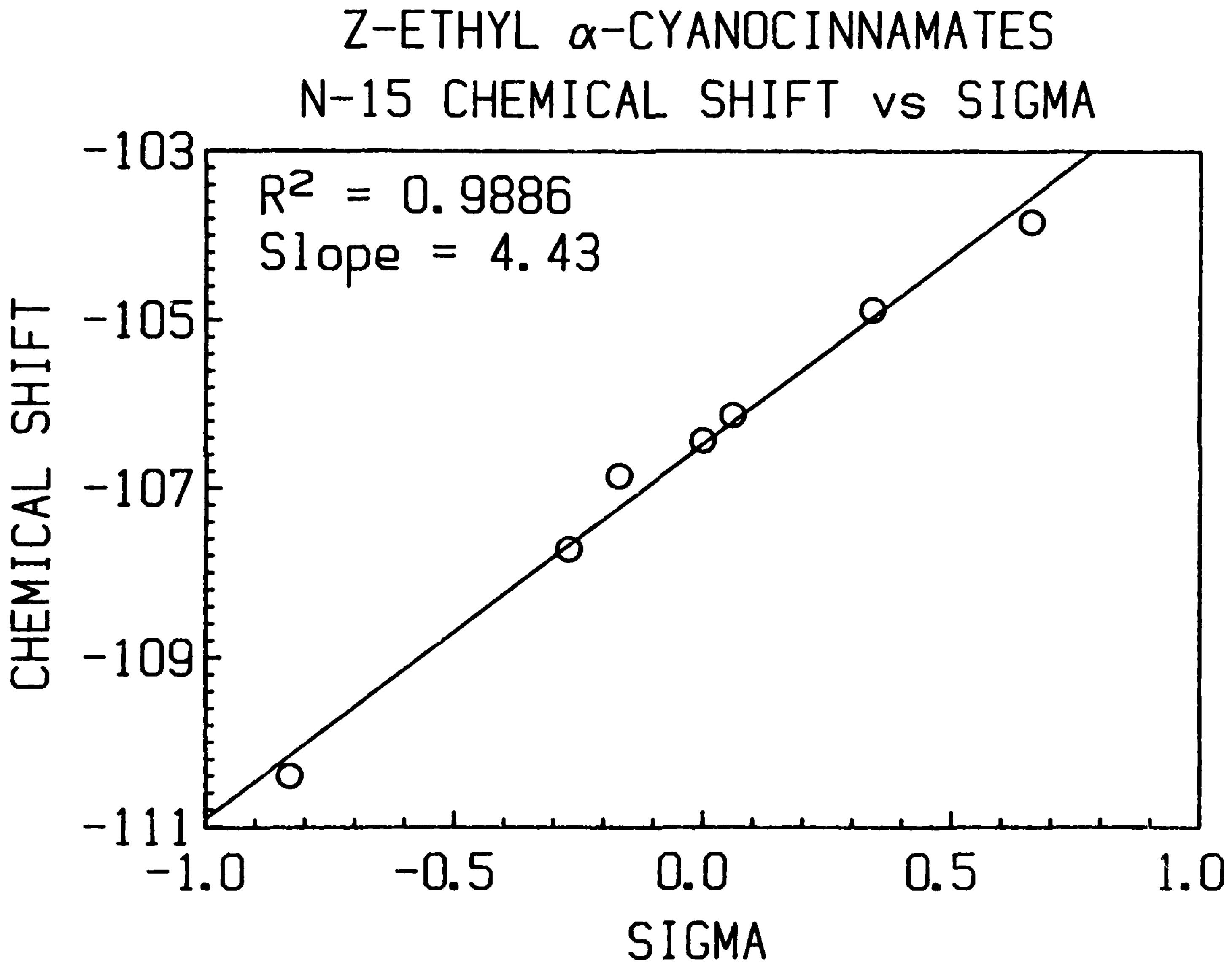
Z-ETHYL α-CYANOCINNAMATES
N-15 CHEMICAL SHIFT vs SIGMA
R^2 = 0.9886
Slope = 4.43
CHEMICAL SHIFT
-103
-105
-107
-109
-111
-1.0
-0.5
0.0
0.5
1.0
SIGMA

FIGURE 12b

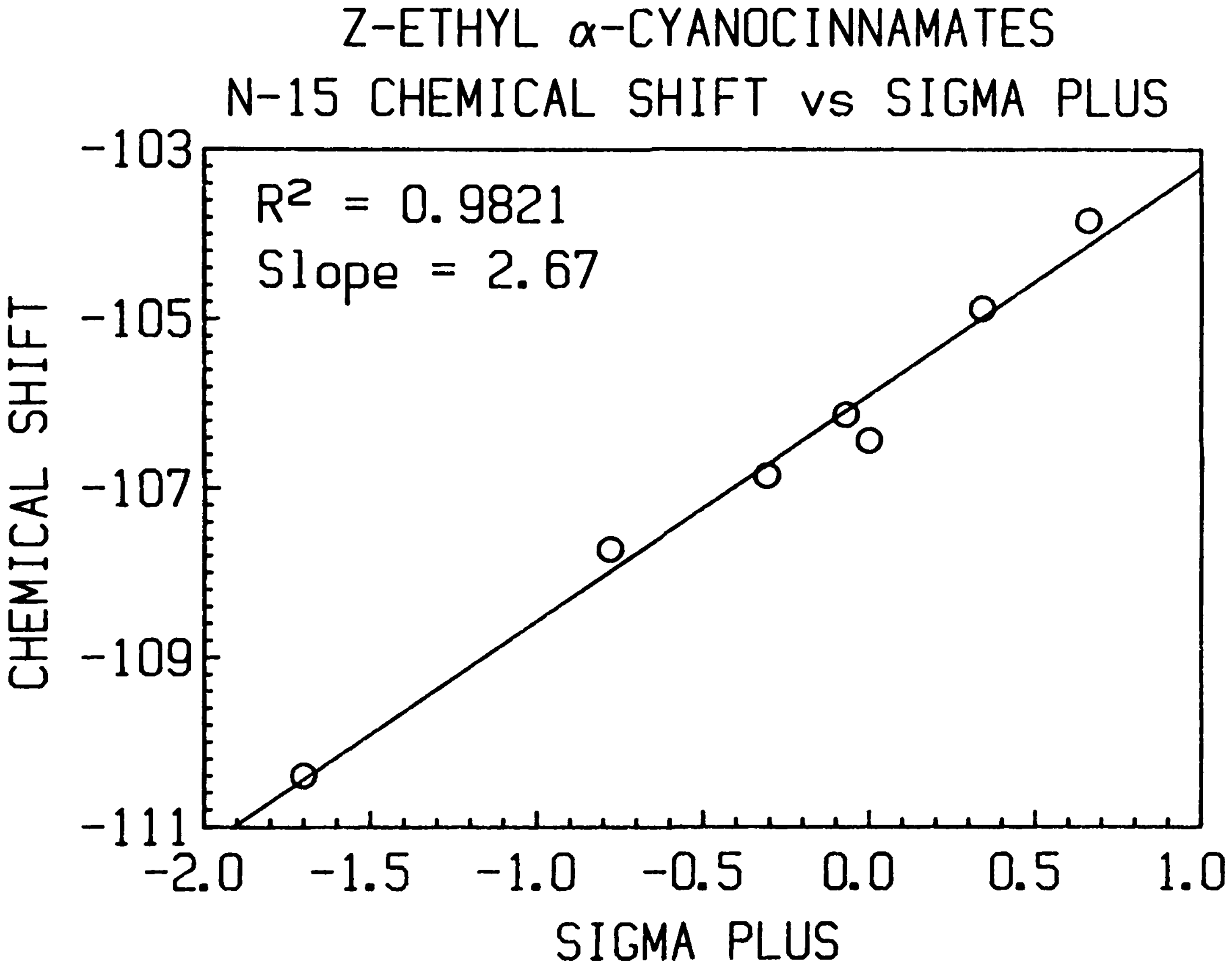
Z-ETHYL α-CYANOCINNAMATES
N-15 CHEMICAL SHIFT vs SIGMA PLUS
R² = 0.9821
Slope = 2.67
CHEMICAL SHIFT
-103
-105
-107
-109
-111
-2.0
-1.5
-1.0
-0.5
0.0
0.5
1.0
SIGMA PLUS

FIGURE 12c

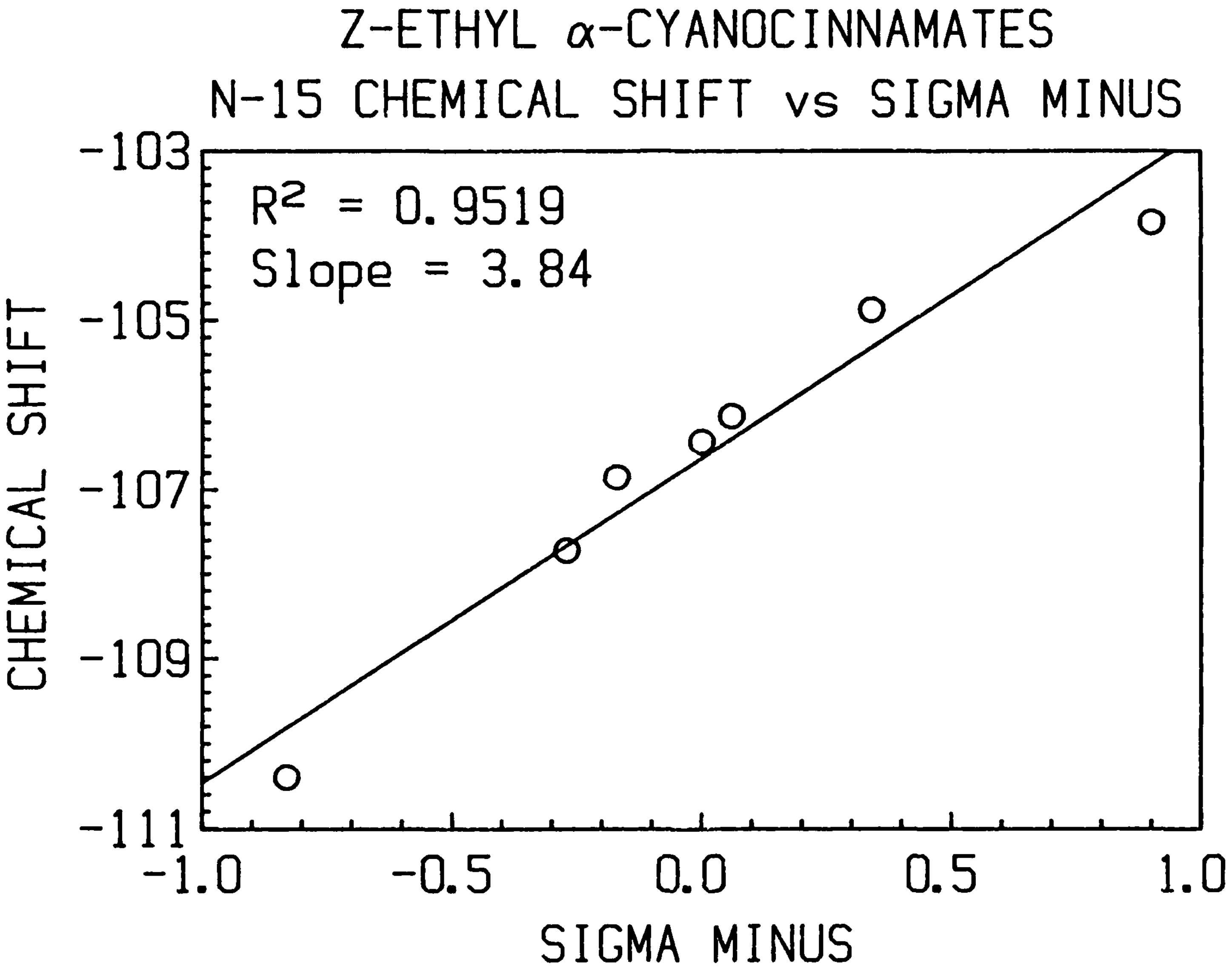
Z-ETHYL α-CYANOCINNAMATES
N-15 CHEMICAL SHIFT vs SIGMA MINUS
R² = 0.9519
Slope = 3.84
CHEMICAL SHIFT
-103
-105
-107
-109
-111
-1.0
-0.5
0.0
0.5
1.0
SIGMA MINUS

FIGURE 12d

General conclusions that can be reached based on these compilations are as follows:

1. A positive slope is again observed.

2. The ^{15}N SCS range covers ≈ 6.5ppm (vs ≈ 12 ppm for the sp^3 hybridized nitrogen in Series A).

3. Consistently excellent correlations were observed for all four substituent scales, in fact the best obtained from all series.

b. Interpretation of the Results

1) Positive Slope

The positive slope is consistent with what is expected from the π-polarization mechanism:

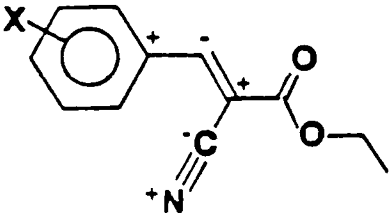

LI

(The unshared electron pair on the nitrile nitrogen is not available for resonance into the styryl system). This finding parallels that observed in the benzonitriles (XXVIII) studied by Pregosin, Randall and White.[33] However, it should be kept in mind that one can also invoke through-resonance from e^- donors into the nitrile system, which qualitatively would also contribute to a positive slope.

2) ^{15}N SCS Range/Correlation Excellence

The relatively narrow but not insignificant range of ^{15}N chemical shifts observed in this compound series indicates a reasonable polarizability of the C≡N bond. The excellent correlations obtained argue for the cyano carbon atom's ability to take on electron density freely as required by the π-polarization phenomenon while simultaneously deshielding the adjacent nitrogen. This tendency to take on electron density is consistent with the generally greater acidity of sp hydridized carbons, over sp^2 or sp^3 carbon.

It should be added that this well-defined behavior of the nitrile carbon was also substantiated at the remote sites in the styryl butadienes (XXXII) where $R = -0.995$ ($R^2 = 0.990$) for C-9 and $R = -0.992$ ($R^2 = 0.984$) for C-10 using the σ^{13} scale.[34]

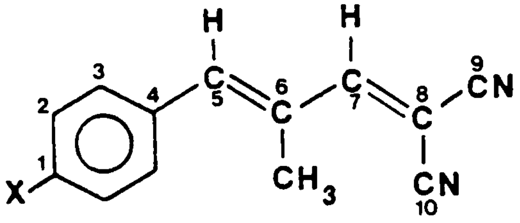

XXXII

The data indicate a well-defined, variable polarizability of the C≡N bond. A further factor that may have aided in these excellent correlations is that the nitrogen atom is held closely and in linear fashion to its nearest neighbors minimizing steric/anisotropic sources of error.

4. Series D

Table 19 lists the ^{77}Se δ's for this series of compounds.

Table 19

^{77}Se Chemical Shifts*/Series D

X	^{77}Se δ E Isomer	Z Isomer
p-N(Me)$_2$	326.83	472.71
p-OMe	338.80	475.16
p-Me	347.50	475.38
p-Ph	351.41	--
p-F	346.60	476.59
H	351.80	475.92
m-OMe	355.10	--
p-Cl	351.30	478.41
m-F	356.75	478.43
m-Cl	356.92	--
p-CO$_2$Me	361.40	--
m-CN	358.46	--
m-CF$_3$	356.00	478.34
p-CF$_3$	360.06	479.90
p-CN	364.50	--
m-NO$_2$	359.03	--
p-NO$_2$	367.45	485.38

*Downfield from external $(CH_3)_2$ Se

a. Isomer Assignments

Seventeen compounds in this series were made, ten of which were composed of both the E and Z isomers. In all cases, except the p-OMe and p-NO$_2$ derivatives, the E compound was either more prevalent or the only isomer. These isomers were differentiated by selective decoupling of the Se/aromatic H's and evaluation of the Se/vinylic ^{1}H coupling constant; for selenium compounds,

^{3}J vinylic ^{1}H/Se (cis) = 6-10 Hz (lit.) [61]
E isomer 6-8 Hz (observed in this series)

^{3}J vinylic ^{1}H/Se (trans) = 1-4 Hz (lit)[61]
Z isomer 4-5 Hz (observed in this series)

b. E Isomers

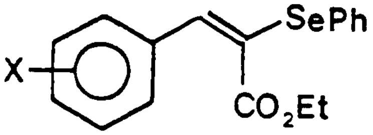

LIIA

1) Summary of the Data

For this isomer series, the Se SCS values ranged over 40 ppm as X was varied from p-N(Me)$_2$ to p-NO$_2$: (Figure 13a-d, pages 139-142)

General conclusions reached based on this data were: (See Table 20, page 143).

1. A large positive slope was observed for all plots.
2. σ^{13} and σ^{+} together provide better correlations than σ and σ^{-}.

2) Interpretation of the Results

a) Large Positive Slope

The significant positive slope verified selenium's strong tendency to interact via resonance donation of its unshared electron pair through the styrene system in analogous fashion to that of nitrogen in the enamines (Series A). Here, however, the ppm range is almost 5 times as great consistent with the greater shielding range of the relatively electron-rich Se atom (3000 ppm) versus N (400 ppm).

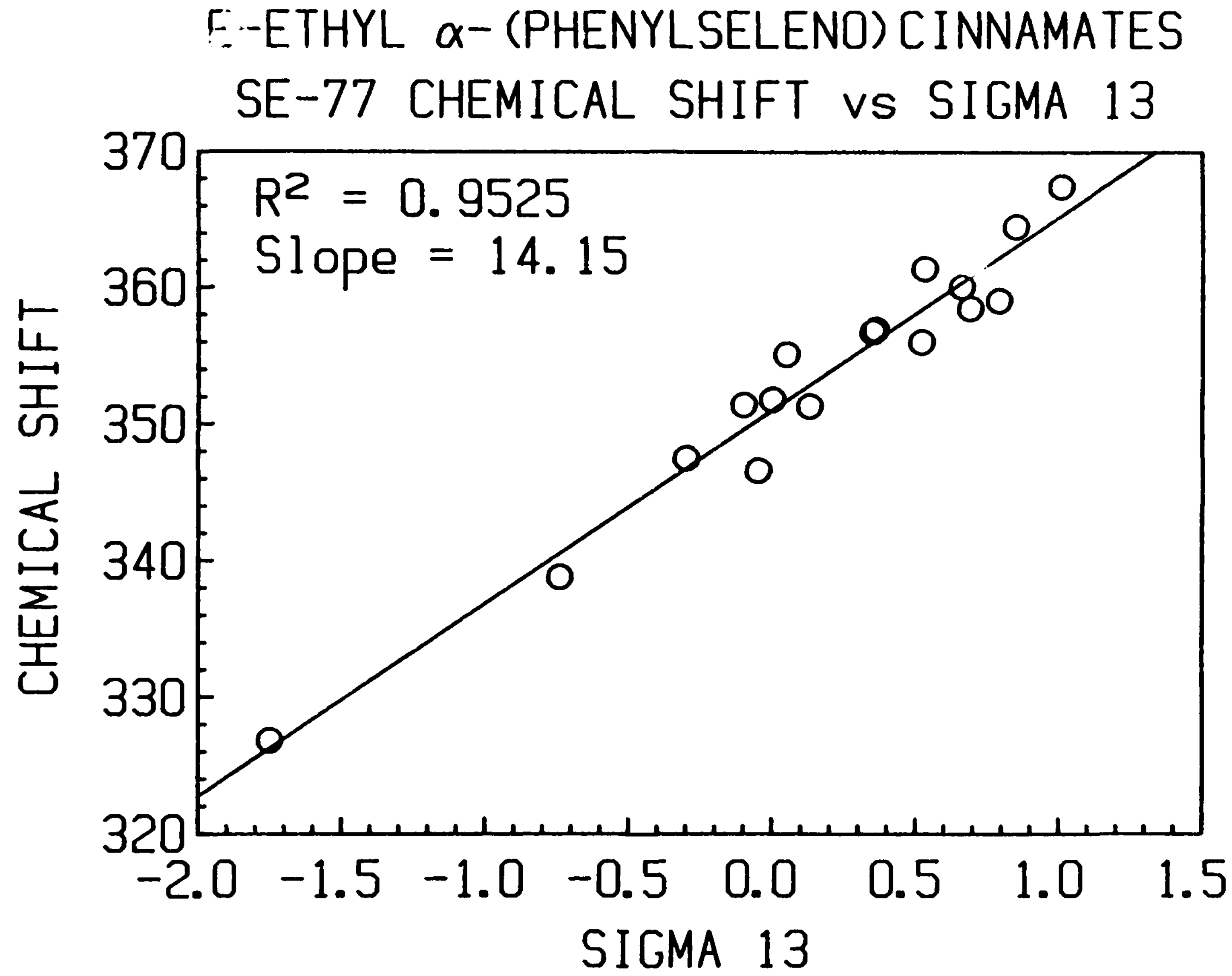
E-ETHYL α-(PHENYLSELENO)CINNAMATES
SE-77 CHEMICAL SHIFT vs SIGMA 13
R² = 0.9525
Slope = 14.15
CHEMICAL SHIFT
370
360
350
340
330
320
-2.0
-1.5
-1.0
-0.5
0.0
0.5
1.0
1.5
SIGMA 13

FIGURE 13a

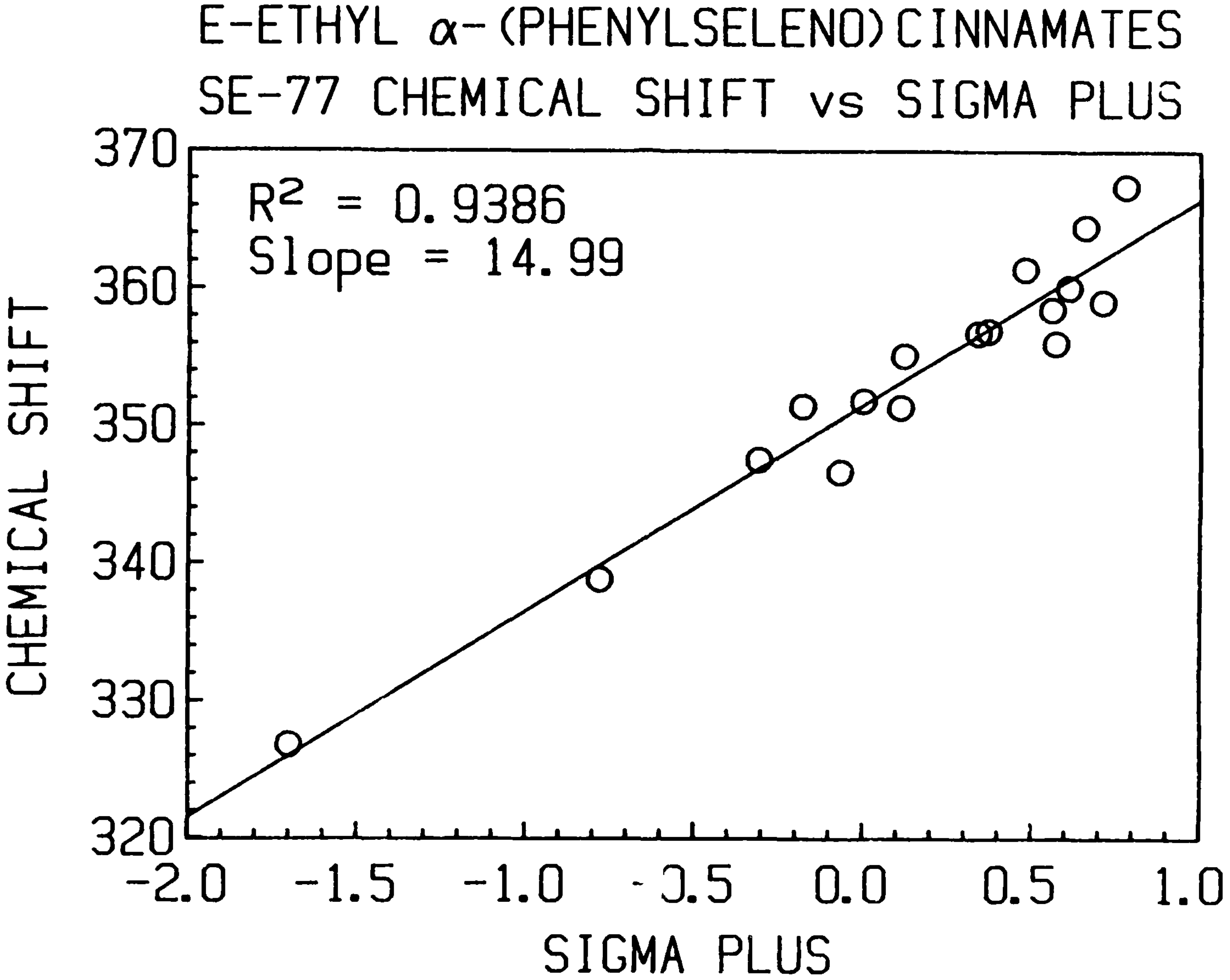
E-ETHYL α-(PHENYLSELENO)CINNAMATES
SE-77 CHEMICAL SHIFT vs SIGMA PLUS
R² = 0.9386
Slope = 14.99
CHEMICAL SHIFT
370
360
350
340
330
320
-2.0
-1.5
-1.0
-0.5
0.0
0.5
1.0
SIGMA PLUS

FIGURE 13b

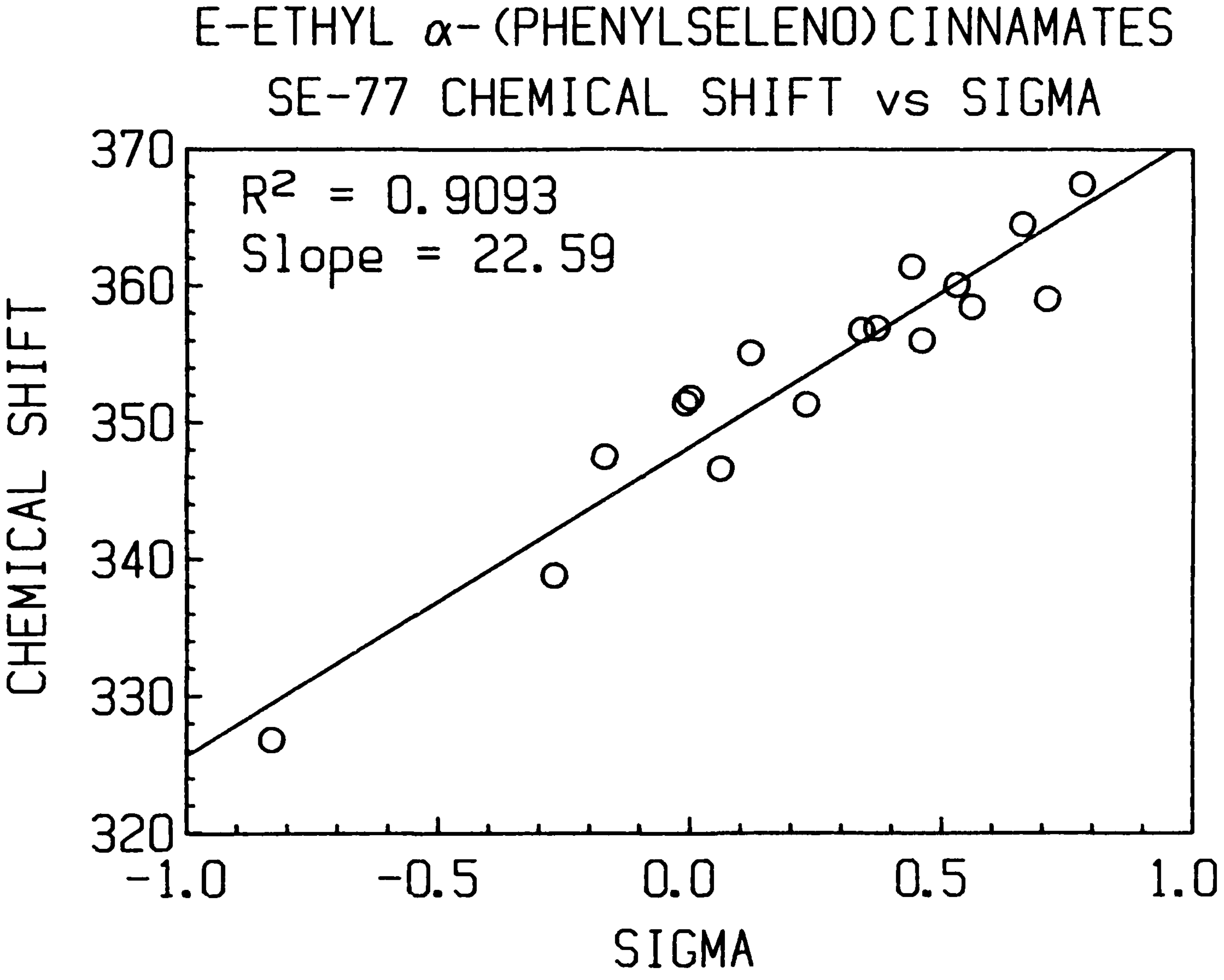
E-ETHYL α-(PHENYLSELENO)CINNAMATES
SE-77 CHEMICAL SHIFT vs SIGMA
R² = 0.9093
Slope = 22.59
CHEMICAL SHIFT
370
360
350
340
330
320
-1.0
-0.5
0.0
0.5
1.0
SIGMA

FIGURE 13c

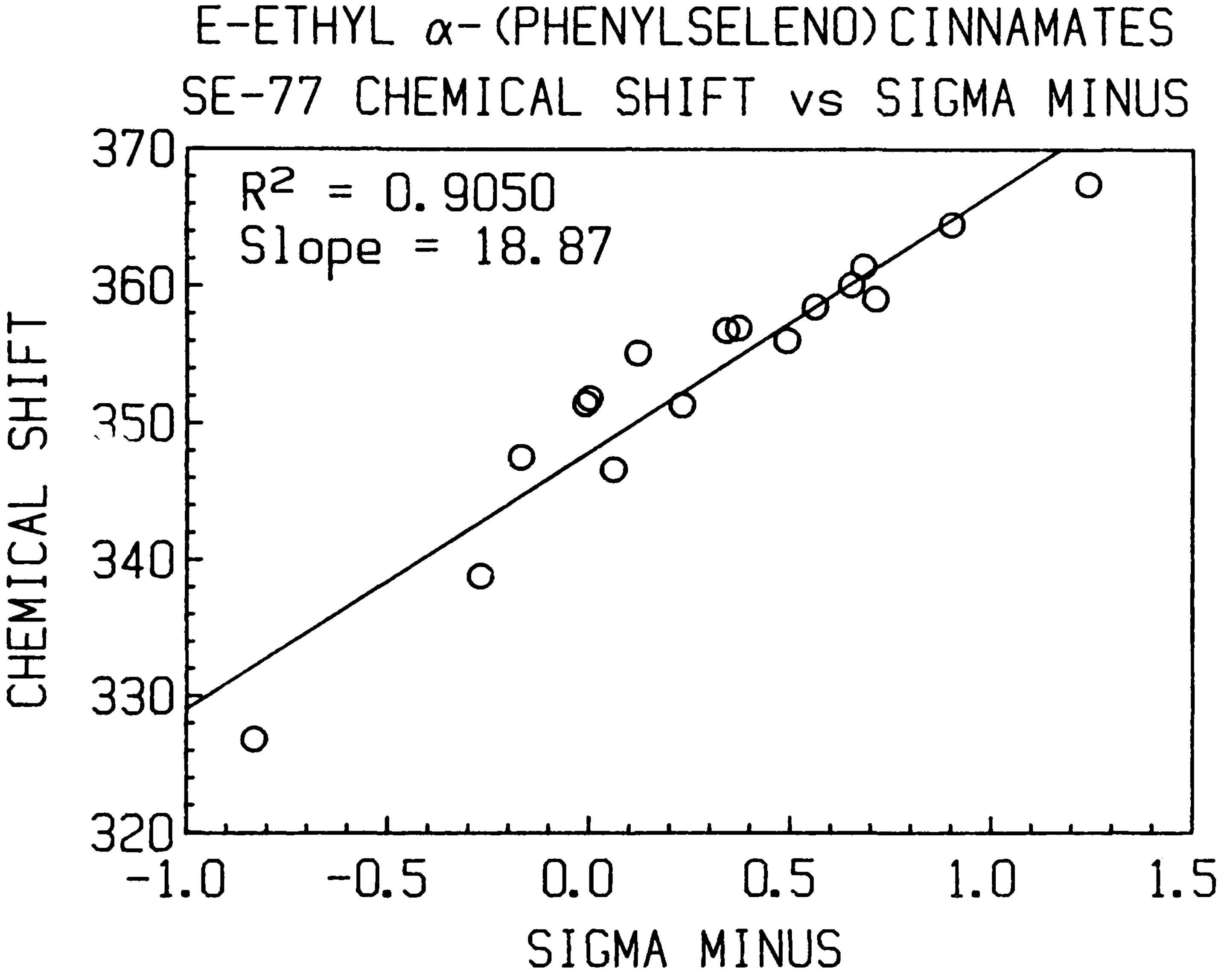
E-ETHYL α-(PHENYLSELENO)CINNAMATES
SE-77 CHEMICAL SHIFT vs SIGMA MINUS
R² = 0.9050
Slope = 18.87
370
360
350
340
330
320
CHEMICAL SHIFT
-1.0
-0.5
0.0
0.5
1.0
1.5
SIGMA MINUS

FIGURE 13d

Table 20

Series D Correlations From Figure 13

Hammett Scale	R^2	Slope	Relative Fit*
σ^{13}	.9525	14.15	100.00%
σ^+	.9386	14.99	98.53%
σ	.9093	22.59	95.46%
σ^-	.9050	18.87	95.01%

*Relative fits of substituent scales compared to best fit (100.0%) (Listed in descending order)

b) Superiority of σ^{13}/σ^+ Correlations Over σ/σ^-

The σ^{13} scale gave the best correlation, but very close in R^2 value to that obtained for σ^+. These two plots also have a very similar appearance. The statistical basis of the σ^{13} scale, incorporating as it does such a wide variety of substitution patterns of the styryl system, including the larger, and more akin to Se, P atom (in the context of the PO_3Et_3 group), gave the best overall fit of the ^{77}Se SCS values. This is logical in that the greater diffuseness and polarizability of selenium would tend to make it more amenable to a statistical analysis of its SCS data.

More useful information is available from contrasting the good σ^{13}/σ^+ correlations with the poorer σ/σ^- correlations. This contrast in σ^+/σ^- correlative behavior from that observed in the ^{15}N data for the enamine series A (where σ^- was much better than σ^+) suggests an important difference in the manner in which Se interacts with the styryl system. The superior σ^+ fit implies the relative importance of selenium acting as an efficient electron acceptor in the case of strongly electron donating substituents. Here, the inductive (-I) and mesomeric (-M) electron withdrawing properties of the SePh group (see page 17) are acting together to accentuate this effect. This argument leads to the following resonance structures (the C-Se-C bond angle is represented linearly for clarity):

LII

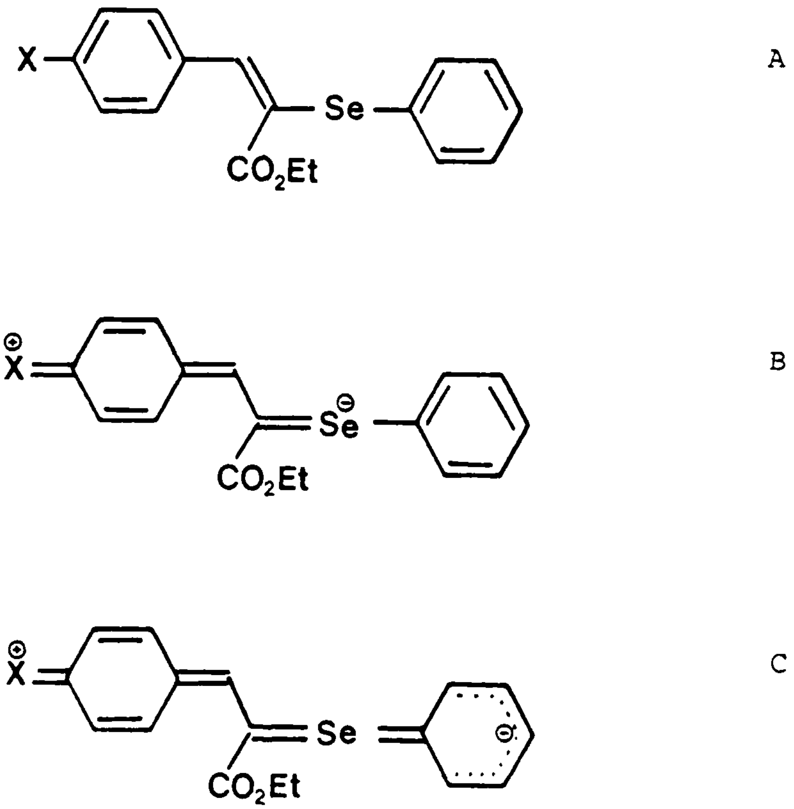

with structures A and B more significant than C. In simplistic terms this resonance model calls for electron donation through the styryl system into Se's empty d orbitals, which would require adequate orbital alignment for both p orbital e^- donation from Se and d orbital acceptance into Se. However, these d orbitals are of very high energy and probably play little role in this e⁻ acceptance, although it is useful to consider this option (see page 161) when scrutinizing the question from several perspectives. What may be of more importance here in accounting for Se's e⁻ acceptance is the phenomenon of negative (σ-π) hyperconjugation as described by Traylor [63] and more recently by Schleyer [64]. These contrasting viewpoints will be discussed subsequently. (See pages 157 to 167). The key element common to them and relevant to the styryl structure is the attainment of some kind of optimal orbital alignment of the SePh unit with the styryl system. This optimal alignment of the phenyl ring adjacent to the selenium atom with the styryl system is more easily accessible in the E (versus Z) configuration, and is required for resonance form LIIC to be significant or its hyperconjugative counterparts (LII D/E) as represented in a valence bond manner:

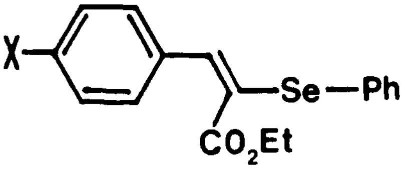

D

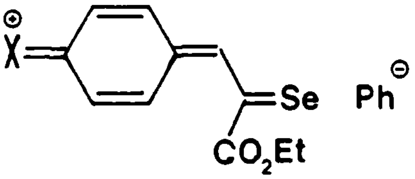

E

In the enamines (Series A), the N atom did not have this capacity to take on e^- density (no accessible empty d orbitals) giving the much poorer σ^+ fit. With the large phenyl moiety attached, and the highly bent C-Se-C bond angle known to be present in dialkyl selenides (≈ 93-97° generally, with Ph-Se-CH_3, as a close example, with an angle of 99.6°)[62], the better isomer for Se/styryl interaction is the E structure, where more room is available for optimal alignment. The contrastingly poor correlative nature of the Z isomer (next section) supports this contention. Also acting in conjunction with this mesomeric effect is the electron withdrawing inductive effect of the SePh group acting through the σ system, which may actually be of greater overall importance.

In contrast, the poorer correlation of the σ^- scale indicates that electron withdrawing substituents do not interact (as effectively) with the non-bonding selenium p-orbitals in such a through-conjugative fashion:

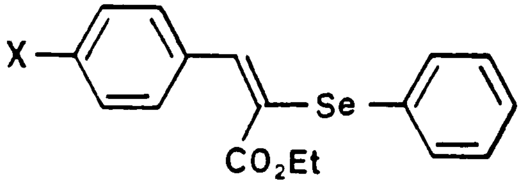

F

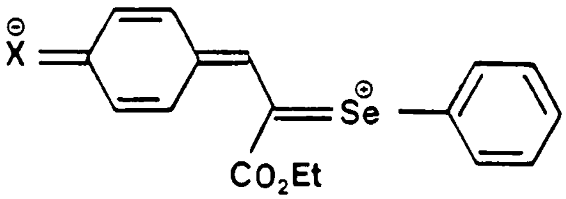

G

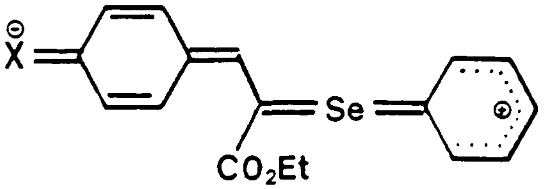

H

(F/G/H not as important as A thru E system, pages 144 and 145).

The slightly concave downward pattern evident in the σ^- correlation supports this view, in that a lessening of importance of resonance structure G means a reduced degree of deshielding of the Se atom with increasing electron withdrawal by X. The determinate error caused by this effect (less than the predicted deshielding for X = electron withdrawers) would give this concave downward result. The through-resonance concept as a means to understand Se's correlative behavior is reinforced by the relative scatter of the σ correlation, where this model is not employed.

These results appear to agree with those of Mullen et al. in studying selenobenzoates (ref 27; page 15) where they found that, while mesomeric donating substituents acted well through the aromatic ring into the electron deficient SeC(O)Ph moiety, electron withdrawing substituents did not interact as effectively with the non-bonding p orbitals on selenium.

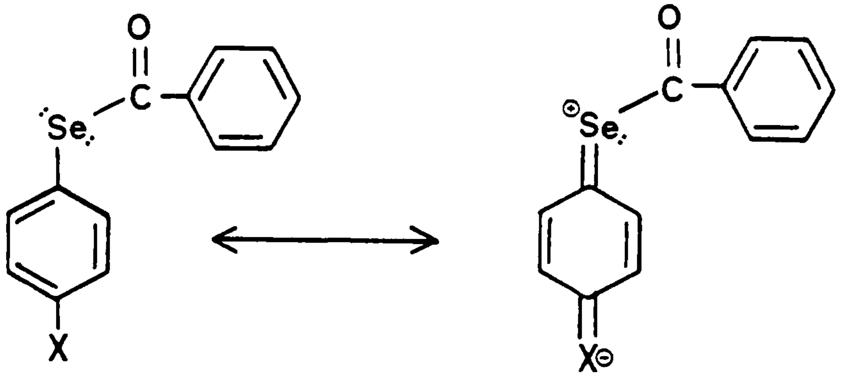

XXVA XXVE

(not as important as resonance structures XXVB through D, page 17).

No doubt, the e⁻ withdrawing influence of the adjacent carbonyl group played a significant part in the unimportance of the above resonance forms, but the same qualitative comparison, using the SePh moiety in these styryl compounds, holds true.

c. Z Isomers/Discussion of the Data In Contrast with the E Isomers

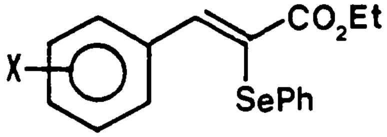

LIIB

One of the most dramatic and interesting observations in this research effort stemmed from the comparison of the ^{77}Se SCS correlations for the E versus Z isomers in the ethyl α-(phenylseleno)cinnamates (Series D). The E isomers, as already discussed, showed a wide ppm range (≈ 40 ppm) with good overall correlations, particularly using σ^{13} and σ^{+}. In stark contrast (see Table 21), the Z isomers showed a much narrower range (≈ 13 ppm), a good correlation only with σ^-, and ^{77}Se chemical shifts of over 100 ppm further downfield than those of the E isomers (Figure 14a-d, page 150-153).

Table 21

Series D (Z Isomer) Correlations From Figure 14

Hammett Scale	R^2	Slope	Relative Fit*
σ^-	0.9467	5.93	100.00%
σ	0.8343	6.77	88.13%
σ^{13}	0.7623	3.82	80.52%
σ^+	0.6952	3.84	73.43%

*Relative fits of substituent scales compared to best fit (100.0%) (Listed in descending order)

A particularly useful way to rationalize this large difference in ^{77}Se NMR behavior between the two isomers is to examine the steric factors operating in both the E and Z configurations. To review, in the E isomers,

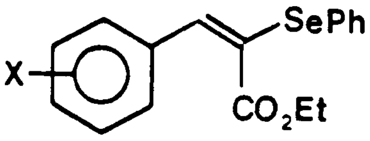

LIIA

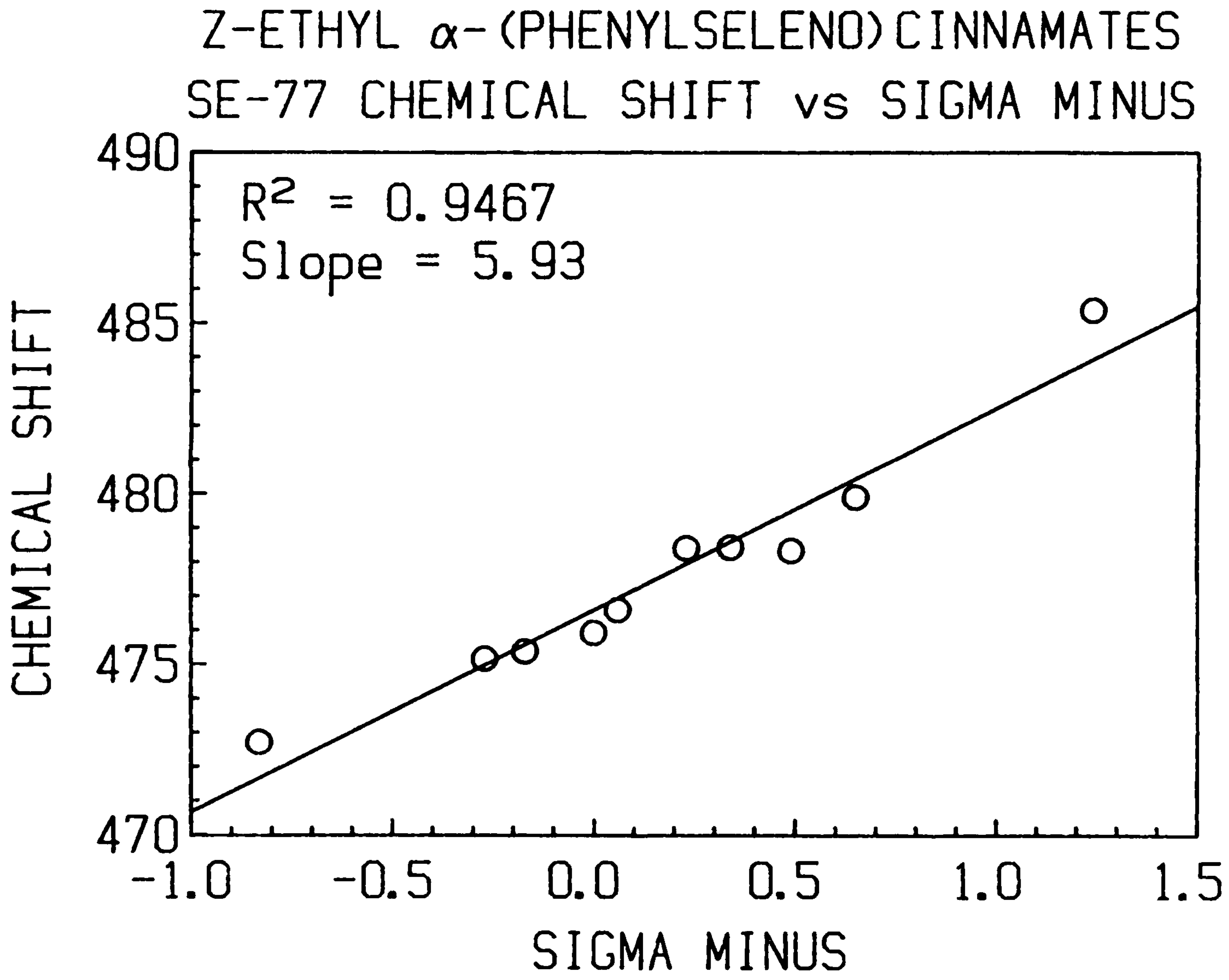
Z-ETHYL α-(PHENYLSELENO)CINNAMATES
SE-77 CHEMICAL SHIFT vs SIGMA MINUS
R² = 0.9467
Slope = 5.93
490
485
480
475
470
CHEMICAL SHIFT
-1.0
-0.5
0.0
0.5
1.0
1.5
SIGMA MINUS

FIGURE 14a

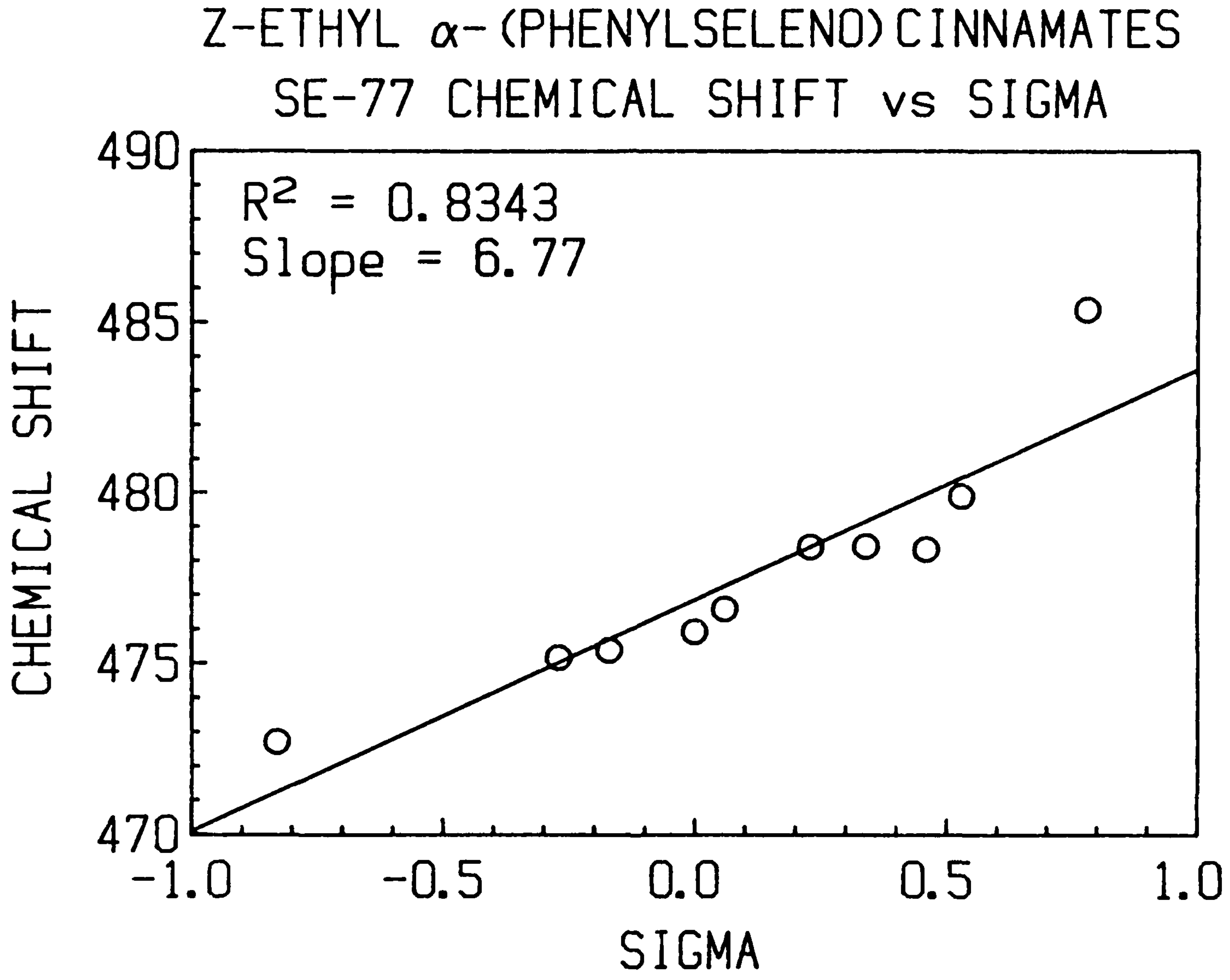
Z-ETHYL α-(PHENYLSELENO)CINNAMATES
SE-77 CHEMICAL SHIFT vs SIGMA
R² = 0.8343
Slope = 6.77
CHEMICAL SHIFT
490
485
480
475
470
-1.0
-0.5
0.0
0.5
1.0
SIGMA

FIGURE 14b

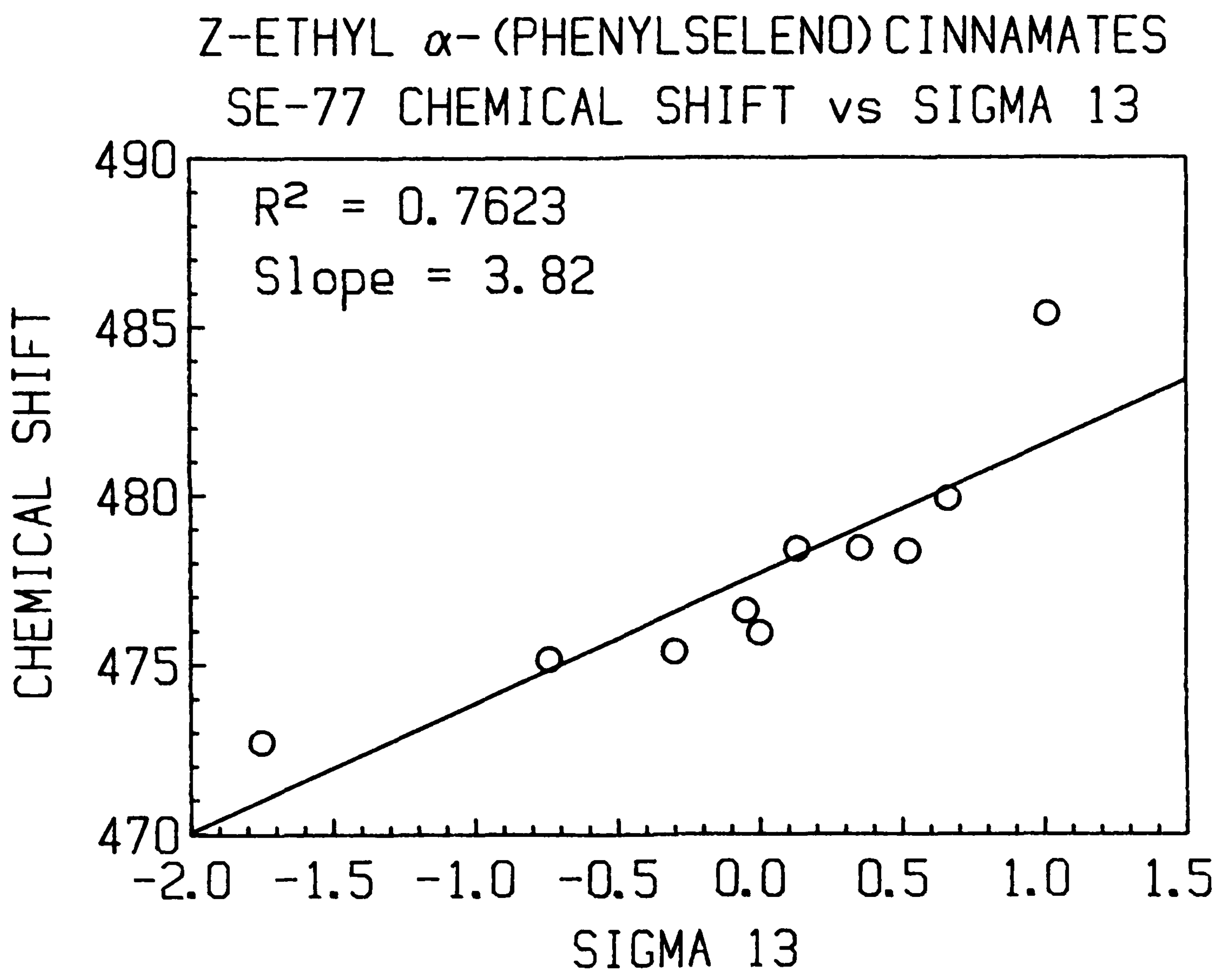
Z-ETHYL α-(PHENYLSELENO)CINNAMATES
SE-77 CHEMICAL SHIFT vs SIGMA 13
R² = 0.7623
Slope = 3.82
490
485
480
475
470
CHEMICAL SHIFT
-2.0
-1.5
-1.0
-0.5
0.0
0.5
1.0
1.5
SIGMA 13

FIGURE 14c

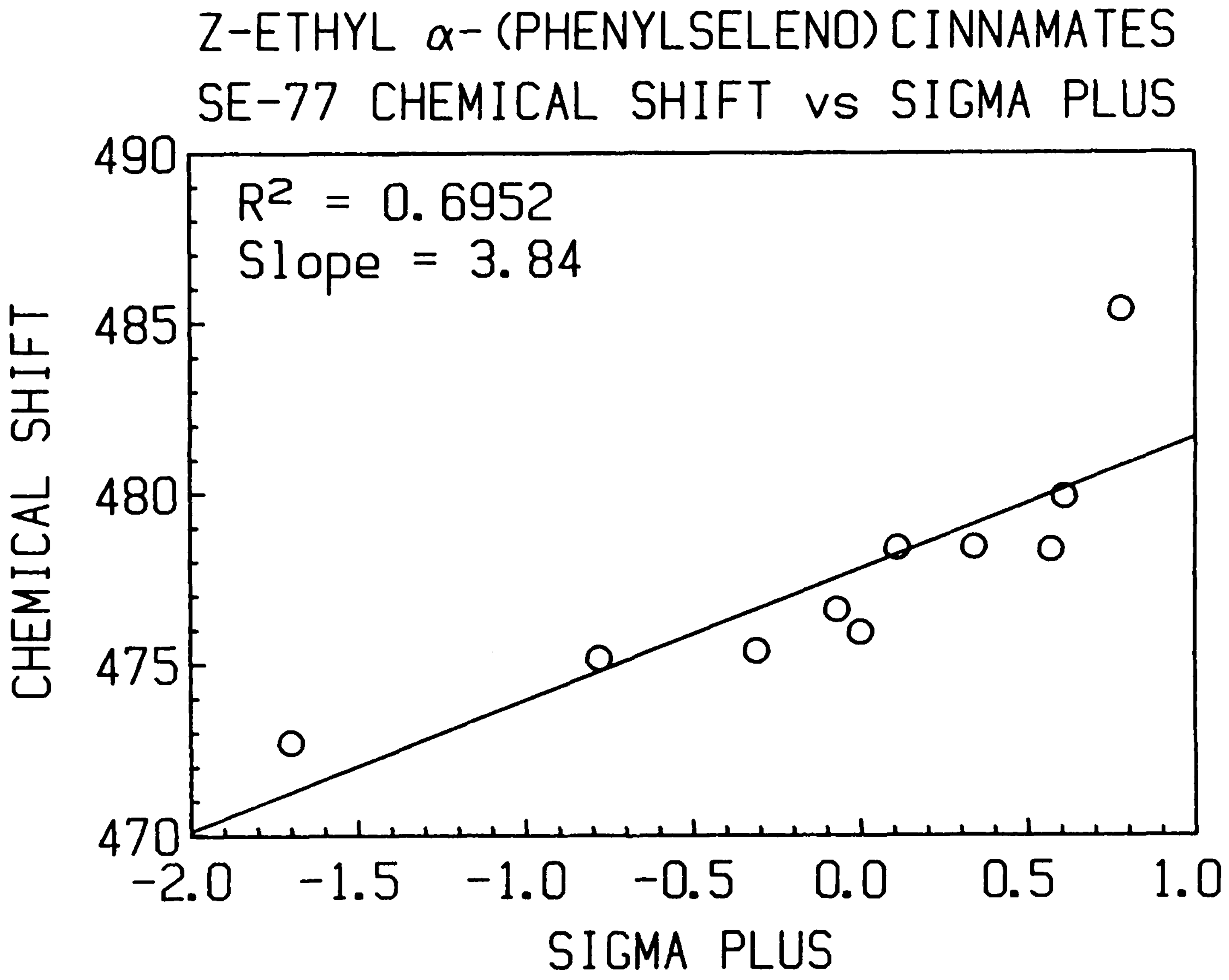
Z-ETHYL α-(PHENYLSELENO)CINNAMATES
SE-77 CHEMICAL SHIFT vs SIGMA PLUS
R² = 0.6952
Slope = 3.84
CHEMICAL SHIFT
490
485
480
475
470
-2.0
-1.5
-1.0
-0.5
0.0
0.5
1.0
SIGMA PLUS

FIGURE 14d

the trans arrangement of the phenylseleno and substituted phenyl systems provides sufficient room for π system optimal alignment including one of selenium's unshared electron pairs. The considerable volume requirement of the SePh group, primarily due to the highly bent C-Se-C bond angle, can be more easily accommodated in the E isomer, while allowing for efficient π-overlap with the selenium unshared electron pair. A large chemical shift range is thus observed. In the Z isomers,

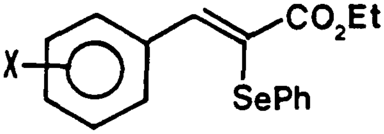

LIIB

the cis arrangement of the aromatic systems increases the steric encumbrance to overlap of the selenium unshared electron pair(s) with the styryl system, and thus the lower SCS range (13 ppm) is observed.

What is more difficult to understand is why σ^- is by far the best scale for the Z ^{77}Se SCS data, while it is the worst scale for the E isomer. To approach this apparent anomaly, molecular models help to contrast the steric hindrance in free rotational volumes of the phenylseleno group in each isomer; the lowest energy conformation available to the E and Z isomers allowing maximum π-overlap between the aromatic systems provides the following:

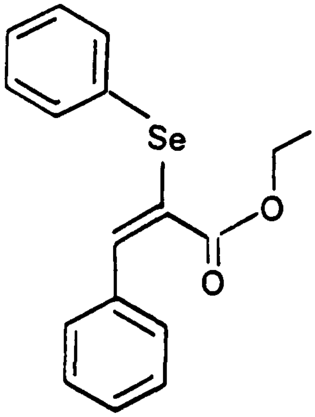

LIIA

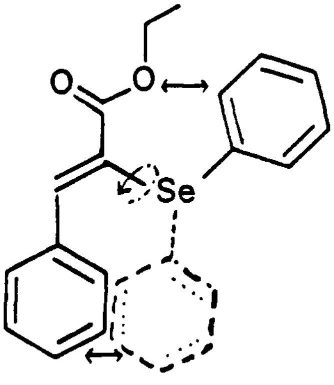

LIIB

coplanarity of phenylseleno/
styryl system

some steric encumbrance (↔)
to complete coplanarity

The highly bent C-Se-C bond angle (≈ 96-100°) would magnify this steric crowding (↔). Any twist out of the π-styryl plane of the SePh phenyl system as a result of this steric crowding would render Se more electronically independent of the Ph moiety due to lessening orbital overlap. Se, apart from mesomeric assistance from the Ph system, now apparently acts as a more effective electron donor by through-resonance (σ^- superiority) and is a poor electron acceptor (σ^+ inferiority).

Qualitatively, this is consistent with the expectation that Se, being an easily polarizable, electron-rich center is ripe for electron donation by through resonance. Its apparent ability to take on electron density in the E isomer is considerably increased with coplanarity of the Ph moiety to help dissipate negative charge buildup. This argues for greater importance for resonance structure LII C, page 144, or the hyperconjugative structures (LII D/E, page 145) in accounting for the E isomer's σ^+ superiority over σ^-. The coplanar conformation discussed above is one possible example of optimal orbital alignment, and is used here since it provides a relatively clear way to contrast these isomers sterically. However, other optimal orbital arrangements are possible. The key point is that in the E isomer this alignment can be more easily achieved due to its greater conformational freedom.

The > 100 ppm deshielding of the ^{77}Se SCS values in the Z isomer relative to E could be due to its greater proximity to the deshielding effect of the substituted phenyl ring. The large size of Se would tend to increase its sensitivity to this effect. This increased influence of the phenyl ring deshielding anisotropy on Se may have also reduced in itself the sensitivity of Se to substituent effects transmitted through the styryl system.

In summary, the SePh moiety acting as a unit from π-styryl optimal alignment available in the E isomer shows a greater proclivity for electron acceptance than donation, while the Se atom itself, in the context of the Z isomer, is more capable of electron donation. It is important to keep in mind that the Z isomer results are only based on 10 data points relative to 17 for the E isomer, and thus must be approached more cautiously.

These contrasts argue for the selenium atom, and the phenylseleno group in particular to be a valuable and sensitive molecular probe for evaluating n-π interaction in sterically conjested systems. These arguments for contrasting the E/Z isomer ^{77}Se NMR behavior are speculative in that crystal structure data would be required to get a definitive idea of the precise steric factors involved, including the degree of SePh twist out of π-styryl plane in the Z isomer. Unfortunately, no pure crystalline Z isomer could be isolated for such a study.

To obtain a better idea of possible ways that Se might act as an electron acceptor in the context of this E/Z isomer contrast, several important precedents in the literature were examined. From them, two perspectives emerge as convenient, if not totally accurate means to rationalize the data.

1) Negative Hyperconjugation

d-orbital participation has been invoked liberally in the literature (see references 67-71) to account for many properties of organic compounds containing transition and representative elements. However, with the development of improved molecular orbital (MO) theoretical calculations, the role of d-orbitals, particularly for large atoms such as Se is increasingly coming under doubt.

A significant alternative model has become reasserted in the literature since its original inception by Roberts to account for the electronic effects of the trifluoromethyl group [65]: negative hyperconjugation. While still controversial, it has become increasingly supported by physical organic chemists, particularly Traylor and Schleyer [63,64].

While hyperconjugation is commonly invoked to account for the increased stability of carbocationic centers α to C-H bonds (via stabilization of the empty p orbital of the cationic center with C-H σ and σ* orbitals of proper symmetry),

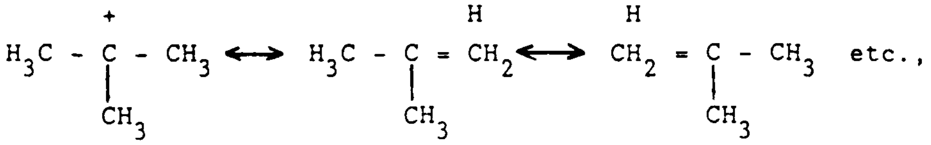

$$H_3C-\underset{|\atop CH_3}{\overset{+}{C}}-CH_3 \longleftrightarrow H_3C-\underset{|\atop CH_3}{C}=\overset{H}{CH_2} \longleftrightarrow \overset{H}{CH_2}=\underset{|\atop CH_3}{C}-CH_3 \quad \text{etc.,}$$

LXXXI

negative hyperconjugation involves the interaction of a filled p orbital with these σ and σ* orbitals and with π and π* orbitals by back-bonding stabilization.[64]

The energetic accessibility of these orbitals appears favorable in contrast to the high energy d-orbitals commonly invoked for period 3 and larger elements. Furthermore, several investigations have indicated a definite conformational dependency for negative hyperconjugation also implying a possible role of this phenomenon in accounting for the Series D E/Z isomer contrast.

Schleyer has asserted that negative hyperconjugation in neutral molecules accounts for the anomeric effect.[64]

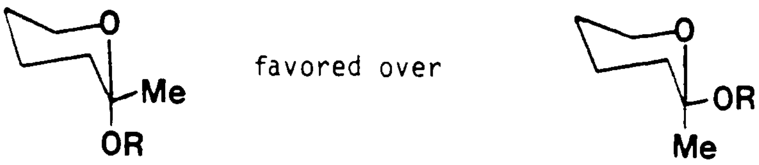

LXXXII

This is also seen in noncyclic structures. The lowest energy conformation for fluoromethylamine is such that the C-F bond and nitrogen lone pair are oriented 180° to each other and can interact hyperconjugatively.

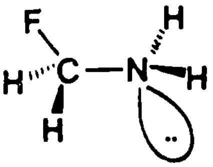

LXXXIII

A more dramatic example of the influence of negative hyperconjugation on molecular configuration was asserted by Weiss et al. in their study at that time of a new class of compounds: bis gem donor-acceptor substituted allenes.[66]

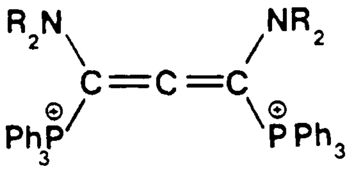

LXXXIV

X-ray characterization of this structure revealed an essentially planar structure, unique compared to the normal orthogonal projections of each half of the allene unit. This was credited partially to the orbital alignment required by negative hyperconjugation.

Finally, Kost and Raban [67] credited negative hyperconjugation with the 2-3 kcal/mole lower than expected barriers to nitrogen inversion in a series of N-benzenesulfenyl-2,2-dimethyl-aziridines:

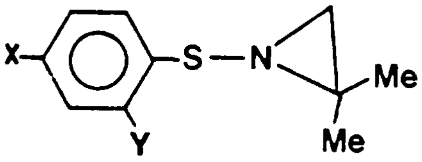

LXXXV

R $\begin{cases} X = OCH_3,\ CH_3,\ H,\ Cl,\ Br,\ NO_2 \\ Y = H,\ NO_2 \end{cases}$

Perturbational analysis indicated that attachment of an electronegative group R lessened the energy difference between the σ and σ* S-R orbitals, allowing a more favorable energy lowering when combined with the N lone pair in negative hyperconjugation. The increased double bond character from this interaction, which can be represented as shown below using the valence bond picture,

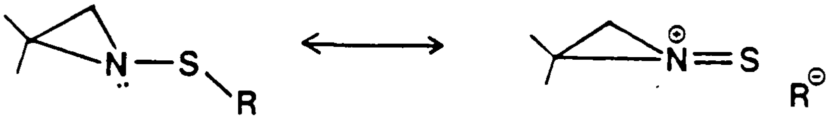

LXXXVI

led to lower inversion barriers. These authors also emphasized the requirement of optimal alignment of the three molecular orbitals involved in this process, π, σ, and σ*. In this case, overlap was maximized when the projection of the S-R bond bisected the CNC angle and the nitrogen lone pair was in a p orbital.

A critical observation made in all these investigations recognized the sensitivity of negative hyperconjugation to optimal orbital alignment. This seemed particularly germane to the E/Z isomer contrast in Series D, based on the steric demand of the SePh group. Whatever orbital alignment may actually be required for negative hyperconjugation to be optimized, more freedom to achieve this conformation is available to the E isomer. It should also be recognized that the strong e^- withdrawing inductive effect of the SePh moiety should further lower the energy of the Se -ipso C σ* orbital [67], increasing the likelihood of favorable negative hyperconjugative interaction. On the other hand, removal of optimal orbital alignment of the Ph system (in the Z configuration) could raise this σ* orbital energy to the point where negative hyperconjugation is no longer favorable, considerably reducing the SCS range of the Se atom in the Z isomer.

2) d-Orbital Involvement in Divalent Se Compounds/Evidence From the Literature

Though negative hyperconjugation is very much more likely to account for Se's e^- accepting tendency, it is useful to consider the possible role of d-orbital participation in this process. The observations related in the following references can be rationalized without invoking d-orbitals, but they are presented here in the interest of both an historical and alternative perspective.

d-orbital participation in divalent selenium compounds has not been extensively studied. It has been observed, however, that the $SeCF_3$ and SCF_3 groups show an e^- withdrawing mesomeric effect (-M) in contrast to the +M effect of the OCF_3 group. This has been credited to the involvement of empty d orbitals in Se and S for e^- accepting conjugation. The weaker -M property of $SeCF_3$ versus SCF_3 has been related to the more diffuse 4d orbitals of Se having a lesser tendency toward $p\pi$ - $d\pi$ conjugation than the 3d orbitals of S.[68] Dipole moments of p-SeMe and p-SMe substituted anilines support this contention:[69]

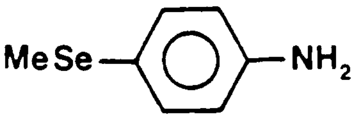

LXXXVII $\mu = 0.43D$

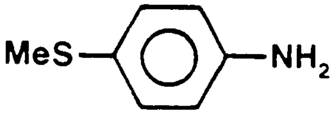

LXXXVIII $\mu = 0.68D$

The question of d-orbital involvement in all bonding schemes of sulfur has been studied extensively. The large acid-enhancing 3d-orbital resonance of the S atom has been argued to be responsible for the $10^2 - 10^3$ increase in the E2 reaction rates of p-substituted β-phenylmercapto chlorides versus their corresponding oxygen analogues.[70]

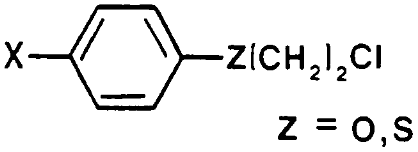

LXXXIX

These same investigators extended this work to evaluate sulfur's non-bonded interaction capability by adding an insulating methylene group:[71]

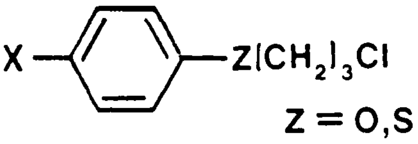

XC

The oxygen compounds gave faster E2 reactions here due to the stronger e^- withdrawing inductive effect of the O atom over that of the S atom.

However, the sulfur series gave a ρ value of 0.37 (R = 0.990), while for the oxygen series, ρ essentially equalled zero. This led the authors to postulate a small non-bonding interaction between a vacant 3d orbital on S and the developing double bond in the E2 transition state. The author's representation of this is shown below:

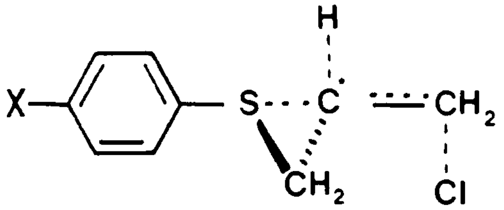

XCI

Here, the S atom is acting as a conduit for delocalization of e⁻ density from the incipient carbanionic-like reaction center(*) into the phenyl ring. The orbital alignment required for this dπ - pπ interaction can be represented as:

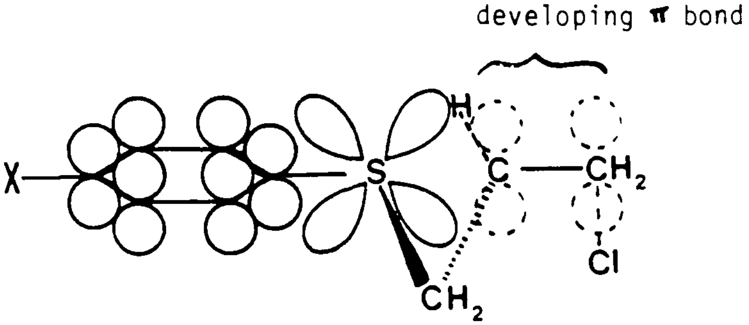

XCII

The increasing reaction rate for X = e⁻ withdrawers (and thus the +ρ value) supports this concept.

3) d-Orbital Participation of Se in Series D[72,73]

The nature of possible Se d-orbital participation in these compounds is difficult to predict. Again, it must be stressed that d-orbital participation is probably of little importance in these compounds. Nevertheless, two models, among others, can be used in the context of the E/Z steric effect. One ignores hybridization and concentrates on optimal orbital overlap. The other argues for an appreciable difference in hybridization of the Se atom in the two configurations, resulting in a change of conjugative efficacy. Reality may reflect a blend of both models, and hard structural data (X-ray) would be required for substantiation.

a) Model 1

Hybridization is ignored and Se's empty d orbitals are assumed to be degenerate. With these starting assumptions, that orbital optimally aligned for $p\pi$ - $d\pi$ overlap with the styryl system should be most favorable for interaction. Using this same d orbital, it can also be seen that further electron donation via the Se into the phenyl ring can occur by direct orbital π overlap. Se is thus acting as a conduit for the transmittal of e^- density. For this to be most effective, however, coplanarity of the entire Se/π system is required. To maximize this specific $p\pi$ - $d\pi$ - $p\pi$ overlap, a linear bonding arrangement also is required. These structural features are shown below:

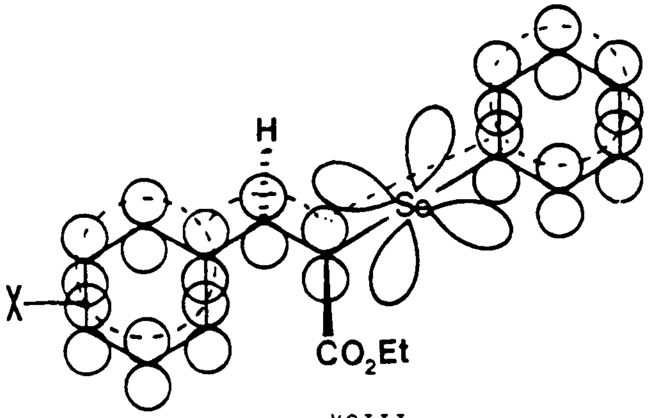

XCIII

This orbital alignment is quite similar to that invoked to account for sulfur's influence on E2 reaction rates in references 70 and 71.

The sp^3 hybridization of the Se valence electrons, of course, requires a much smaller C-Se-C bond angle than the linear arrangement optimizing d-orbital overlap. Attenuated but effective lateral overlap could still occur with the phenyl system as long as coplanarity could be maintained (shown below). This coplanarity is more accessible in the E (versus Z) configuration, thus making more likely this d-orbital participation. (It should be kept in mind that with d-orbital overlap, more latitude from coplanarity is possible.)

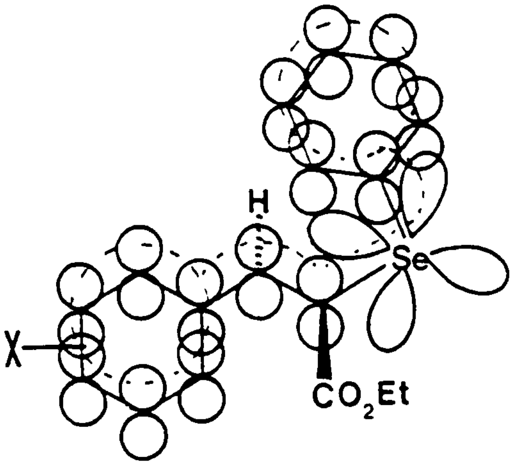

XCIV

Any increased participation of the d-orbital in this bonding picture within the substituent series may be expected to increase the observed C-Se-C bond angle, since greater importance of the linear structure is involved. X-ray crystal structure data of the p-NO_2 versus p-$N(Me)_2$ derivatives could be evaluated for any appreciable increase in bond angle as predicted by this model. (Qualitatively, the resonance structures LII B-C, page 144, using simple VSEPR (Valence Shell Electron Pair Repulsion) rules, call for a 109° to 120° bond angle increase, consistent with the increase in bond angle predicted using this d-orbital participation model.)

b) Model 2

In this model, Se is involved in appreciably different hybridization schemes in the two configurations. The greater planarity of the E isomer may allow greater orbital mixing, providing somewhat increased sd^3 character to the original sp^3 hybridization. This in turn could allow greater p character to that orbital involved in accepting e^- density from the π-styryl system, increasing efficacy of conjugation. The quotation below from Cotton and Wilkinson's Advanced Inorganic Chemistry may be applicable in this case to Se:[74]

> The two hybridization schemes giving a set of tetrahedrally directed orbitals, namely, sp^3 and sd^3, are only extremes, and it is possible to have a set of tetrahedral hybrids using one s orbital and portions of each of the sets d_{xy} d_{xz} d_{yz} and $p_xp_yp_z$. For carbon, the amount of d character is doubtless negligible since the lowest available d orbitals, the 3d's, are so far above the 2p's that their use could only be a great energetic disadvantage. With silicon, germanium, tin, and lead, this will not be so clear cut. Outer d orbitals may well play at least some part in the bonding in these MX_4 compounds.

In the Z configuration, less orbital mixing may occur, requiring a more pure, and thus higher energy d-orbital to act as the e^- acceptor, reducing the conjugative ability in this direction.

Experimentally, the influence of this effect may be more difficult to detect since sp^3 versus sd^3 hybridization involves similar bond angles.

In the context of this hybridization model, it should be stressed that while "pure" d-orbitals are possibly not involved directly in Se e^- acceptance, perturbational molecular orbital treatment shows that d-orbitals may play a significant role in stabilizing the energy levels of the σ and σ^* orbitals. This in many cases can lead to increased σ^*-n mixing, and thus a stronger negative hyperconjugative effect.[75]

C. Dual Substituent Parameter Analysis

1. General Comments

The ^{15}N SCS data from Series A and B, as well as the ^{77}Se SCS data from Series D (E isomer only) were subjected to Dual Substituent Parameter treatment using the REG (regression analysis) procedure incorporated in the statistical analysis package from the SAS Institute.[76] This was done in an effort to evaluate separately the polar and resonance components of substituent effects in these compound series. Generally, the ^{77}Se data gave good to moderate correlations using both the Swain-Lupton, [77]

$$\delta = f\mathcal{F} + r\mathcal{R} + h$$

where

δ = ^{77}Se chemical shift

f,r = weighting factors (relative DSP contribution)

$\mathcal{F},\mathcal{R}$ = polar and resonance constants for substituent, respectively

h = ^{77}Se chemical shift for parent compound

and Taft dual parameter techniques,[78]

$$\delta = \rho_I\sigma_I + \rho_R\sigma_R + h$$

where

ρ_I, ρ_R = weighting factors (relative DSP contribution, see Table 1, page 3)

σ_I = aliphatic polar substituent constant

σ_R = any of four resonance scales: $\sigma_R°$, σ_{R+}, σ_{R-}, $\sigma_{R+/-}$

The physical basis for each of these Taft resonance scales, which will be drawn upon in later discussion, is shown in Table 22.[79] In the Taft DSP treatment, the $\sigma_R°$ values were first employed to obtain a standard of comparison for the other resonance scales. (The $\sigma_R°$ scale is thought to be the best Taft scale for NMR correlations because the refined constants come from NMR analyses.)

With the ^{15}N SCS data only marginal to poor DSP results were obtained for Series A. The only exception to this was with the σ_R-

Table 22

Taft Resonance Models [79]

Resonance Scale	Resonance Model	Interpretations
$\sigma_R^{\bullet}$	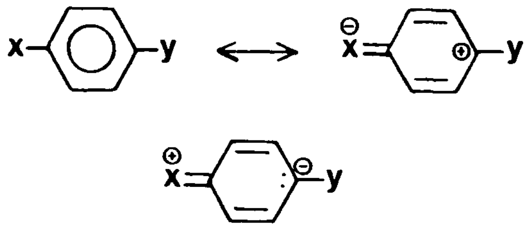 X = general substituent Y = probe site	Series for which neither e^- donating or withdrawing substituent effects from the para position are enhanced or retarded by quinoidial resonance effects (p-substituted fluorobenzene ^{19}F NMR shifts are included in the $\sigma_R\bullet$ basis set indicating that weakly interacting Y π-electron donor groups are also included.
σ_R^{+}	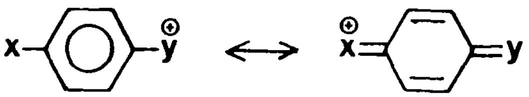	Y is a strongly interacting π-electron acceptor; NOTE: para quinoidal resonance is magnified for all groups compared to σ_R°; this effect is particularly strong for X = strong e^- donors.

Table 22 (Continued)

Resonance Scale	Resonance Model	Interpretations
σ_{R^-}	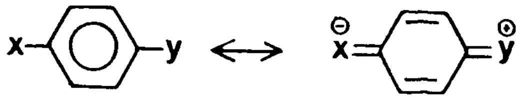	Y is a strongly interacting π-electron donor; NOTE: para quinoidal resonance is magnified for all groups compared to $\sigma_{R\bullet}$; this effect is particularly strong for X = strong e^- acceptors.
$\sigma_{R^{+/-}}$	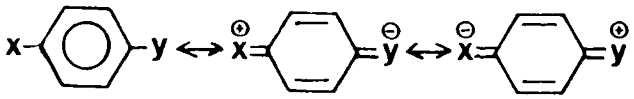	Y behaves both as a strong π acceptor and donor depending on electron supply and demand from X (extreme values from both scales employed)

scale employed in the Taft treatment of the Z isomer (a close parallel to the single substituent results). This, however, did involve a relatively limited data set. For Series B, very poor DSP results were observed, consistent with the poor quality of the single substituent correlations. With better and more meaningful results coming from the ^{77}Se data, this area will be presented first.

It must be stressed that the following discussion only covers possible interpretations that could be made if each of the derived DSP equations were, for whatever reason, expected to be the "correct" one. With no method to substantiate this, this discussion must be purely speculative, and these interpretations are certainly not advanced as defensible proposals.

2. ^{77}Se DSP Analysis/Series D (E Isomers)

Table 23 lists the $\sigma_I/\sigma_R°$ values (Taft treatment) and the *F/R* values (Swain-Lupton treatment) for the substituents used in this series.

The para and meta substituent chemical shifts were treated separately in the DSP equations, since they each give a different mix of resonance and polar/field demands. The results follow:

$(\lambda = \frac{\rho_R}{\rho_I}$ or $\frac{r}{f})$ [80]:

Para substituents

Taft

$$\delta_{Se} = 14.748\sigma_I + 43.329\ \sigma_R° + 351.934$$

$$R^2 = 0.9905 \qquad \lambda = 2.94$$

Table 23

DSP Parameters

X	σ_I	σ_{R°	F	R
para				
H	0.00	0.00	0.00	0.00
p-CO_2Me	0.20	0.16	0.47	0.67
p-Cl	0.46	-0.18	0.72	-0.24
p-CN	0.56	0.08	0.90	0.71
p-N(Me)$_2$	0.06	-0.55	0.69	-3.81
p-F	0.50	-0.31	0.74	-0.60
p-MeO	0.27	-0.42	0.54	-1.68
p-Me	-0.04	-0.13	-0.01	-0.41
p-NO_2	0.65	0.15	1.00	1.00
p-CF_3	0.42	0.08	0.64	0.76
p-Ph			0.25	-0.37
meta				
m-Cl	0.46	-0.18	0.72	-0.24
m-CN	0.56	0.08	0.90	0.71
m-F	0.50	-0.31	0.74	-0.60
m-MeO	0.27	-0.42	0.54	-1.68
m-NO_2	0.65	0.15	1.00	1.00
m-CF_3	0.42	0.08	0.64	0.76

Swain

$$\delta_{Se} = 5.955F + 8.178R + 351.340$$

$R^2 = 0.9645$ $\lambda = 1.37$

Meta substituents

Taft

$$\delta_{Se} = 10.953\sigma_I + 0.148\sigma_{R^\circ} + 351.832$$

$R^2 = 0.9756$ $\lambda = 0.014$

Swain

$$\delta_{Se} = 7.122F + 0.210R + 351.676$$

$R^2 = 0.9925$ $\lambda = 0.029$

The $\sigma_R \cdot$ scale does not invoke charge transfer through the π system by para-quinoidal through-resonance interaction of the Se atom. With this basis, the substituent's polar (σ_I) effect on Se can be evaluated in the context of an otherwise unperturbed π-system. In trying to invoke a physical model, it is known that the polar effect of X can be manifested in the styryl backbone by the π-polarization phenomenon. This was verified for this series of compounds by the alternating slopes of the $^{13}C/\sigma$ correlations, as shown below:

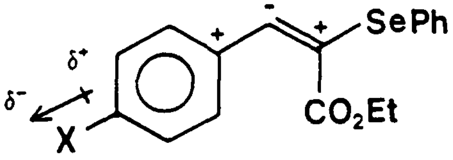

LIIA

The Taft DSP equation shows that the polar effect on the ^{77}Se chemical shift results in greater deshielding, augmenting the deshielding resonance effect. Possibly, this deshielding may stem from some degree of polarization of the β-carbon/selenium bond; but how may this occur?

This raises a complex issue. Even for the much smaller and presumably simpler F atom, much debate has centered not only over the best way to account for a substituent's polar effect on the C-F bond, but also whether this effect is accurately reflected in ^{19}F SCS values.[81] For fluoroaromatics, this debate has largely centered on the relative influence of direct through-space field effects versus π-polarization acting via the π-orbital framework.

Reynolds has shown that both these effects can be involved in the polar component of ^{19}F SCS values. However, in studies of structures XCV through XCVII,[82]

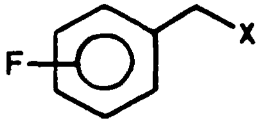

XCV

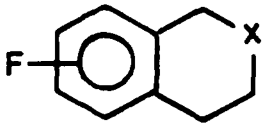

XCVI

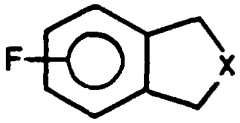

XCVII

a close parallel was seen between the polar effects on ^{19}F chemical shifts, and polar effects on the corresponding ^{13}C chemical shift in the unsubstituted analogue. Reynolds goes on to state:[83]

> Since the latter undoubtedly reflected aromatic π polarization effects, this suggested that π-polarization was also responsible for the ^{19}F chemical shifts [84]. Calculations indicated proportional changes in fluorine (q_F^{π}) and carbon (q_C^{π}) π electron densities,
>
> $$q_F^{\pi} \approx 0.1\ q_C^{\pi}$$
>
> indicating that π polarization at the carbon induced correspondingly smaller changes at fluorine, presumably by inducing π electron transfer from fluorine to the aromatic ring, that is, field-induced resonance.[84]

The unshared electron pairs on Se provide some analogy with F in terms of the possibility of this "field-induced resonance" process, although here the presence of the styryl system changes the molecular model. It should also be kept in mind that, while the styryl backbone may be responding to the polar effect by π-polarization, the Se atom itself may be affected by an entirely different polar mechanism, one perhaps unique to the diffuse but abundant electron density of the Se atom. One possibility may be that the Se can interact more directly through space with the substituent dipole rather than interacting strictly via the π system.

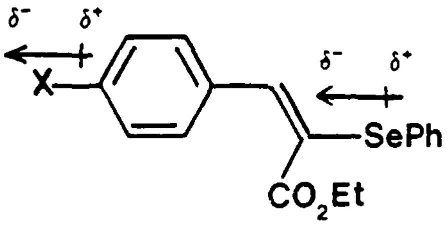

LIIA

The Swain DSP equation shows a greater balance of resonance and polar effects (57.9% resonance/42.1% polar) for para substituents. However, both the Swain and Taft equation for meta substituents indicate a complete reversal of the relative importance of resonance versus polar effects. The Swain equation shows a 97.1% polar/2.9% resonance balance and indicates that not only does the polar effect result in a deshielding of Se, but also that this deshielding effect can indeed act independently of the charge-transfer via through-resonance phenomenon since this kind of interaction is not possible with meta substituents. Se's highly sensitive nature to polar as well as resonance effects is shown here.

The Taft DSP equation was also used employing the σ_{R^+}, σ_{R^-}, and $\sigma_{R^{+/-}}$ scales for the para substituents listed in Table 24.

Table 24

Taft Resonance Scale Values

X	σ_{R^+}	σ_{R^-}	$\sigma_{R^{+/-}}$
H	0.00	0.00	0.00
Cl	0.11	0.23	0.11
CN	0.66	0.90	0.90
$N(Me)_2$	-1.70	-0.83	-1.70
F	-0.07	0.06	-0.07
MeO	-0.78	-0.27	-0.78
Me	-0.31	-0.17	-0.31
NO_2	0.78	1.24	1.24

For comparison, the DSP treatment using the $\sigma_R^\bullet$ scale was repeated for these eight substituents. The resulting DSP equations, in decreasing order of R^2 follow:

$$\delta_{Se} = -5.520\sigma_I + 15.267\sigma_{R^{+/-}} + 352.209$$

$$R^2 = 0.9942 \qquad \lambda = -2.77$$

$$\delta_{Se} = 14.530\sigma_I + 44.657\sigma_R^\bullet + 352.471$$

$$R^2 = 0.9920 \qquad \lambda = 3.07$$

$$\delta_{Se} = -14.869\sigma_I + 24.017\sigma_{R^-} + 350.437$$

$$R^2 = 0.9742 \qquad \lambda = -1.62$$

$$\delta_{Se} = -1.313\sigma_I + 16.418\sigma_{R^+} + 352.440$$

$$R^2 = 0.9655 \qquad \lambda = -12.50$$

With the σ_I term an essentially constant factor between these equations, this Taft DSP approach could be exploited to evaluate which single resonance scale is most appropriate in describing Se's behavior in this compound series. The overall picture one may obtain from these DSP equations is that whenever para-quinoidal resonance interaction is invoked (see Table 22), a counteracting shielding effect (negative coefficient) arises from the polar term. Mechanistically, this would be consistent with a buildup of negative charge on Se as a result of the δ+ (generated by the π-polarization mechanism) on the adjacent sp^2 carbon. This would constitute a polarization pattern opposite to that seen using the $\sigma_{R\cdot}$ scale.

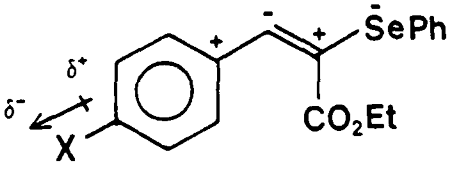

LIIA

However, these negative σ_I coefficients may to a certain extent be artifacts of the exaggerated deshielding resonance interaction embodied in the chosen σ_R scale. The use of σ_{R^+}, which incorporates a greater relative importance to Se's acting as an electron acceptor for those X's that are highly electron donating via resonance (i.e., p-N(Me)$_2$ and p-MeO),

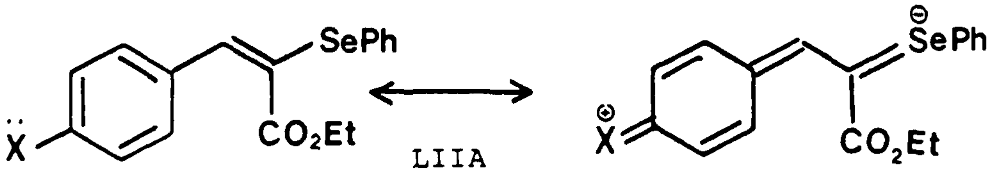

LIIA

only requires a small shielding contribution ($\rho_I = -1.313$) from the σ_I component (recall that all para-quinoidal resonance is favored using σ_{R+}, including the deshielding influence.) In contrast, when the σ_{R-} scale is employed, accentuating the deshielding effect of through conjugation for X=strong electron withdrawers by resonance (X=NO_2, CN),

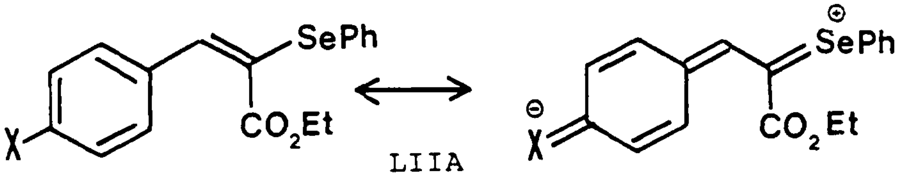

LIIA

a much larger shielding contribution (ρ_I = -14.869) is required from the polar term. That the σ_{R+} may better estimate the nature of para-quinoidal resonance is also supported by its much larger λ value (-12.50) versus that for σ_{R-} (-1.62).

However, to say that the σ_{R+} scale is "better" than the σ_{R-} scale is made difficult by the R^2 comparisons of the DSP equations; R^2 (σ_{R-}) = 0.9742 > R^2 (σ_{R+}) = 0.9655 (page 176). Perhaps of greater value is recognizing the overall flexibility of Se in terms of its resonance ability in both directions as indicated by the excellent (and best) fit of the $\sigma_{R+/-}$ scale (R^2 = 0.9942), with a moderate reverse σ_I effect (ρ_I = -5.520, λ = -2.77). One could conclude from these comparisons that the best single resonance scale to describe Se's mesomeric behavior in this series would be a scale somewhere between σ_{R+} and $\sigma_{R+/-}$. Specifically, this scale would retain the exaggerated values for X = electron donors, but attenuate those values for X = strong electron withdrawers.

3. ^{15}N DSP Analysis/Series A and B

Series A and B were subjected in like manner to DSP analyses of the ^{15}N chemical shift data. For both series, only the para substituent data was analyzed, since not enough meta substituents were available for a meaningful analysis. As with the ^{77}Se data, the $\sigma_R°$ scale was first employed in the Taft equation for subsequent comparison to the other resonance scales.

a. Series A

The ^{15}N chemical shift data for the (E) and (Z) enamine isomers from Series A gave the following initial DSP results:

Z Isomer

Taft

$$\delta_N = 5.902\sigma_I + 12.920\sigma_R° - 327.412$$

$R^2 = 0.9682$ $\lambda = 2.19$

Swain

$$\delta_N = 2.523F + 2.428R - 327.656$$

$R^2 = 0.9308$ $\lambda = 0.96$

E Isomer

Taft

$$\delta_N = 7.245\sigma_I + 11.592\sigma_R° - 300.255$$

$R^2 = 0.8926$ $\lambda = 1.60$

Swain

$$\delta_N = 4.806F + 2.125R - 301.269$$

$R^2 = 0.8184$ $\lambda = 0.44$

These results, particularly in the context of Z/E isomer comparisons must be treated more cautiously than previous series; the important p-NO_2 substituent value was unavailable for the Z isomer. Thus, any apparent superiority of the DSP results for the Z isomer could largely be due to this exclusion.

However, for both isomers it does appear that the Taft DSP equation using the simple σ_R° scale for unperturbed aromatic systems gives a better result than the Swain treatment. The Taft approach also puts more emphasis on the substituent resonance effect, while Swain accentuates the polar term. Finally, in all cases, no "reverse" effect is noted (an opposite sign before the σ_I or F variable). In the context of the resonance scale used here (σ_R°, calling for small resonance donation by N into the styryl π system) the polar effect in some fashion augments the deshielding of the N atom as observed using σ_R° for Se.

The Taft treatment was extended to the σ_{R^+}, σ_{R^-}, and $\sigma_{R^{+/-}}$ scales, excluding the p-CO_2Me, p-CF_3, and p-Ph substituents. (The values for these groups were not available for analysis.) The results for each isomer in decreasing order of R^2 were:

Z Isomer (also excludes p-NO_2)

$$\delta_N = -3.233\sigma_I + 8.038\sigma_{R^-} - 327.636$$

$R^2 = 0.9968$ $\lambda = -2.49$

$$\delta_N = 6.142\sigma_I + 13.609\sigma_R^{\circ} - 327.217$$

$R^2 = 0.9688$ $\lambda = 2.22$

$$\delta_N = 0.018\sigma_I + 4.478\sigma_{R^{+/-}} - 327.385$$

$R^2 = 0.9516$ $\lambda = 248$

$$\delta_N = 0.715\sigma_I + 4.567\sigma_{R^+} - 327.386$$

$R^2 = 0.9117$ $\lambda = 6.39$

E Isomer (includes p-NO_2)

$$\delta_N = -0.088\sigma_I + 6.681\sigma_{R^-} - 300.797$$
$R^2 = 0.8978$ $\lambda = -75.92$

$$\delta_N = 7.719\sigma_I + 11.202\sigma_{R^\bullet} - 300.475$$
$R^2 = 0.8692$ $\lambda = 1.45$

$$\delta_N = 3.205\sigma_I + 3.395\sigma_{R^{+/-}} - 300.827$$
$R^2 = 0.7900$ $\lambda = 1.06$

$$\delta_N = 4.028\sigma_I + 3.281\sigma_{R^+} - 300.957$$
$R^2 = 0.7307$ $\lambda = 0.82$

Because of the lack of a common substituent series between these two isomers, interisomer comparisons will not be attempted. However, within each isomer series, common trends were observed from the best to the worst fitting resonance scale: $\sigma_{R^-} > \sigma_{R^\bullet} > \sigma_{R^{+/-}} > \sigma_{R^+}$. The only excellent correlation result obtained from all of Series A employed the σ_{R^-} scale for the Z isomer using a relatively limited substituent set. This was consistent with the superior fit obtained using the σ^- single substituent scale and clearly indicated strong through-resonance of the diethylamino nitrogen to be a dominant electronic property of these compounds. However, the degree of deshielding invoked by this full through-resonance effect was compensated by the mathematical artifact of a significant shielding polar term (negative σ_I coefficient) as seen earlier with the ^{77}Se data. The physical explanation for this mathematical artifact may be that steric encumbrance may be reducing somewhat the level of N's through-resonance, requiring the compensating polar term in the DSP treatment. It is tempting, in continuing this line of argument, that for the E isomer (where this steric encumbrance to through-resonance donation is less of a factor) a much lower shielding compensating polar term is required. The much poorer R^2 value (and lack of a common substituent set) makes this comparison, however, quite tenuous.

The worst fitting by σ_{R+} for both isomers, conversely, revealed the lack of electron acceptance of nitrogen by through resonance (being a second-period element, nitrogen can not expand its valence shell, like Se can, to take on additional electron density). Finally, it should be pointed out that the E isomer DSP results were all poor, paralleling the correlative nature of this isomer in the single substituent parameter treatment.

b. Series B

The DSP results for the benzylidene azlactones (Series B) were very poor, as obtained from the single substituent treatment:

Taft

$$\delta_N = -1.717\sigma_I - 1.020\sigma_{R^\circ} - 141.487$$

$R^2 = 0.8334$ $\lambda = 0.59$

Swain

$$\delta_N = -0.705\mathcal{F} - 0.338\mathcal{R} - 141.627$$

$R^2 = 0.8464$ $\lambda = 0.48$

At the very best, these expressions illustrate the predominant influence of the polar effect on these ^{15}N δ's, due to lack of resonance interaction of the unshared electron pair of the nitrogen atom. The negative coefficients observed are consistent with negative charge buildup (greater shielding) associated with π-polarization phenomenon at N:

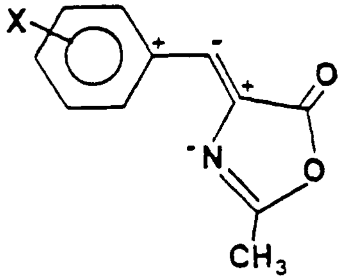

L

To evaluate the other resonance scales in the Taft treatment, DSP analysis was repeated for the above substituents (except p-CO_2Me, since this value was unavailable), giving the following results (listed in decreasing order of R^2):

$\delta_N = -0.976\sigma_I - 0.554\sigma_{R+} - 141.654$

$R^2 = 0.9320$ $\lambda = 0.57$

$\delta_N = -0.960\sigma_I - 0.461\sigma_{R+/-} - 141.603$

$R^2 = 0.8923$ $\lambda = 0.48$

$\delta_N = -1.620\sigma_I - 1.915\sigma_{R\bullet} - 141.568$

$R^2 = 0.8474$ $\lambda = 1.18$

$\delta_N = -0.901\sigma_I - 0.607\sigma_{R-} - 141.498$

$R^2 = 0.8255$ $\lambda = 0.67$

Perhaps the most useful information from these results is that σ_{R+} gives the best fit, and σ_{R-} the worst. Qualitatively, this parallels the single substituent parameter results in that σ^- gave by far the worst correlation indicating complete lack of any through resonance donation by nitrogen into the styryl system of the benzylidene structure (prohibited due to orthogonality of the unshared electron pair to the π styryl system).

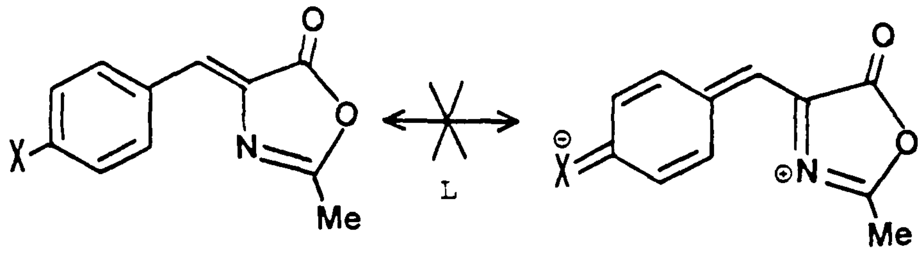

The relatively "good fit" of the σ_{R^+} scale implies that the following resonance structures (with its increased shielding effect) may have some limited importance:

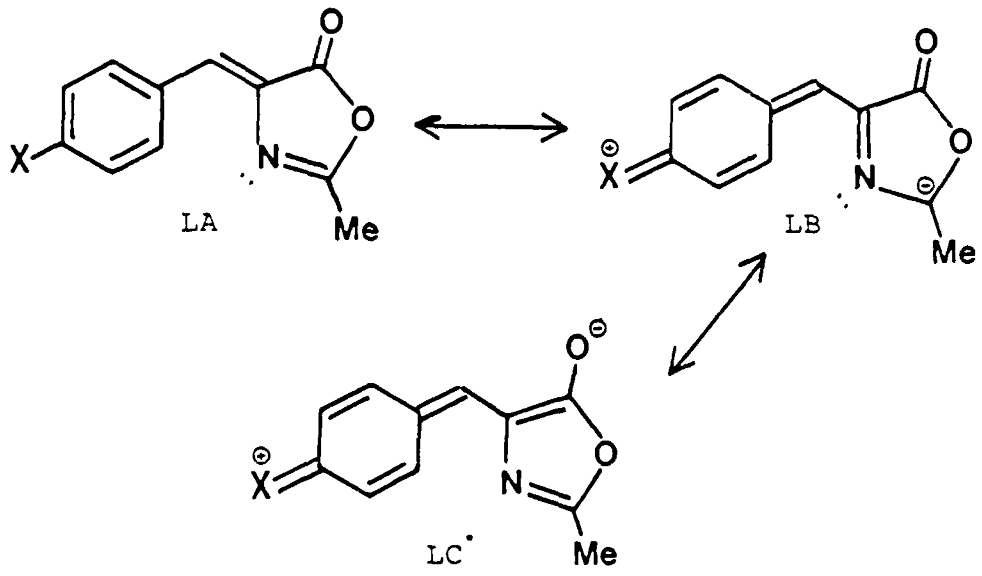

Here increased charge density of the azlactone ring can be accommodated due to the imino enolate contributing structure (*). This resonance structure is also further stabilized by aromaticity of the heterocyclic ring. The particularly good σ^+ correlations of the

C-7 and C-8 carbons cited in reference 60 also supports this concept. This increased charge density would increase shielding of the N.

The inferiority of the σ^- scale also suggests that through-resonance e^- donation from the oxazolone oxygen atom is not an important resonance phenomenon,

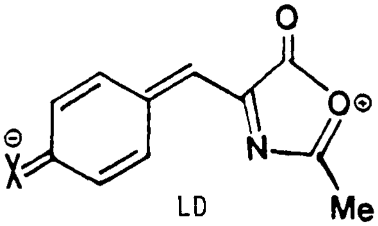

LD

although one can recognize that any influence of this process would further scramble the data, since it is acting in a direction opposing that characterized by σ^+.

The overall poor N DSP correlations indicate the probable influence of the phenyl ring anisotropy on the unshared electron pair of the N atom, again paralleling the single substituent parameter results.

In summary, DSP treatment appeared to be more useful for Se versus N in terms of improving the correlations. The more complex electronic nature of the Se atom would logically render it more amenable to clarification by DSP treatment. Specifically, the flexibility of Se acting as an e^- donor and acceptor was more clearly shown (using the $\sigma_{R^{+}/-}$ Taft resonance scale), than with the single substituent method, where more bias was placed on Se's e^- accepting role.

For N, DSP analysis was less useful, perhaps to some extent due to the simpler nature of this atom, and that fewer substituents were used in the analysis. Results for Series A closely paralleled those from single substituent treatment. However, for Series B, DSP analysis indicated significantly more importance for the iminoenolate resonance form; a significant improvement using the σ_{R^+} Taft scale ($R^2 = 0.9320$) was observed versus the best single substituent scale (σ), ($R^2 = 0.8016$).

D. ^{13}C Correlations

1. Series A/General Comments

Correlations of the ^{13}C chemical shift data for both the Z and E isomers were carried out principally to gain further understanding of the interplay of the through-resonance and π-polarization mechanisms. A comprehensive assignment table for Series A is given in Table 26, page 188 (Z isomer) and Table 27, page 189 (E isomer). These assignments were made based on substituent effects observed in a large variety of β,β- disubstituted styryl systems.

Table 25 below lists the correlation results (in order of decreasing R^2) for selected carbon nuclei of each isomer.

a. General Interpretation of the Data

The alternating signs of the correlation slopes going from carbons 6 through 4 for both isomers indicates the overall predominance of the π-polarization mechanism in accounting for this ^{13}C SCS data, consistent with results obtained from many other β,β-disubstituted styryl series. A more detailed analysis here, however, can provide some assessment of the effect on the ^{13}C shieldings of the through-resonance phenomenon from the N nucleus acting in conjunction with the π-polarization mechanism.

Table 25

Correlation Results For Selected ^{13}C Nuclei/Series A

Z	E
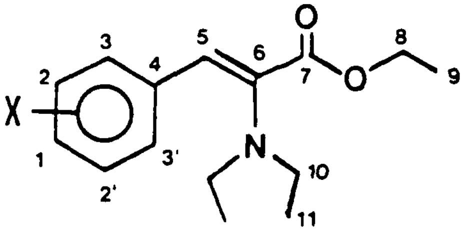	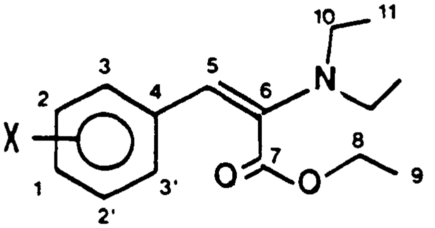

	Z			E		
	Scale	R^2	Slope	Scale	R^2	Slope
#6	σ	0.923	6.81	σ	0.944	3.65
	σ^{13}	0.914	4.06	σ^-	0.944	2.98
	σ^-	0.887	5.44	σ^{13}	0.929	2.17
	σ^+	0.883	4.30	σ^+	0.898	2.30
#5	σ^+	0.704	-3.04	σ^-	0.567	-2.46
	σ	0.701	-4.70	σ	0.494	-2.82
	σ^{13}	0.699	-2.81	σ^{13}	0.427	-1.57
	σ^-	0.608	-3.56	σ^+	0.407	-1.65
#4	σ^-	0.879	10.25	σ^+	0.939	7.87
	σ^+	0.872	8.09	σ^{13}	0.923	7.25
	σ^{13}	0.872	7.51	σ	0.906	11.99
	σ	0.858	12.44	σ^-	0.860	9.49
#10	σ^+	0.011	-.03	σ^-	0.740	0.699
	σ	0.008	-.04	σ	0.659	0.810
	σ^{13}	0.008	+.008	σ^{13}	0.636	0.477
	σ^-	0.004	-.02	σ^+	0.597	0.498

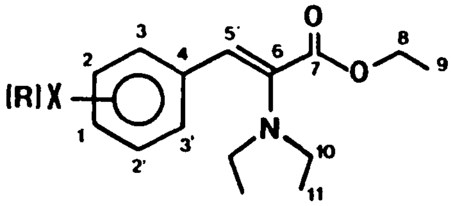

Table 26

^{13}C Assignments (J_{C-F} in Hz)

(Z) Ethyl-2-diethylamino-3-phenyl-2-propenoates

#C	$pN(Me)_2$	pMeO	pMe	pPh	pF	H	pCl	mF	mCl	pCO_2Me*	mCN	pCF_3	pCN	pNO_2
1	151.66	160.86	139.37	141.86	163.78 (246.8)	130.39	134.14	117.07 (23.0)	130.07	130.35	132.40	130.34 (32.1)	111.23	149.01
2'								131.15 (8.4)	130.21		131.93			
2	111.99	114.30	129.57	127.96	116.18 (21.5)	129.24	128.93	163.99 (241.9)	138.19	130.35	113.54	126.20 (3.33)	132.86	124.90
3'								127.66 (2.7)	129.08		136.62			
3	133.09	132.94	131.07	130.16	133.61 (8.0)	131.22	132.22	116.12 (21.6)	130.27	130.89	135.23	131.32	130.92	129.68
4	123.73	130.74	133.34	135.95	133.38 (3.2)	136.64	134.90	139.37 (8.3)	140.57	144.67	137.45	141.06	141.49	145.59
5	135.59	128.71	131.84	128.83	130.10 (0.0)	129.43	128.66	128.09 (0.0)	127.76	126.35	126.09	128.05	129.20	126.94
6	133.91	136.65	138.08	139.87	139.63 (2.3)	139.56	139.71	141.33	140.97	141.66	144.85	142.28 (5.3)	142.57	145.59
7	167.54	167.37	167.28	168.10	168.25	167.96	167.03	168.18	167.01	167.94	167.88	168.11	167.52	168.47
8	60.55	60.89	60.95	61.76	61.92	61.59	61.22	62.15	61.32	52.80	64.31	62.22	62.03	65.76
9	14.73	14.65	14.61	14.77	14.79	14.69	14.57	14.75	14.53		14.70	14.71	14.59	14.03
10	47.74	47.58	47.43	47.81	47.91	47.59	47.35	47.85	47.26	47.65	47.73	47.71	47.41	47.73
11	13.97	13.92	13.89	14.12	14.08	14.00	13.85	14.06	13.85	14.02	14.02	14.02	13.91	13.13
R	40.07	55.47	21.37	138.23(1) 127.74(o) 131.96(m) 130.07(p)						168.53 52.61	120.07		120.04	

*^{13}C assignments for (Z) Methyl-2-diethylamino-3-(4-carbomethoxyphenyl)-2-propenoate

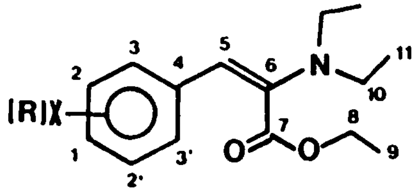

Table 27

^{13}C Assignments (J_{C-F} in Hz)

(E) Ethyl-2-diethylamino-3-phenyl-2-propenoates

#C	pN(Me)$_2$	pMeO	pMe	pPh	pF	H	pCl	mF	mCl	pCO$_2$Me*	mCN	pCF$_3$	pCN	pNO$_2$
1	149.47	160.47	135.06	141.53	162.02 (241.6)	129.16	136.00	113.89 (21.8)	128.64	128.93	130.88	129.29 (32.6)	107.29	147.27
2'								131.15 (8.4)	134.42		129.98			
2	113.17	114.50	129.50	127.80	116.09 (21.6)	129.24	128.93	164.34 (241.5)	134.33	130.74	113.26	126.35 (3.73)	132.98	125.14
3'								123.83 (2.5)	124.89		131.97			
3	128.46	133.03	127.41	128.20	129.56 (7.6)	127.70	128.79	112.21 (21.2)	125.60	126.96	130.43	127.65	127.25	126.94
4	126.60	131.08	135.68	136.98	135.81 (2.9)	139.06	137.57	142.08 (8.9)	143.72	142.12	140.94	143.77	144.31	144.99
5	129.93	129.20	129.57	129.88	130.10 (0.0)	129.59	128.93	128.09 (0.0)	126.80	126.35	128.94	127.65	124.14	126.98
6	140.30	141.68	142.16	143.43	143.59 (0.0)	143.13	143.23	144.43	143.78	144.47	145.06	145.11	145.28	146.54
7	169.02	168.70	168.52	169.15	169.24	168.98	168.11	169.07	168.00	168.17	168.64	168.82	168.16	168.47
8	61.57	61.87	61.69	62.65	61.92	62.34	62.00	63.01	62.07	53.23	63.06	63.08	62.92	63.59
9	13.97	13.92	13.89	14.12	14.18	14.05	13.91	14.17	13.93		14.16	14.11	14.00	14.13
10	43.98	43.97	44.02	44.58	44.61	44.37	44.16	44.79	44.23	44.96	44.83	44.91	44.81	45.37
11	12.32	12.38	12.44	12.74	12.80	12.69	12.56	12.65	12.59	12.89	12.86	12.91	12.91	13.13
R	40.59	54.64	20.97	138.49(i) 127.63(o) 128.20(m) 128.77(p)						169.38 52.53	120.42		120.62	

*^{13}C assignments for (E) Methyl-2-diethylamino-3-(4-carbomethoxyphenyl)-2-propenoate

Qualitatively, the electron donating through-resonance effect acting from the N nucleus into the styryl system will tend to lessen the δ^+/δ^- charge segregation stemming from the π-polarization mechanism alone (shown below for E isomer).

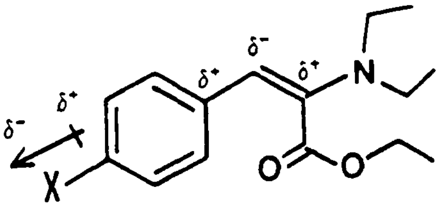

XLIXA

π-polarization effect alone

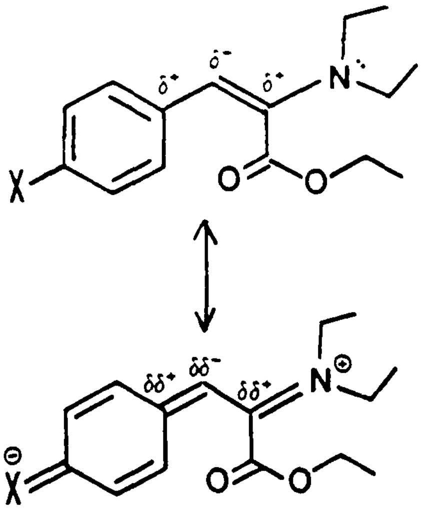

π-polarization effect attenuated by through-resonance

As a result, a lower SCS range (and resultant slope) would occur in conjunction with a stronger through-resonance effect. Consistently, a lower slope was observed for all correlations of E isomer ^{13}C nuclei versus their Z isomer counterparts.

As further evidence, an E/Z comparison of the #10 carbon correlations (the methylene carbons attached to the ^{15}N nucleus) shows that a meaningful (albeit very crude) correlation is seen only for the E isomer. In complete contrast, no correlation is seen in the Z isomer. This argues that steric encumbrance of optimal deshielding alignment of the $N(\underline{Et})_2$ ethyl groups is indeed greater in the Z versus E configuration. (Molecular models suggest this possibility.)

In the E isomer, sufficiently greater through-resonance occurs (perhaps aided by lack of steric encumbrance) to allow some slight observance of greater deshielding for these ^{13}C nuclei.

The #7 carbon (carbonyl) data revealed a complete lack of any substituent effect in both isomers.

b. Specific Aspects of the Data

1) #6 Carbon Correlations

For both isomers, the σ scale gave the best correlation result (σ^- tied with it in the E isomer). This could reflect an overall balance of the influences of deshielding π-polarization and shielding through-resonance, which would be particularly strong at this site. In the E isomer, where through-resonance is more pronounced, σ^- is comparable to σ with R^2 values greater than any in the Z correlations; for Z where through-resonance is less pronounced the σ^{13} scale placed second with σ^- third. σ^+ being last for both isomers was consistent with the #6 carbon being adjacent to a through-resonance electron donor.

2) #5 Carbon Correlations

For each isomer, the individual Hammett scale correlations were so poor that no definite conclusions could be reached concerning the relative merits of these scales for each isomer; the scatter was so significant that little confidence could be placed in the absolute difference in R^2 values. It can be said that as a group, the Z R^2 values appeared better than those of the E isomer, in opposite fashion to the #6 correlation.

To rationalize this comparison, the δ^- inherent in #5 carbon shielding can be understood to be related to the δ^+'s generated on either side of it at C4 and C6. The more intense and well-defined the δ^+ at C6, the better should be the correlative behavior at C5. It has been shown that through-resonance counteracts the π-polarization effect, lessening the δ^+ at C6 and thus causing a reduced correlation at C5. For the E isomer, where through-resonance is more important, the #5 R^2 values are indeed lower. For Z, the greater δ^+ at C6 due to a lesser influence of through-resonance allows a more significant δ^- at C5 and a better correlation.

3) #4 Carbon Correlations

For the Z isomer, all four scales are essentially equivalent in R^2 value reflecting a balance from the effects of attenuated $N(Et)_2$ electron donation and CO_2Et electron acceptance, the same factors attributed to the Z isomer's overall better ^{15}N SCS correlation, page 118.

The E isomer shows a significant R^2 superiority of σ^+ over σ^-. This difference in correlative behavior from the #4 carbon of the Z isomer (where essentially equivalent R^2's were found) is difficult to rationalize. One could argue that the #4 carbon is far enough removed from the push/pull trade-off of the $N(Et)_2/CO_2Et$ system to reflect that process best stabilizing the δ^+ at this site: σ^+.

4) The #5 and #6 Carbon Shieldings

For both isomers, the α carbon (#5) was more shielded than the β carbon (#6), with the exception of the Z p-N(Me)$_2$. This confirms the greater influence of the N(Et)$_2$ effecting the carbon-carbon double-bond polarization over that of the carboxylate group:

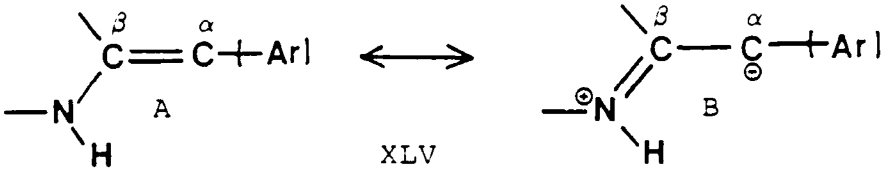

XLV

This is consistent with what was observed in the aryl methylenehydantoins, reference 38, page 28.

Another interesting observation was that the difference in chemical shift between the α and β carbons was consistently greater (except for the m-CN compound) in the E isomer versus the Z. This could reflect the greater push/pull influence of the N(Et)$_2$ and CO$_2$Et moieties of the E isomer. However, poor correlations were obtained for all four substituent scales for the #5 carbon in both isomers, unlike the good σ^- and σ correlation results observed for this nucleus in the aryl methylenehydantoins.[38] The lack of a rigidly planar system in the Series A enamines would appear to be a major reason for these inferior correlations.

2. Series D (E isomers)

^{13}C correlations were also carried out for the #6, #5, and #4 carbons of the ethyl α-(phenylseleno)cinnamates (E isomers). A comprehensive assignment table for Series D (E isomers) is given in Table 29, page 195. Table 28 below lists the correlation results (in order of decreasing R^2) for these nuclei.

Table 28

Correlation Results For Selected ^{13}C Nuclei/
Series D (E Isomers)

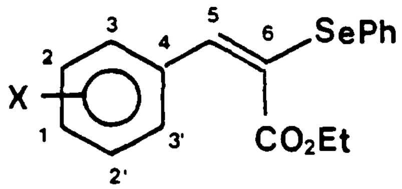

	Scale	R^2	Slope
#6	σ^+	0.961	11.54
	σ^{13}	0.959	10.80
	σ	0.911	17.19
	σ^-	0.873	14.10
#5	σ	0.966	-4.67
	σ^-	0.911	-3.80
	σ^{13}	0.909	-2.78
	σ^+	0.876	-2.91
#4	σ^{13}	0.841	6.13
	σ^+	0.838	6.53
	σ^-	0.798	8.17
	σ	0.781	9.65

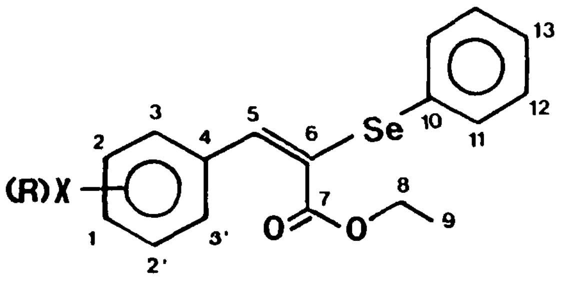

Table 29

^{13}C Assignments (J_{C-F} in Hz)

(E) Ethyl-3-phenyl-2-phenylseleno-2-propenoates

#C	pN(Me)$_2$	pOMe	p-Me	p-Ph	p-F	H	m-OMe	p-Cl	m-F	m-CL	p-COOMe	m-CN	m-CF$_3$	p-CF$_3$	p-CN	m-NO$_2$	p-NO$_2$
1	150.66	160.80	139.96	142.19	163.14 (251.4)	129.45	115.59	135.37	116.21 (21.2)	129.17	130.28	132.20	125.68 (3.8)	130.73 (32.8)	112.21	123.52	147.51
2'							129.14		129.63 (8.1)	129.31		128.97	128.61			129.01	
2	111.05	113.61	128.88	126.76	115.27 (21.9)	128.12	159.21	128.39	162.88 (245.6)	134.04	129.27	112.43	130.54 (32.2)	125.07 (4.07)	131.76	147.82	123.37
3'							122.95		126.05 (2.7)	128.14		133.11	126.63 (3.8)			135.54	
3	133.06	132.47	130.38	130.85	132.31 (8.2)	130.18	114.87	131.43	116.52 (22.3)	129.74	129.82	133.94	133.00	130.07	130.20	124.47	129.27
4	115.28	121.28	122.85	126.91	123.83 (0.00)	128.27	129.27	125.04	128.56	126.37	132.07	128.05	128.75	132.14	132.16	128.49	132.48
5	147.62	145.58	145.27	144.46	143.78	144.78	144.49	143.28	142.73	142.45	142.61	140.98	142.21	142.15	141.06	140.64	140.57
6	111.70	120.47	128.17	131.00	131.15 (3.4)	130.92	131.64	133.44	135.59	136.75	139.43	136.27	135.80	138.62	139.46	136.56	141.51
7	167.28	166.78	166.63	166.55	166.46	166.51	166.53	166.32	166.28	166.20	166.18	165.94		166.16	165.91	165.93	165.99
8	61.42	61.66	61.69	61.78	61.85	61.76	61.79	61.88	61.91	61.91	61.92	62.12	62.02	62.04	62.09	62.14	62.27
9	13.79	13.77	13.75	13.76	13.77	13.73	13.75	13.75	13.73	13.74	13.70	13.80	13.76	13.75	13.72	13.78	13.76
10	129.61	129.61	129.18	129.26	129.31	129.24	130.91	129.34	129.36	130.31	129.27	129.78	129.46	129.48	129.75	129.61	131.31
11	130.39	131.09	131.45	131.64	131.56	131.66	131.71	131.73	131.95	132.01	132.07	132.20	132.11	132.20	132.22	132.28	132.48
12	128.94	129.01	128.99	129.04	129.08	129.00	129.02	129.08	129.08	129.06	129.06	129.21	129.11	129.14	129.14	129.13	129.27
13	126.27	126.75	126.89	127.00	127.09	127.01	127.05	127.19	127.26	127.27	127.33	127.54	127.37	127.45	127.56	127.55	127.77
R	40.06	55.23	21.41	140.15(1) 127.00(o) 128.79(m) 127.69(p)			55.22				166.41 52.18	118.27			118.43		

The π-polarization mechanism is again asserted by the alternating positive and negative slopes. The excellent correlations of σ^+ and σ^{13} at the #6 carbon are consistent with these being the best scales for the ^{77}Se SCS data. For this series, the correlations are also generally good at the #5 α carbon, unusual for styryl systems. This is attributable to the polarizability of Se setting up a well-defined charge alternation down the styryl backbone. This influence of the Se atom appears, however, to decrease with distance, as seen in the lowering R^2 values in going from C6 to C4.

The slopes of the #6 correlations in this series are considerably greater than those for the #6 carbon for the E isomer in Series A. This is understandable in terms of the much greater shielding range experienced by the #6 carbon adjacent to the highly polarizable Se atom. The #5 slopes are more comparable in magnitude to Series A with the #4 slopes essentially equivalent, again implying a lessening influence of Se further down the styryl backbone.

3. Series B

^{13}C δ correlations were also carried out for selected nuclei of the benzylidene azlactones using data previously compiled from 17 compounds in this series.[60] The predominance of the π-polarization mechanism in this structure could give a useful contrast to the Series A/D correlations, where the influence of the through-resonance mechanism was evaluated. Table 30 lists the correlation results (in order of decreasing R^2) for these nuclei.

The dominance of the π-polarization mechanism is revealed in two aspects of the data:

Table 30

Correlation Results for Selected ^{13}C Nuclei/ Series B

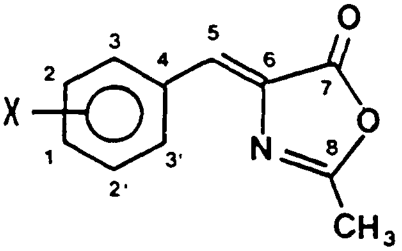

	Scale	R^2	Slope
#8	σ^{13}	.9909	2.15
	σ	.9816	3.45
	σ^+	.9666	2.29
	σ^-	.9356	2.86
#7	σ	.9859	-1.16
	σ^{13}	.9552	-0.706
	σ^+	.9312	-0.750
	σ^-	.9298	-0.953
#6	σ^{13}	.9985	3.03
	σ^+	.9850	3.23
	σ	.9618	4.79
	σ^-	.9077	3.95
#5	σ	.8984	-3.73
	σ^-	.8680	-3.11
	σ^{13}	.7873	-2.16
	σ^+	.7429	-2.26
#4	σ^+	.9087	6.59
	σ^{13}	.8997	6.08
	σ	.8153	9.36
	σ^-	.7980	7.86

1) A precise alternation between positive and negative slopes from C4 through the conjugated system to C7 and C8 (as illustrated in the structure).

2) The overall superiority of σ^{13} illustrating an efficient transmission of substituent effects through the styryl system.

This second aspect of the data is underscored by the excellent correlations for the C8 and C7 (carbonyl) nuclei, in spite of their remote locations from the substituent X. The presence of complete planarity and conjugation between X and these probe nuclei appear vital for this efficient transmission.

While the through-resonance effect is not prominent in this structure, it can be said that any effect there is from this transmission mechanism favors σ^+ over σ^-; for all carbons, except the "anomalous" C5, σ^+ gives a better R^2 value than σ^-. This discernable albeit slight preference for the σ^+ scale can be rationalized by invoking the imino enolate resonance hybrid, made possible by e^- donation from X.

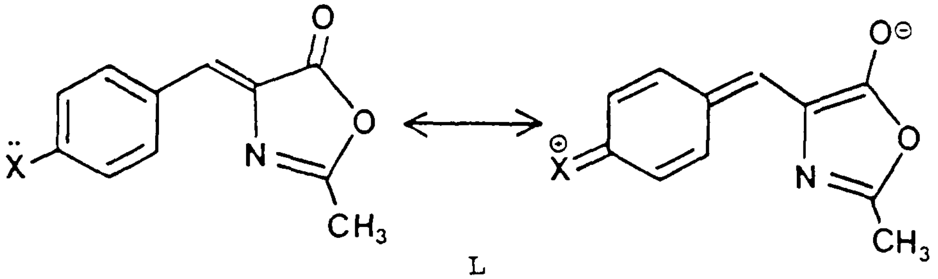

L

As stated on page 129, this structure is further stabilized by aromaticity of the heterocyclic ring. However, the fact that σ^+ gives lower R^2 values than σ^{13} (and usually σ) in all cases except C4 indicates this resonance form not to be very important. The Series C

^{13}C δ correlations, again verifying the π-polarization mechanism, have been discussed elsewhere.[34]

CHAPTER V

CONCLUSION

It must be stressed in perspective that the modest R^2 values obtained for the linear free energy correlations evaluated in this study implied the simultaneous operation of many effects. (Statisticians often insist on an R value of 0.99 or better for a "definitive" correlation.) The inclusion of two functional groups (N/Se and CO_2R) probably complicated the correlation analysis. Considering this, it is fortunate that meaningful comparisons could still be seen between the single substituent correlations applied to the same isomer and between the E/Z geometrical isomers (Series A and D).

Most investigations of the styrene probe have involved e^- deficient atoms attached to the β carbon. In these studies, the transmission of π-polarization effects could be evaluated without the interfering influence of through-resonance. This research has provided a complement to this body of work in that through-resonance effects from electron rich centers (N and Se) were shown to be meaningfully evaluated, particularly in the context of geometrical isomerism. This supports the contention that the styrene probe can be a useful way to evaluate the orientational dependency of the transmission of substituent effects, whether relating to electronic and/or steric factors.

For example, Adcock, Khor [85,86] and Reynolds [87] found with β, β-difluorostyrenes

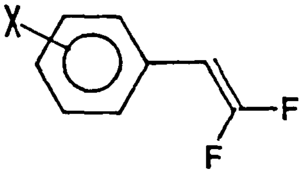

XCVIII

an angular dependence of polar effects which was consistent with a direct field mechanism. (The direct field component was greater at the E C-F bond where an increased ρ_I value was observed.) In this study of diethylamino and phenylseleno cinnamates, the through-resonance tendency of the E isomer appeared greater, though in these cases, steric factors appeared to be of primary importance.

Further interesting aspects of structural chemistry were evident in the results. Phenyl ring anisotropy provided a useful means to rationalize the relative shieldings of the E vs Z nitrogen nuclei in the diethylaminocinnamates. Also, the diethylamino moiety provided a fairly sensitive structure for evaluating steric factors leading to loss of styryl coplanarity, and a potential means to evaluate in more detail the nature of repulsive interaction between nitrogen's lone pair and a carbanionic α site.

In light of these concepts, a very interesting area for follow-on work would be a series of ethyl α-dimethylborocinnamates,

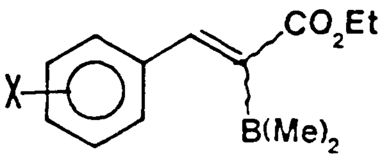

XCIX

where the planar arrangement and electron deficiency of the boron atom would provide an intriguing parallel to the nitrogen series. At the other extreme, a phenyltelluro group attached at the β carbon would provide a useful extension to the phenylseleno system. A key question here would be whether the TePh group would also be more deshielded in the Z versus the E configuration (as observed for SePh), or if the greater size of Te could cause twisting of the phenyl ring in such a manner as to shield the Te nucleus (relative to E).

More insight was achieved regarding the electronic properties of the SePh moiety. The contrast in behavior of this group in the E vs Z isomers (Series D) reflected a high sensitivity to molecular conformation effects. If, indeed, negative hyperconjugation were contributing to the wider chemical shift range of the Se in the E versus Z isomer, the geometrical dependence of this phenomenon must be closely related to the conformational differences of these isomers. The greater conformational freedom of the SePh unit in the E isomer evidently allows an optimal orbital arrangement to be achieved whatever model is invoked (d-orbitals or negative hyperconjugation). X-ray crystal structure determination is certainly needed to elucidate this question.

Shortcomings and utility of DSP analysis were evident from this work. For N, particularly in the nonrigid enamines (Series A), the σ_{R^-} Taft scale superiority (for Z) strongly supported the same conclusion from single substituent treatment. Otherwise, little or no improvement was seen. For the Series B azlactones, a modest improvement using the σ_{R^+} Taft scale versus the single substituent treatment implied a greater importance of the iminoenolate resonance form. This was a useful qualitative contrast, and may have been due to the greater planarity/rigidity of this structure allowing a more useful evaluation of substituent effects in terms of polar and resonance components.

The more complex nature of Se appeared to lend it more amenable to constructive DSP analysis. R^2 values above 0.99 were achieved in many cases. Of particular value here was the indication of Se's through-resonance ability in both an e^- accepting and donating mode. The wide chemical shift range (40 ppm) supported this viewpoint. This also indicates that heavy nuclei can be usefully evaluated using the DSP technique.

REFERENCES

REFERENCES

1. W. F. Reynolds, Prog. Phys. Org. Chem., 14, 165 (1983).

2. D. J. Craik and R. T. C. Brownlee, Prog. Phys. Org. Chem., 14, 1 (1983), pg. 3.

3. G. J. Martin, M. L. Martin, and S. P. Gouesnard, ^{15}N NMR Spectroscopy, Berlin, Springer-Verlag, 1981.

4. D. G. Craik, in Annual Reports on NMR Spectroscopy, 15 (G.A. Webb, ed), Academic Press, London, 1983, pg. 9.

5. R. L. Lichter and J. D. Roberts, Org. Magn. Reson., 6, 636 (1974).

6. T. Axenrod and M. J. Wieder, Org. Magn. Reson., 8, 350 (1976).

7. T. I. Schuster, S. H. Doss, and J. D. Roberts, J. Org. Chem., 43, 4693 (1978).

8. P. W. Westerman, R. E. Botto, and J. P. Roberts, J. Org. Chem., 43, 2590 (1978).

9. R. E. Botto and J. D. Roberts, J. Org. Chem., 44, 140 (1979).

10. T. Axenrod, X. H. Luang, and C. Watnick, Tetrahedron Lett., 27, 11 (1986).

11. T. B. Patrick and R. D. Willaredt, J. Org. Chem., 48, 4415 (1983).

12. Ref. 3, pages 99-101.

13. R. J. Shamberger, Biochemistry of Selenium, (Ed., E. Frieden), Plenum Press, 1983.

14. D. Liotta and R. Monahan III, Science, 231, 356 (1986).

15. N. P. Luthra and J. D. Odom, in The Chemistry of Organic Selenium and Tellurium Compounds, Volume I, (S. Patai and Z. Rappoport, eds.), John Wiley and Sons, Chichester, England, 1986.

16. Ibid., p. 206.

17. W. Gombler, *Z. Naturforsch.*, *36b*, 535 (1981).

18. V. V. Bairov, G. A. Kalabin, M. L. Alpert, V. M. Bzhezovskii, I. D. Sadekov, B. A. Trofimov and V. I. Minkin, *Zh. Org. Khim.*, *14*, 617 (1978).

19. J. W. Baker, G. F. Barrett and W. T. Tweed, *J. Chem. Soc.*, 2831 (1952).

20. G. Llabres, M. Baiwir, L. Christiaens, J. Denoel, L. Laitem and J. L. Piette, *Can. J. Chem.*, *56*, 2008 (1978).

21. G. A. Kalabin, D. F. Kushnarev, V. M. Bzesovsky and G. A. Tschmutova, *Org. Magn. Reson.*, *12*, 598 (1979).

22. W. McFarlane and R. J. Wood, *J. Chem. Soc.* (A), 1397 (1972).

23. L. M. Litvinenko, *Izv. Akad. Nauk. SSSR, Ser. Khim.*, 1737 (1962).

24. L. M. Litvinenko, A. F. Popov, R. S. Popova and L. D. Snagoshenko, *Reakts. Sposobnost Org. Soedin*, *5*, 744 (1968).

25. J. Gosselck, *Angew. Chem* (Intern. Ed.), *2*, 660 (1963).

26. L. D. Pettit, A. Royston, C. Sherrington, and R. J. Whewell, *J. Chem. Soc.* (B), 588 (1968).

27. G. P. Mullen, N. P. Luthra, R. B. Dunlap, and J. D. Odom, *J. Org. Chem.*, *50*, 811 (1985).

28. J. I. Musher, *J. Amer. Chem. Soc.*, *94*, 1370 (1972).

29. R. A. McClelland and M. Leung, *J. Org. Chem.*, *45*, 187 (1980).

30. I. D. Sadekov and A. Ya. Bushkov, *Zh. Obshchi Khim.*, *47*, 631 (1977); E.E. 576.

31. D. Seebach, *Angew. Chem.*, 91, 259 (1979).

32. J. Bromilow and R. T. C. Brownlee, *Tetrahedron Lett.*, 2113 (1975).

33. P. S. Pregosin, E. W. Randall, and A. I. White, *J. Chem. Soc. Perkins Trans. II*, 513 (1972).

34. C. N. Robinson, C. D. Slater, J. S. Covington III, C. R. Chang, L. S. Dewey, J. M. Franceschini, J. L. Fritzsche, J. E. Hamilton, C. C. Irving, Jr., J. M. Morris, D. W. Norris, L. E. Rodman, V. I. Smith, G. E. Stablein, and F. C. Ward, *J. Magn. Reson.*, *41*, 293 (1980).

35. J. A. Pople and M. Gordon, *J. Am. Chem. Soc.*, *89*, 4253 (1967).

36. S. Fliszar, J. Am. Chem. Soc., 94, 7386 (1972).

37. W. Schwotzer and W. von Phillipsborn, Helv. Chim. Acta, 60, 1501 (1977).

38. S. Tan, K. Ang, H. Jayachandra and Y. Fong, J. Chem. Soc. Perkins Trans. II, 1043 (1987).

39. C. N. Robinson and C. C. Irving, Jr., J. Heterocyclic Chem., 16, 921 (1979).

40. C. N. Robinson and G. E. Stablein, private communication.

41. D. J. Craik, R. T. C. Brownlee and M. Sadek, J. Org. Chem., 47, 657 (1982).

42. L. Horner and E. O. Renth, Liebigs Ann. Chem., 703, 37 (1967).

43. Organic Synthesis, Collective Volume 2, (ed. A. H. Blatt), John Wiley and Sons, New York, 1943, p. 1.

44. R. H. Siddiqui and Salah-Ud-Din, J. Indian Chem. Soc., 18, 636 (1941); procedure modified as discussed in Ref. 33, page 300.

45. H. Yokoyama, W. J. Hsu, S. Poling and E. Hayman, ACS Symp. Ser., 181, 153 (1982).

46. W. Lehnert, Tetrahedron, 30, 301 (1974).

47. D. H. Wadsworth and M. R. Detty, J. Org. Chem., 45, 4611 (1980).

48. K. B. Sharpless, R. F. Lauer, J. Am. Chem. Soc., 95, 2697 (1973).

49. G. C. Levy and R. L. Lichter, Nitrogen-15 Nuclear Magnetic Resonance Spectroscopy, John Wiley and Sons, New York, 1979, p. 31.

50. L. Gelbaum, private communication.

51. L. P. Hammett, J. Am. Chem. Soc., 59, 96 (1937).

52. H. C. Brown and Y. Okamoto, J. Am. Chem. Soc., 80, 4979 (1958).

53. H. H. Jaffe', Chem. Rev., 53, 191 (1953).

54. J. Bromilow and R. T. C. Brownlee, J. Org. Chem., 44, 1261 (1979).

55. Dr. Peter Bridson, private communication.

56. U. Vogeli and W. von Phillipsborn, Org. Magn. Reson., 7, 617 (1975).

57. H. Krabbenhoff, J. Org. Chem., 43, 1830 (1978).

58. T. Yokoyama, I. Hanazome, M. Mishima, M. J. Kamlet, and R. W. Taft, J. Org. Chem., 52, 163 (1987).

59. C. E. Johnson and F. A. Bovey, J. Chem. Phys., 29, 1012 (1958).

60. Dr. Charles N. Robinson, private communication.

61. I. Johannson, L. Henriksen and H. Eggert, J. Org. Chem., 51, 1657 (1986).

62. C. Glidewell, A. G. Robiette and G. M. Sheldrick, Chem. Phys. Letters, 16, 526 (1972).

63. T. G. Traylor, W. Hanstein, H. J. Berwin, N. A. Clinton, and R. S. Brown, J. Amer. Chem. Soc., 93, 5715 (19721).

64. P. V. R. Schleyer, A. J. Kos, Tetrahedron, 39, 1141 (1983).

65. J. D. Roberts, R. L. Webb, and E. A. McElhill, J. Am. Chem. Soc., 72, 408 (1950).

66. R. Weiss, H. Wolf, V. Schubert and T. Clark, J. Am. Chem. Soc., 103, 6142 (1981).

67. D. Kost and M. Ruban, J. Am. Chem. Soc., 98, 8333 (1976).

68. E. V. Titov, N. G. Korzhenevskaya, L. M. Kapkan, L. N. Sedova, L. Z. Gandel'sman, Yu. A. Fialkov and L. M. Yagupol'skii, Zh. Org. Chim., 7, 2552 (1971); E.E. 2651.

69. A. E. Lutskii, E. M. Obukhova, L. M. Yagupol'skii and V. G. Volashchuk, Zh. Strukt. Khim., 10, 349 (1969).

70. S. Oae and Y. Yano, Tetrahedron, 24, 5721 (1968).

71. Y. Yano and S. Oae, Tetrahedron, 26, 67 (1970).

72. Dr. Randy Johnston, private communication.

73. Dr. Larry Houk, private communication.

74. F. A. Cotton and G. Wilkinson, Advanced Inorganic Chemistry, John Wiley and Sons, Inc., 1972, pg. 94.

75. C. G. Pitt, J. Organometallic Chem., 61, 49 (1973).

76. SAS Institute Inc., Box 8000, Cary NC 27511.

77. C. G. Swain and E. C. Lupton, Jr., J. Am. Chem. Soc., 90, 4328 (1968).

78. R. W. Taft, Jr., and I. C. Lewis, J. Am. Chem. Soc., 80, 2436 (1958).

79. S. Ehrenson, R. T. C. Brownlee, and R. W. Taft, Prog. Phys. Org. Chem., 10, 1973, pp. 42-43.

80. All DSP calculations were performed by Dr. Carl Slater, Northern Kentucky University.

81. R. T. C. Brownlee and D. J. Craik, Org. Magn. Reson., 15, 248 (1981).

82. W. F. Reynolds and G. K. Hamer, J. Amer. Chem. Soc., 98, 7296 (1976).

83. W. F. Reynolds, Prog. Phys. Org. Chem., 14, (1983), pg. 186.

84. R. T. C. Brownlee and D. J. Craik, J. Chem. Soc., Perkin II, 760 (1981).

85. W. Adcock and T. C. Khor, Tetrahedron Lett., 3063 (1976).

86. W. Adcock and D. P. Cox, J. Org. Chem., 44, 3004 (1979).

87. W. F. Reynolds, V. G. Gibb, and N. Plavac, Canad. J. Chem., 58, 839 (1980).

APPENDICES

APPENDIX A

General Experimental Methods

Melting points were determined on an Electrothermal® melting point apparatus and are uncorrected. Thin-layer chromatography was performed on silica gel F-254 (type 60, E. Merck) precoated on aluminum sheets. All eluting solvent mixtures are given as volume to volume ratios. Column chromatography was carried out on silica gel 60 (70-230 mesh, E. Merck.). Gas chromatography was performed with a Hewlett-Packard 5890-A interfaced with a Hewlett-Packard 5950-A Mass Selective Detector. Infrared spectra were recorded on a Mattson Polaris FT infrared spectrophotometer. All NMR's were obtained as described in the Experimental section of the dissertation (Chapter 3). Elemental analyses were performed by Galbraith Laboratories, Inc., Knoxville, TN, and by Desert Analytics, Tuscon, AZ.

Appendix B

^{1}H NMR

Series A

Table 31 summarizes the chemical shift data for both Z and E isomers in this series. Isomer preponderance could be followed most clearly by comparison of the relative intensities of the triplet and quartet patterns of the aliphatic region, as indicated below.

Within the aromatic region, para-substituted splitting patterns were usually observed for all p-X's. When this pattern for both isomers could be identified, these have been individually listed. Otherwise (and including the m-X compounds), the entire aromatic multiplet chemical shift region is listed.

Impurities evident in the NMR's to varying degrees were

a) ethyl diethylaminoacetate starting compound

b) stopcock grease

c) ethyl phenylpropiolate derivative, formed from Hoffman elimination of the N-oxide intermediate probably occurring during high-temperature vacuum distillation: (only evident for p-NO_2 and m-CN).

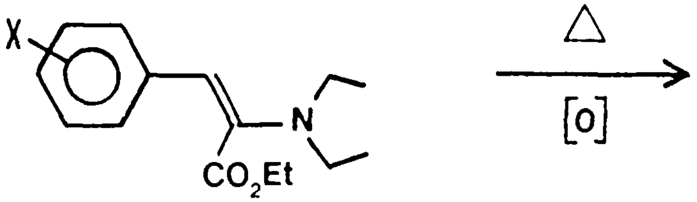

Table 31

'H NMR Chemical Shifts*

Series A: (E+Z) Ethyl 2-diethylamino-3-phenyl-2-propenoates
(δ, ppm downfield from TMS)

X $( )^1$	Aromatic(m)	Vinylic(s) Z	Vinylic(s) E	OCH_2CH_3(q) (overlapping)	$N(CH_2CH_3)_2$ (q) Z	$N(CH_2CH_3)_2$ (q) E	OCH_2CH_3(t) Z J=7.06-7.20	OCH_2CH_3(t) E 7.07-7.09(Hz)	$N(CH_2CH_3)_2$(t) Z J=7.26-7.20	$N(CH_2CH_3)_2$(t) E 7.26-7.06(Hz)	X Z	X E
p-$N(Me)_2$ (Z)	7.94-6.60	7.21	5.45	4.20-4.13	3.03-2.96 (overlapping)		1.30-1.26	1.20-1.10	1.04-0.99	1.10-1.04	2.89	2.82
p-MeO (Z)	7.97-6.86(Z) 7.30-7.01(E)	7.15	5.02	4.23-4.16	3.10-2.95 (overlapping)		1.32-1.27	1.15-1.10	1.04-0.99	1.11-1.06	3.76	3.73
p-Me (Z)	7.82-7.07	6.99	5.43	4.22-4.15	3.02-2.94	3.09-3.02	1.31-1.26	1.12-1.06	1.03-0.98	1.12-1.06	2.28	2.23
p-Ph (Z)	7.99-7.17	7.05	5.16	4.28-4.21	3.07-3.00	3.18-3.11	1.36-1.31	1.23-1.18	1.07-1.02	1.16-1.11		
p-F (Z)	7.98-6.94	7.06	5.44	4.26-4.19	3.02-2.95	3.13-3.06	1.34-1.29	1.15-1.11	1.03-0.99	1.13-1.09		
H (Z)	7.89-7.08	6.99	5.47	4.27-4.20	3.04-2.97	3.16-3.10	1.34-1.29	1.17-1.13	1.04-0.99	1.15-1.10		
p-Cl (Z)	7.86-7.29(Z) 7.19-7.03(E)	6.96	5.38	4.25-4.16	3.01-2.94	3.13-3.06	1.33-1.28	1.17-1.12	1.03-0.98	1.13-1.08		
m-F (Z)	7.82-6.75	6.95	5.42	4.27-4.20	3.04-2.97	3.16-3.10	1.34-1.30	1.21-1.16	1.04-0.99	1.15-1.10		
m-Cl (Z)	7.97-6.97	6.89	5.35	4.26-4.18	3.02-2.95	3.14-3.07	1.33-1.28	1.19-1.14	1.04-0.99	1.13-1.09		
p-CO_2Me (Z)	8.01-7.82(Z) 7.47-7.11(E)	6.86	5.44	3.79(s) 3.76(s) (β-CO_2CH_3)	3.03-2.95	3.18-3.11			1.03-0.98	1.15-1.11	3.88	3.84
m-CN (E)	8.21-7.27	6.88 (?)	5.40	4.26-4.21	3.04-2.96	3.19-3.12	1.36-1.31	1.23-1.18	1.05-1.00	1.17-1.12		
p-CF_3 (E)	7.94-7.60(Z) 7.49-7.20(E)	6.89	5.42	4.26-4.18	3.04-2.97	3.19-3.12	1.34-1.29	1.19-1.14	1.04-0.99	1.16-1.11		
p-CN (E)	7.86-7.64(Z) 7.52-7.15(E)	6.75	5.39	4.29-4.24	3.05-2.97	3.23-3.16	1.36-1.31	1.25-1.21	1.05-1.00	1.18-1.13		
p-NO_2 (E)	8.16-7.56(Z) 8.04-7.15(E)	6.72	5.24	4.32-4.25(E) 4.15-4.05(Z)	3.07-3.00	3.27-3.20	1.38-1.33	1.30-1.25	1.06-1.01	1.21-1.16		

---

[1] Indicates predominant isomer whose chemical shift assignments are underlined.

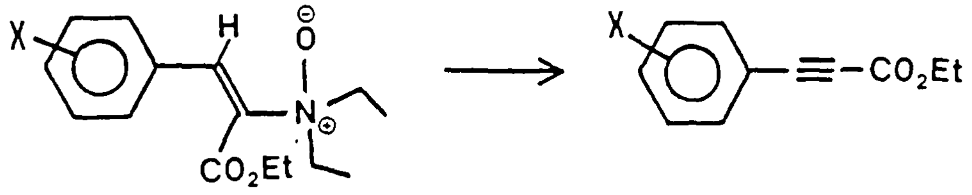

Other than these impurities, the only anomalous result evident in this table was the reverse intensity of the vinylic H's for the m-CN compound, indicated by ?. This compound was clearly predominantly E, as shown by the triplet and quartet relative intensities (and further corroborated by ^{13}C and ^{15}N NMR). The other three compounds showing E preponderance (p-CF_3, p-NO_2 and p-CN) showed the more shielded vinylic ^{1}H to be more intense, as expected.

The following abbreviations will be used in Table 31:
m = multiplet, s = singlet, q = quartet, t = triplet.

Series D

Common patterns observed in the ^{1}H NMR of the phenylseleno cinnamate esters were as follows: (pattern, assignment, chemical shift range (approximate). Additional information is given in the footnotes.

a^1. singlet, vinylic ^{1}H (E isomer), 8.02 - 8.43δ

b^2. multiplet, aromatic ^{1}H's (E/Z isomers), 8-7δ (fine splitting pattern from ^{77}Se/^{1}H coupling)

c^3. quartet, ethyl ester methylene ^{1}H's (E/Z isomers), 4.1 - 4.0δ

d^3. triplet, ethyl ester methyl ^{1}H's (E/Z isomers), 1.1 - 1.0δ

[1]Occasionally, when both E and Z isomers were present in a sample, an additional singlet absorption (7.3 - 6.9δ) was detected, presumably the vinylic ^{1}H of the Z isomer.

[2]The phenylseleno protons absorbed from ≈ 7.4-7.1δ, and were characterized by two sets of peaks, each displaying a fine splitting pattern from ^{77}Se/^{1}H coupling:

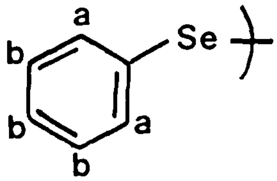

a = 7.37-7.35

b = 7.21-7.19

For p-X phenyl protons, the para-substituted splitting pattern was often apparent, though sometimes obscured by the SePh system.

[3]Whenever both isomers were present, these patterns usually overlapped, but occasionally appeared in close succession.

Table 32 summarizes the ^{1}H NMR chemical shifts for this series. In all cases except p-NO_2 and p-OMe the E isomer was the preponderant or only isomer present. The entire range of aromatic ^{1}H chemical shifts is presented for each compound. In many cases, this obscured the Z-isomer vinylic ^{1}H absorption, preventing definitive assignment. The same abbreviations are employed as in Table 31.

Table 32

^1H NMR Chemical Shifts*

Series D: (E+Z) Ethyl-2-phenylseleno-3-phenyl-2-propenoates

*(δ, ppm downfield from TMS)

X	Aromatic(m)	Vinylic(s)		OCH_2CH_3(q) (overlapping)	OCH_2CH_3(t) (overlapping) J=7.11-7.15 Hz	X	
		E	Z			E	Z
p-$N(Me)_2$	7.82-6.64	8.23		4.24-4.07	1.10-1.06	2.99(s)	2.96(s)
p-MeO	7.74-6.81	8.17	7.08	4.11-4.03	1.08-1.03	3.82(s)	3.79(s)
p-Me	7.65-7.15	8.15		4.03-4.08	1.05-1.02	2.36(s)	2.31(s)
p-Ph	7.76-7.18	8.19		4.10-4.05	1.06-1.02		
p-F	7.69-7.00	8.12		4.11-4.05	1.08-1.03		
H	7.70-7.06	8.15	7.06	4.10-4.00	1.10-0.99		
m-MeO	7.41-6.91	8.11		4.03-4.01	1.06-1.02	3.79(s)	
p-Cl	7.60-7.19	8.07	7.34	4.10-4.05	1.07-1.03		
m-F	7.64-6.93	8.05		4.10-4.01	1.07-1.02		
m-Cl	7.63-7.20	8.02		4.10-4.05	1.07-1.04		
p-CO_2Me	8.06-7.19	8.10		4.10-4.05	1.07-1.04	3.92(s)	
m-CN	7.87-7.19	8.03		4.14-4.08	1.11-1.08		
m-CF_3	7.86-7.15	8.10	6.94	4.13-4.01	1.10-1.01		
p-CF_3	7.66-7.17	8.06	6.90	4.08-3.99	1.05-0.98		
p-CN	7.68-7.19	8.03		4.11-4.05	1.09-1.05		
m-NO_2	8.13-7.11	8.43		4.13-4.07	1.13-1.05		
p-NO_2	8.21-7.21	8.06	6.84	4.12-4.02	1.10-1.04		

Series A/^{1}H NMR's

NOTE: These were obtained using CD_3NO_2 solvent and TMS referencing standard.

(Z+E) ethyl 2-diethylamino-3-(4-dimethylaminophenyl)-2-propenoate

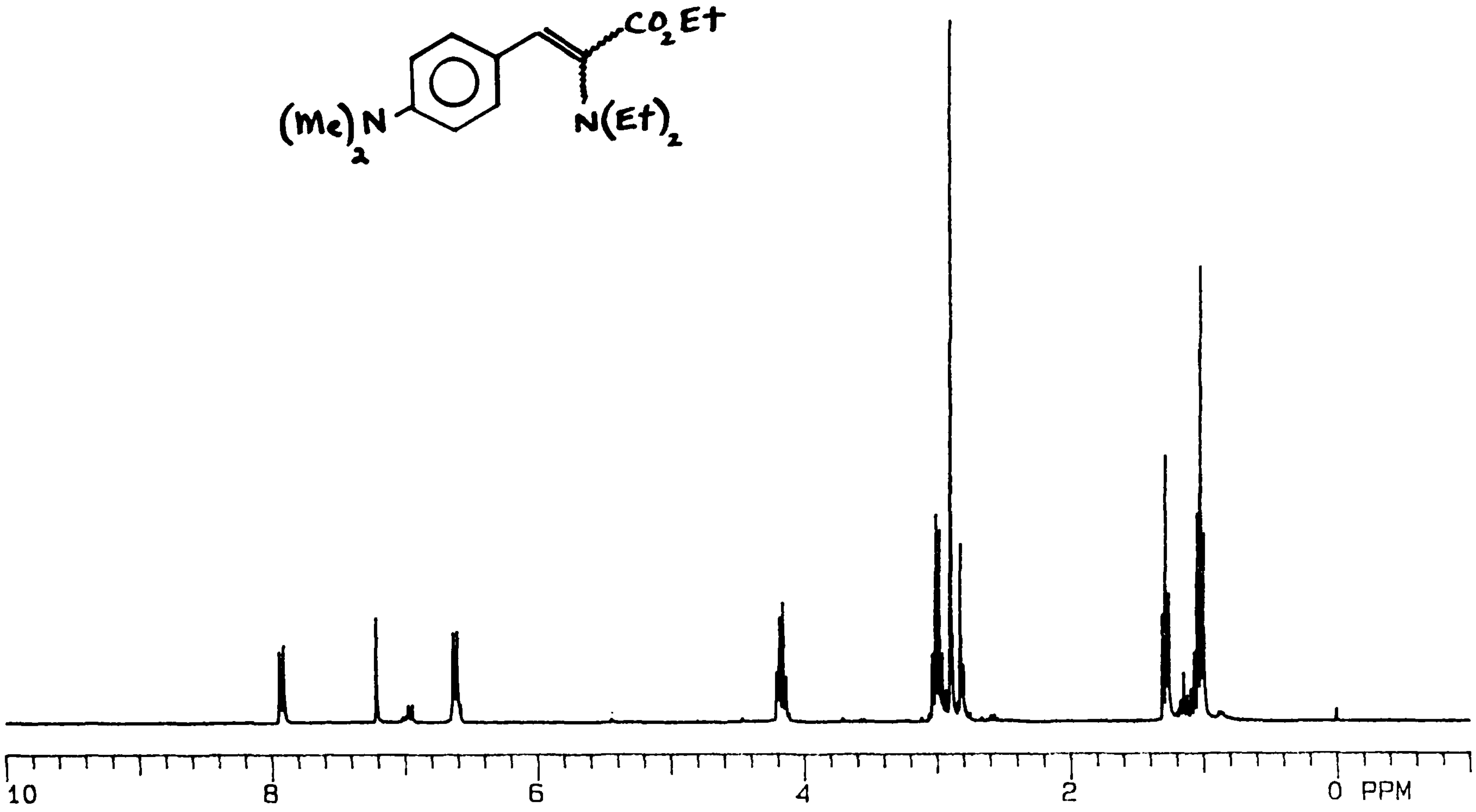

(Z+E) ethyl 2-diethylamino-3-(4-methoxyphenyl)-2-propenoate

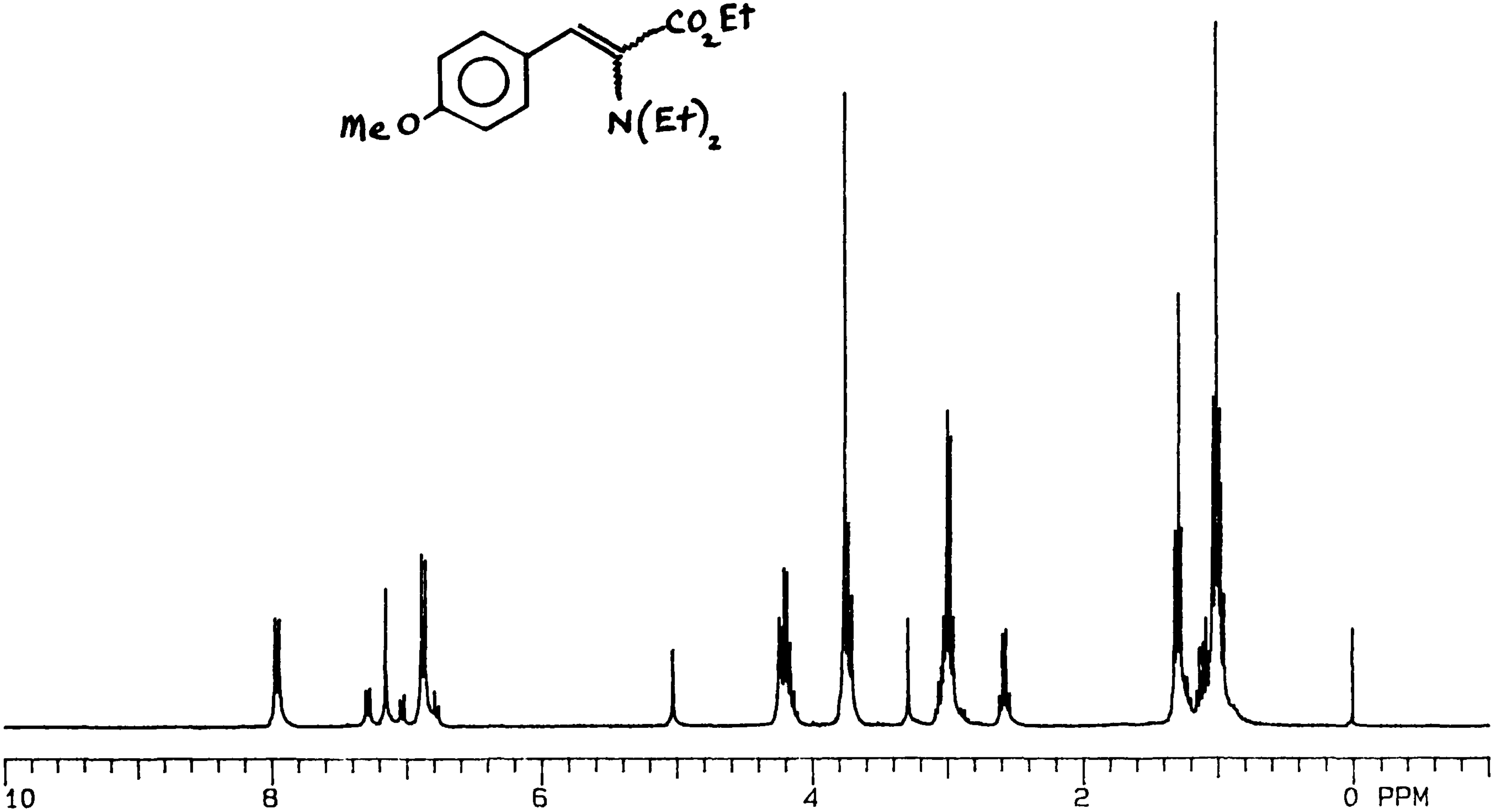

(Z+E) ethyl 2-diethylamino-3-(4-methylphenyl)-2-propenoate

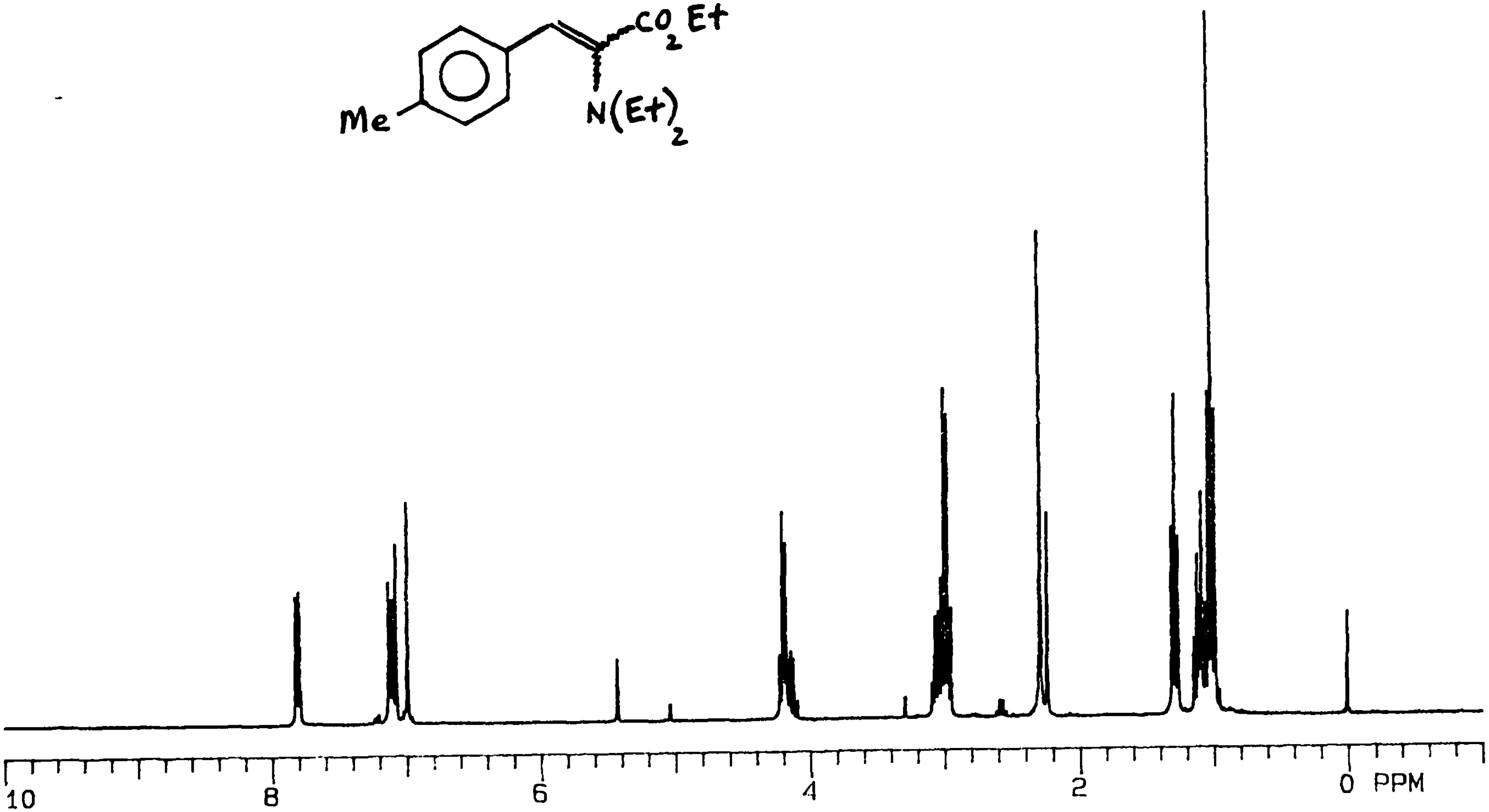

(Z+E) ethyl 2-diethylamino-3-(4-phenylphenyl)-2-propenoate

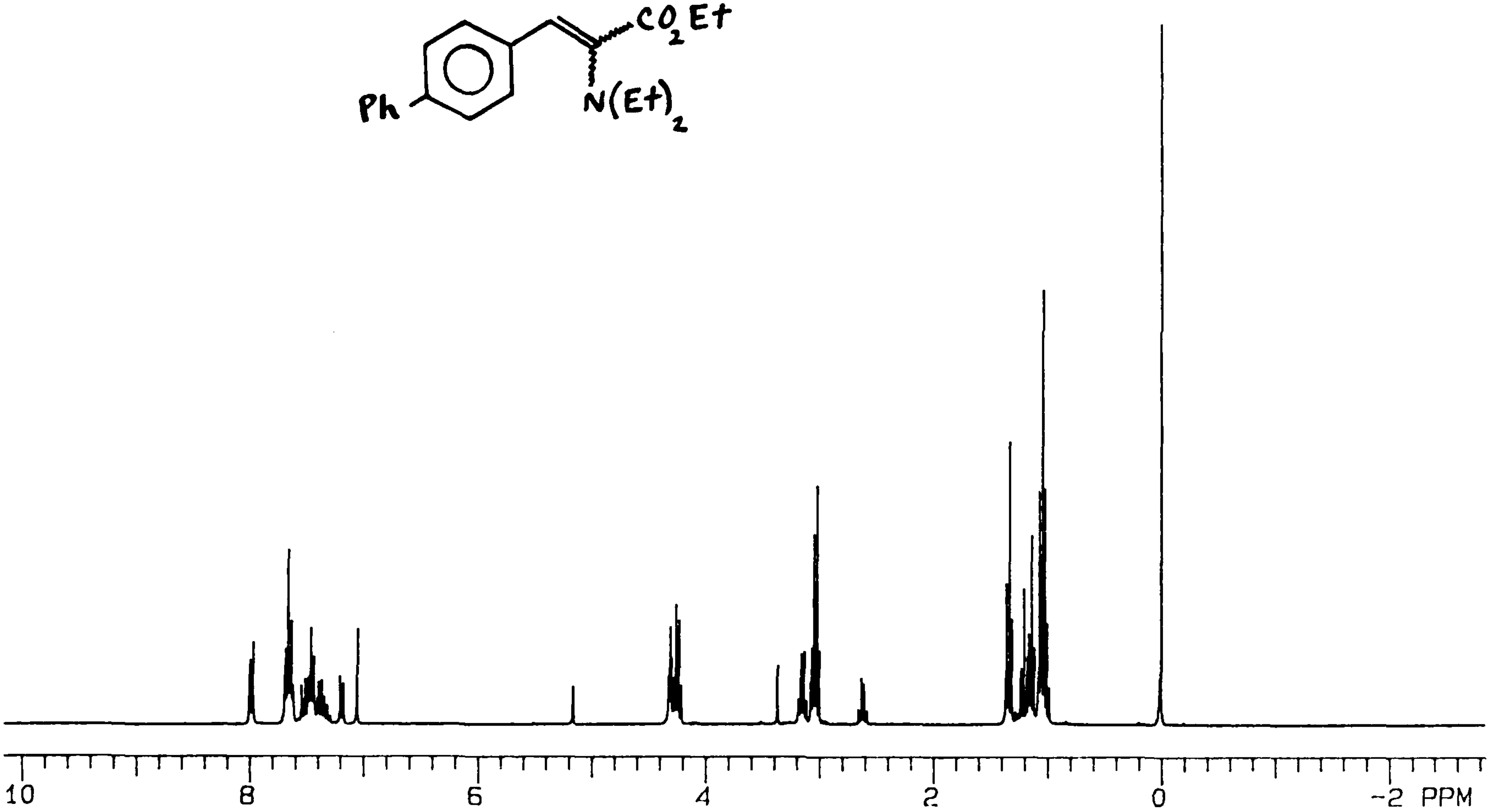

(Z+E) ethyl 2-diethylamino-3-(4-fluorophenyl)-2-propenoate

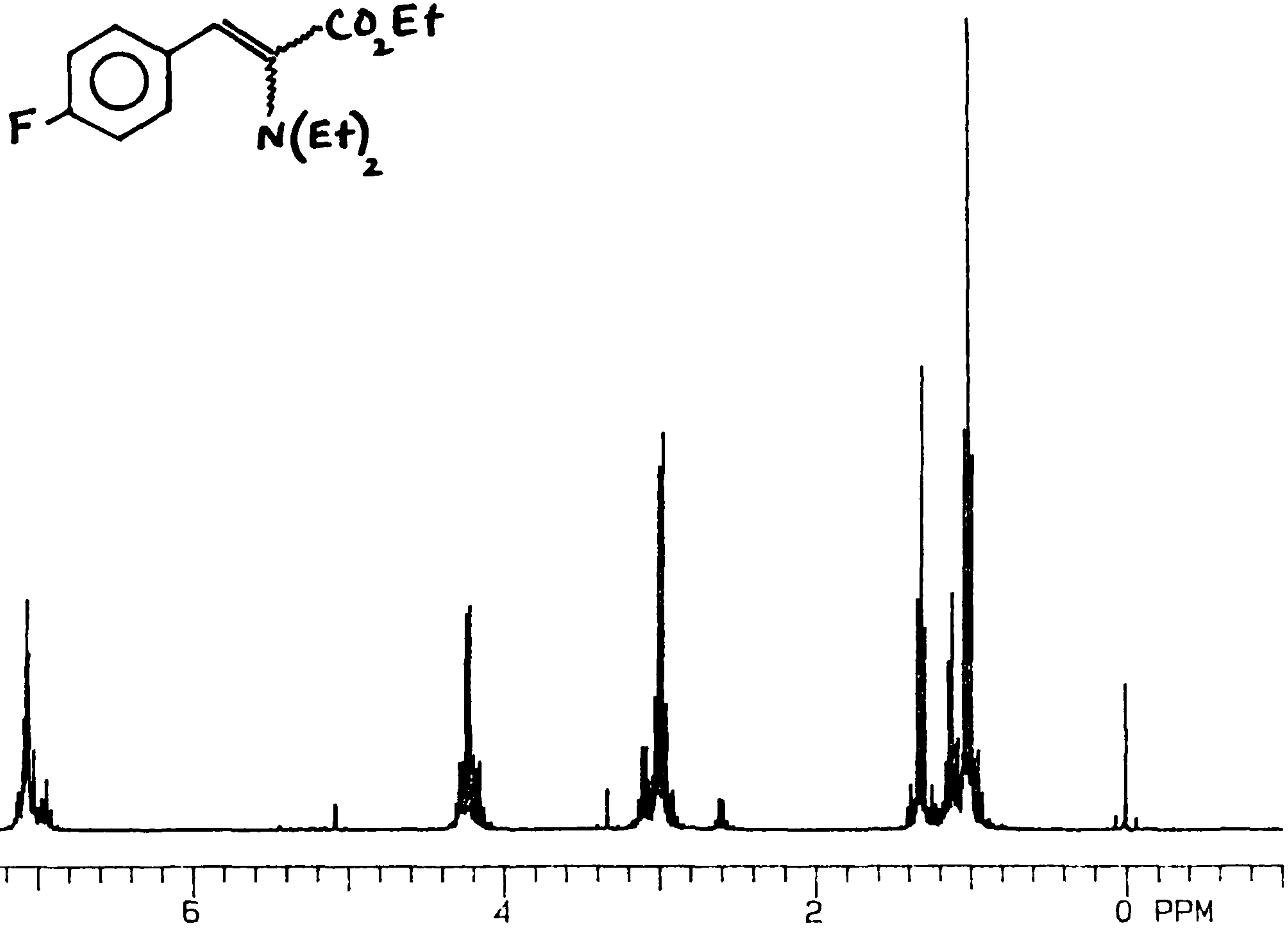

(Z+E) ethyl 2-diethylamino-3-phenyl-2-propenoate

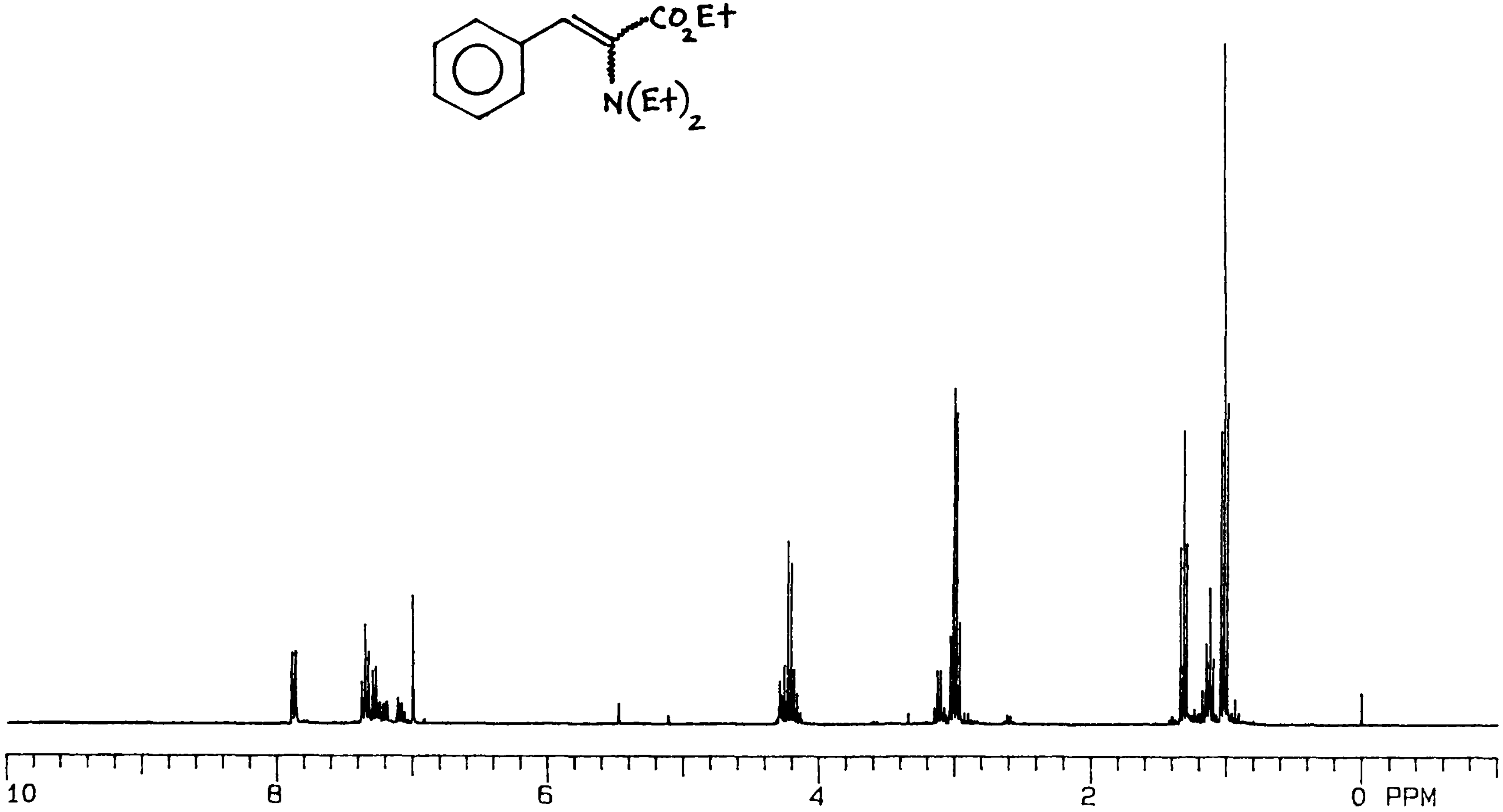

(Z+E) ethyl 2-diethylamino-3-(4-chlorophenyl)-2-propenoate

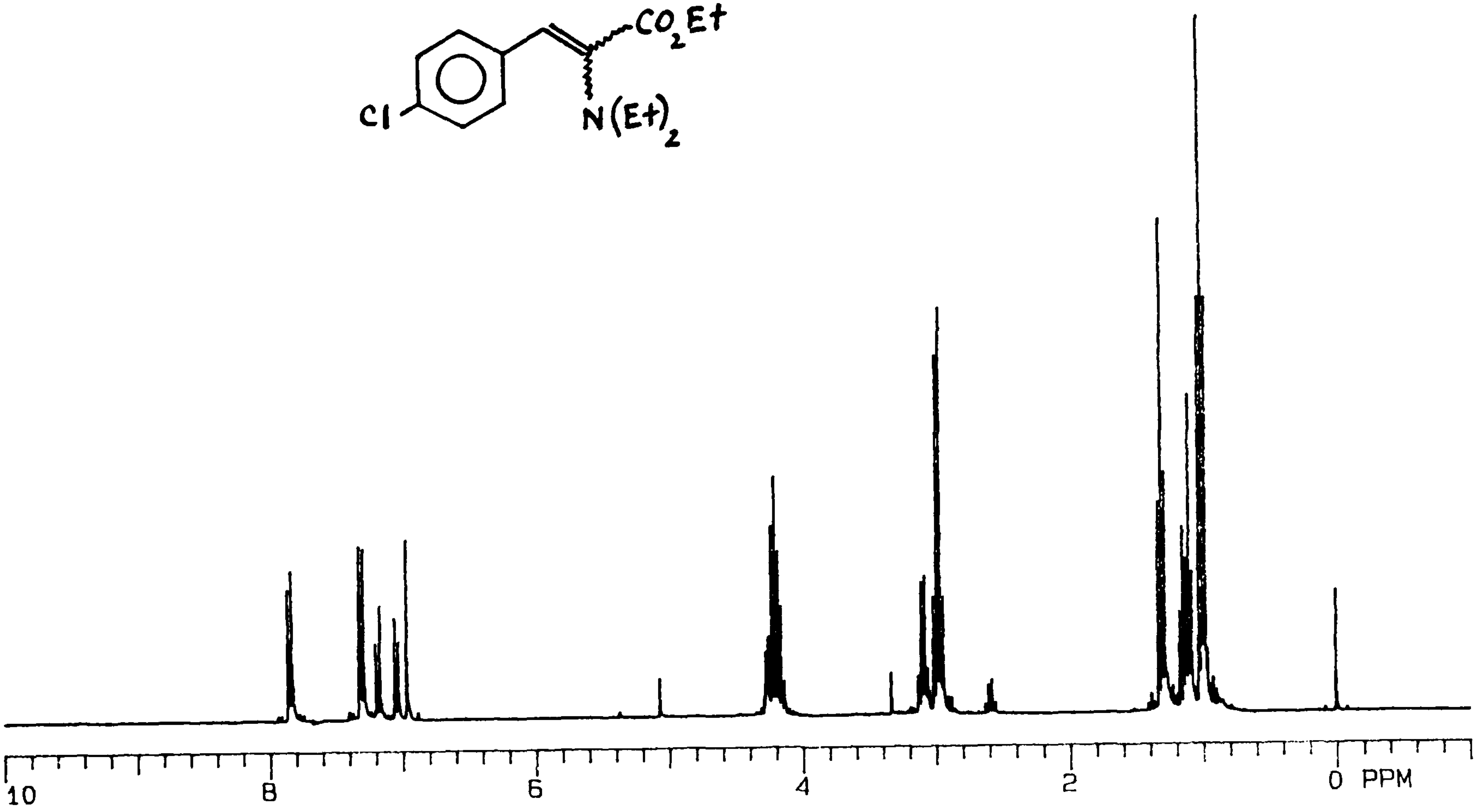

(Z+E) ethyl 2-diethylamino-3-(3-fluorophenyl)-2-propenoate

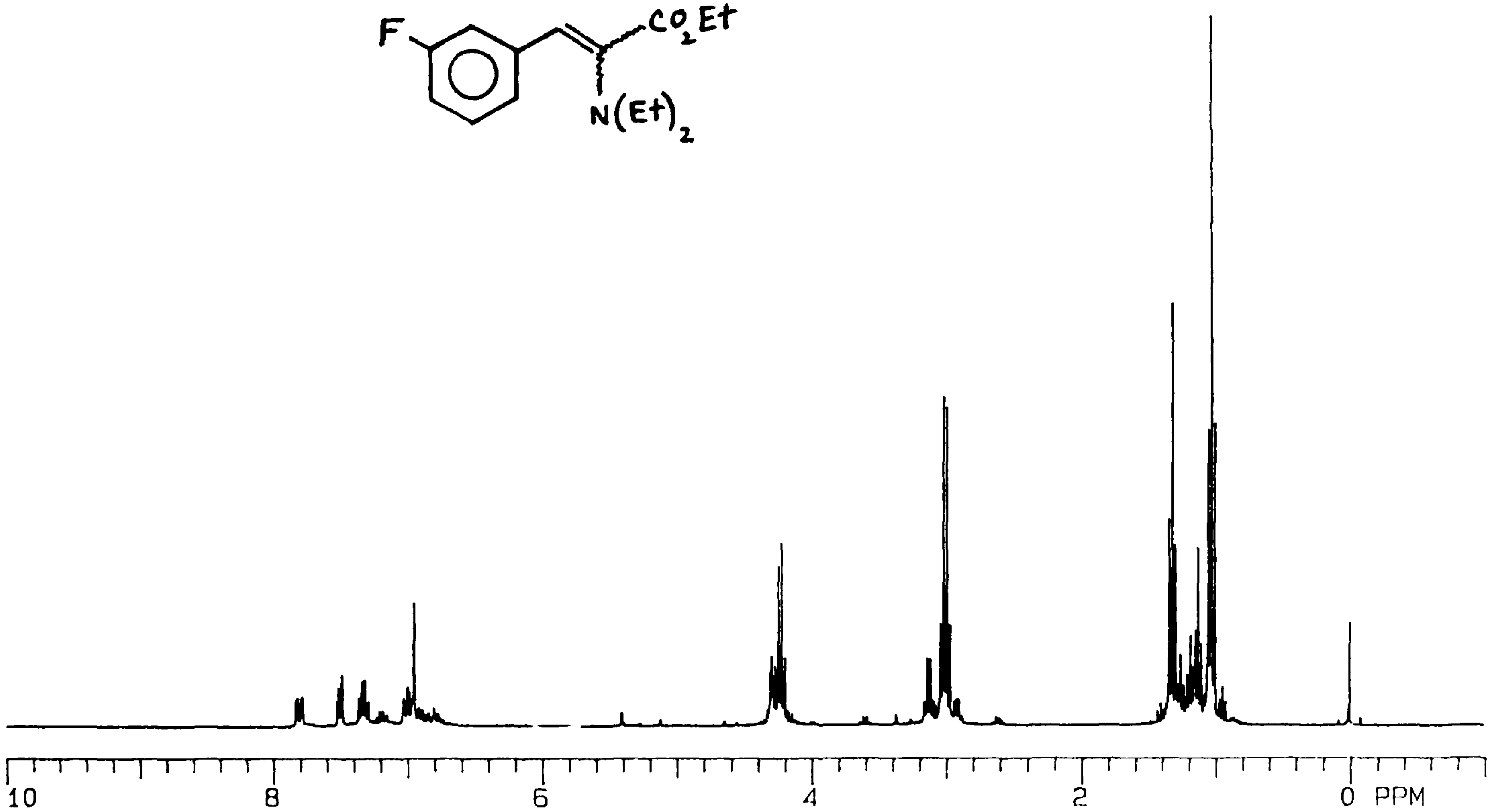

(Z+E) ethyl 2-diethylamino-3-(3-chlorophenyl)-2-propenoate

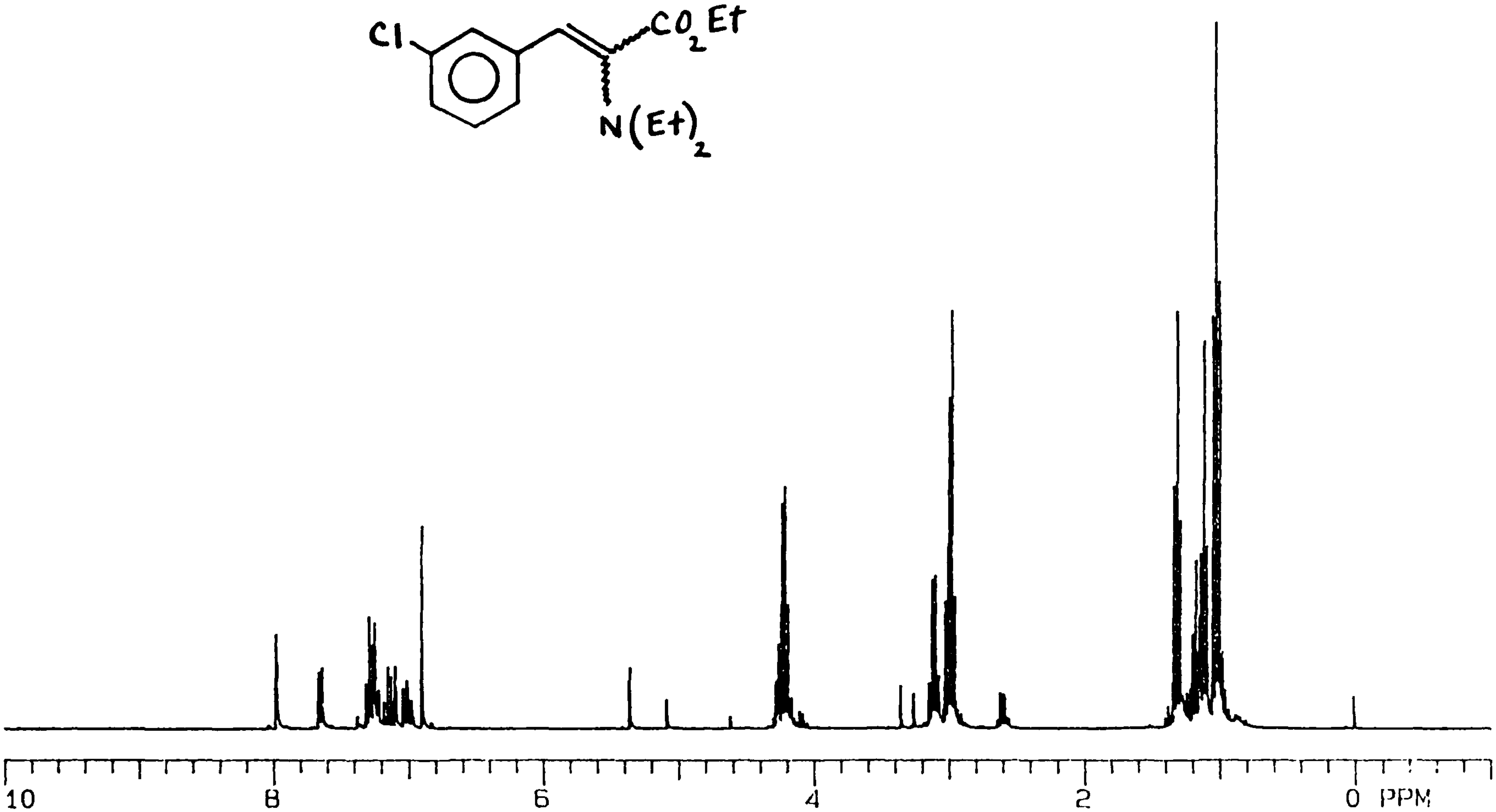

(Z+E) methyl 2-diethylamino-3-(4-carbomethoxyphenyl)-2-propenoate

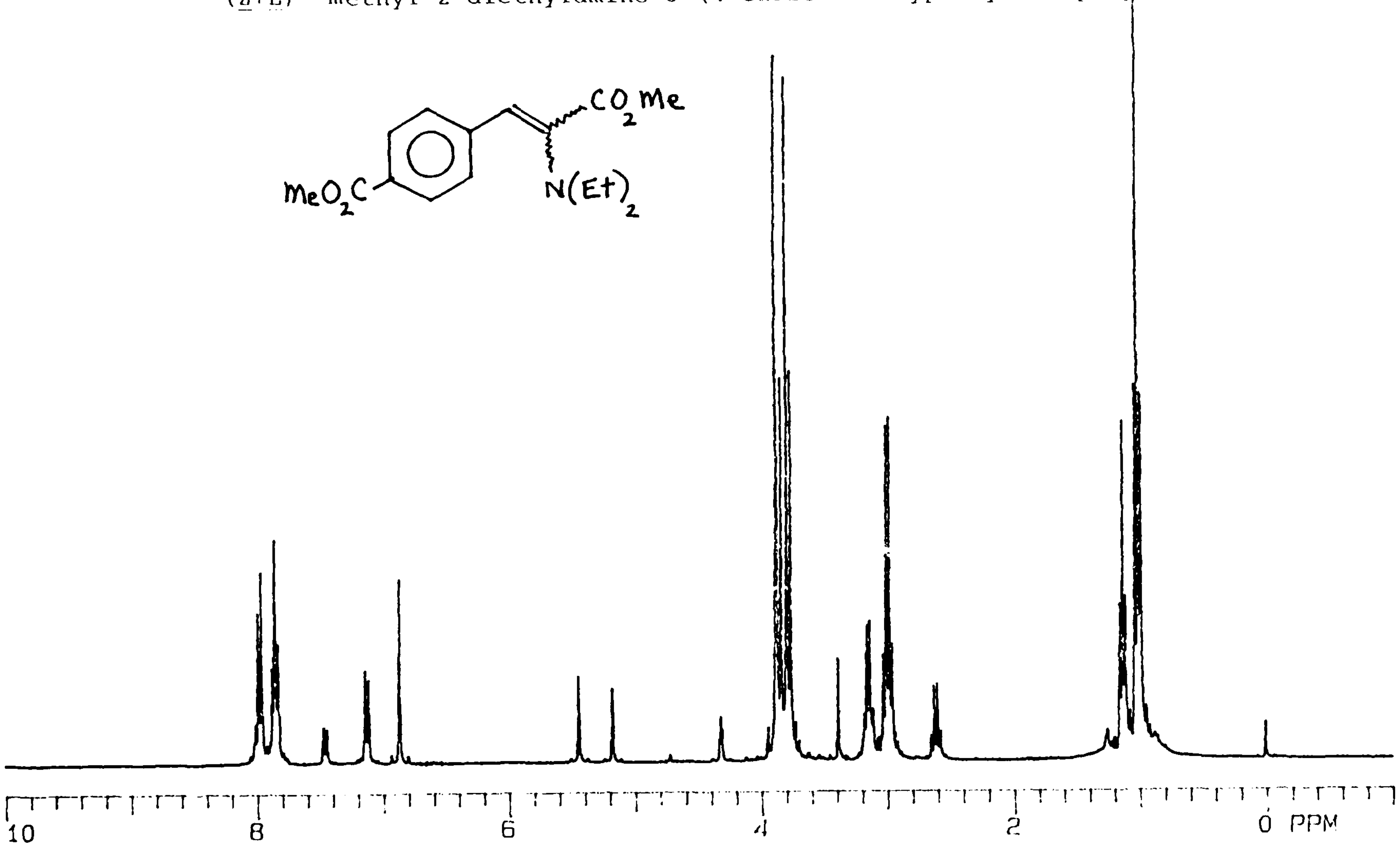

(E+Z) ethyl 2-diethylamino-3-(3-cyanophenyl)-2-propenoate

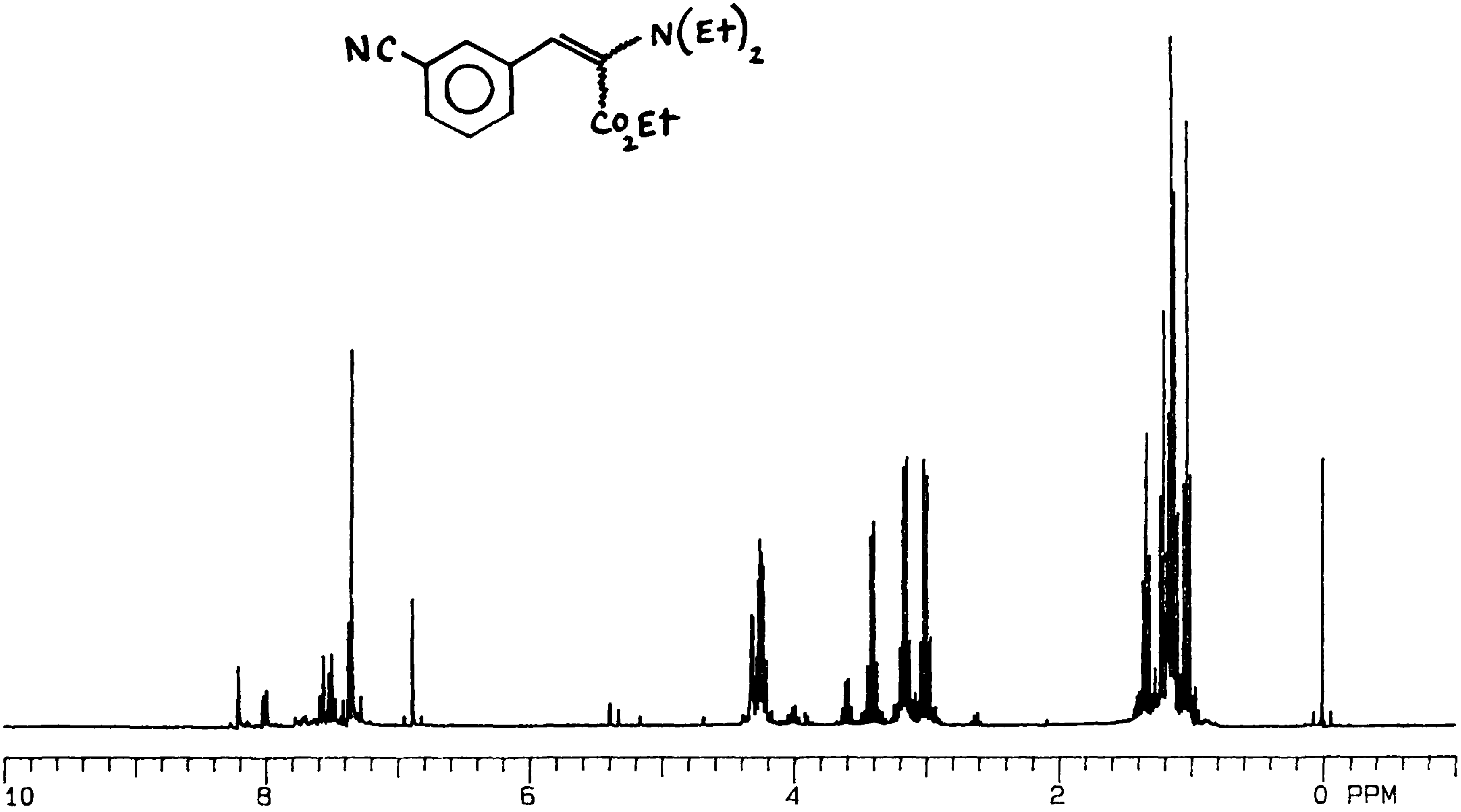

(E+Z) ethyl 2-diethylamino-3-(4-trifluoromethylphenyl)-2-propenoate

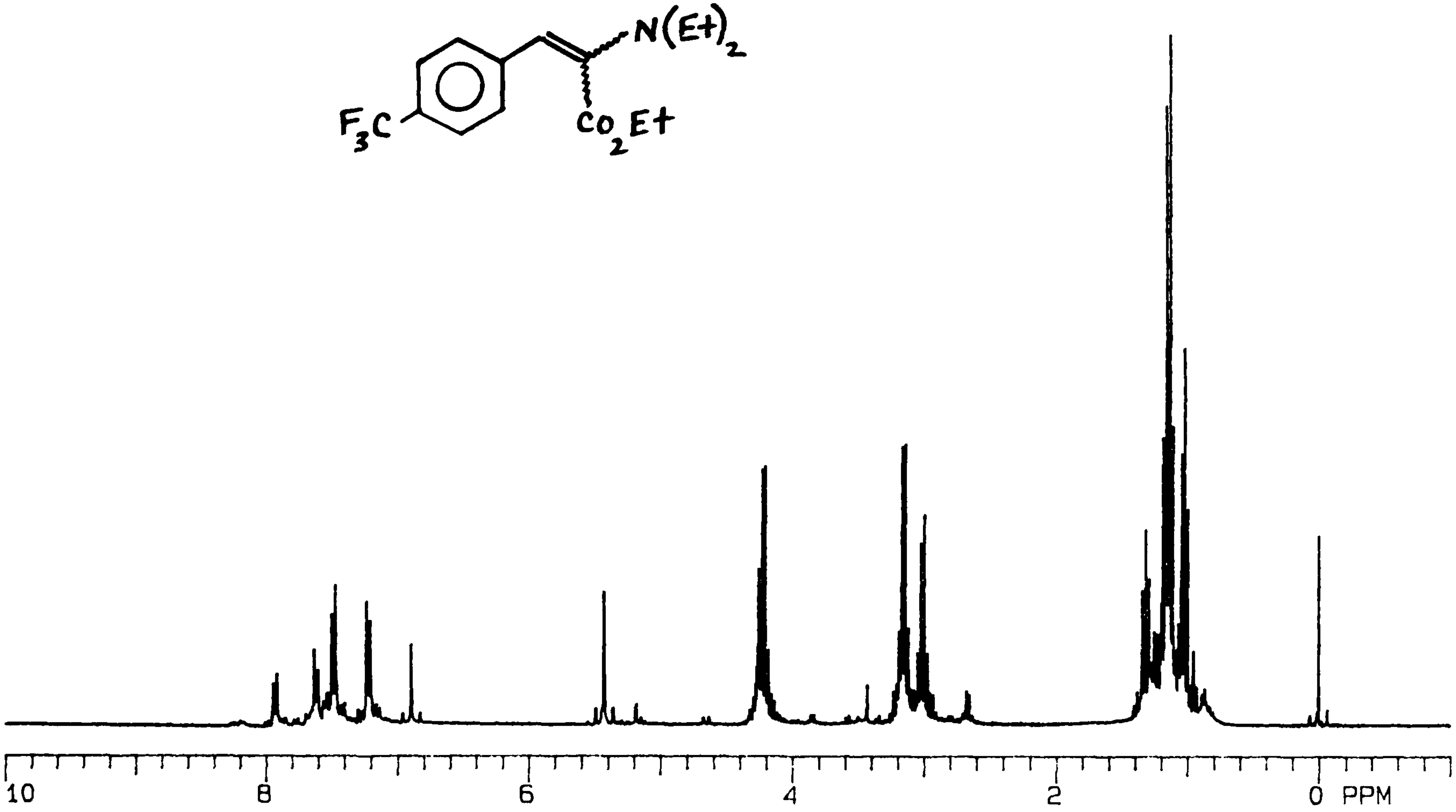

(E+Z) ethyl 2-diethylamino-3-(4-cyanophenyl)-2-propenoate

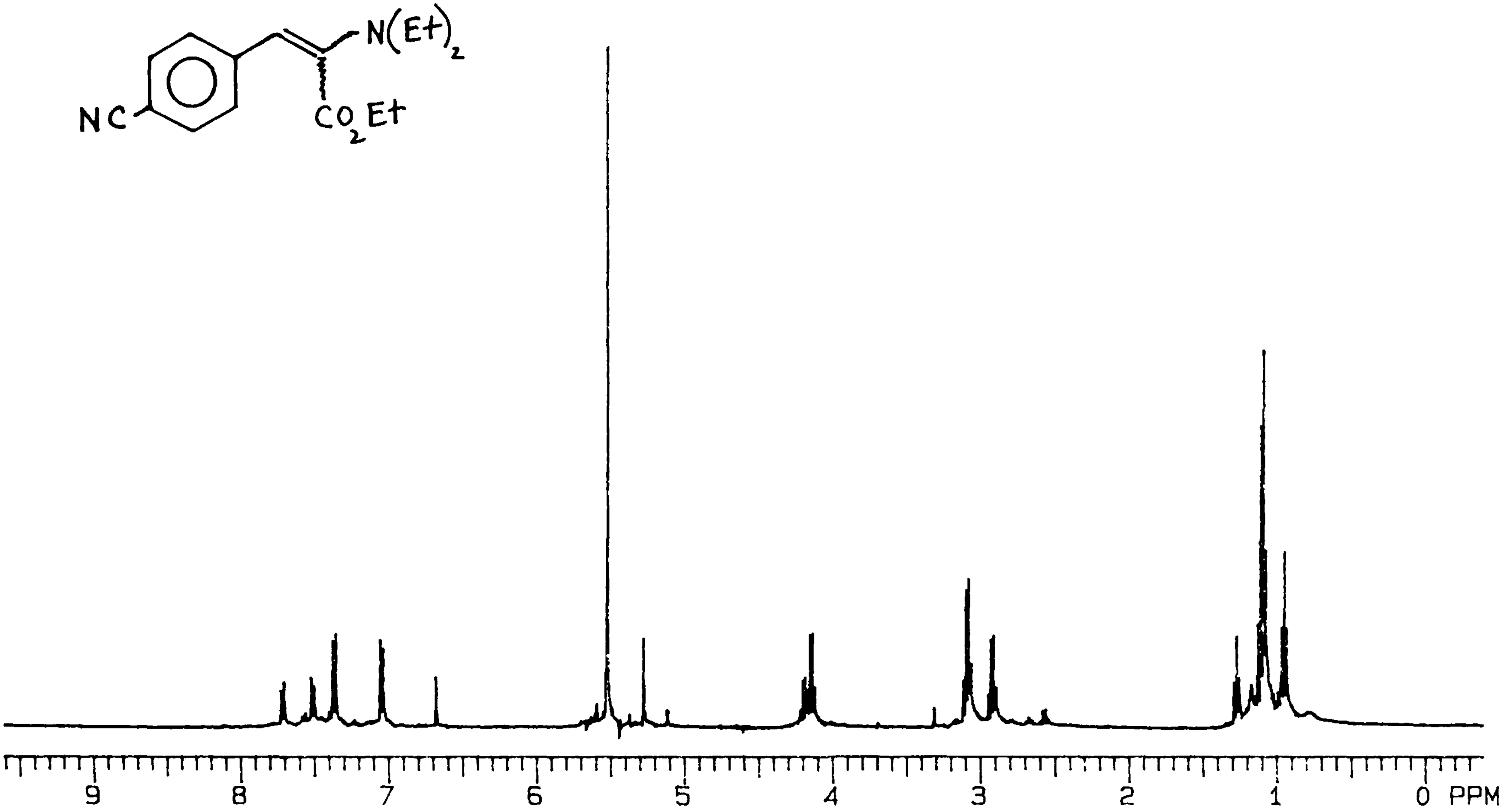

(E+Z) ethyl 2-diethylamino-3-(4-nitrophenyl)-2-propenoate

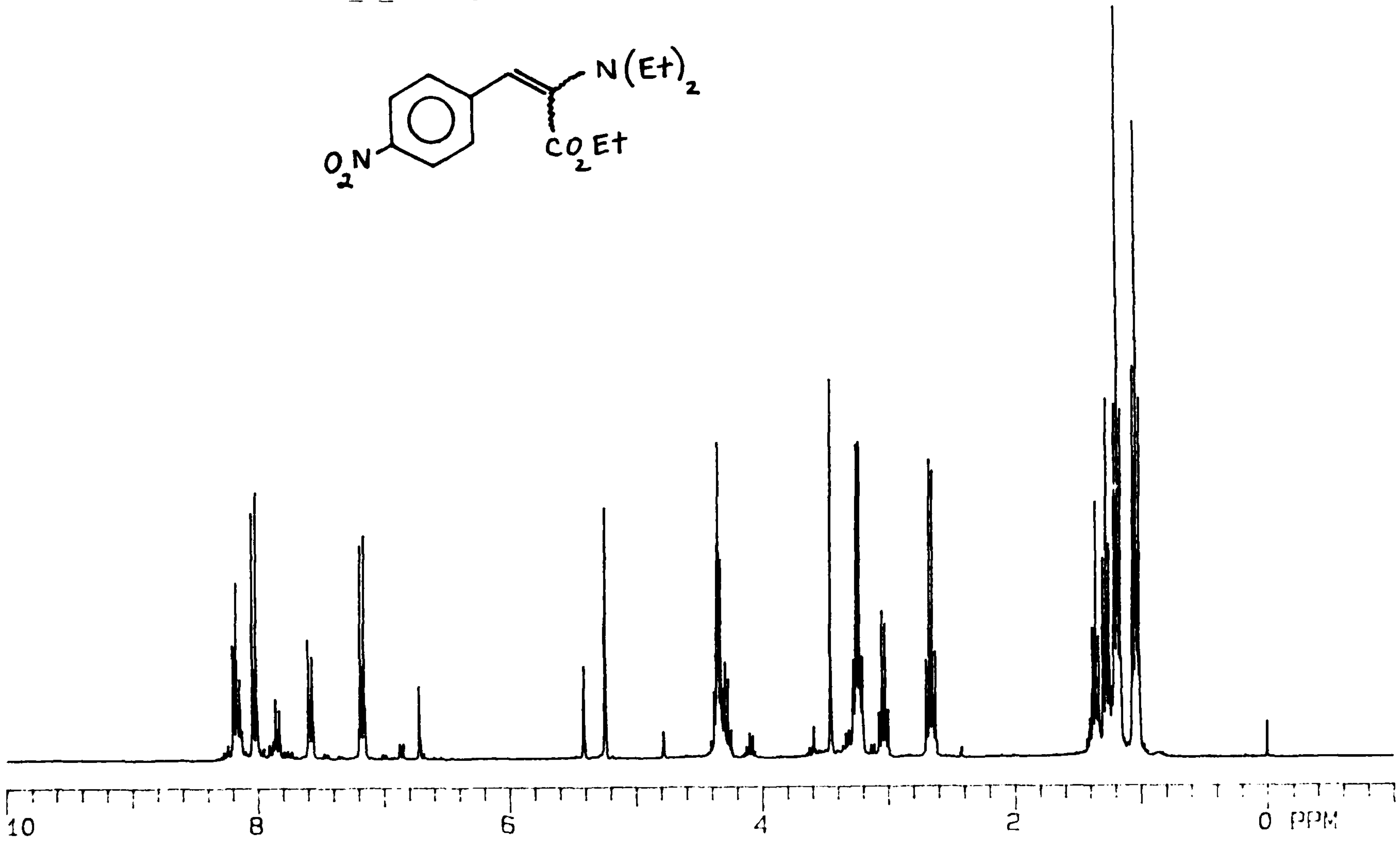

Series D/^{1}H NMR's

NOTE: These were obtained using $CDCl_3$ solvent and TMS referencing standard.

(E+Z) ethyl 2-phenylseleno-3-(4-dimethylaminophenyl)-2-propenoate

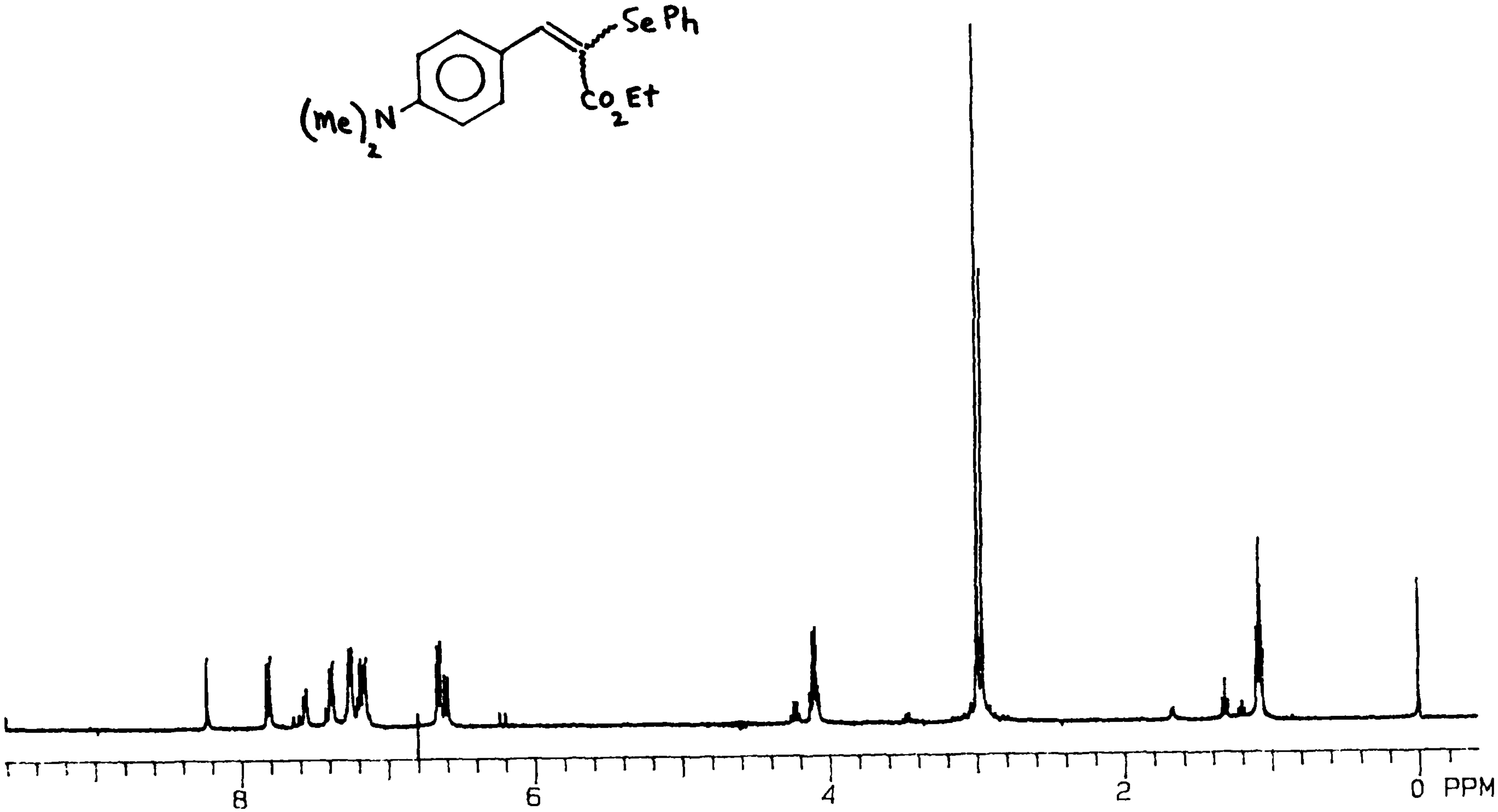

(E+Z) ethyl 2-phenylseleno-3-(4-methoxyphenyl)-2-propenoate

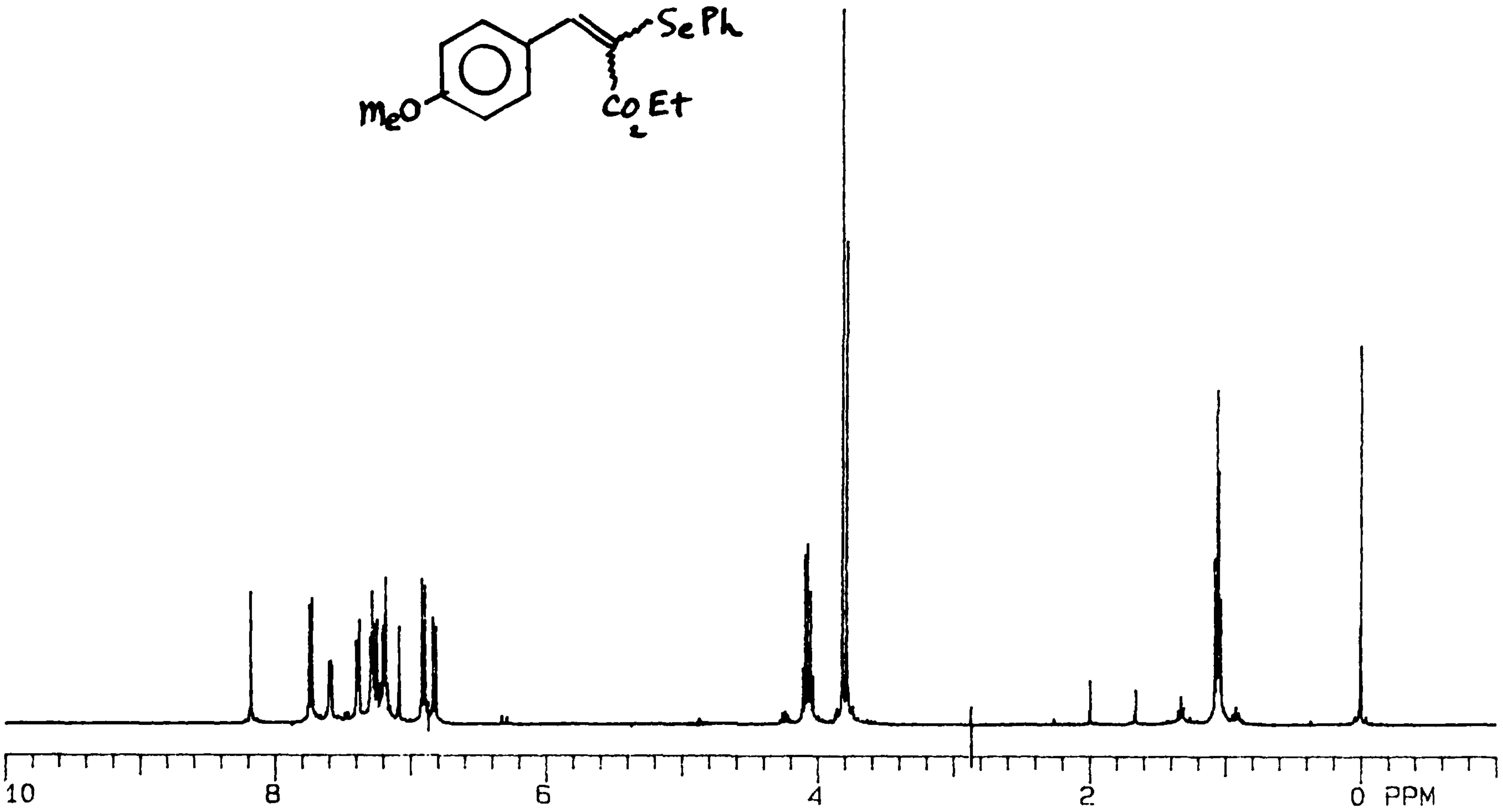

(E+Z) ethyl 2-phenylseleno-3-(4-methylphenyl)-2-propenoate

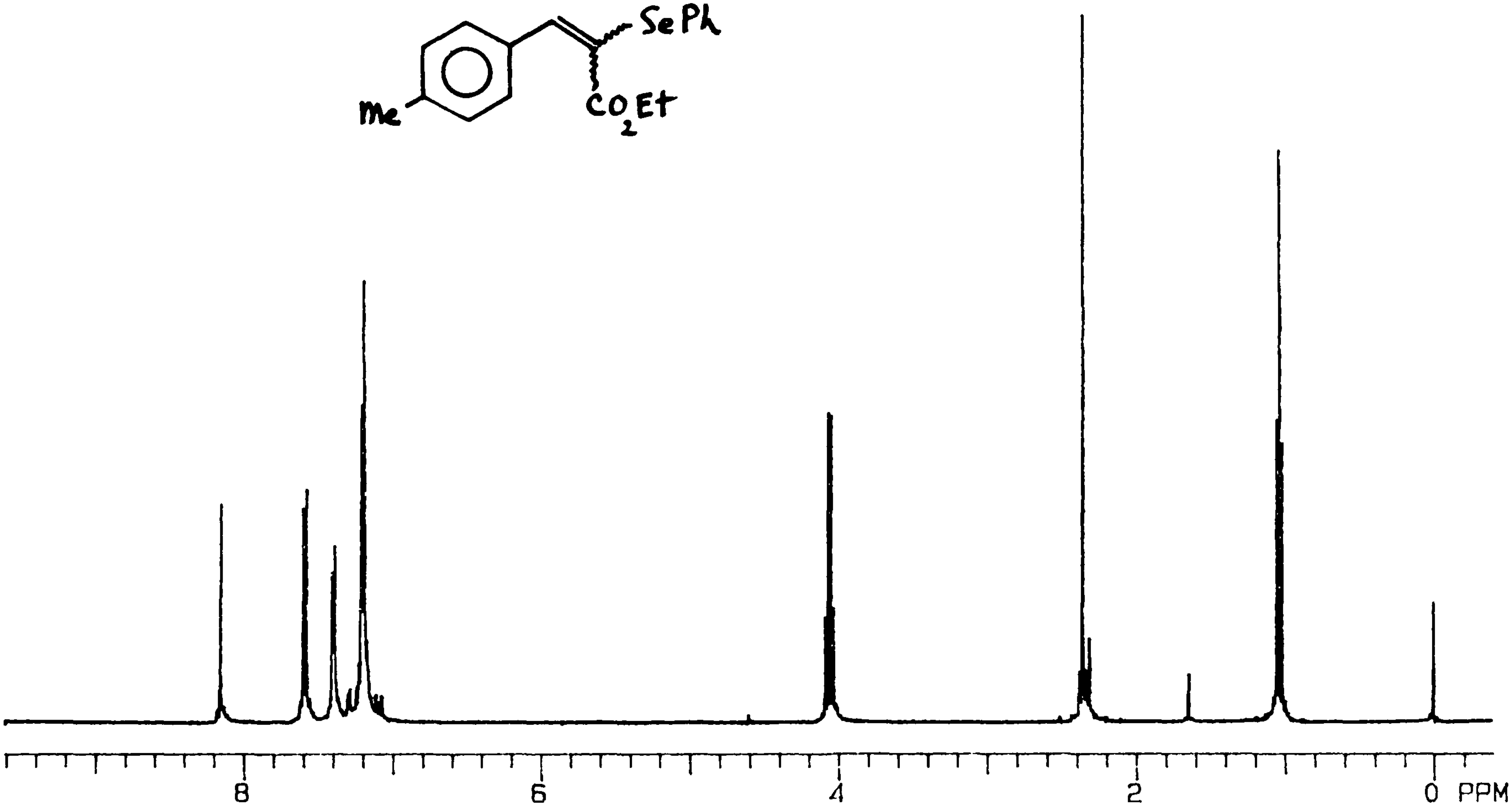

(E+Z) ethyl 2-phenylseleno-3-(4-phenylphenyl)-2-propenoate

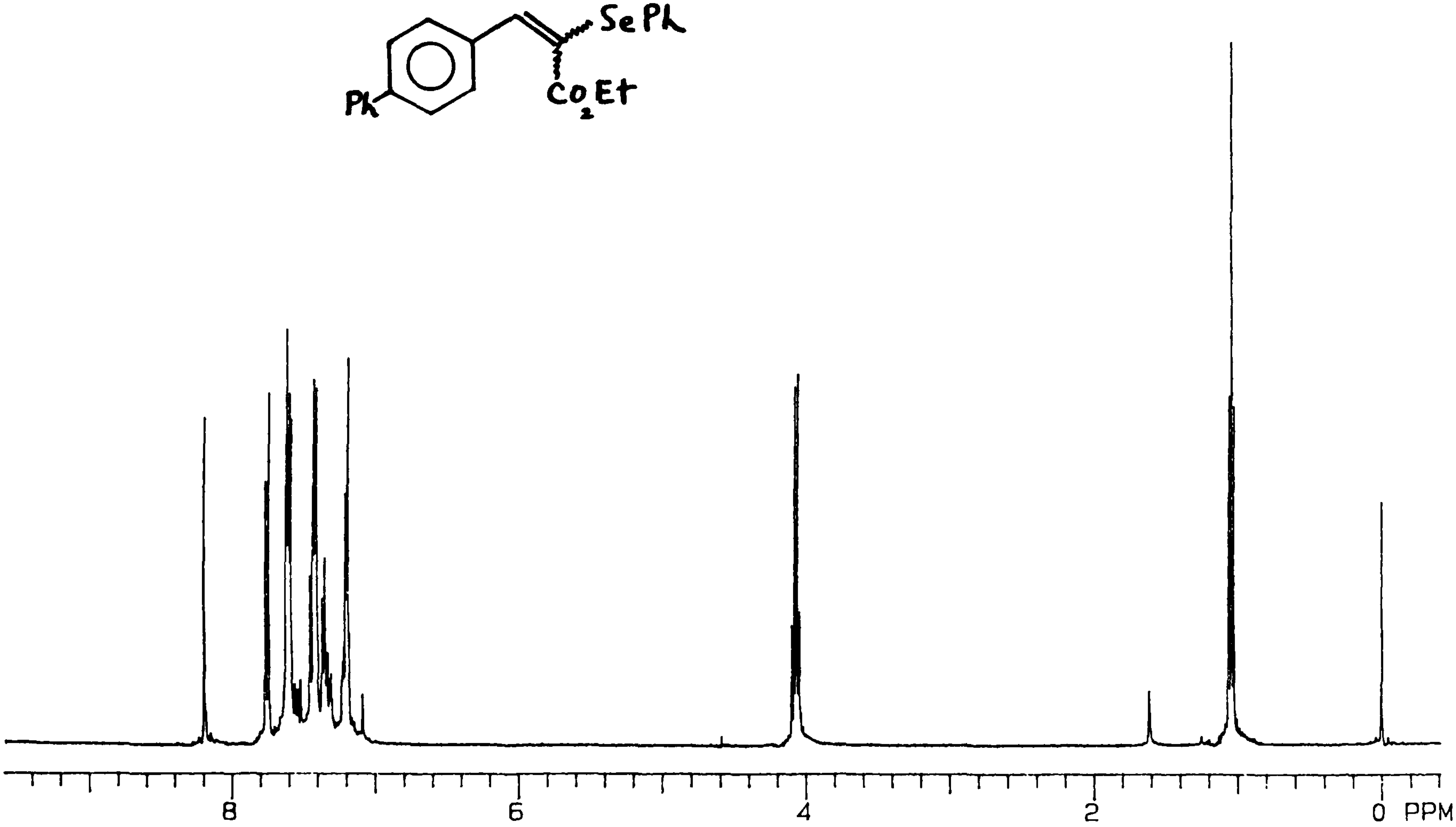

(E+Z) ethyl 2-phenylseleno-3-(4-fluorophenyl)-2-propenoate

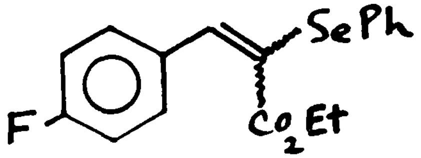
F
SePh
CO2Et

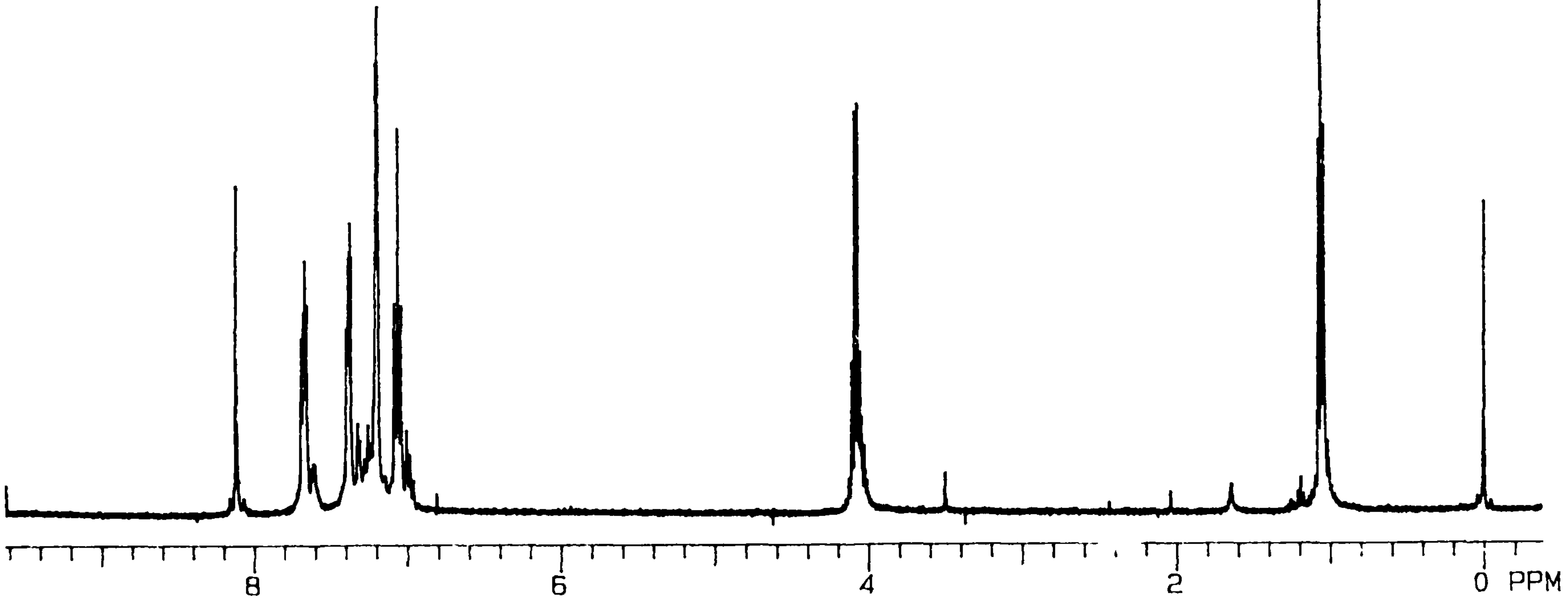

(E+Z) ethyl 2-phenylseleno-3-phenyl-2-propenoate

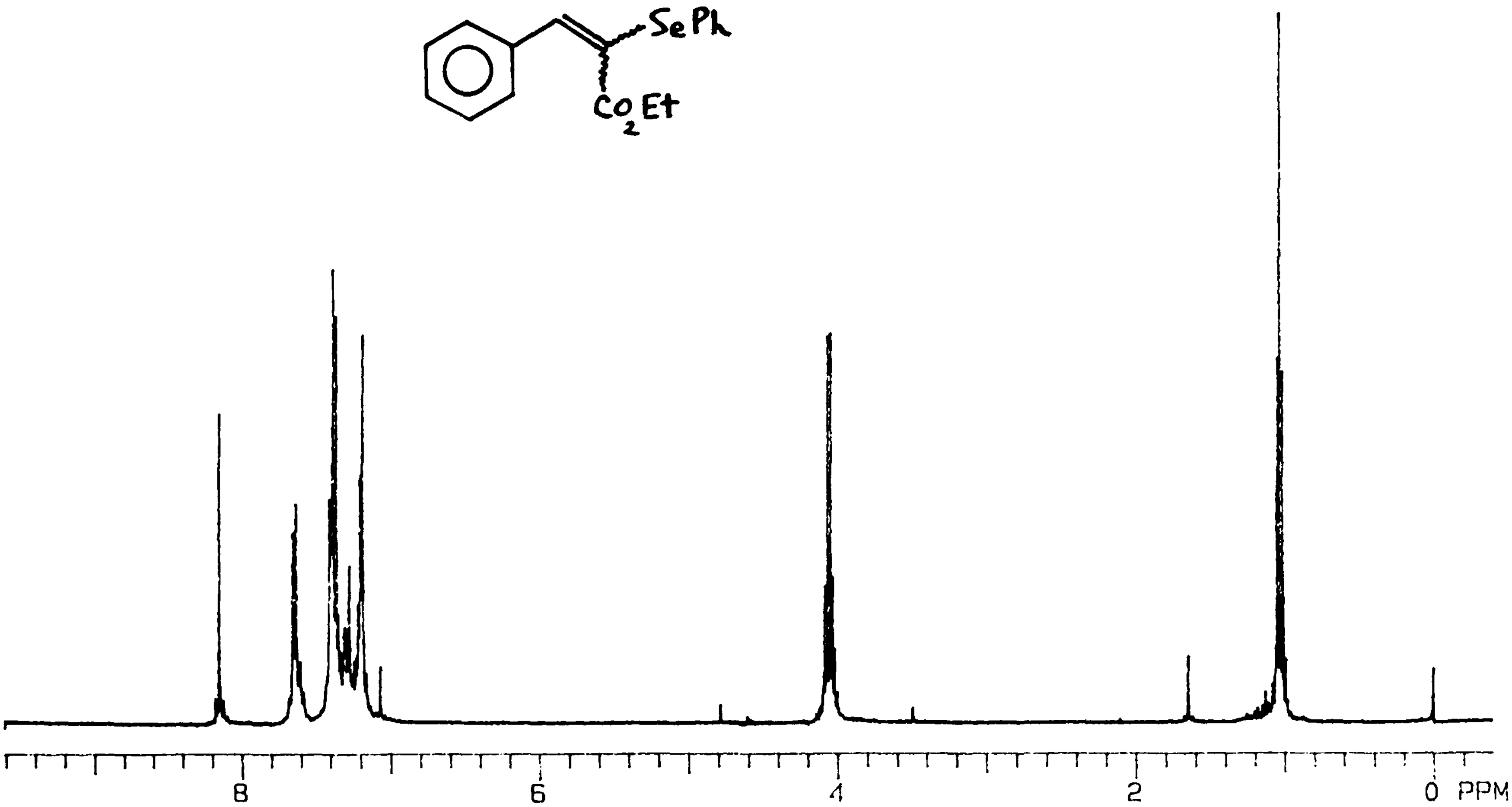

(E+Z) ethyl 2-phenylseleno-3-(3-methoxyphenyl)-2-propenoate

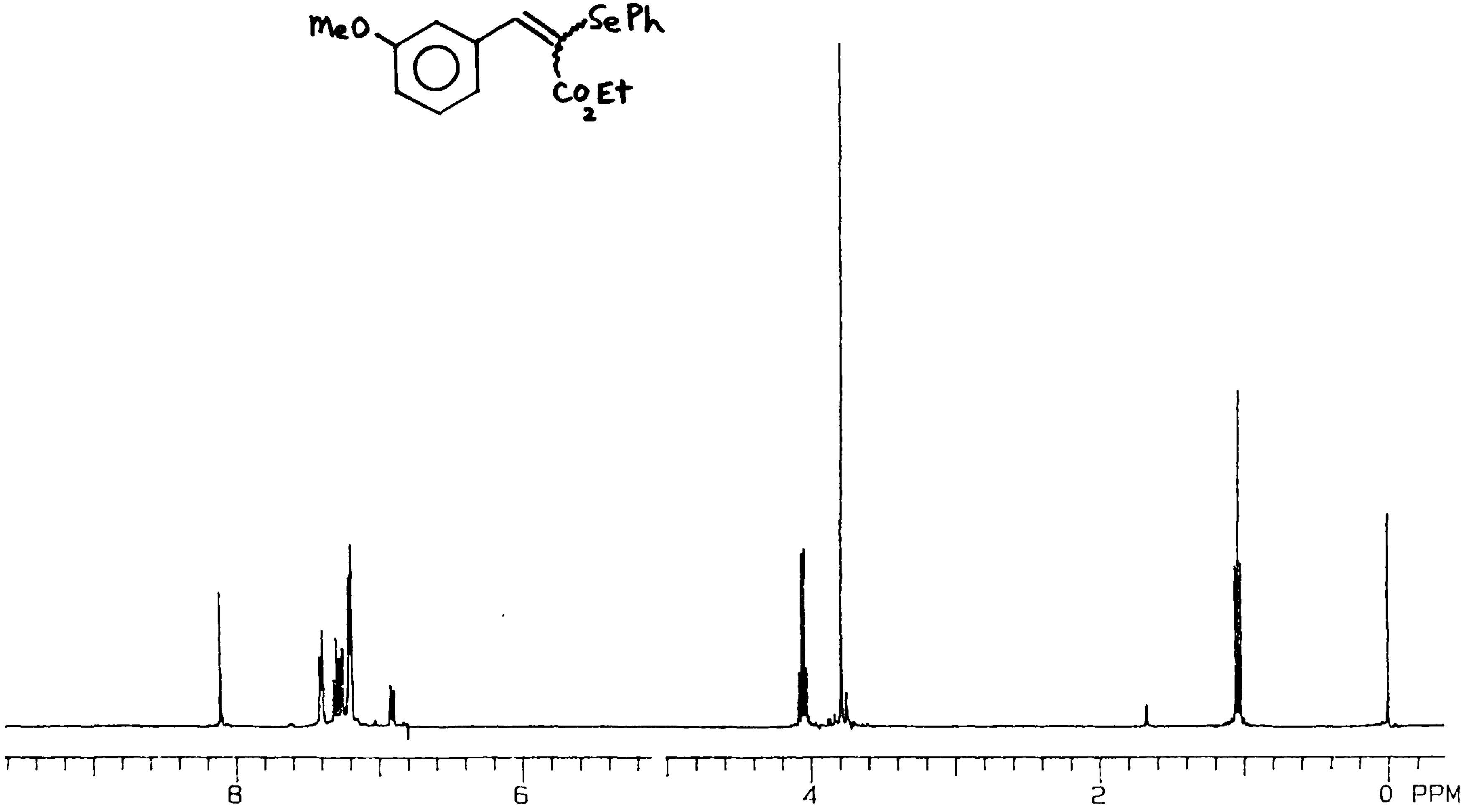

(E+Z) ethyl 2-phenylseleno-3-(4-chlorophenyl)-2-propenoate

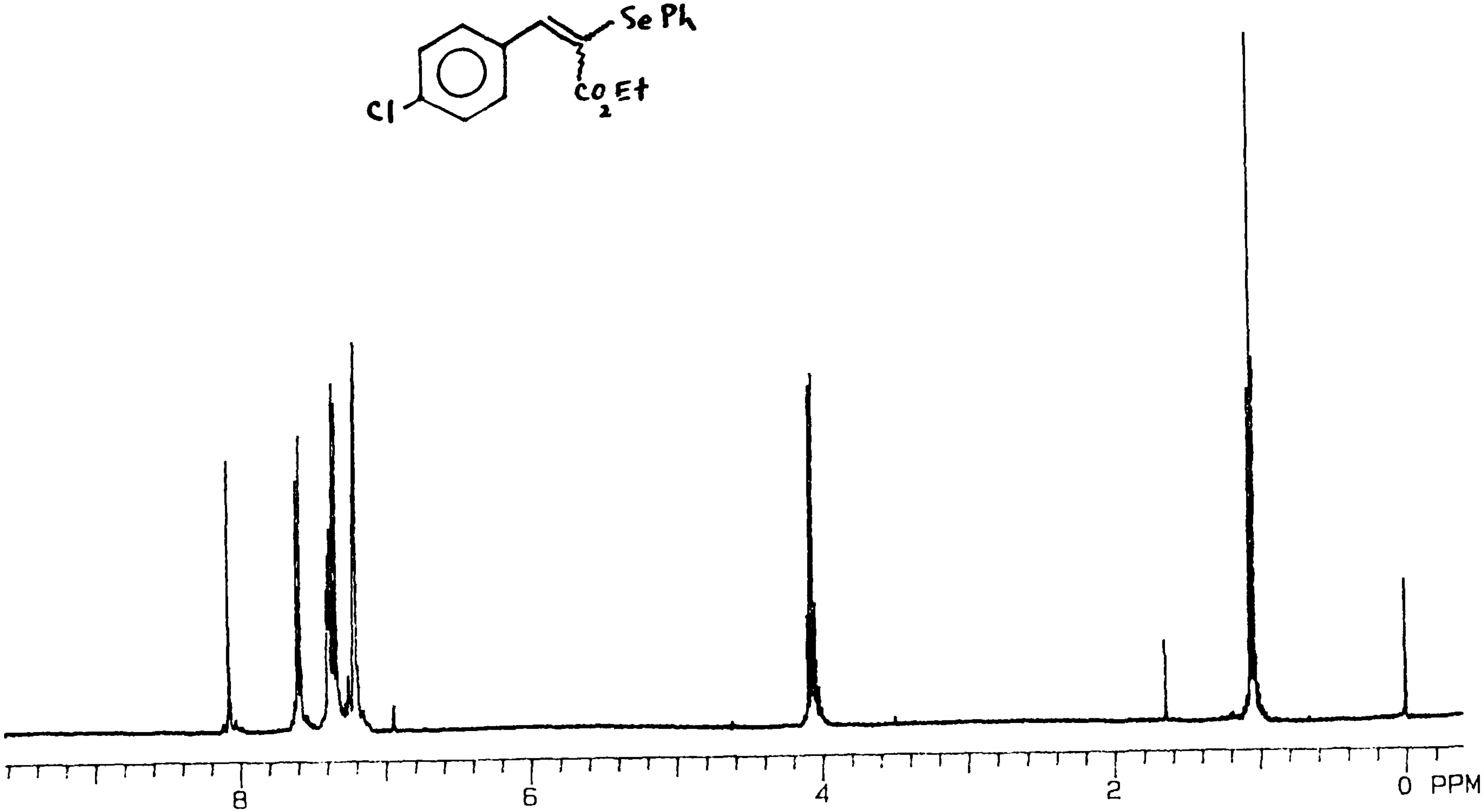

(E+Z) ethyl 2-phenylseleno-3-(3-fluorophenyl)-2-propenoate

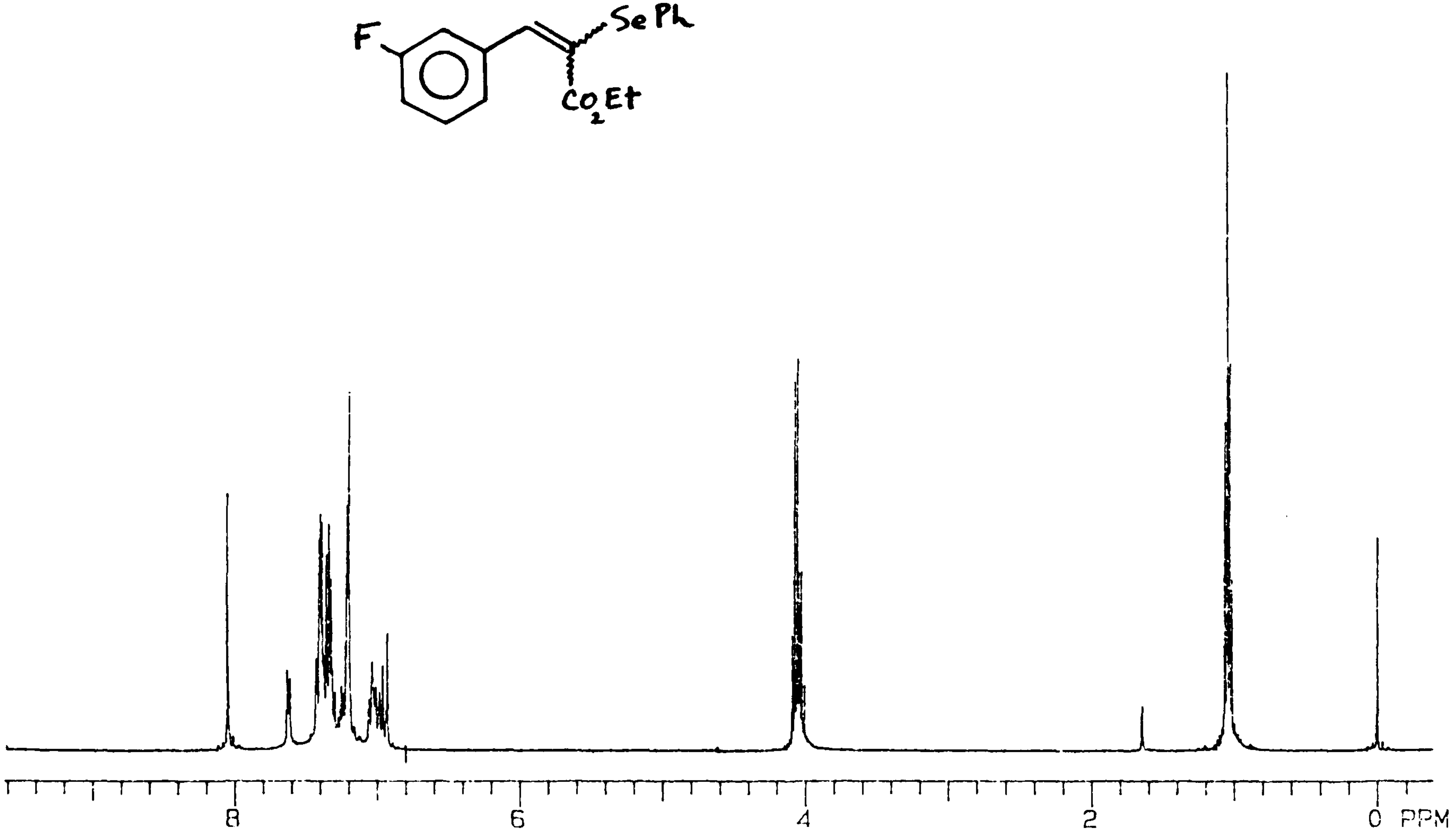

(E) ethyl 2-phenylseleno-3-(3-chlorophenyl)-2-propenoate

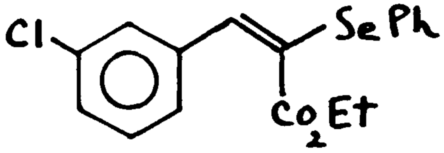
Cl
SePh
CO2Et

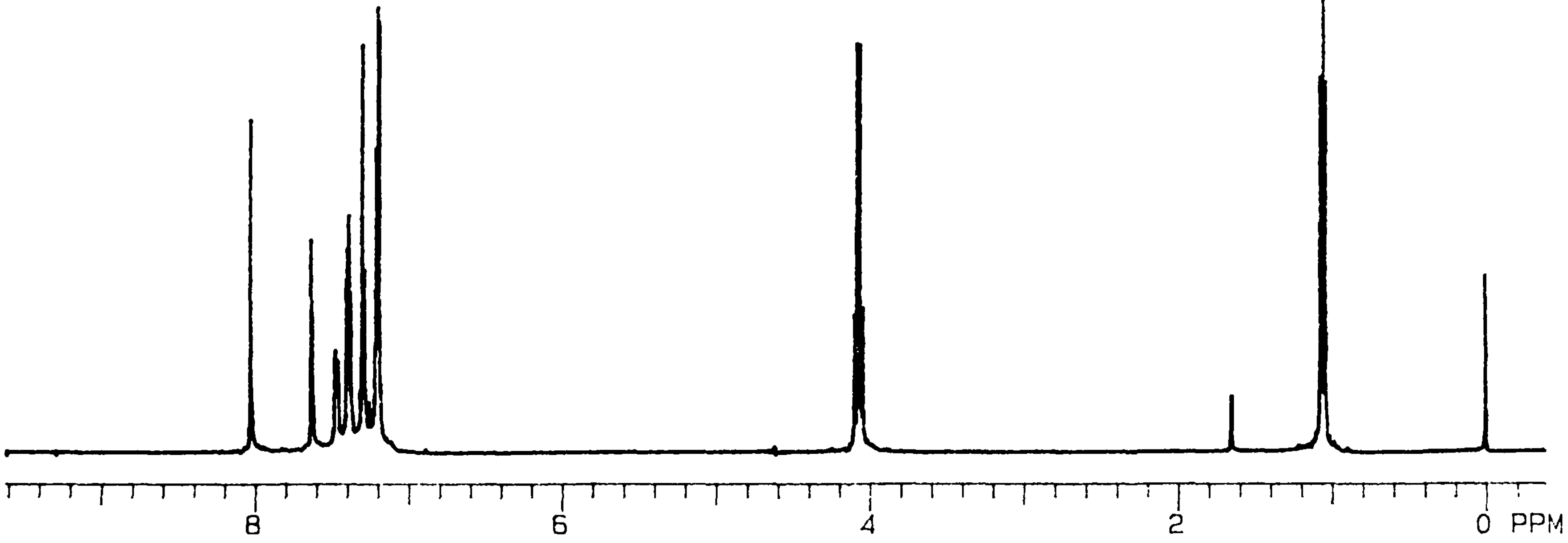

(E) ethyl 2-phenylseleno-3-(4-carbomethoxyphenyl)-2-propenoate

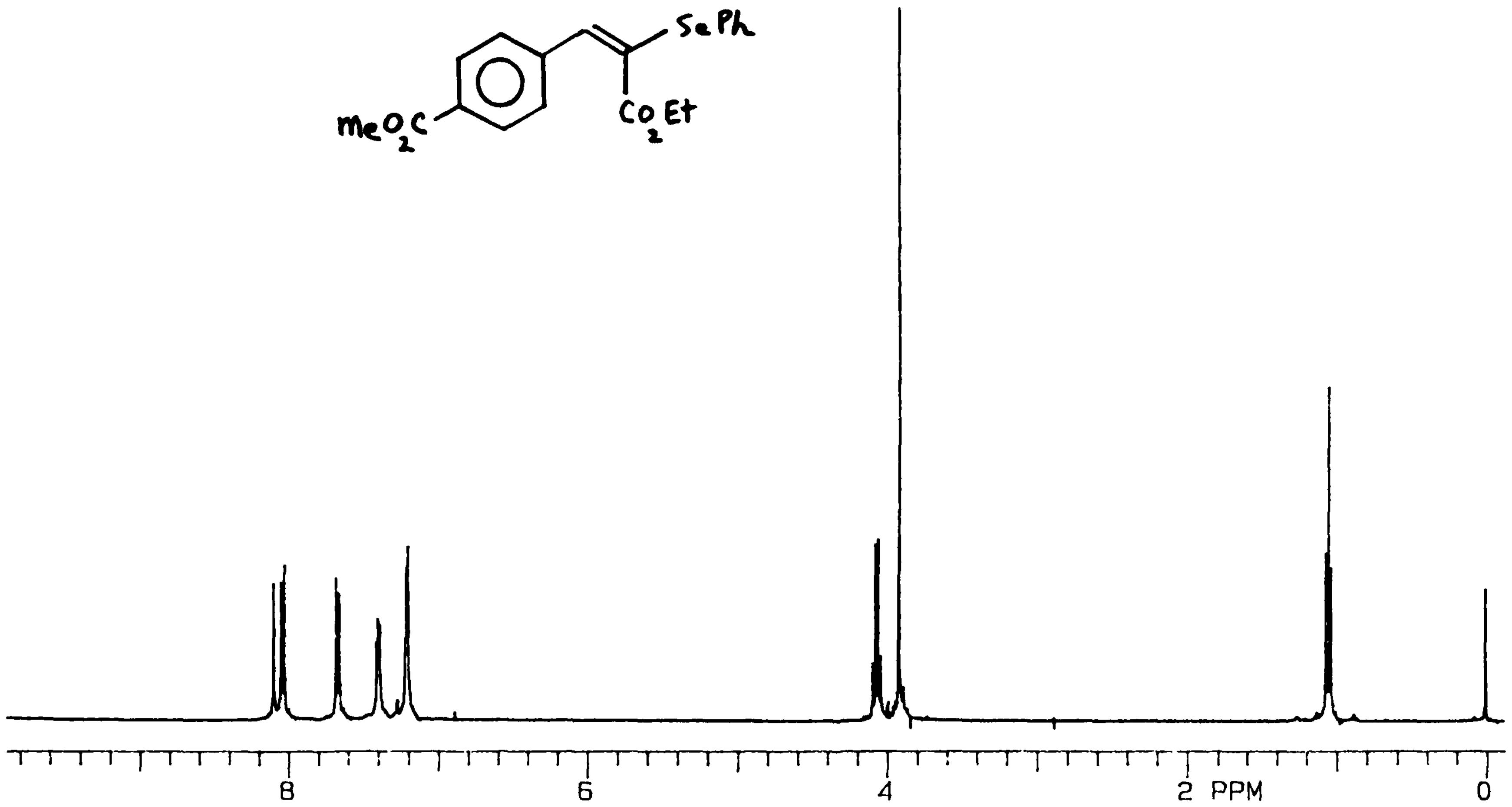

(E) ethyl 2-phenylseleno-3-(3-cyanophenyl)-2-propenoate

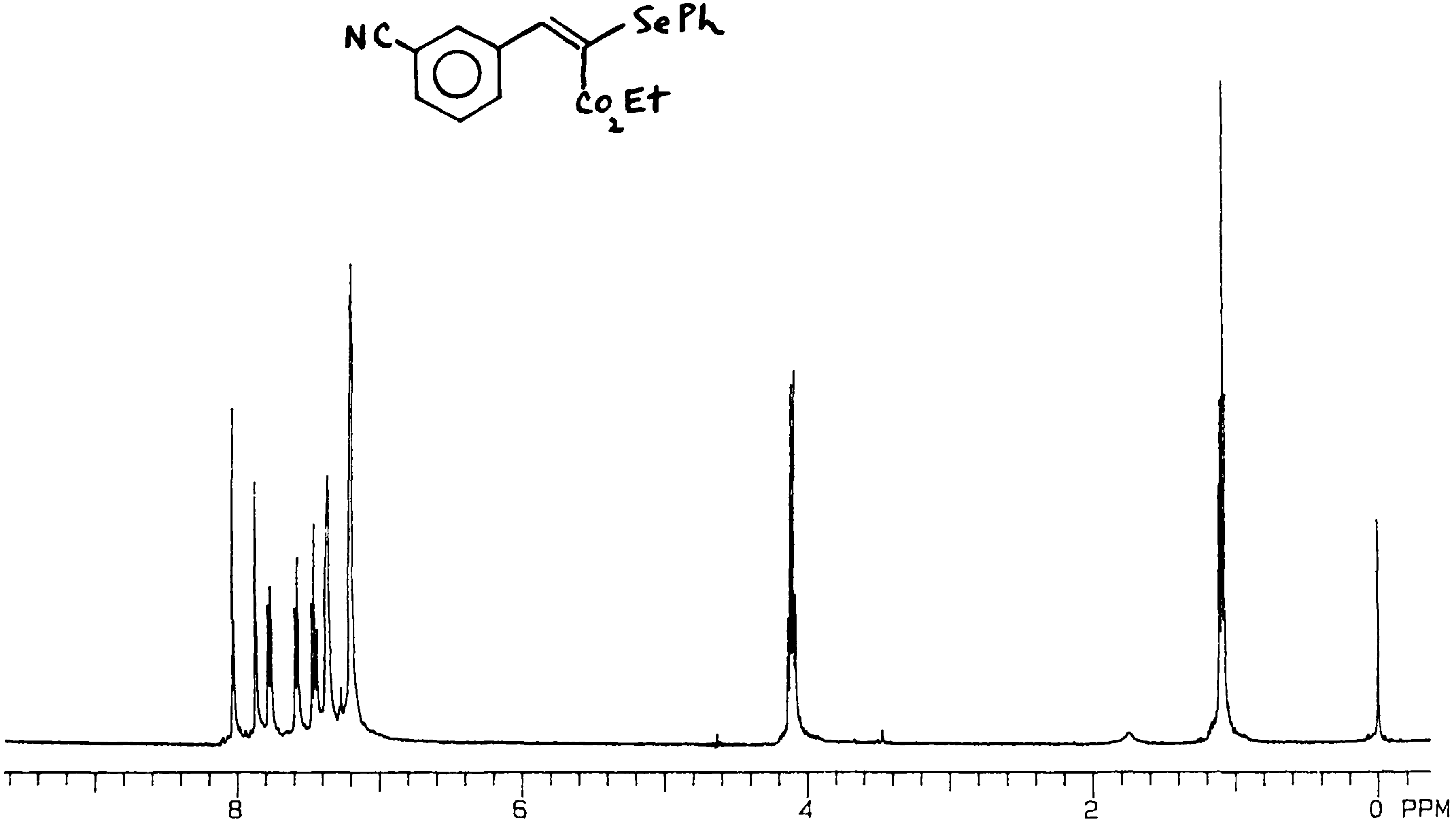

(E+Z) ethyl 2-phenylseleno-3-(3-trifluoromethylphenyl)-2-propenoate

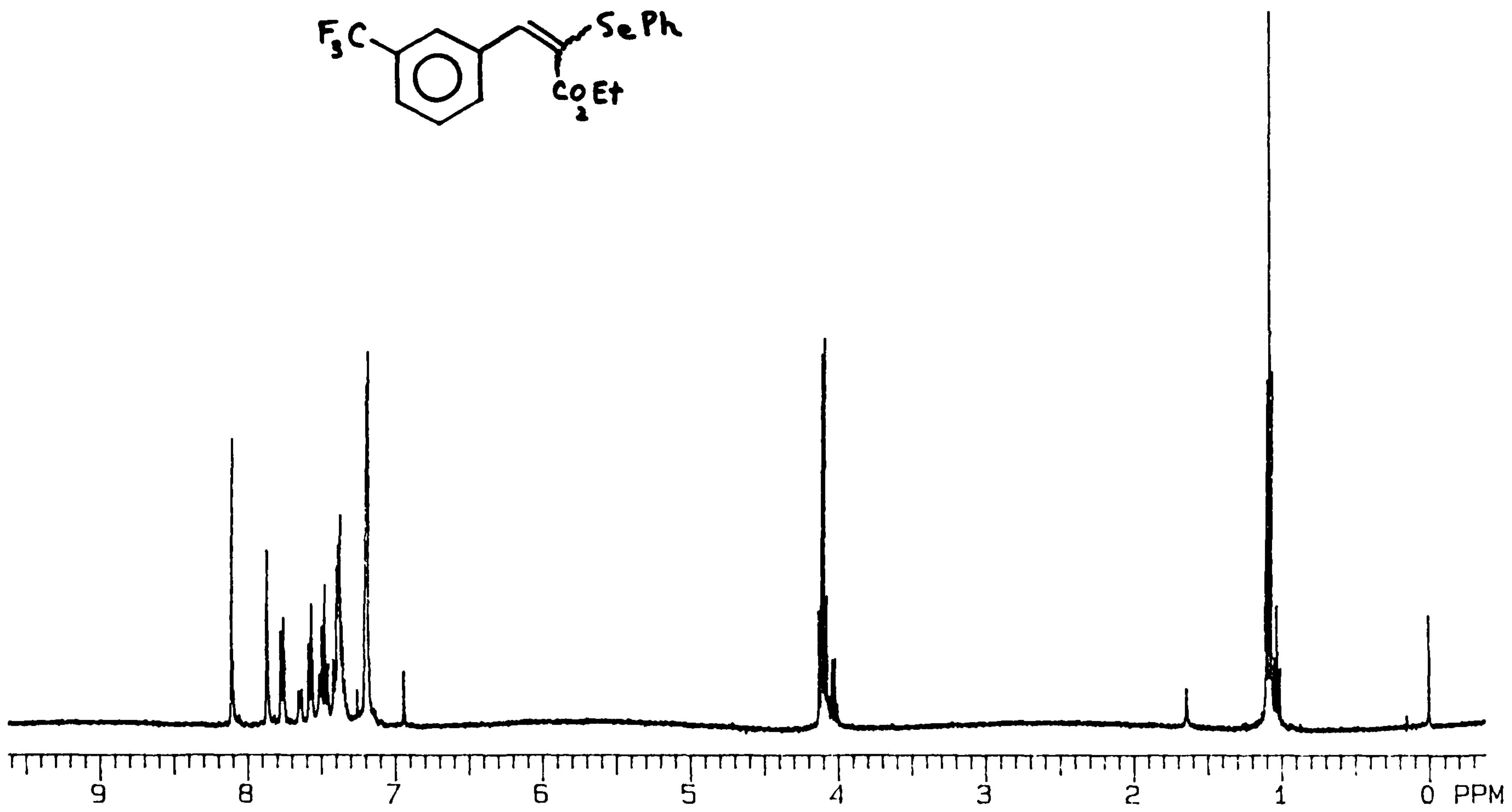

(E+Z) ethyl 2-phenylseleno-3-(4-trifluoromethylphenyl)-2-propenoate

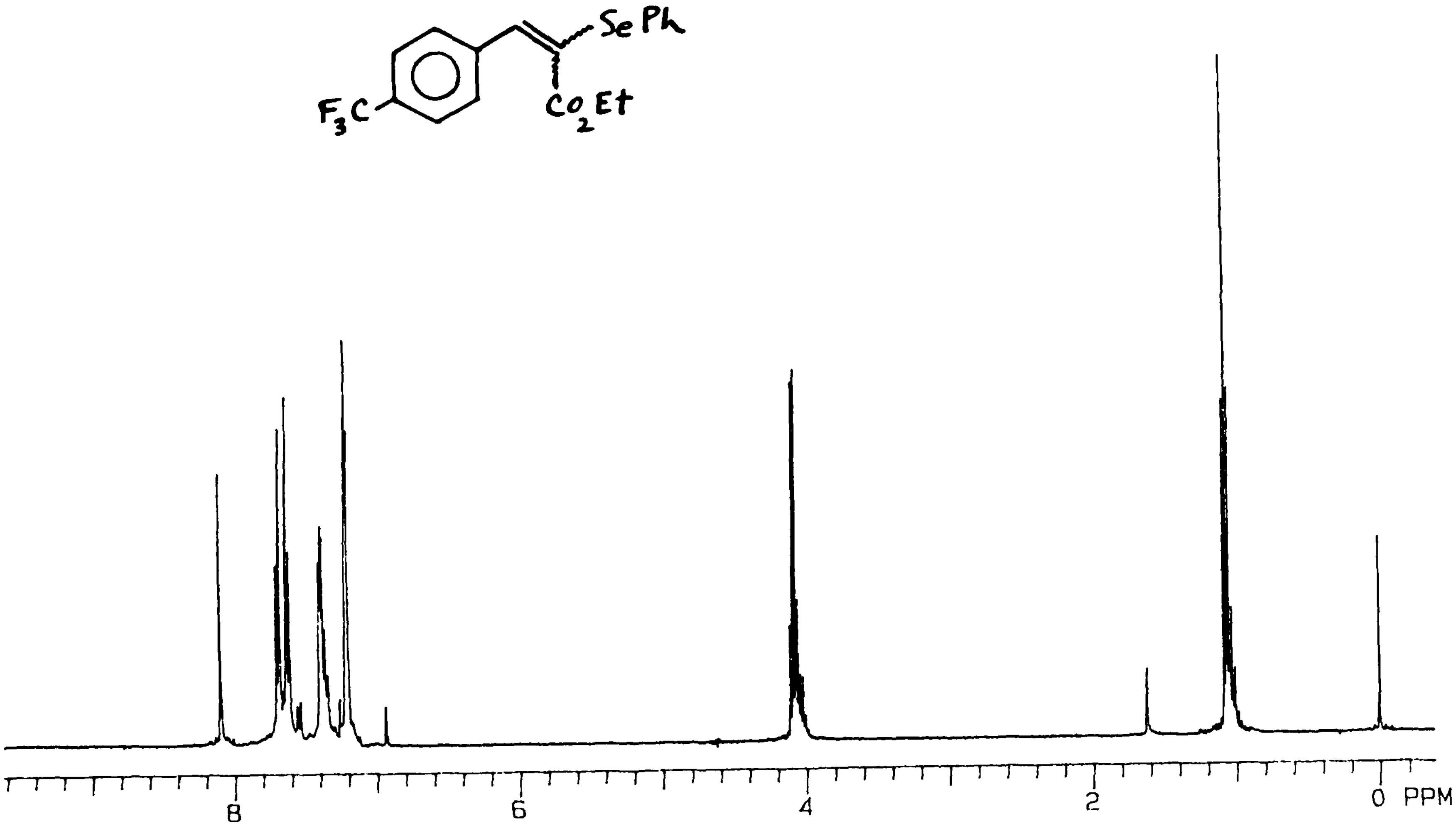

(E̲) ethyl 2-phenylseleno-3-(4-cyanophenyl)-2-propenoate

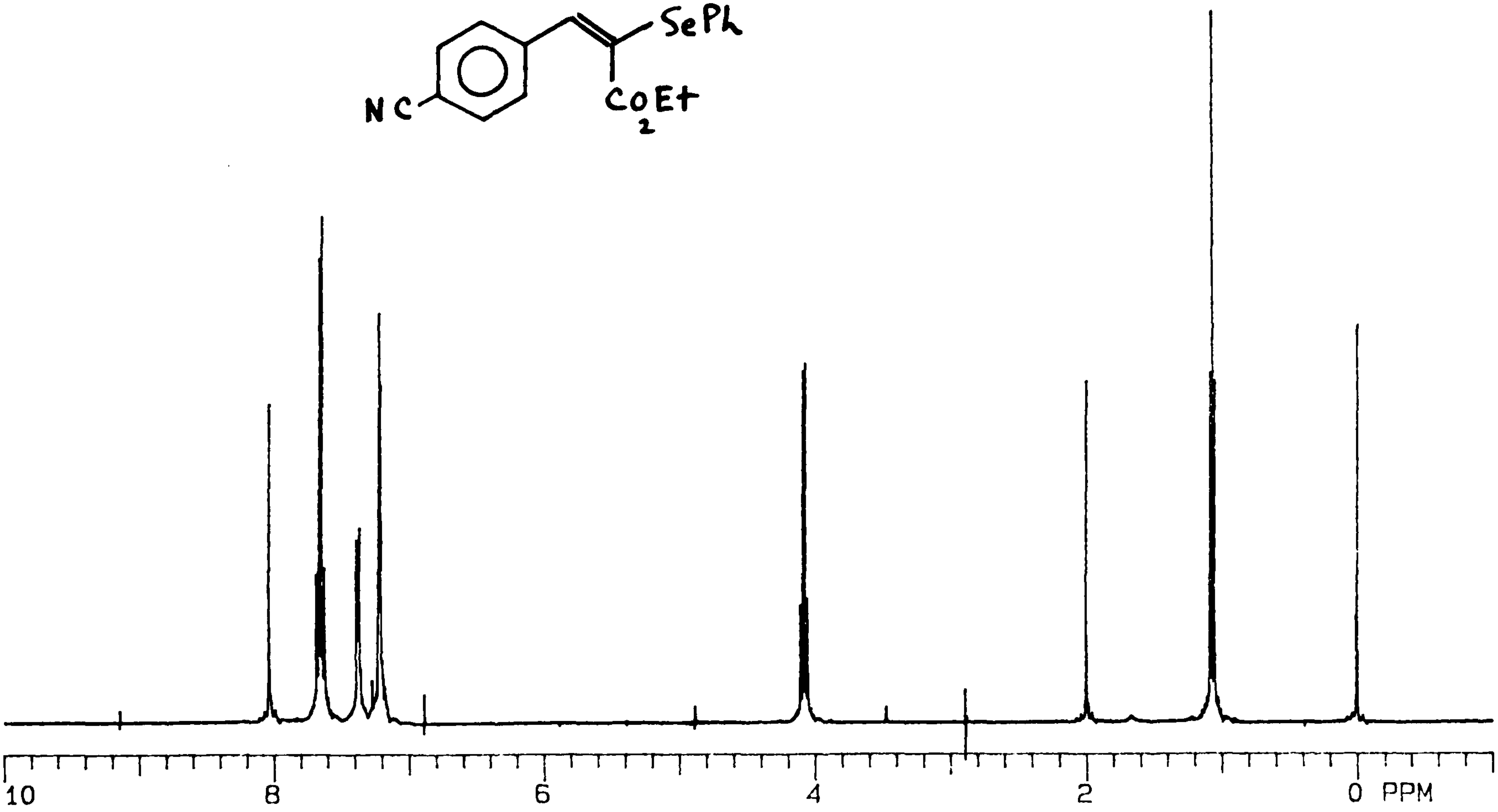

(E) ethyl 2-phenylseleno-3-(3-nitrophenyl)-2-propenoate

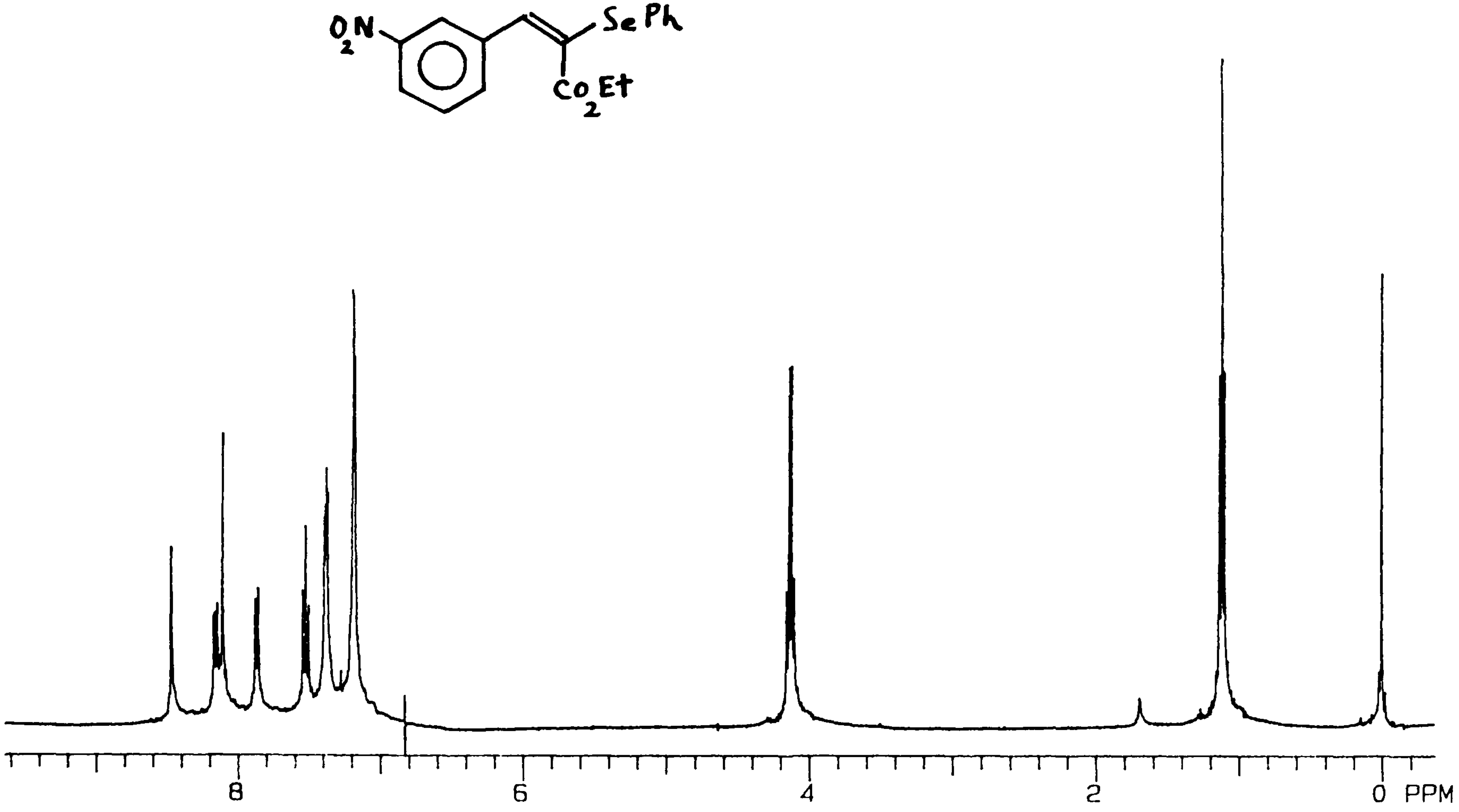

(Z+E) ethyl 2-phenylseleno-3-(4-nitrophenyl)-2-propenoate

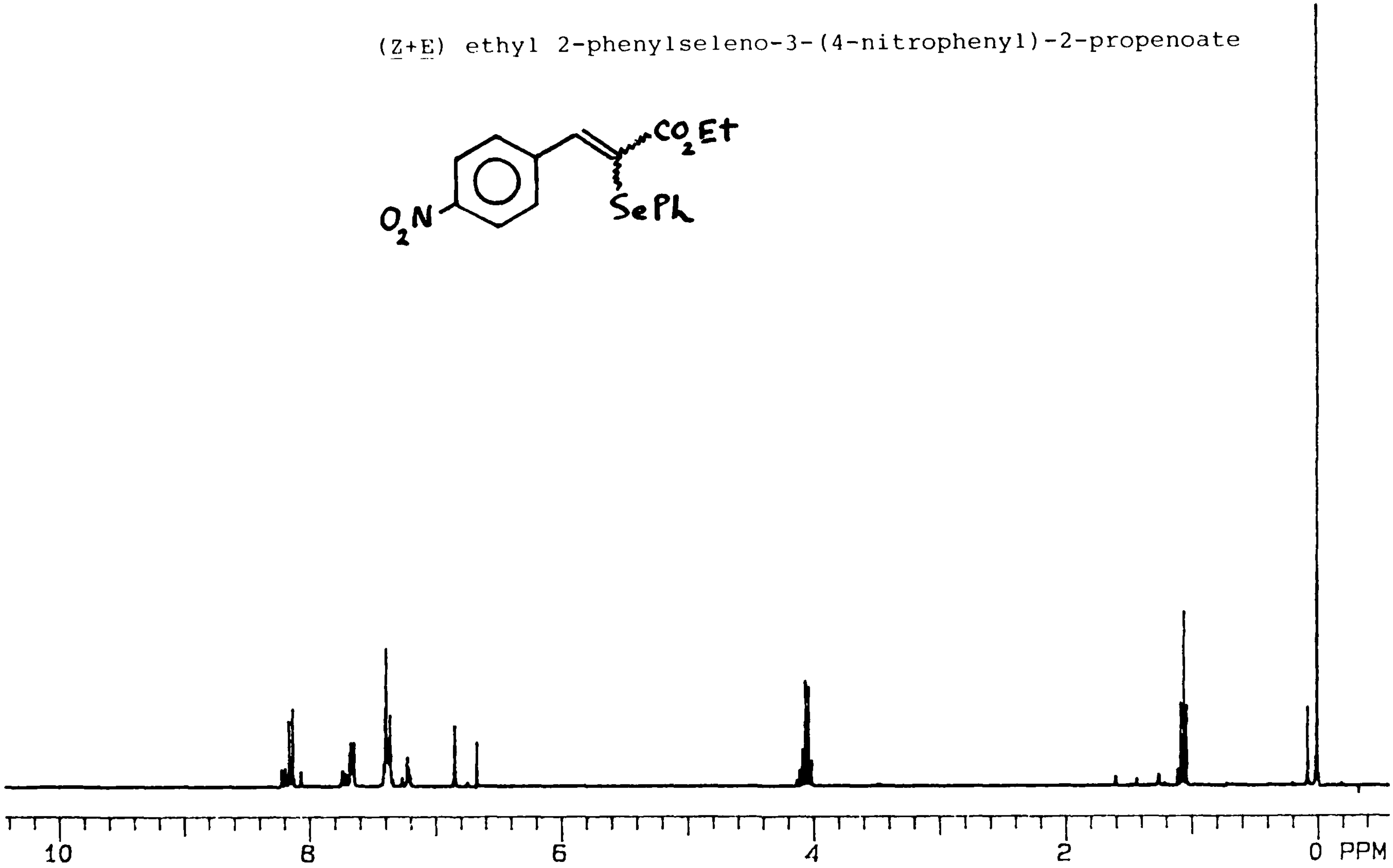

Appendix C

^{13}C NMR

Series A

^{13}C NMR spectra for the Series A compounds follow:

NOTE: These were obtained using CD_3NO_2 solvent and TMS referencing standard.

(Z+E) ethyl 2-diethylamino-3-(4-dimethylaminophenyl)-2-propenoate

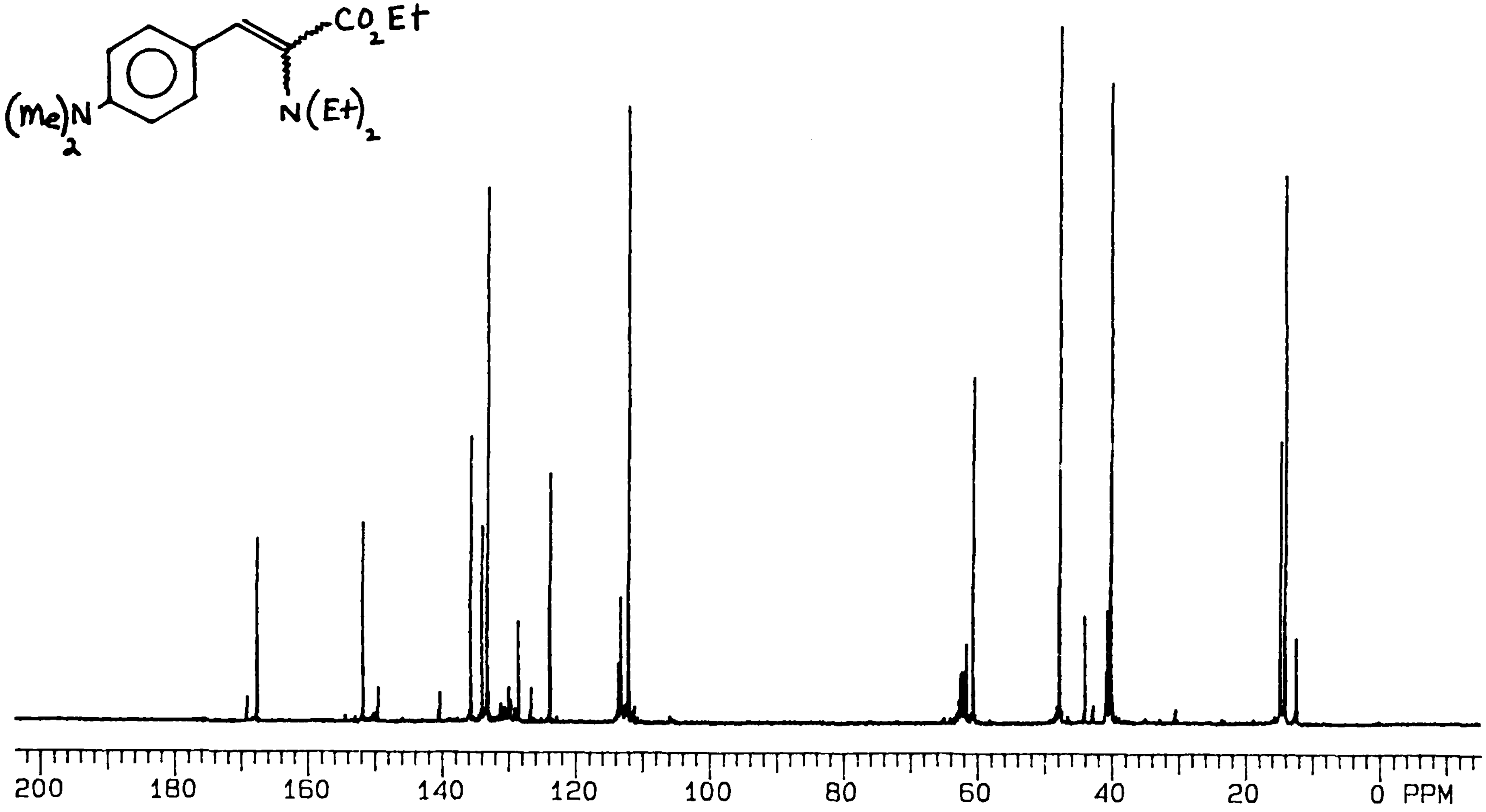

(Z+E) ethyl 2-diethylamino-3-(4-methoxyphenyl)-2-propenoate

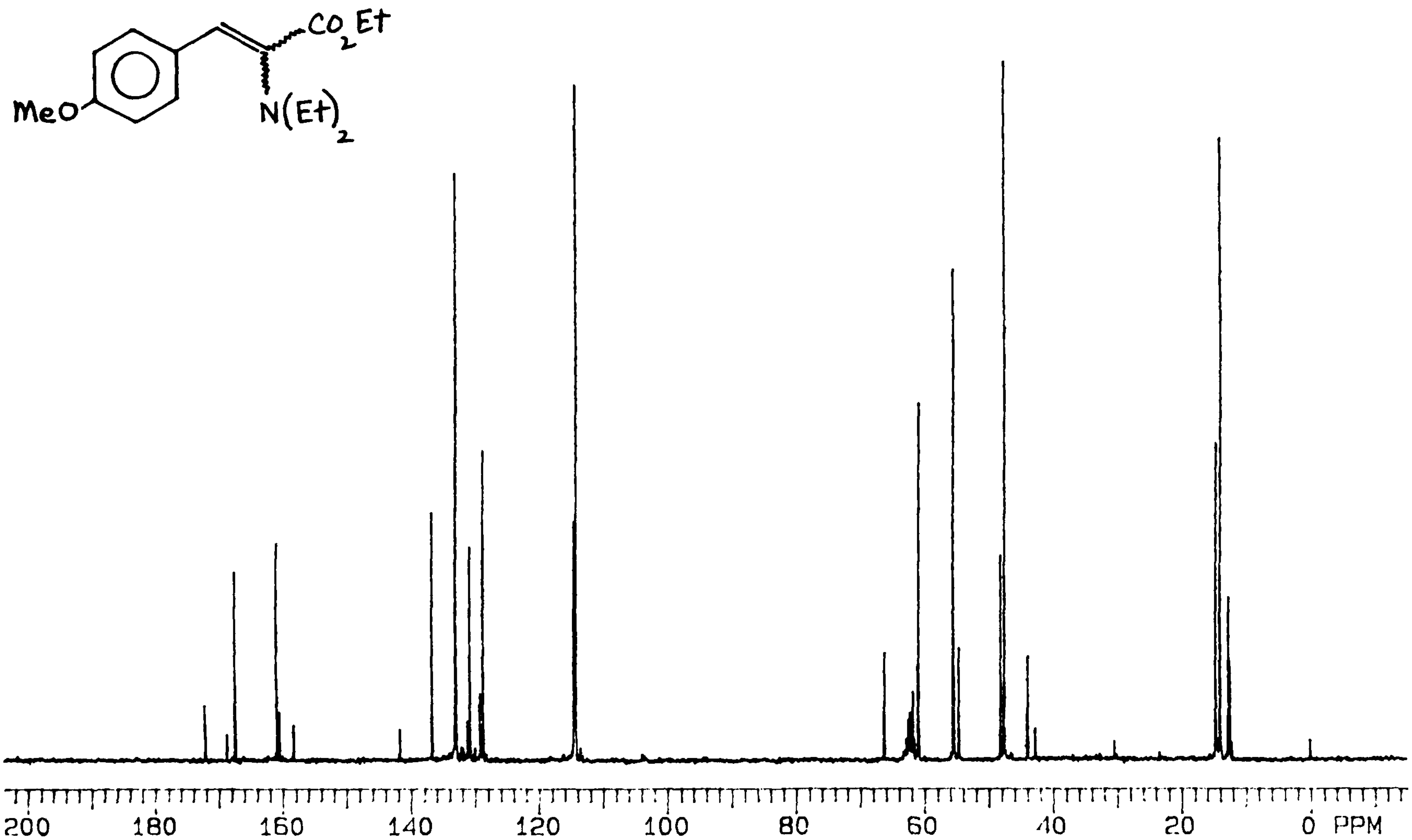

(Z+E) ethyl 2-diethylamino-3-(4-methylphenyl)-2-propenoate

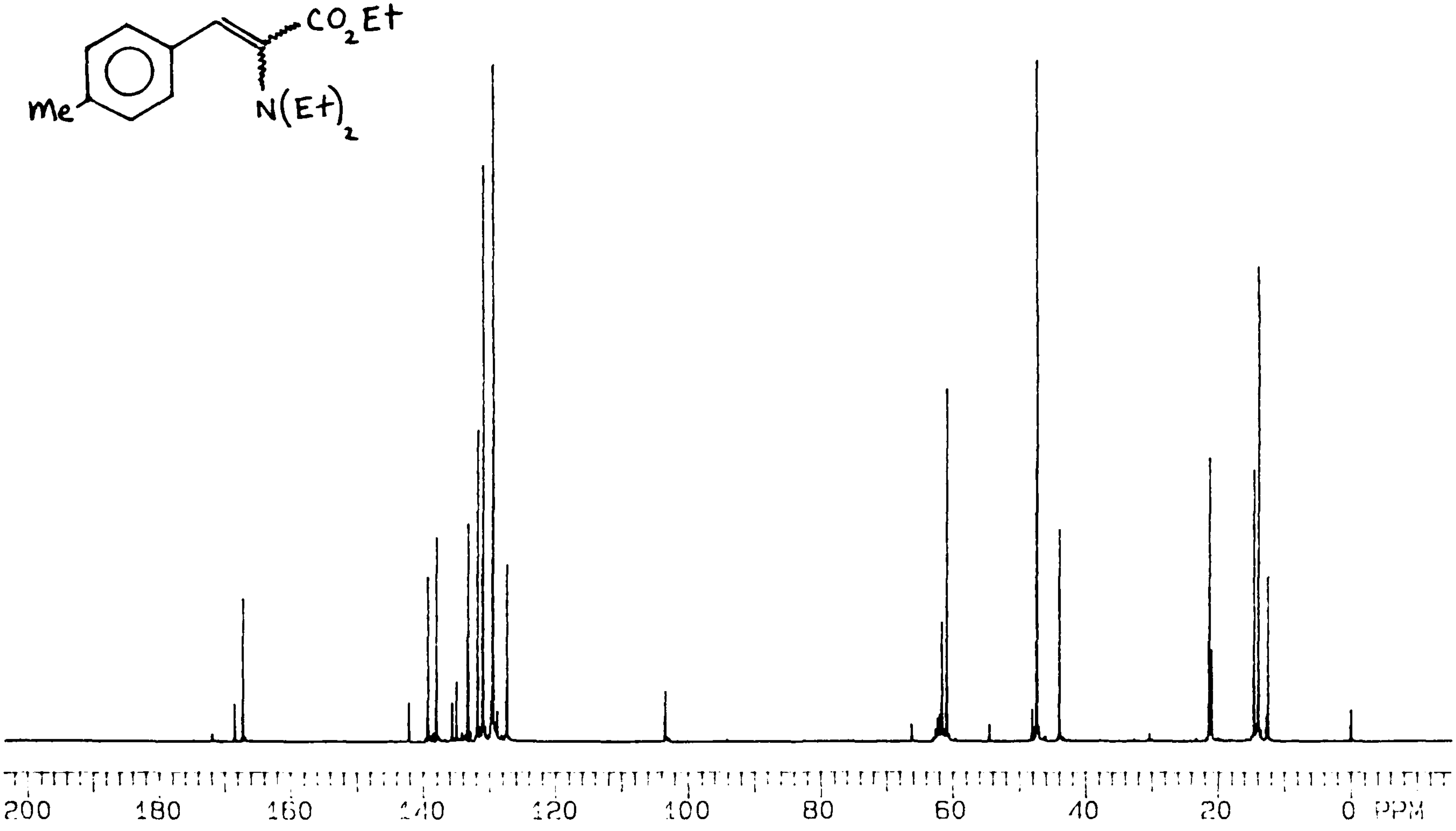

(Z+E) ethyl 2-diethylamino-3-(4-phenylphenyl)-2-propenoate

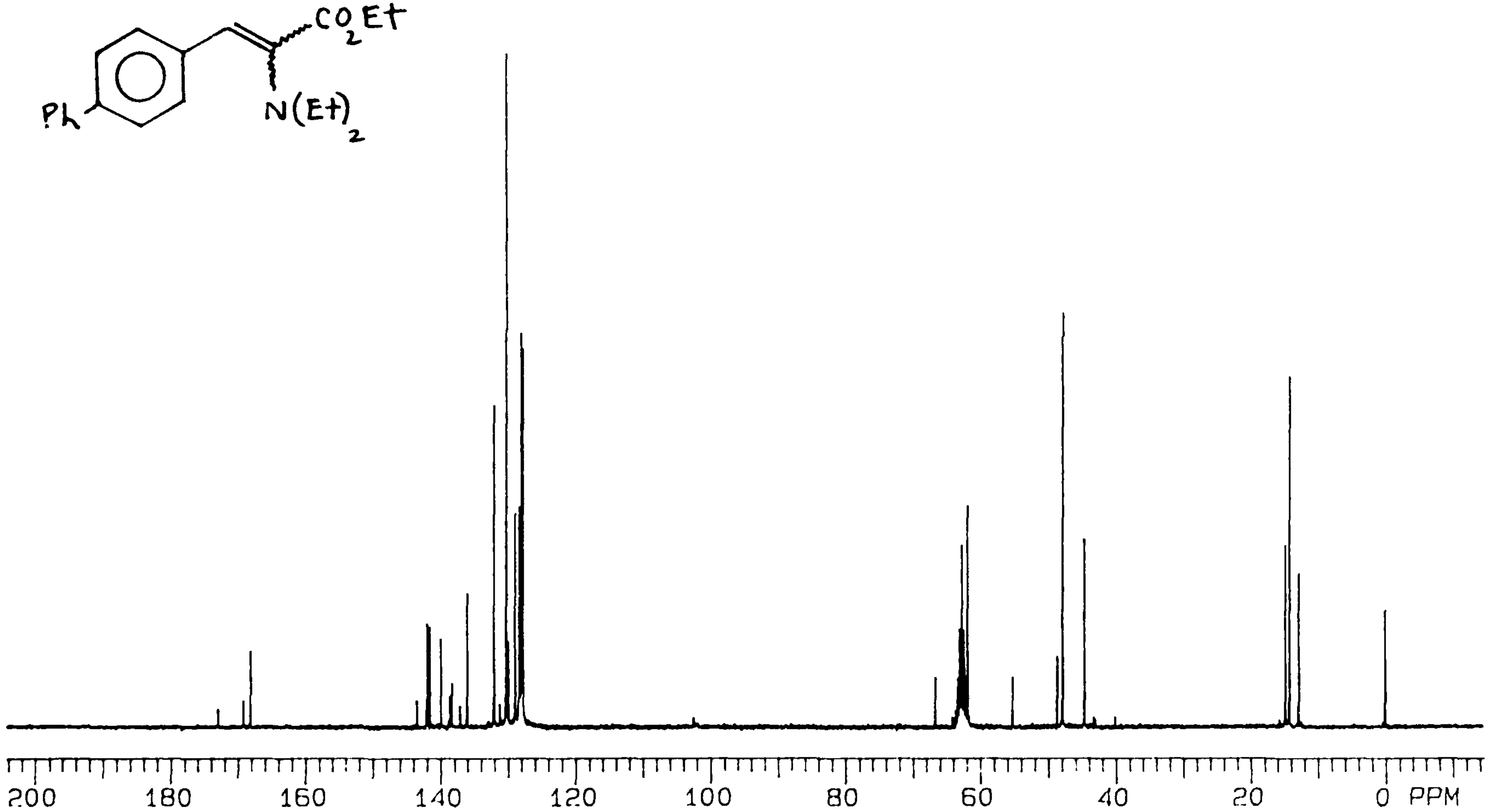

(Z+E) ethyl 2-diethylamino-3-(4-fluorophenyl)-2-propenoate

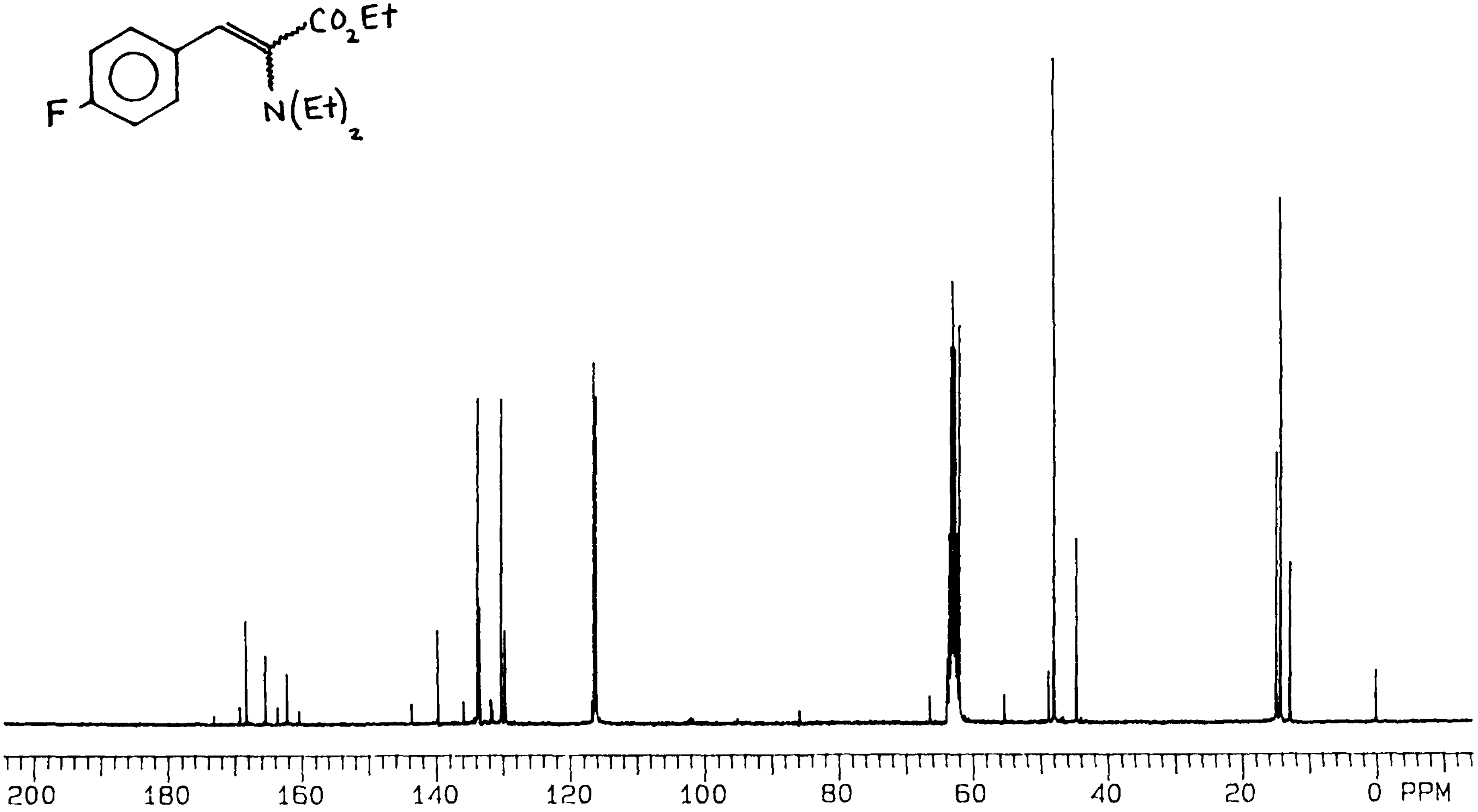

(Z+E) ethyl 2-diethylamino-3-phenyl-2-propenoate

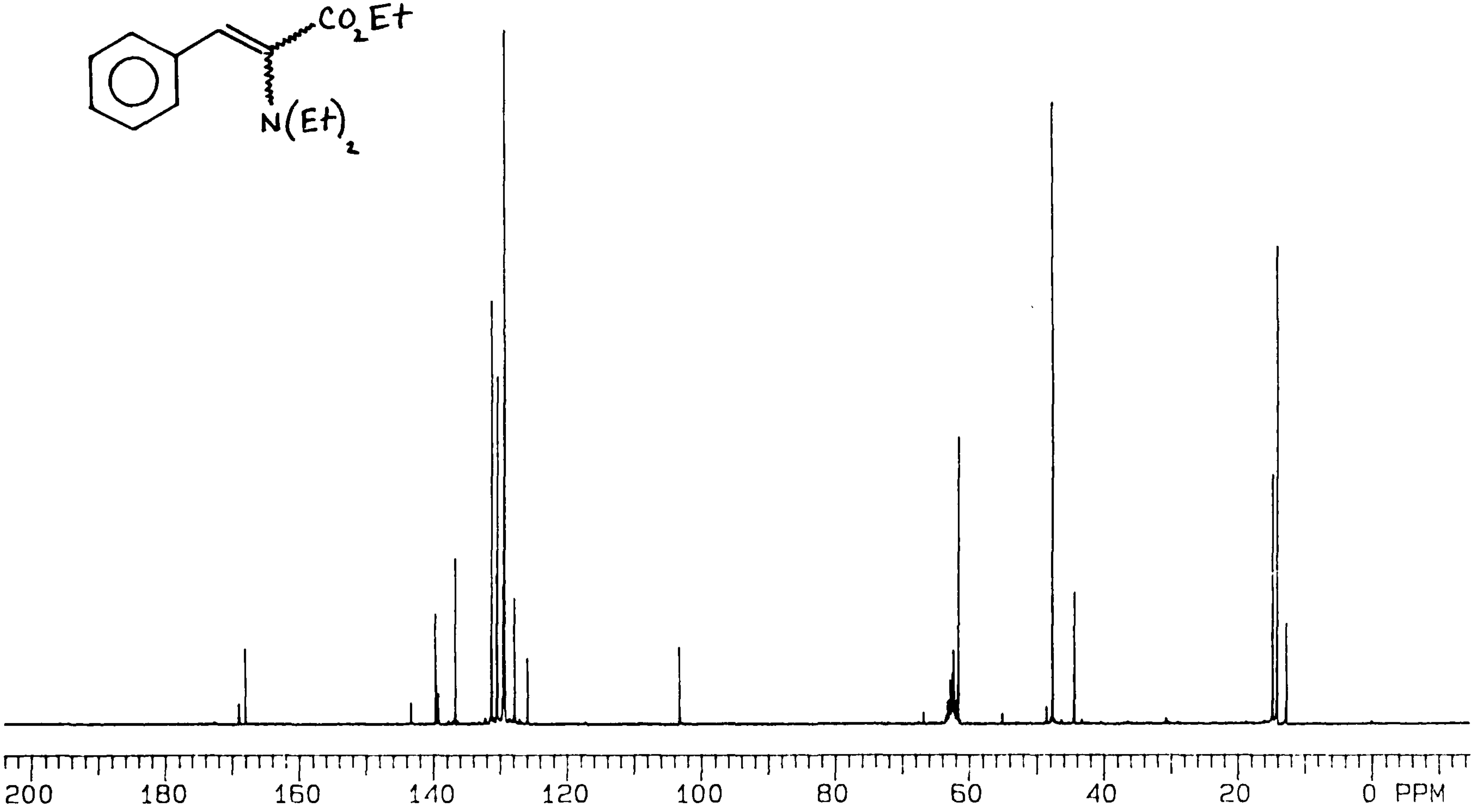

(Z+E) ethyl 2-diethylamino-3-(4-chlorophenyl)-2-propenoate

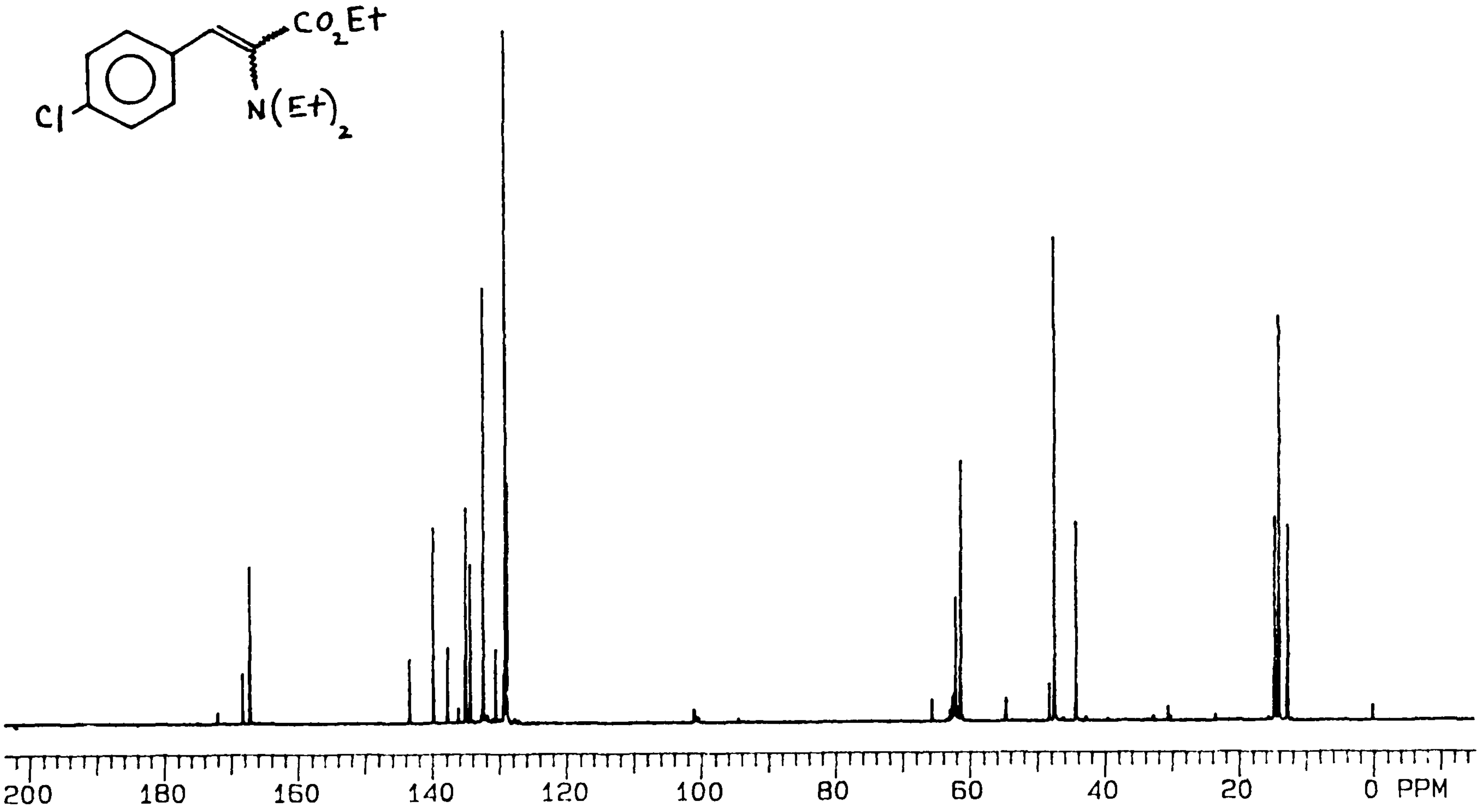

(Z+E) ethyl 2-diethylamino-3-(3-fluorophenyl)-2-propenoate

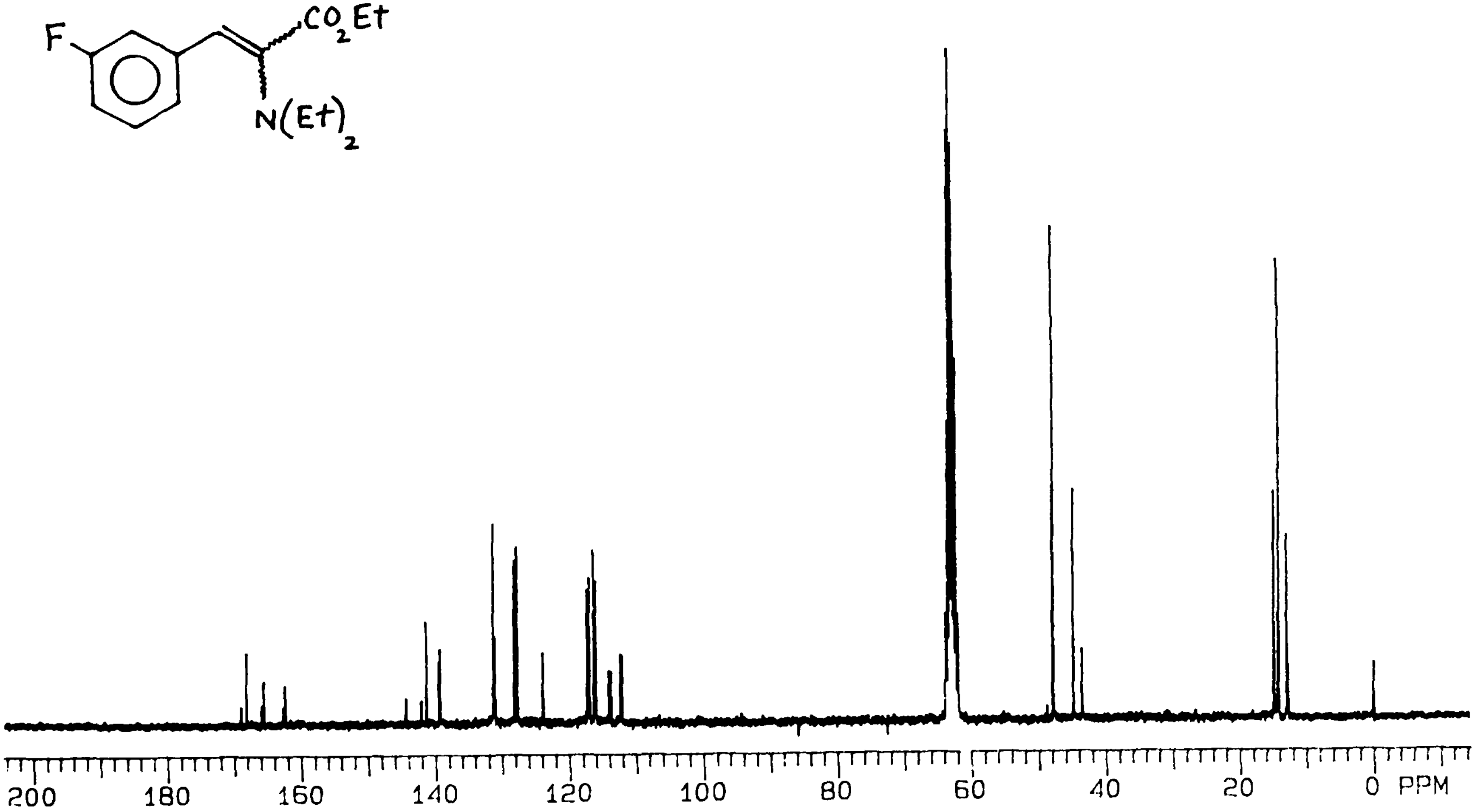

(Z+E) ethyl 2-diethylamino-3-(3-chlorophenyl)-2-propenoate

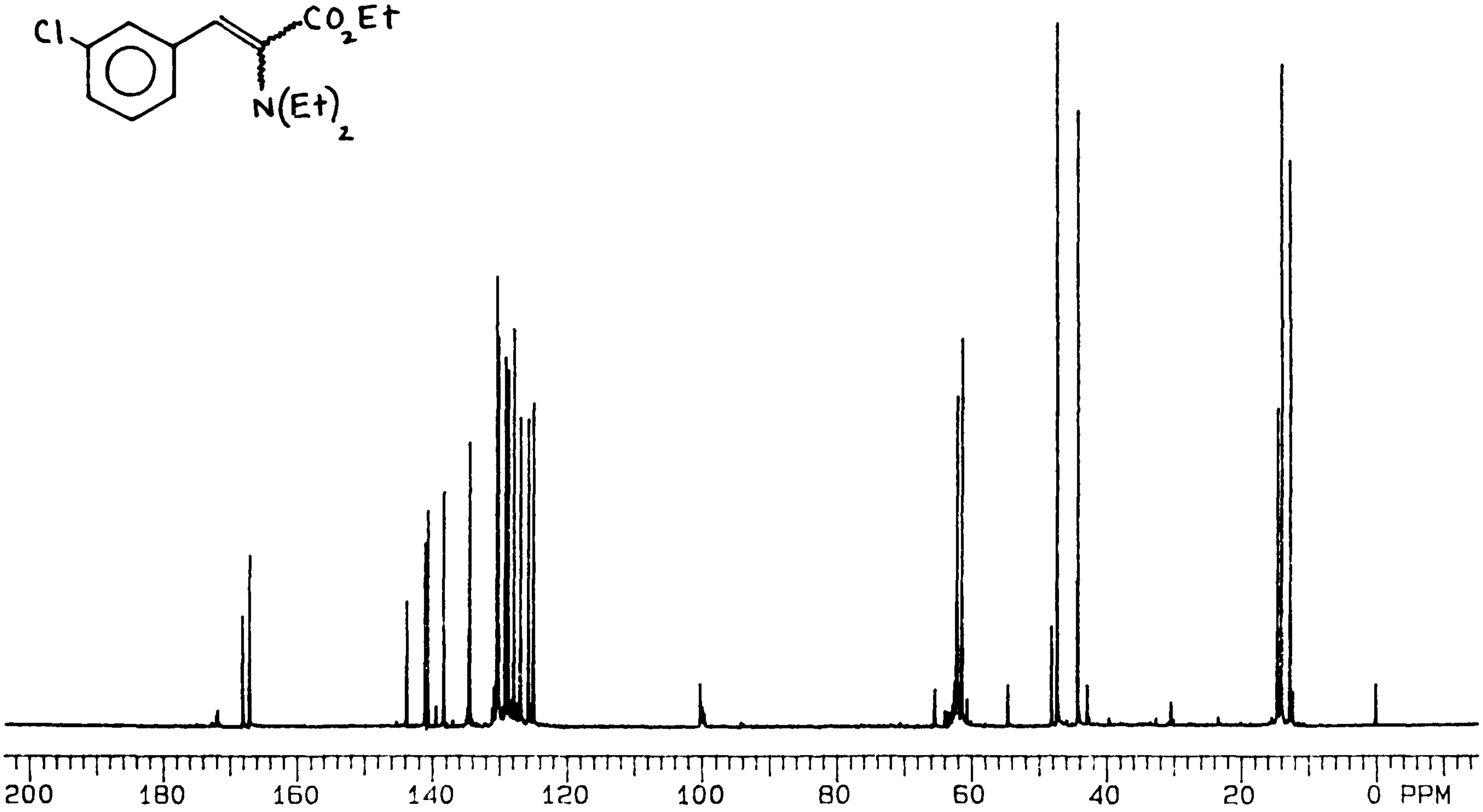

(Z+E) methyl 2-diethylamino-3-(4-carbomethoxyphenyl)-2-propenoate

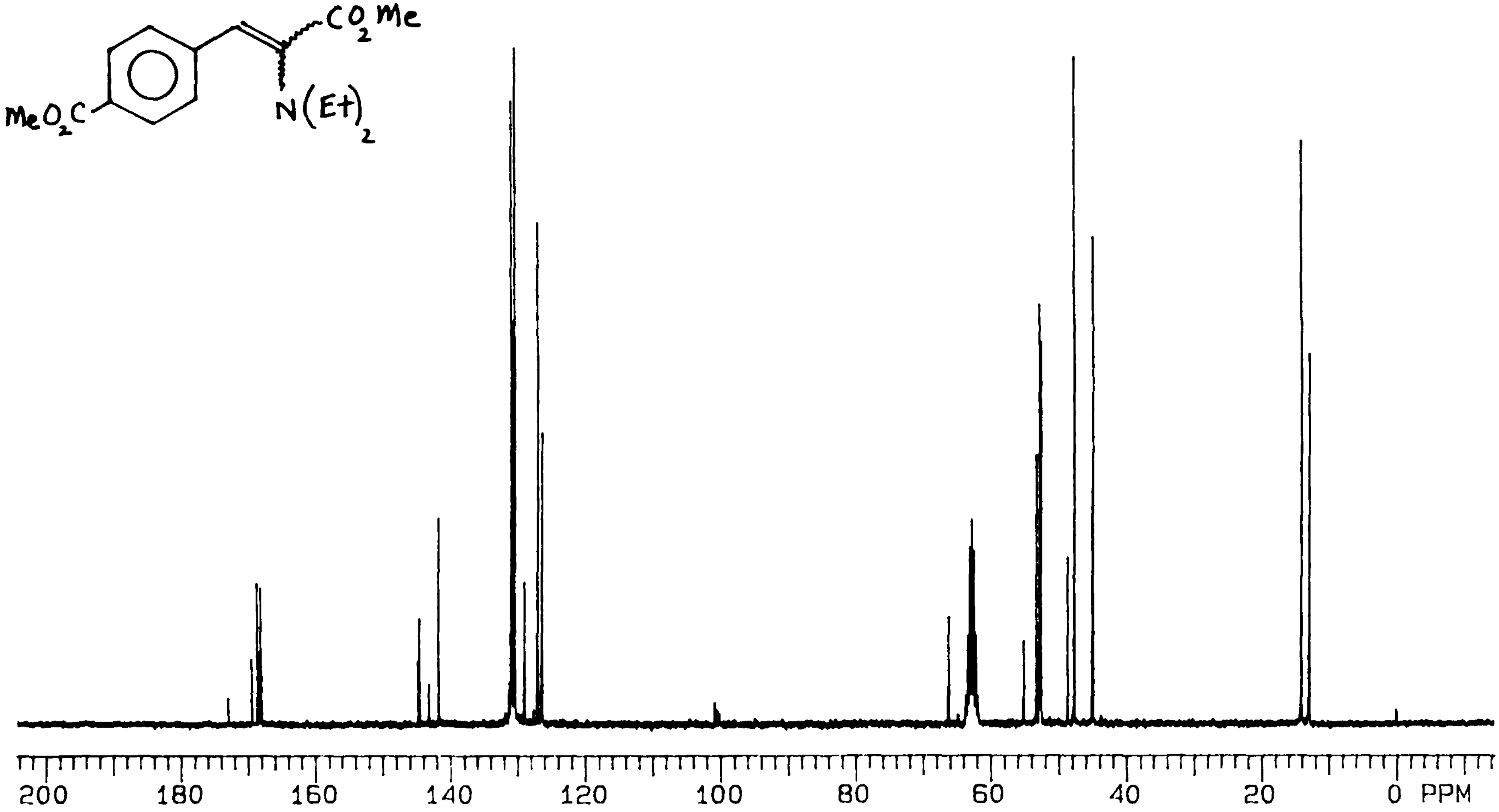

(E+Z) ethyl 2-diethylamino-3-(3-cyanophenyl)-2-propenoate

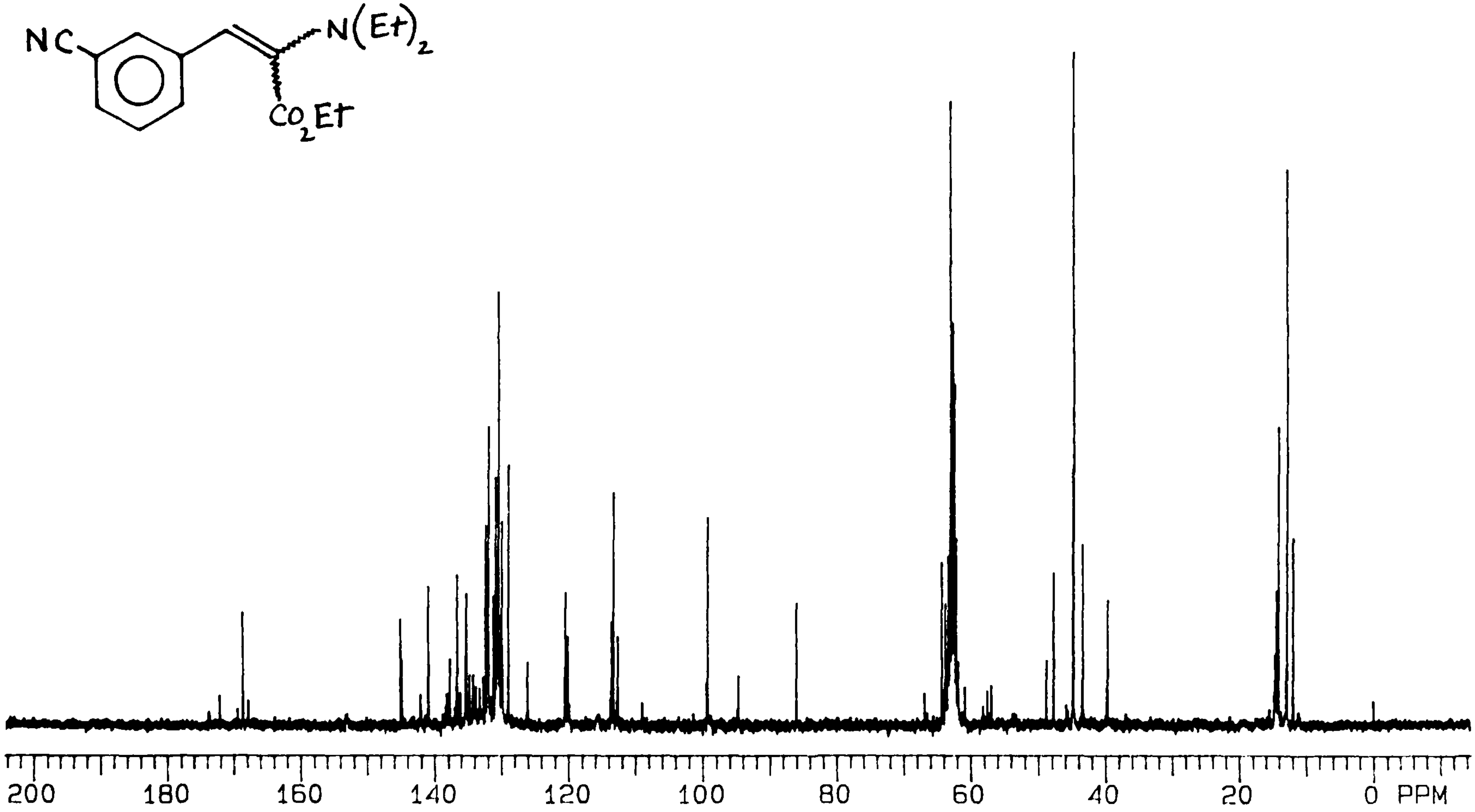

(E+Z) ethyl 2-diethylamino-3-(4-trifluoromethylphenyl)-2-propenoate

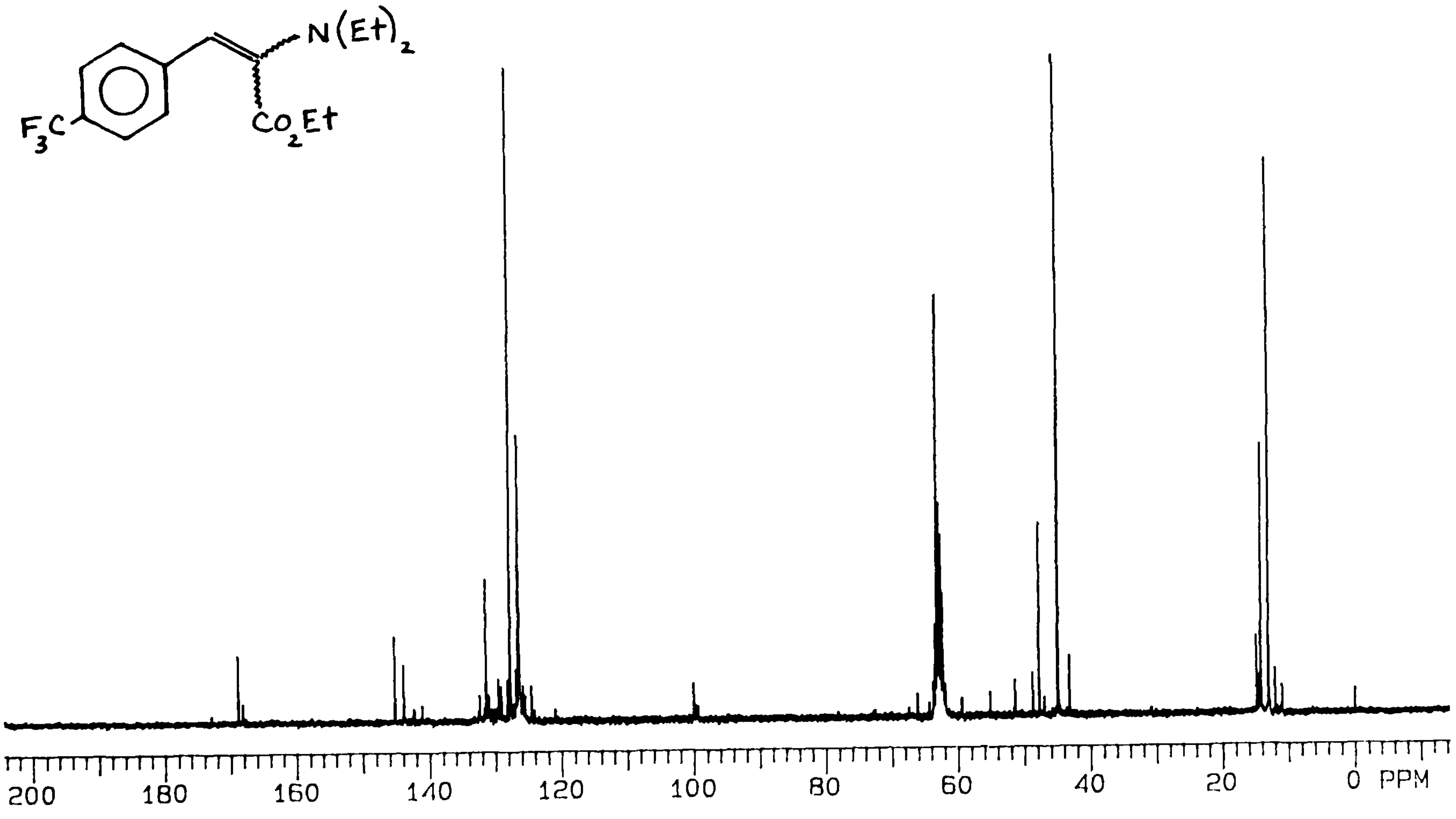

(E+Z) ethyl 2-diethylamino-3-(4-cyanophenyl)-2-propenoate

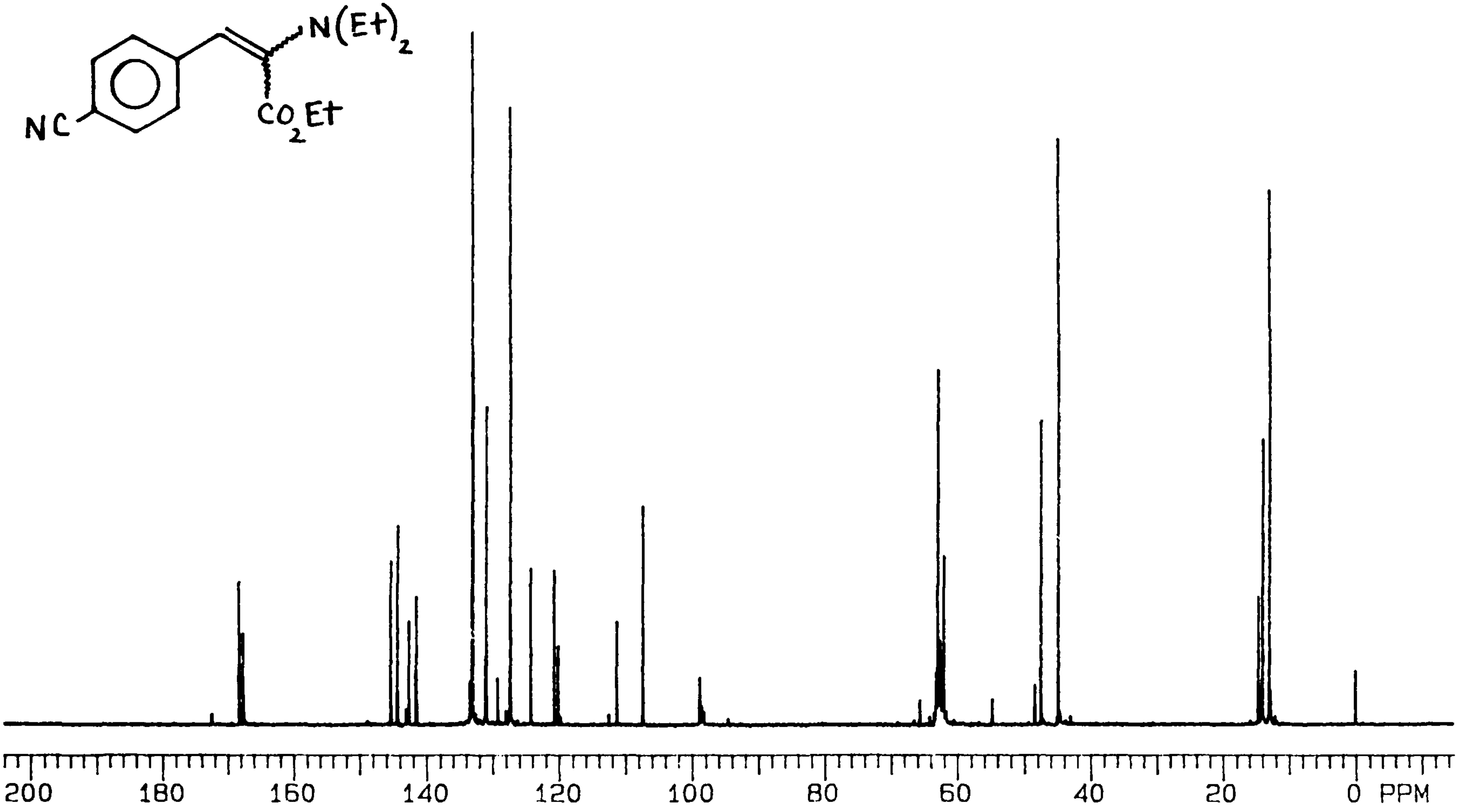

(E+Z) ethyl 2-diethylamino-3-(4-nitrophenyl)-2-propenoate

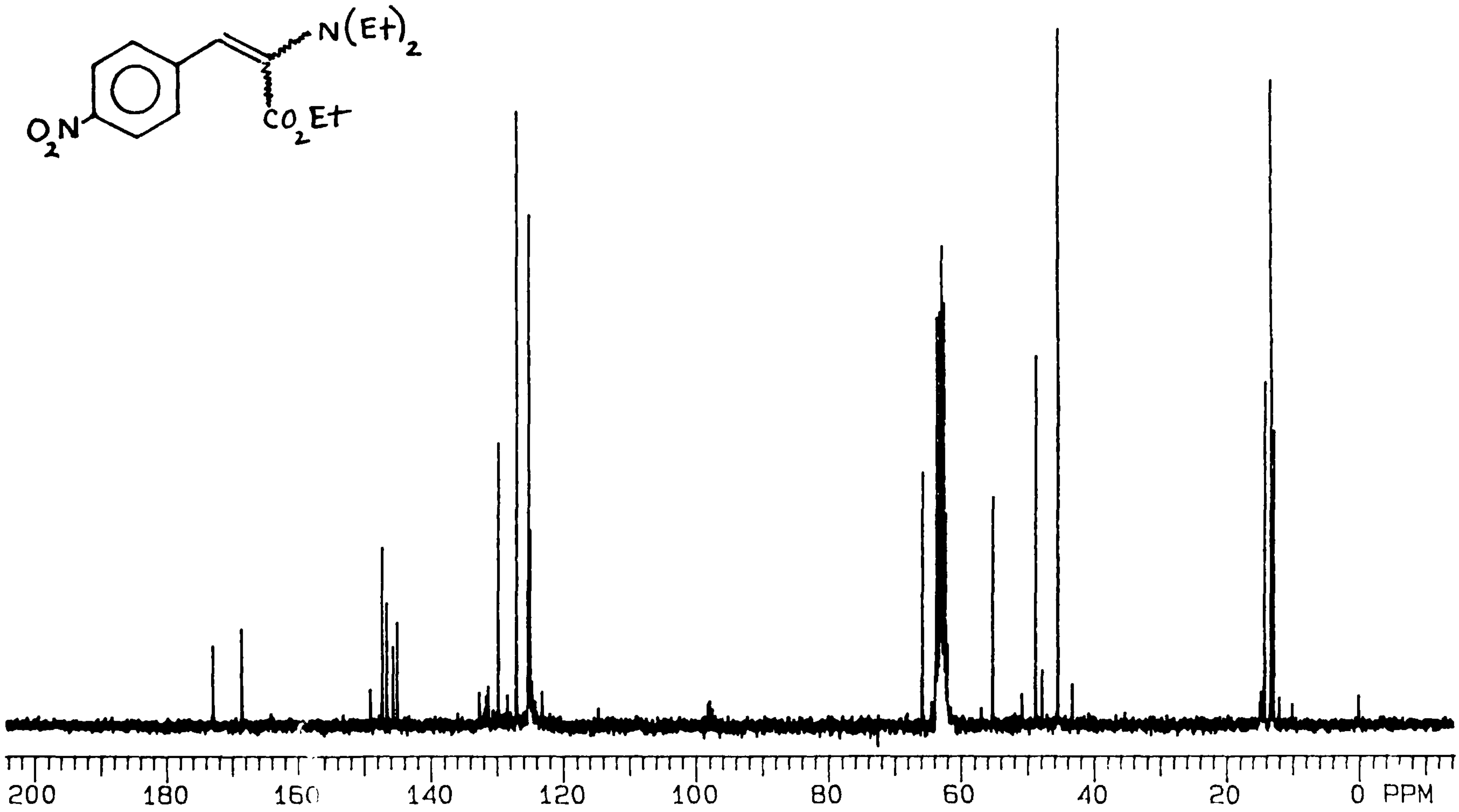

Series D

^{13}C NMR spectra for the Series D compounds follow:

NOTE: These were obtained using $CDCL_3$ solvent and the central peak of the $CDCL_3$ triplet at 77.0 ppm as the referencing standard.

(E+Z) ethyl 2-phenylseleno-3-(4-dimethylaminophenyl)-2-propenoate

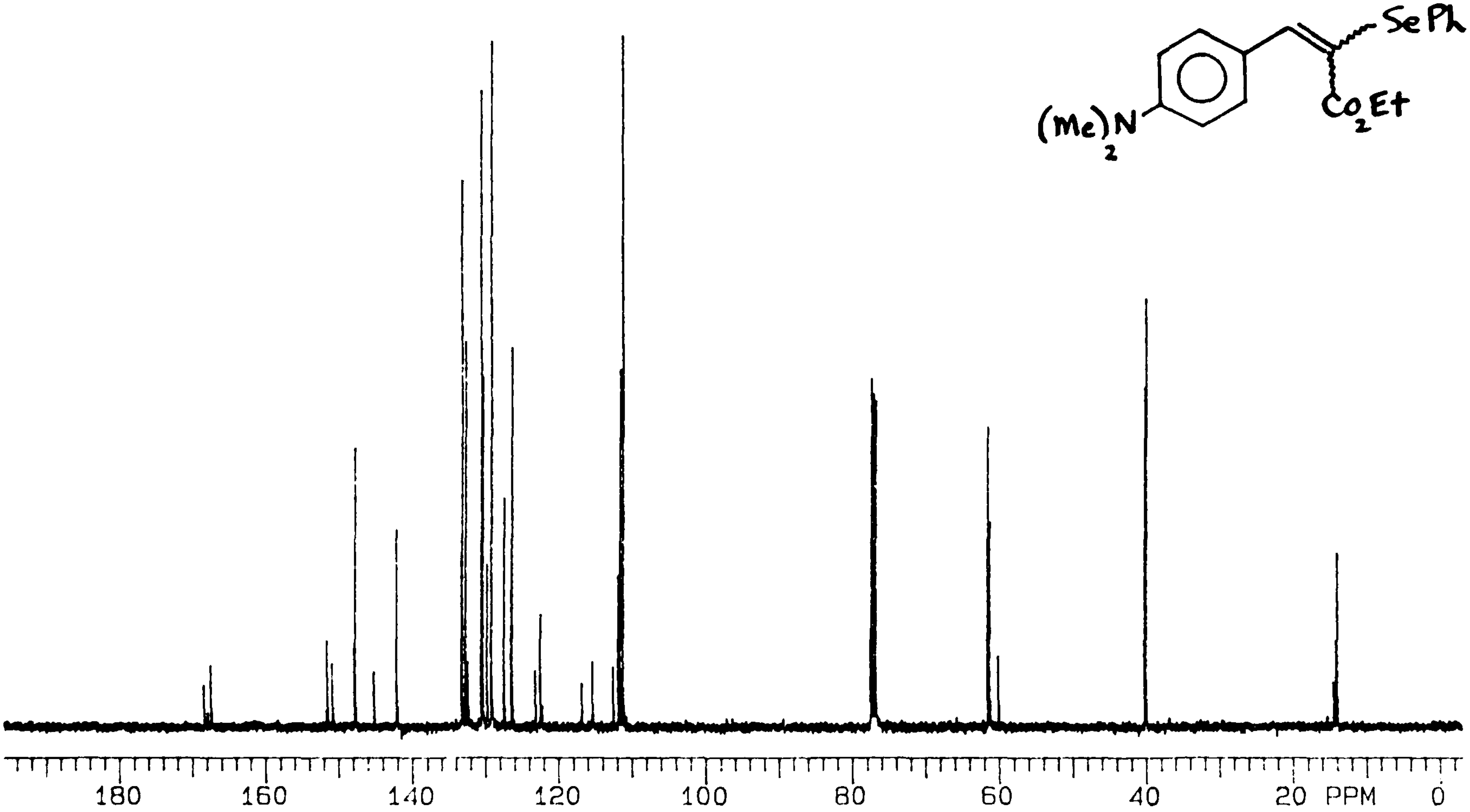

(E+Z) ethyl 2-phenylseleno-3-(4-methoxyphenyl)-2-propenoate

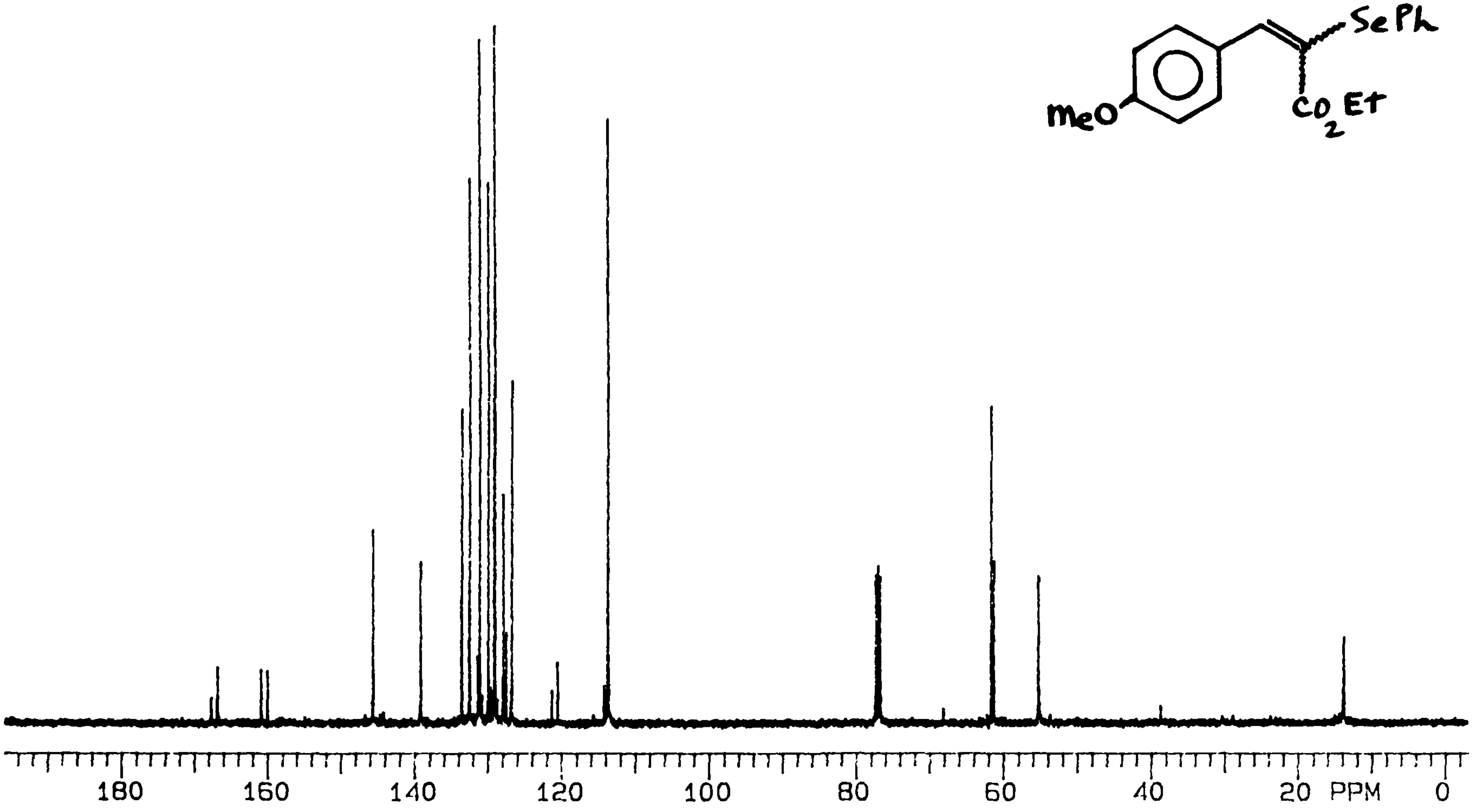

(E+Z) ethyl 2-phenylseleno-3-(4-methylphenyl)-2-propenoate

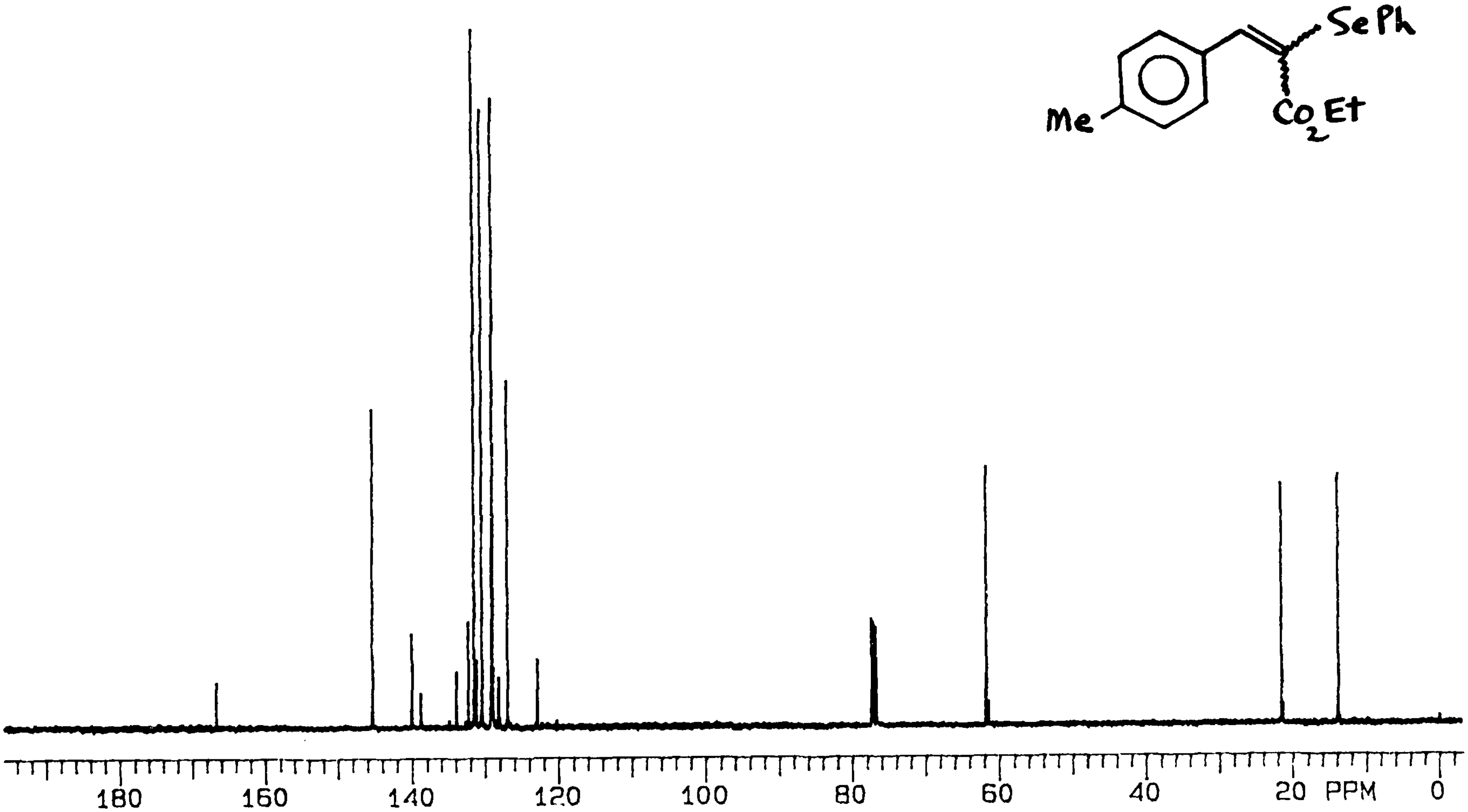

(E+Z) ethyl 2-phenylseleno-3-(4-phenylphenyl)-2-propenoate

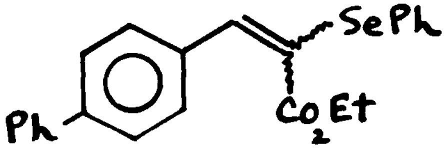
SePh
CO2Et
Ph

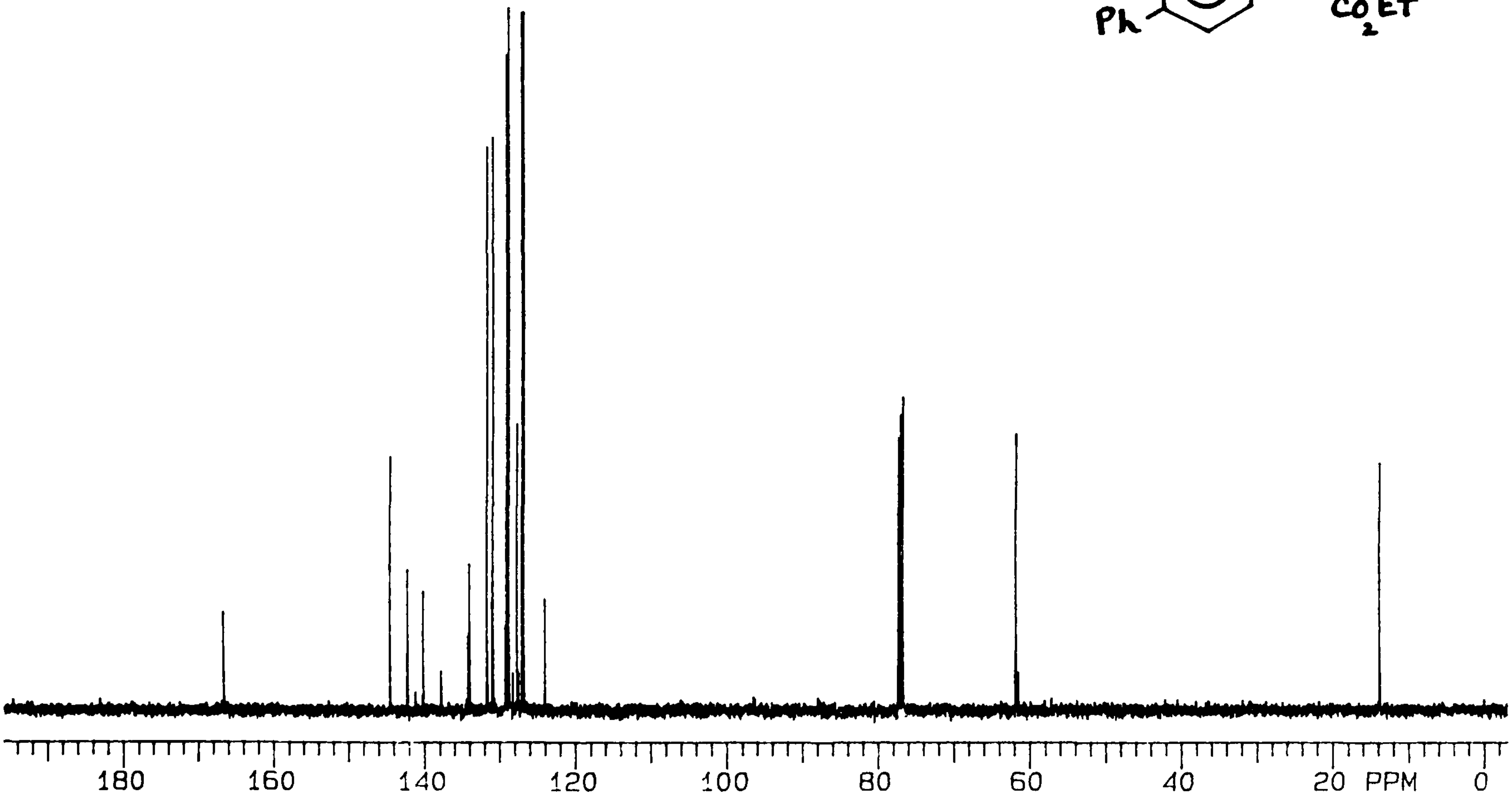

(E+Z) ethyl 2-phenylseleno-3-(4-fluorophenyl)-2-propenoate

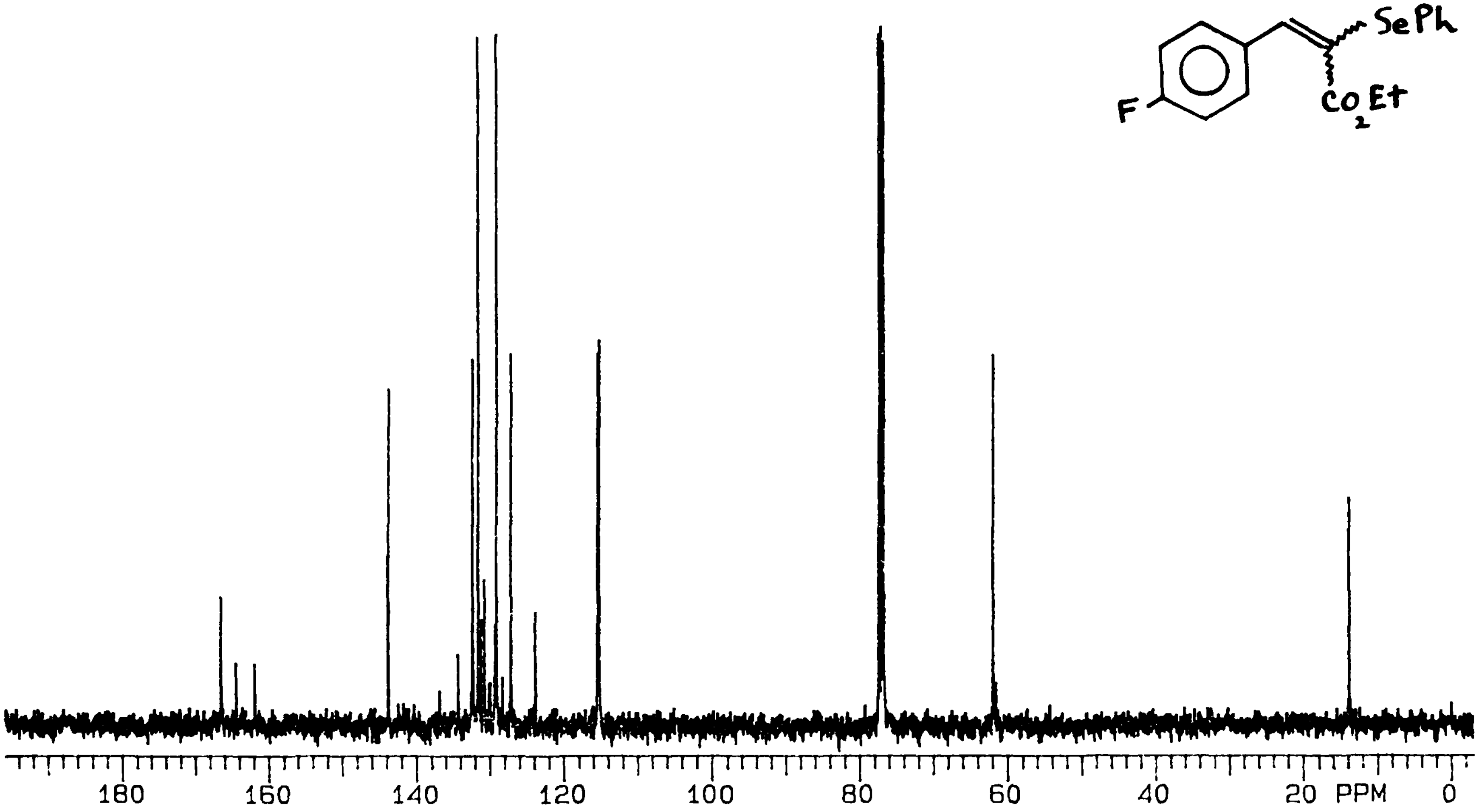

(E+Z) ethyl 2-phenylseleno-3-phenyl-2-propenoate

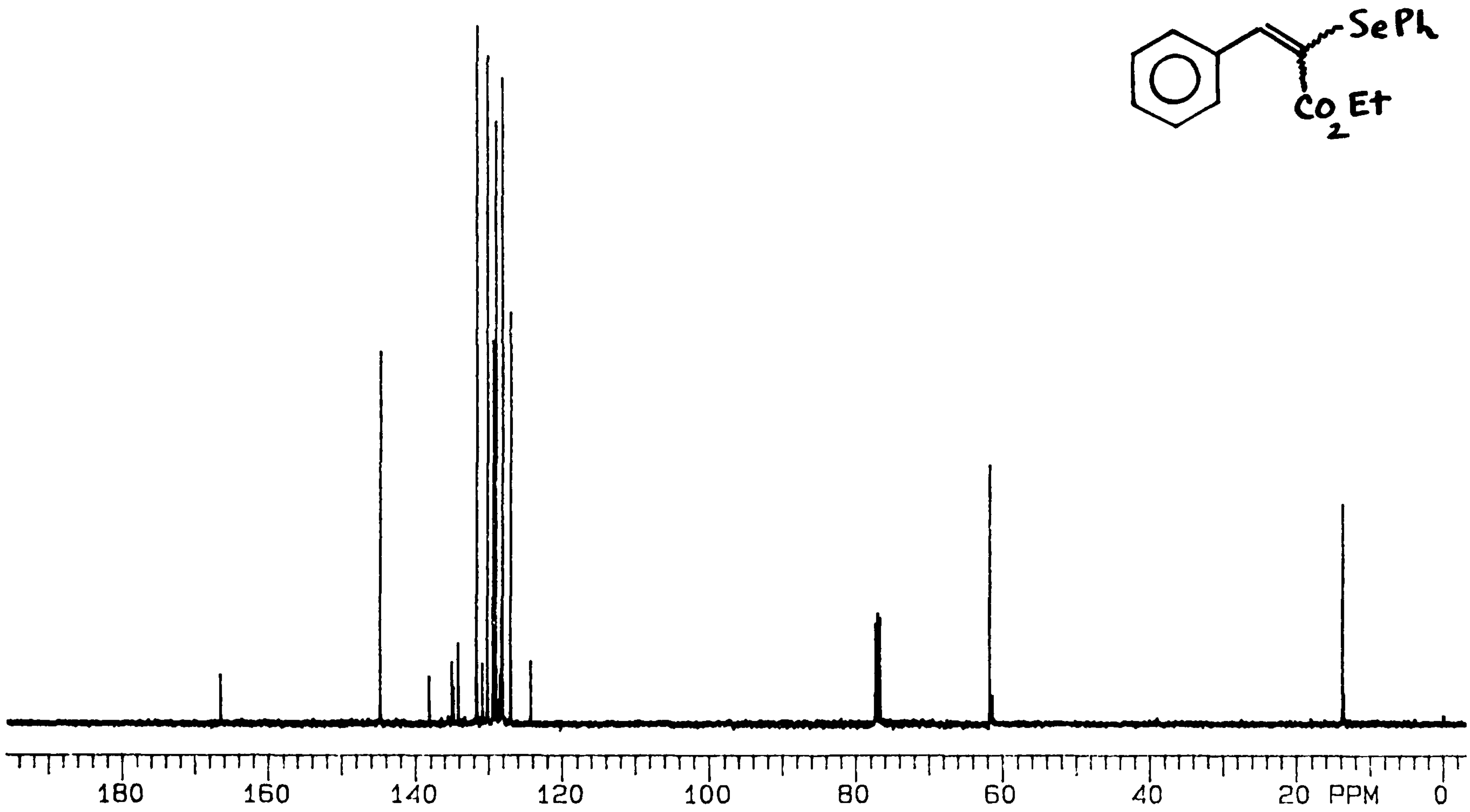

(E+Z) ethyl 2-phenylseleno-3-(3-methoxyphenyl)-2-propenoate

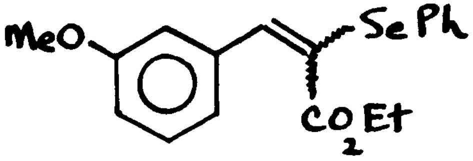
MeO
SePh
CO2Et

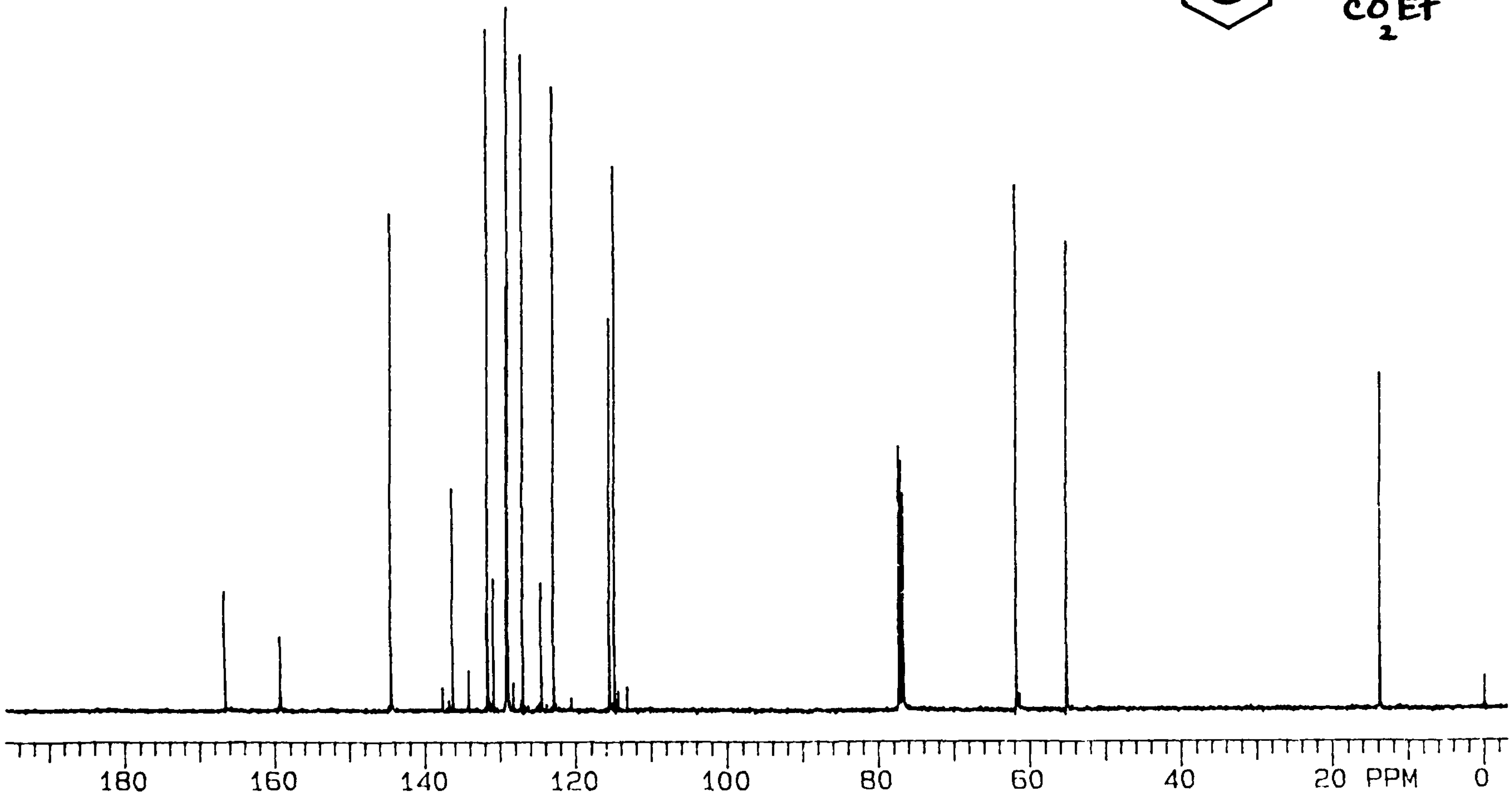

(E+Z) ethyl 2-phenylseleno-3-(4-chlorophenyl)-2-propenoate

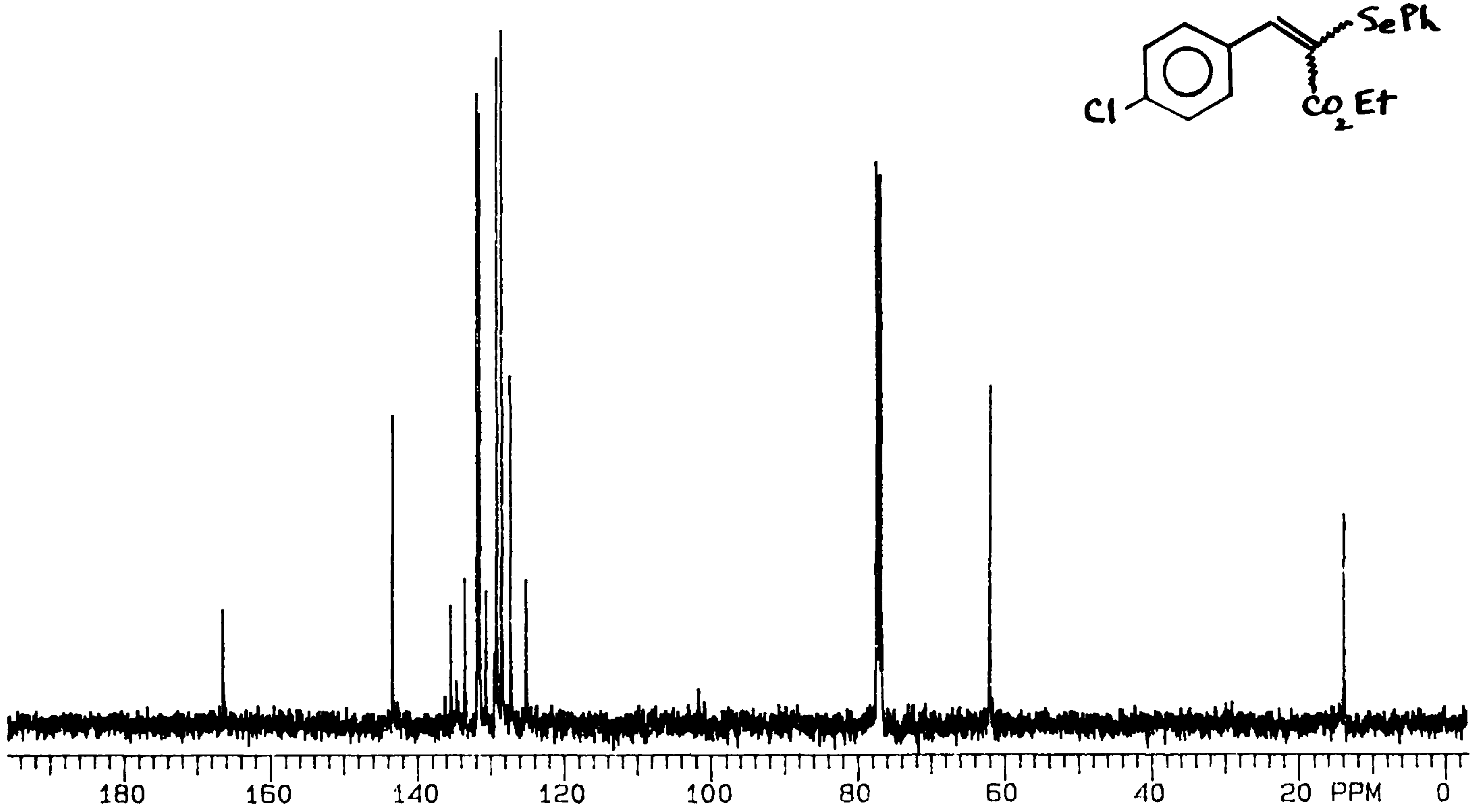

(E+Z) ethyl 2-phenylseleno-3-(4-fluorophenyl)-2-propenoate

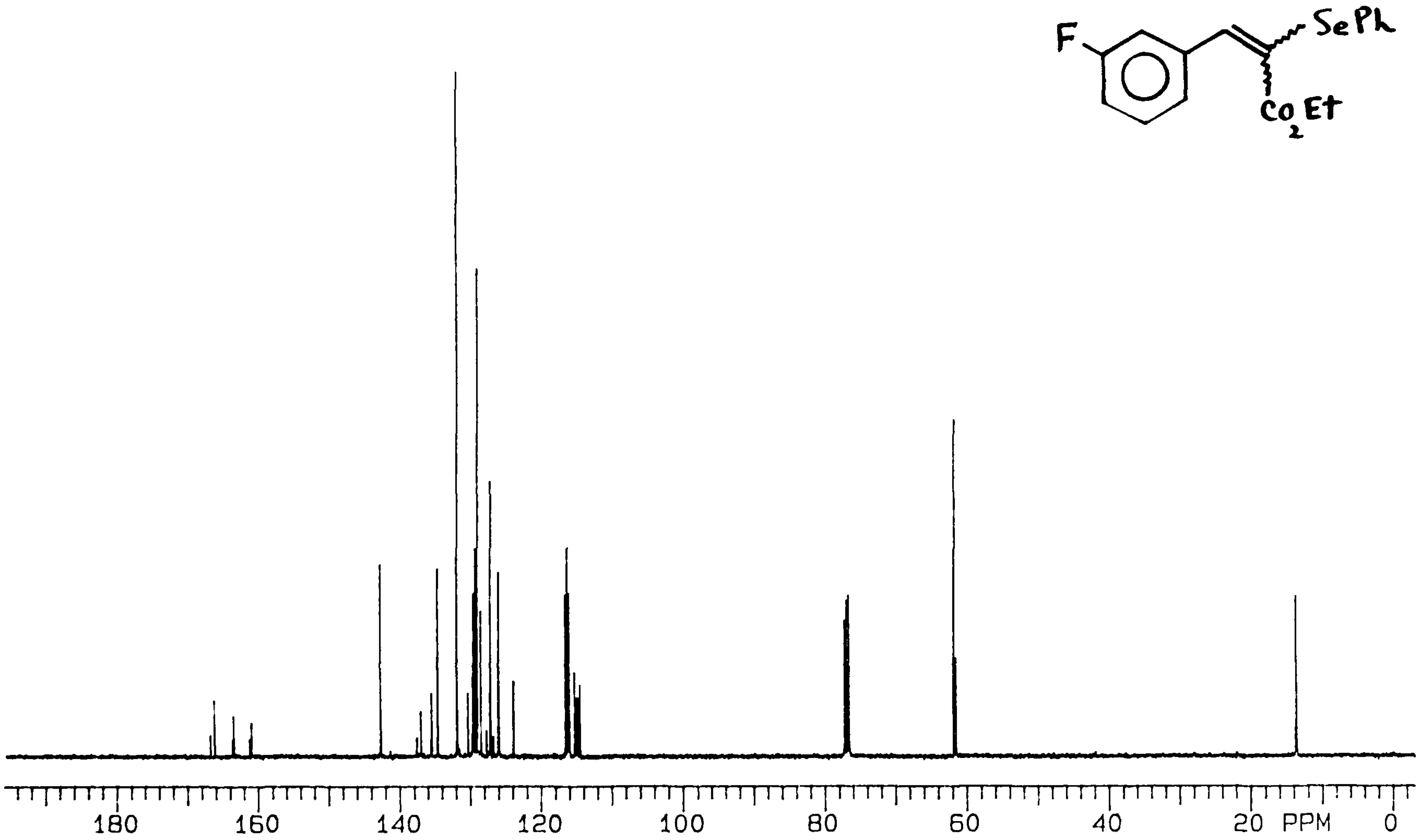

(E) ethyl 2-phenylseleno-3-(3-chlorophenyl)-2-propenoate

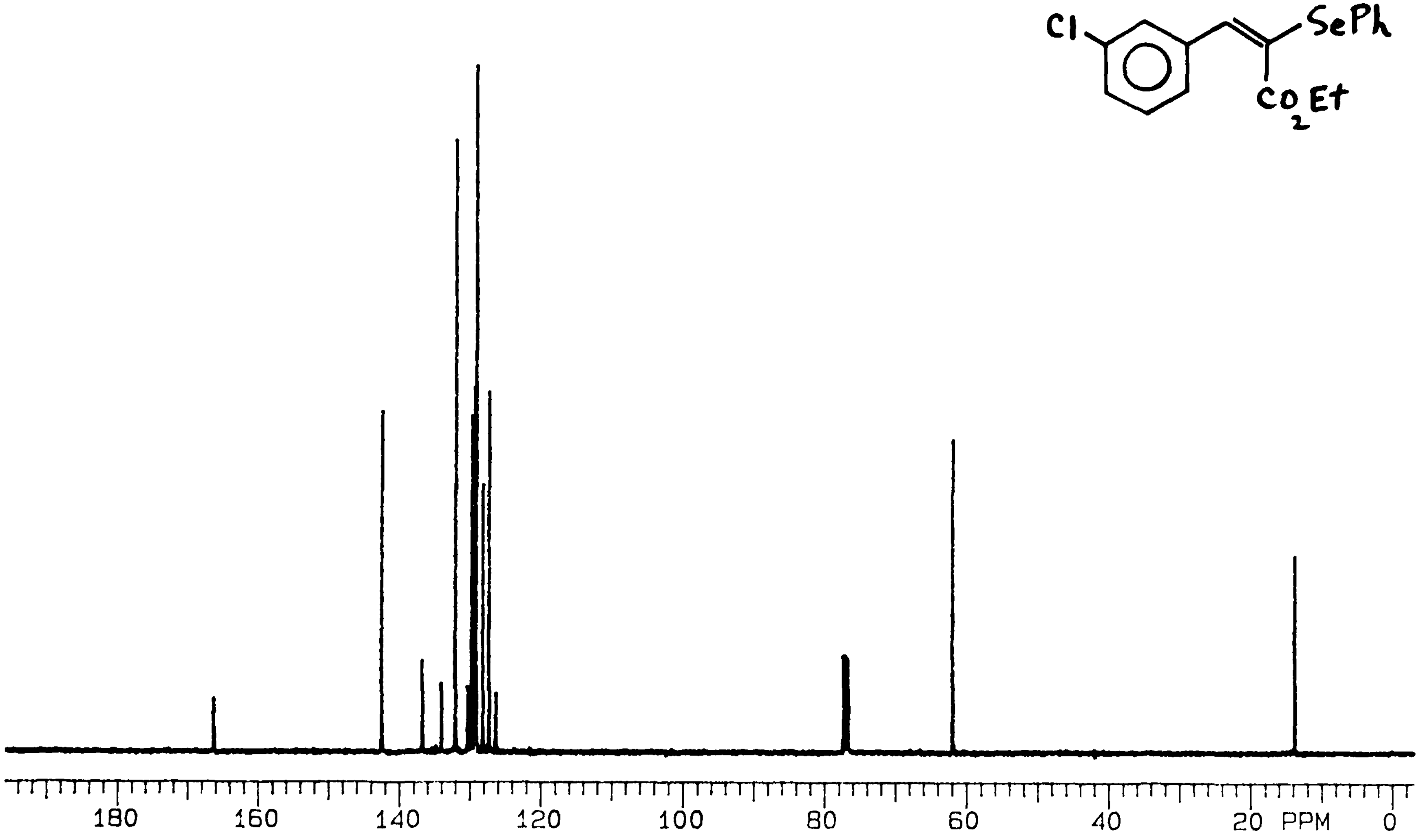

(E) ethyl 2-phenylseleno-3-(4-carbomethoxyphenyl)-2-propenoate

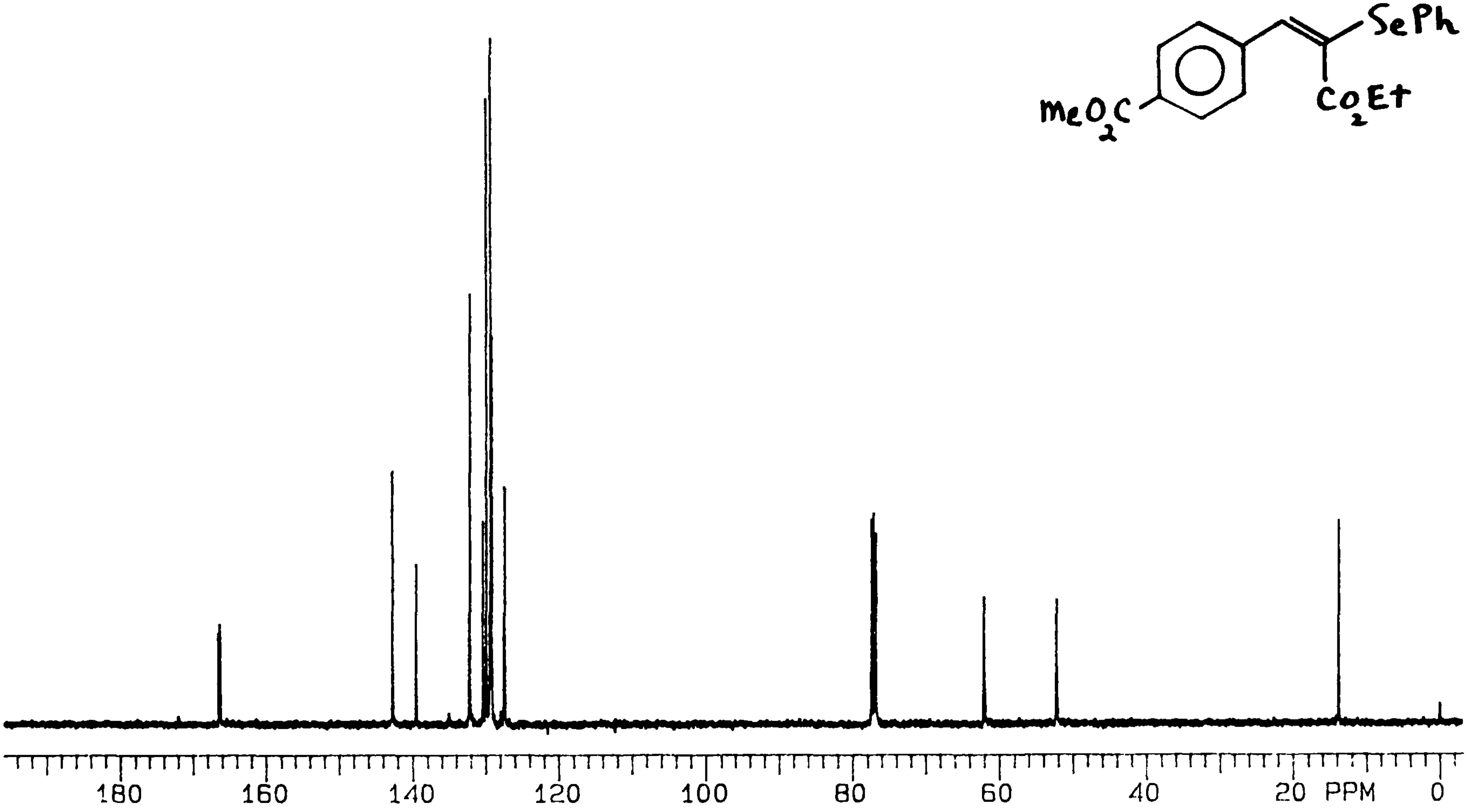

(E) ethyl 2-phenylseleno-3-(3-cyanophenyl)-2-propenoate

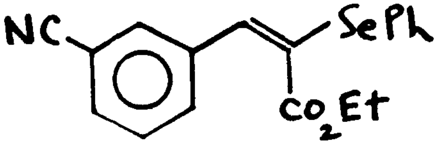
NC
SePh
CO2Et

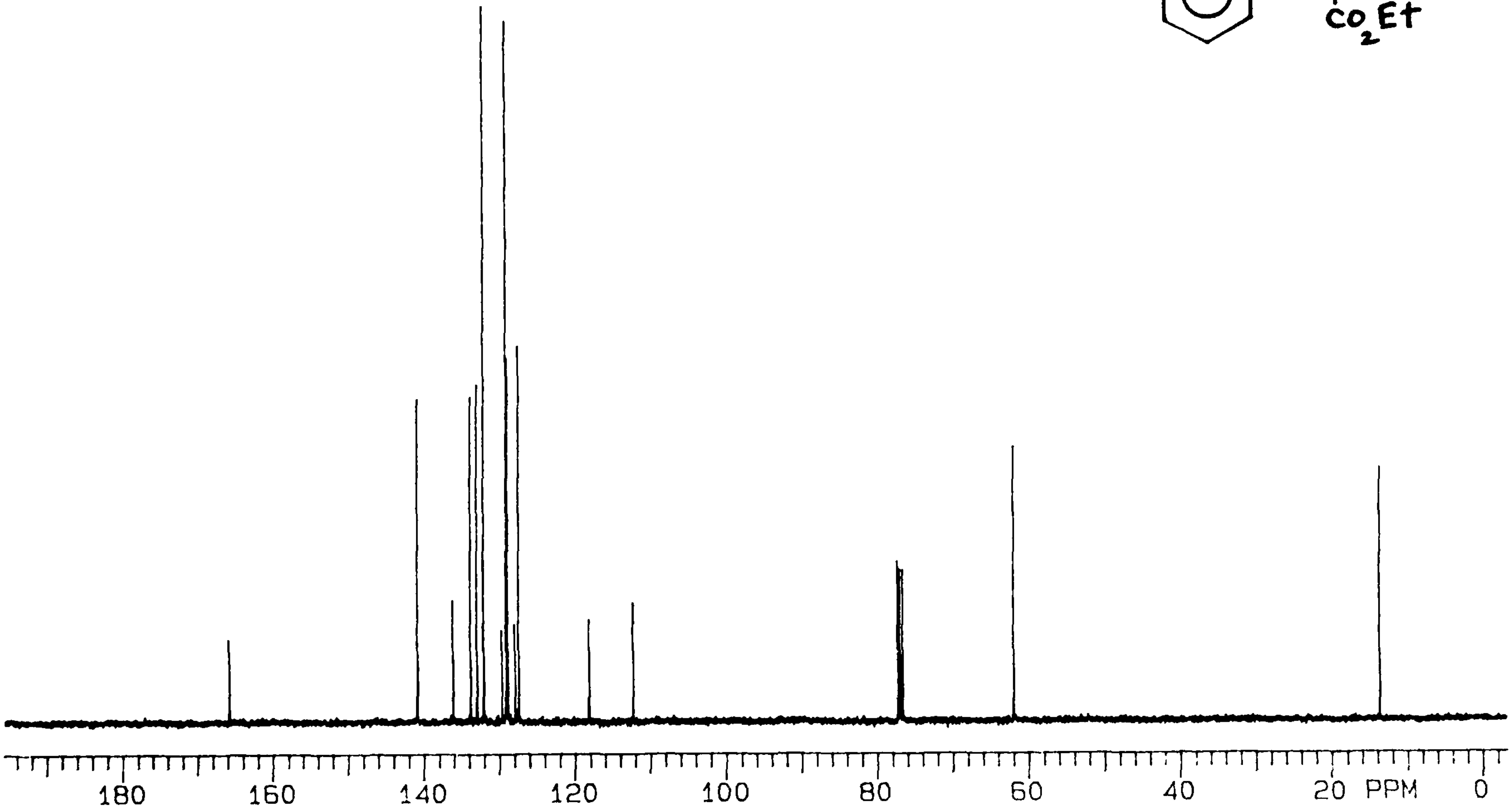

(E+Z) ethyl 2-phenylseleno-3-(3-trifluoromethylphenyl)-2-propenoate

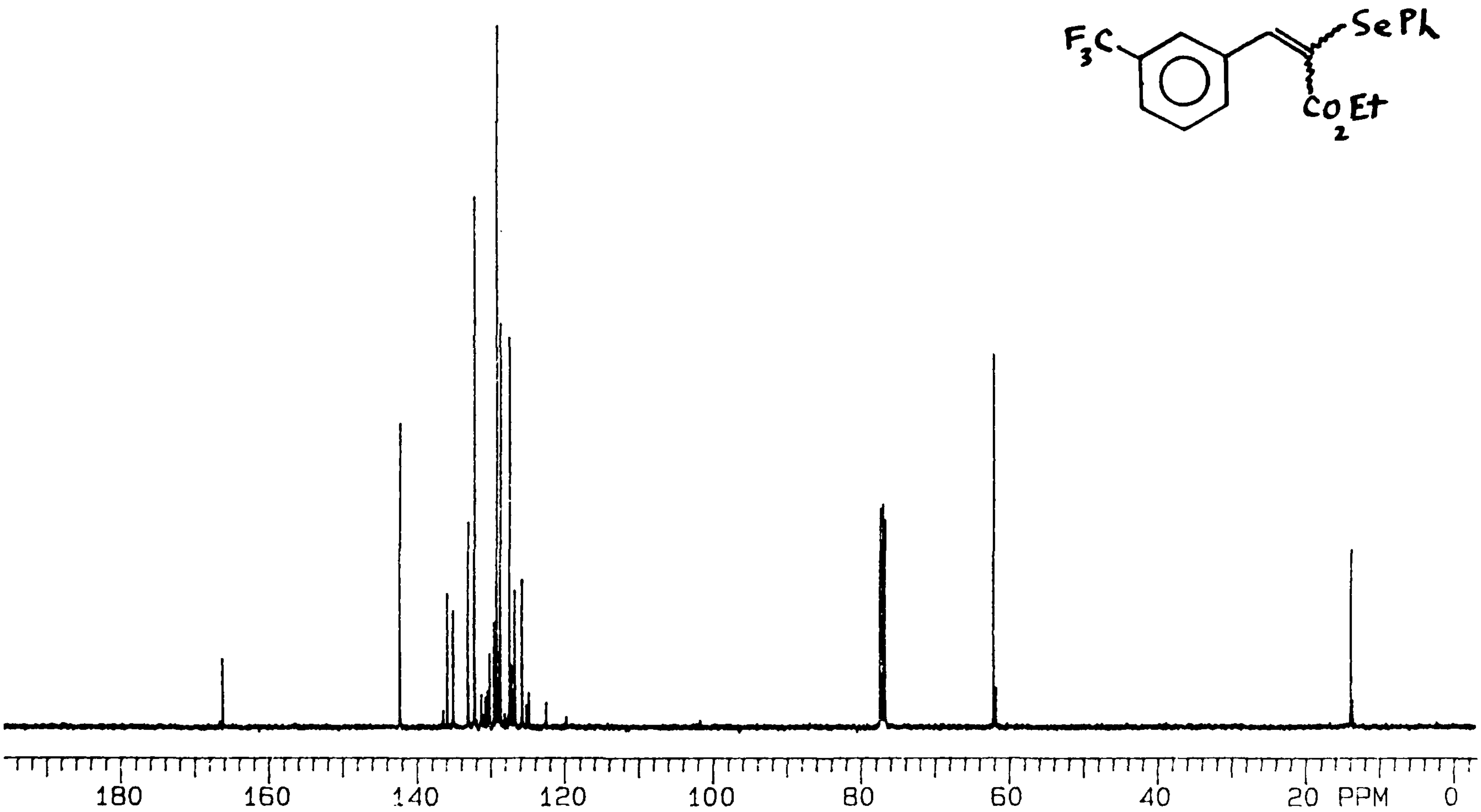

(E+Z) ethyl 2-phenylseleno-3-(4-trifluoromethylphenyl)-2-propenoate

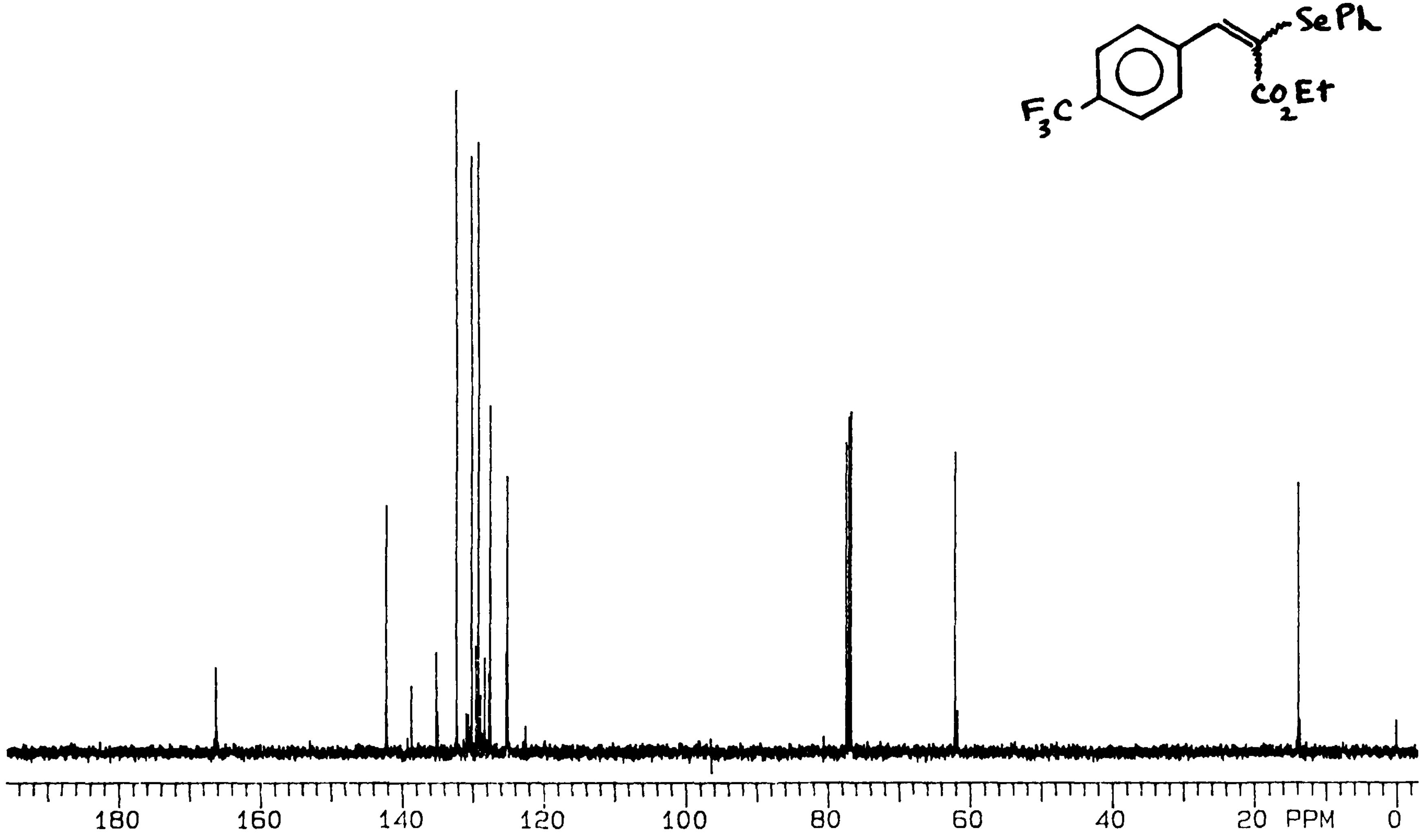

(E) ethyl 2-phenylseleno-3-(4-cyanophenyl)-2-propenoate

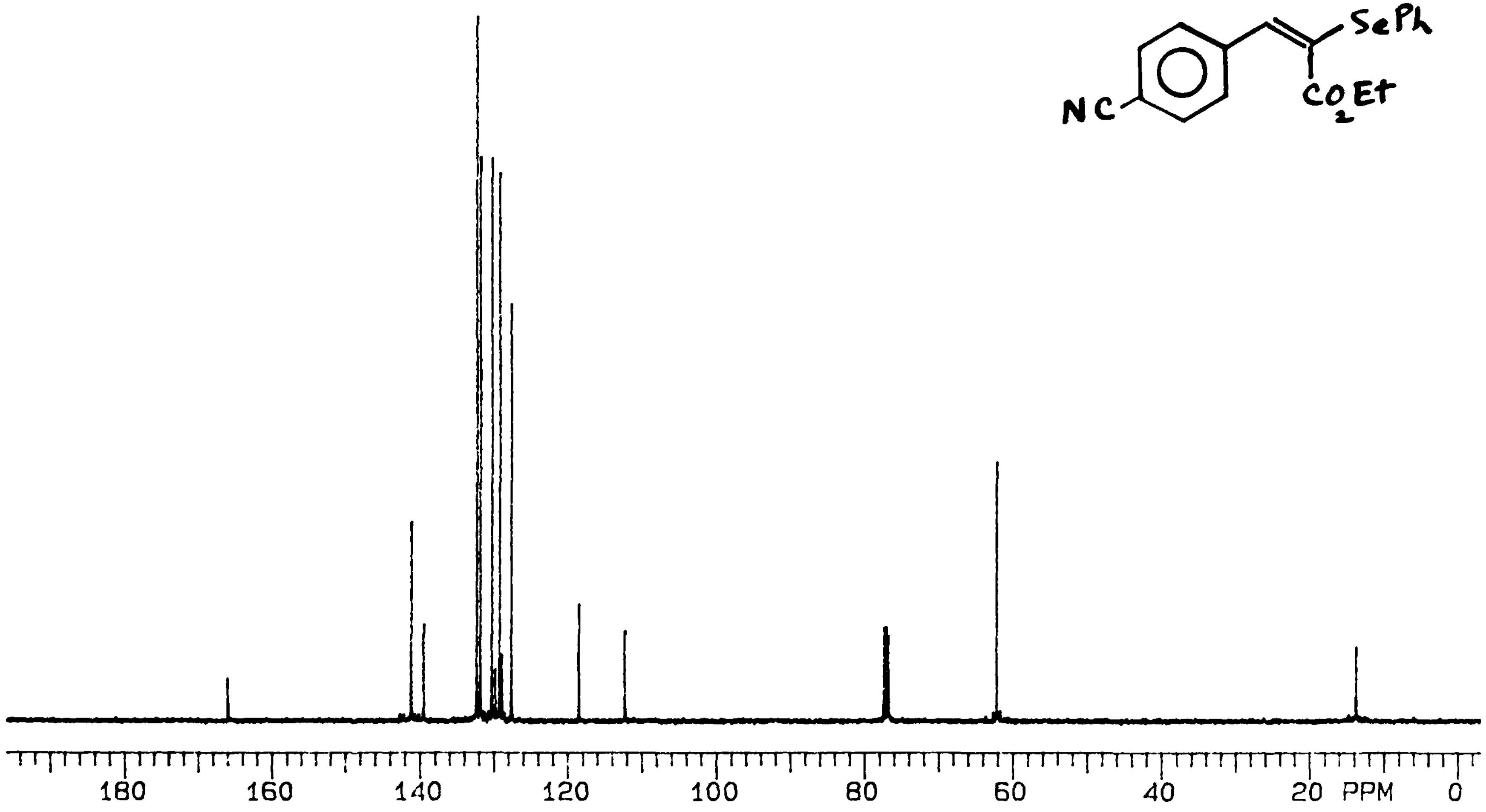

(E) ethyl 2-phenylseleno-3-(3-nitrophenyl)-2-propenoate

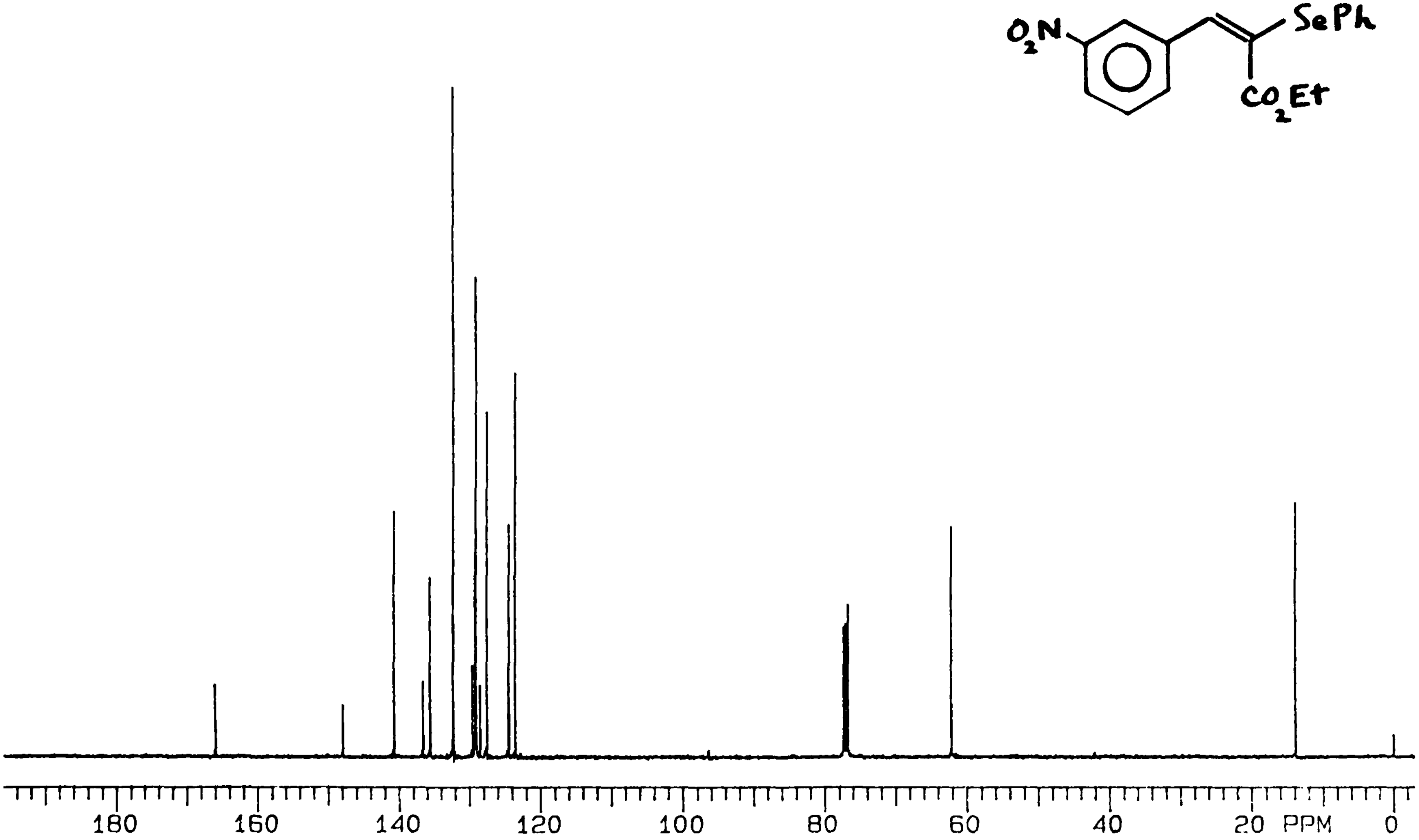

(Z+E) ethyl 2-phenylseleno-3-(4-nitrophenyl)-2-propenoate

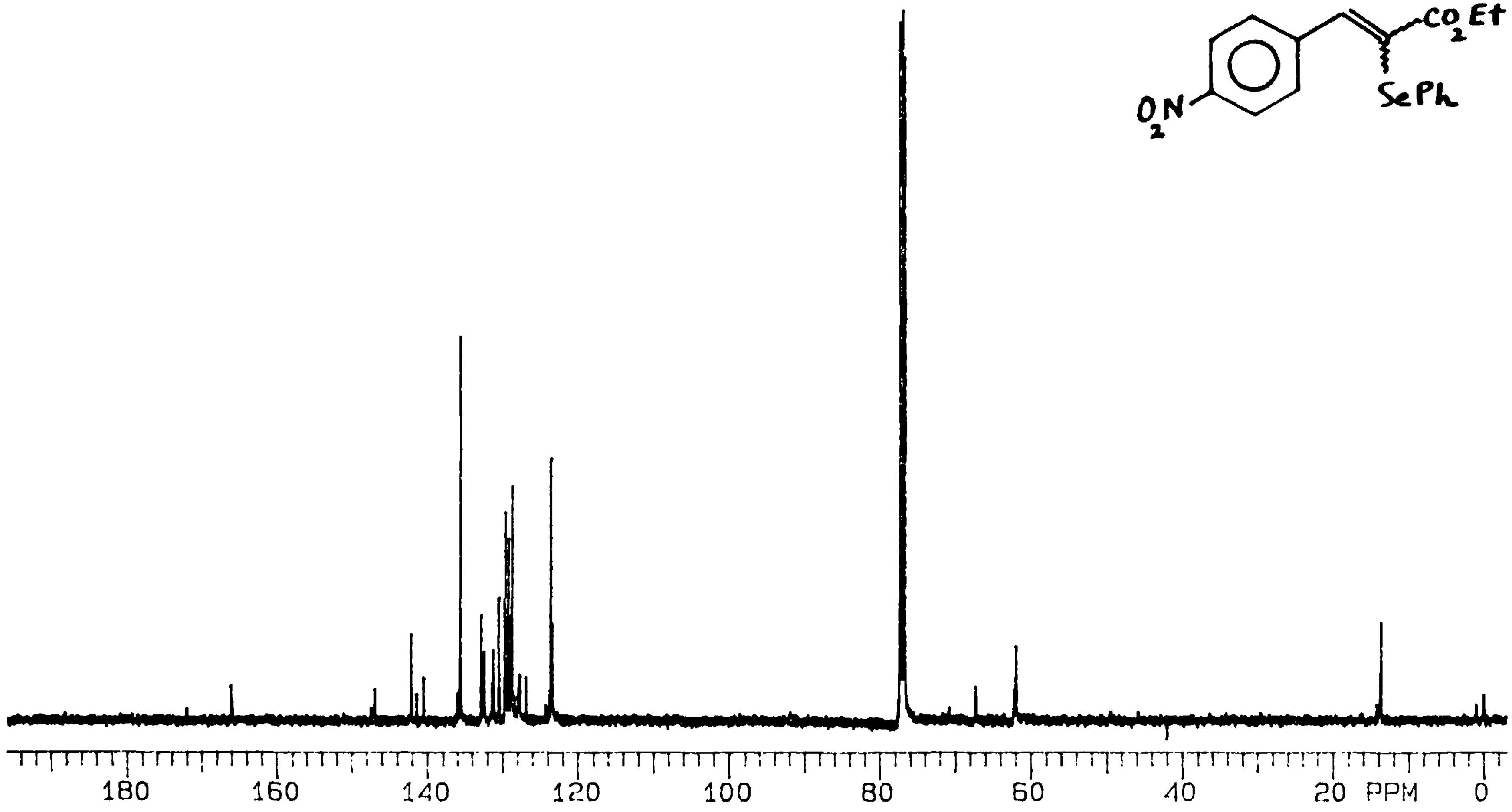

Appendix D

Mass Spectra/Gas Chromatography

Series A

Mass Spectra/General Comments (MS)

Several important fragmentation patterns were evident for the enamines of Series A. The most common were:

a) loss of Et and CO_2Et fragments from the molecular ion

b) loss of $HN(Et)_2$ fragment via Hoffmann elimination from the cinnamic acid intermediate

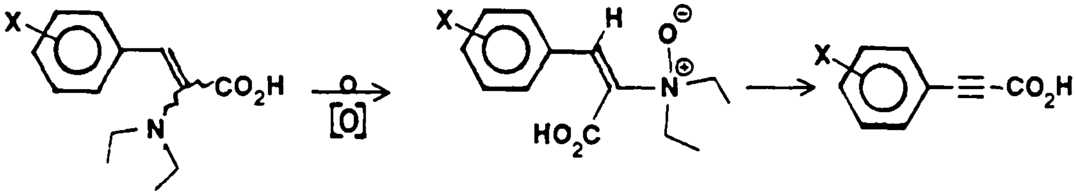

c) initial decarboxylative eliminition from the cinnamic acid,

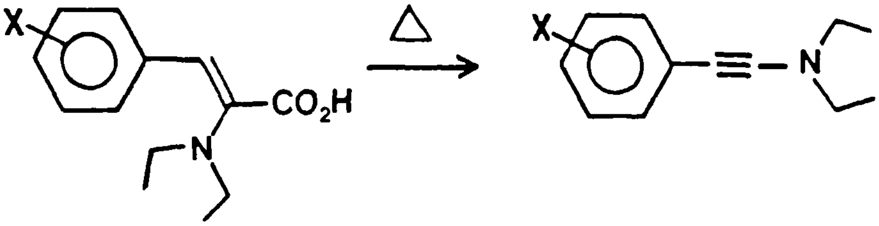

followed by loss of Et groups from N-C bond cleavage

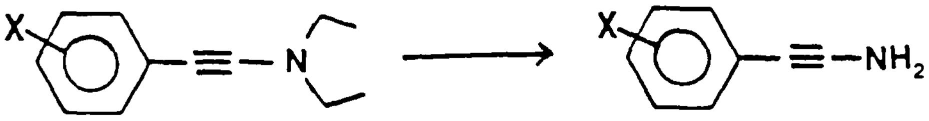

The phenylpropionic acid (from b) and the phenylethynylamine (from c) degradation products accounted for most of the base peaks in the mass spectra.

The mass spectra for the E and Z isomers of each enamine gave essentially identical fragmentation patterns. Only that for the Z isomers will be presented.

Gas Chromatography/General Comments (GC)

In all cases, except for the p-Me compound, the Z and E isomers eluted as separate components at 200°C oven temperature, although the differences in retention times were usually less than 1 minute. (Only 1 peak eluted for the p-Me compound even as low as 125°C).

For X=e^- withdrawing groups (from p-F through to p-NO_2), the Z isomer eluted first. This is consistent with the overall greater balance of the various dipoles generated within the Z molecule (versus E) due to the resonance and field effects of the three functional groups, as shown:

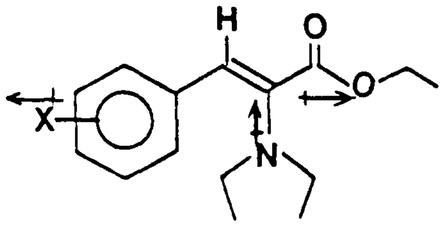

XLIXB

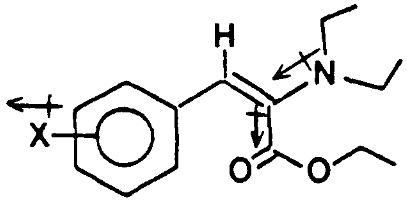

XLIXA

dipole moment of Z < E

The greater molecular dipole of E would increase its relative retention on the column.

However, for X = e$^-$ donating groups (p-N(Me)$_2$, p-MeO, and p-Ph), the E isomer eluted first, suggesting the following contrast:

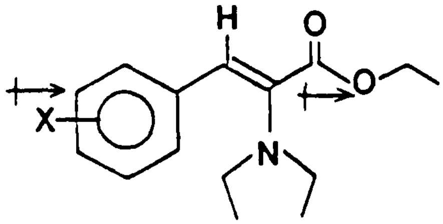

XLIXB

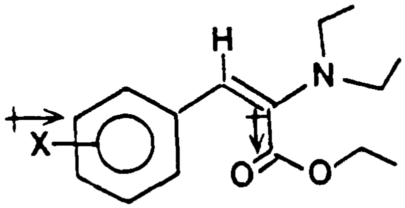

XLIXA

dipole moment of Z > E

Format for Reporting MS/GC Results

The following format will be used for reporting this information: X; m/e (relative intensity, fragment assignment), etc. Note: the base peak m/e will be underlined

G.C.; (isomer assignment, retention time, relative ion abundance).

p-N(Me)$_2$; 291 (6.6, M$^+$ +1), 290 (35.0, M$^+$), very small peaks at 275 and 261 corresponding to loss of Me and Et respectively, but below 3% abundance, 217 (17.4, M$^+$ - CO$_2$Et), 189 (10.3, 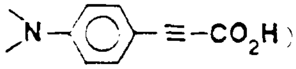), 159 (100, 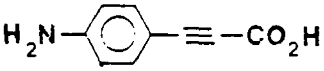).

GC; (E, 4.56 min., 15.9%), Z, 5.54 min, 100.0%).

p-MeO; 278 (4.4, M$^+$ +1), 277 (27.3, M$^+$), 262 (5.3, M$^+$ - Me), 248 (21.0, M$^+$ - Et), 204 (26.4, M$^+$ - CO$_2$Et), 132 (35.3, [M$^+$ - CO$_2$Et] - N(Et)$_2$), 175 (34.4, 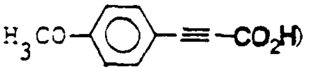, 146 (89.5, 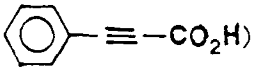, 121 (100, 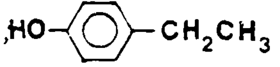).

GC; (E, 2.64 min, 38.3%), (Z, 2.82 min, 100%).

p-Me; 262 (8.2, M$^+$ + 1), 261 (48.4, M$^+$), 246 (9.1, M$^+$ - Me) 232 (56.6, M$^+$ - Et), 188 (41.1, M$^+$ - CO$_2$Et), 160 (88.4, 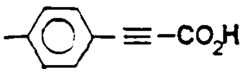, 105 (100, 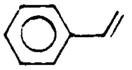).

GC; (one peak only, 1.62 min.).

p-Ph; 323 (24.2, M$^+$), 294 (20.2, M$^+$ - Et), 222 (21.9, 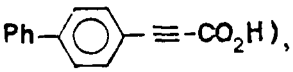, 192 (100, 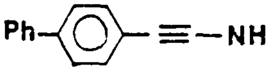).

GC; (E, 2.04 min., 4.6%), (Z, 3.06 min., 100.0%).

p-F; 266 (5.5, M$^+$ + 1), 265 (34.6, M$^+$), 250 (9.7, M$^+$ - Me), 236 (63.6, M$^+$ - Et), 192 (40.3, M$^+$ - CO$_2$ Et), 164 (91.4, 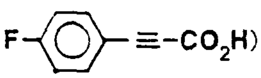, 135 (100, 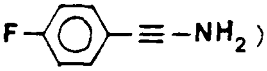.

GC; (Z, 5.48 min., 100%), (E, 5.68 min., 37.4%).

m-F; essentially identical to p-F pattern.

GC; (Z, 1.16 min., 100%), (E, 1.28 min., 38.5%).

H; 248 (5.9, M^+ + 1), 247 (37.8, M^+), 232 (9.5, M^+ - Me), 218 (66.6, M^+ - Et), 174 (30.2, M^+ - CO_2Et), 146 (57.4, 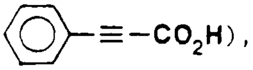), 117 (100, 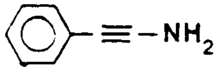).

GC; (Z, 5.28 min., 100%), (E, 5.48 min., 3.0%).

p-Cl; 283 (11.6, M^+ + 2), 282 (5.9, M^+ + 1), 281 (35.3, M^+), 266 (6.2, M^+ -Me), 252 (49.4, M^+ - Et), 208 (35.7, M^+ - CO_2Et), 180 (100.0, 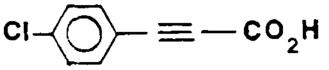).

GC; (Z, 2.04 min., 100%), (E, 2.14 min., 23.8%).

m-Cl; essentially identical to p-Cl pattern.

GC; (Z, 1.90 min., 100%), (E, 2.10 min., 98.5%).

p-CO_2Me; 292 (5.2, M^+ + 1), 291 (37.7, M^+), 276 (45.5, M^+ - Me), 262 (11.7, M^+ - Et), 232 (37.0, M^+ - CO_2Me), 260 (14.3, M^+ - OMe), 175 (M^+ - 2 (CO_2Me)), 144 (100.0, 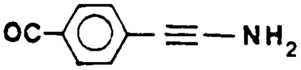).

GC; (Z, 3.64 min., 100%), (E, 4.42 min., 12.7%).

p-CF_3; 315 (8.4, M^+), 286 (24.0, M^+ - Et), 242 (20.2, M^+ - CO_2Et), 214 (77.4, 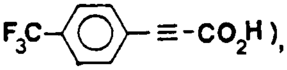), 185 (100.0, 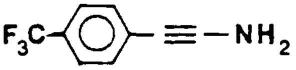).

GC; (Z, 1.14 min., 11.9%), (E, 1.26 min., 100%).

p-CN; 273 (7.1, M^+ + 1), 272 (34.2, M^+), 257 (11.8, M^+ - Me), 243 (69.2, M^+ - Et), 199 (37.6, M^+ - CO_2Et), 171 (100.0, 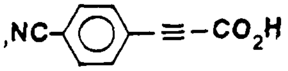) 142 (72.6, 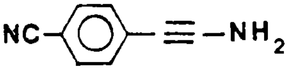).

GC; (Z, 2.93 min., 23.3%), (E, 3.60 min., 100%).

m-CN; essentially identical to p-CN pattern.

GC; (Z, 2.62 min., 36.5%), (E, 3.06 min., 100%).

p-NO$_2$; 293 (5.4, M$^+$+1), 292 (33.5, M$^+$), 277 (14.5, M$^+$ - Me), 263 (81.8, M$^+$ - Et), 219 (27.6, M$^+$ - CO$_2$Et), 191 (100.0, 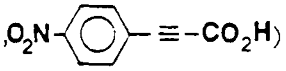), 163 (68.8, 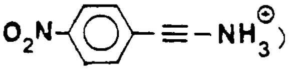).

GC; (only E isomer appears in appreciable abundance, 6.18 min).

Series D

Mass Spectra/General Comments

A cluster of peaks due to the six natural isotopes of Se was observed about the molecular ion, consistent with the presence of one selenium atom in the molecule. The six naturally occurring isotopes of Se are:

nuclide	% abundance	atomic mass
$_{34}Se^{74}$	0.87	73.9225
$_{34}Se^{76}$	9.02	75.9192
$_{34}Se^{77}$	7.58	76.9199
$_{34}Se^{78}$	23.52	77.9173
$_{34}Se^{80}$	49.82	79.9165
$_{34}Se^{82}$	9.19	81.9167

The resolution of the instrument prevented a quantitative correlation of the relative peak heights of these clusters for all the isotopes, although a qualitative correlation could be seen. For example, for the parent (H) selenide compound, the following relative peak intensities were found with the molecular ion, corresponding to the nuclide shown:

nuclide	Se^{74}	Se^{76}	Se^{77}	Se^{78}	Se^{80}	Se^{82}
m/e		328.00	329.10	330.00	332.05	334.05
observed rel. int.		10.5	9.6	26.1	49.4	9.4
theor. rel. int. (from Se only)	0.87	9.0	7.6	23.5	49.8	9.2

Some error, of course, was due to isotope effects from other elements involved (^{13}C, ^{2}H, and ^{17}O particularly).

Of most value was the approximately 2:1 ratio between the two most abundant isotopes (Se^{80} and Se^{78}), which provided a convenient recognition flag for the monoselenium compound. These will be reported along with the Se^{82} peak, as the $M^{+}+2$, M^{+}, and $M^{+}-2$ peaks in the following mass spectra.

The most common fragmentation patterns observed for the selenide compounds involved loss of CO_2Et, SePh, and OC_2H_5 groups from the molecular ion. The base peak was often found at 157 mass units, consistent with PhSeH byproduct from fragmentation process. In some cases the base peak appeared to be the allylic alcohol, perhaps generated by reduction of the carboxylate moiety by the PhSeH byproduct, which itself would be oxidized to PhSeOH. All fragmentations from the molecular ion of >200 mass units involved peak clusters since Se was always a factor in the mass difference. Thus, for brevity in the format for reporting fragmentation patterns, only the single greatest intensity peak of each cluster (and its relative intensity) will be reported.

The E and Z isomers (when both were present) gave essentially identical fragmentation patterns. Only the E isomer pattern will be reported. Also, the fragmentation patterns listed are generally directly from the molecular ion with the exception of the base peak.

Gas Chromatography/General Comments

Whenever both E and Z isomers were present, the Z isomer was found to elute first through the column, followed (usually within one minute at 250°C column temperature) by the E isomer. This elution order is logical in that the Z isomer,

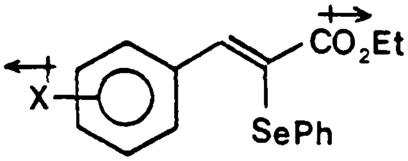

LIIA

has less of an overall molecular dipole moment since the polar groups are facing in opposite directions. In the E isomer

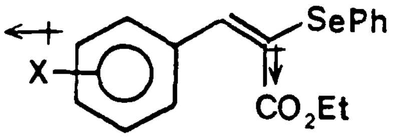

LIIA

there is a greater molecular dipole moment and thus greater retention by the column since these polar groups are now facing a more common direction.

The same format for reporting MS/GC results will be used as in Series A.

p-N(Me)$_2$; 377 (10.6, $M^+ + 2$), 375 (49.6, M^+), 373 (29.2, $M^+ - 2$), 330 (3.5, M^+ - N(Me)$_2$), 302 (7.7, $M^+ - CO_2Et$), 295 (92.3, M^+ - Se), 223 (26.3, M^+ - SePh), 144 (100, 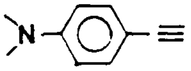).

GC; (Z, 10.16 min., 91.2%), (E, 11.20 min., 100%).

p-MeO; 364 (7.6, $M^+ +2$), 362 (37.4, M^+), 360 (19.4, $M^+ - 2$), 289 (9.4, $M^+ - CO_2Et$), 208 (23.0, M^+ - SePh), 165 (100, 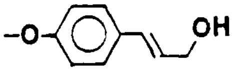).

GC; (Z, 7.02 min., 100%), (E, 7.38 min., 98.8%).

p-Me; 348 (8.5, $M^+ + 2$), 346 (40.9, M^+), 344 (20.9, $M^+ - 2$), 273 (15.6, $M^+ - CO_2Et$), 192 (47.3, M^+ - SePh), 149 (73.0, [M^+ - SePh] - OEt), 115 (100, 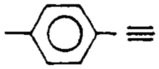).

GC; (Z, 6.06 min., 24.5%), (E, 6.36 min., 100%).

p-Ph; 410 (8.1, $M^+ + 2$) 408 (42.2, M^+), 406 (17.8, $M^+ - 2$), 334 (10.8, $M^+ - CO_2Et$), 254 (45.9, M^+ - SePh), 178 (100.0, 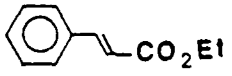).

GC; (Z, 16.56 min., 5.9%), (E, 17.74 min., 100%).

p-F; 352 (12.3, $M^+ + 2$), 350 (61.8, M^+), 348 (31.3, $M^+ - 2$), 305 (3.8, M^+ - OEt), 277 (21.8, $M^+ - CO_2Et$), 196 (89.5, M^+ - SePh), 153 (100.0, 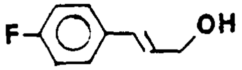).

GC; (Z, 5.20 min., 14.3%), (E, 5.46 min., 100.0%).

p-Cl; 368 (43.4, M^+ + 2), 366 (99.3, M^+), 364 (50.0, M^+ - 2), 291 (35.3, M^+ - CO_2Et), 258 (55.9, [M^+ - CO_2Et] - Cl), 212 (49.3, M^+ - SePh), 169 (100, 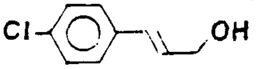).

GC; (Z, 5.02 min., 31.9%), (E, 5.18 min., 100%).

m-MeO; 364 (3.7, M^+ + 2), 362 (18.6, M^+ - OEt); unusually weak high mw fragmentation pattern; 289 (5.3, M^+ - CO_2Et), 208 (100, M^+ - SePh).

GC; (Z, 8.48 min. 0.40%), (E, 8.80 min., 100%).

m-F; 352 (9.4, M^+ + 2), 350 (48.2, M^+), 348 (25.3, M^+ - 2), 303 (4.5, M^+ - OEt), 277 (24.5, M^+ - CO_2Et), 196 (100, M^+ - SePh), 157 (57.6, PhSeH).

GC; (Z, 5.38 min., 42.9%), (E, 5.94 min., 100%).

m-Cl; 368 (38.9, M^+ + 2), 366 (76.1, M^+), 364 (43.6, M^+ - 2), 321 (5.8, M^+ - OEt), 292 (34.2, M^+ - CO_2Et), 258 (53.1, [M^+ - CO_2Et] - Cl), 212 (83.4, M^+ - SePh), 157 (100, PhSeH).

GC; (E only, 9.04 min.).

p-CO_2Me; 392 (11.9, M^+ + 2), 390 (65.0, M^+), 388 (32.9, M^+ - 2), 359 (7.0, M^+ - OMe), 345 (3.5, M^+ - OEt), 316 (20.3, M^+ - CO_2Et), 285 (19.6, [M^+ - CO_2Et] - OMe), 258 (32.9, [M^+ - CO_2Et] - CO_2Me), 236 (27.3, M^+ - SePh), 193 (100.0, 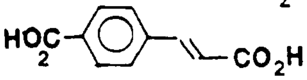), 157 (70.6, PhSeH).

GC; (Z, 8.36 min., 28.6%), (E, 8.60 min., 100%).

m-CN; 359 (12.7, $M^+ + 2$), 357 (72.7, M^+), 355 (34.8, $M^+ - 2$), 312 (6.4, $M^+ - OEt$), 284 (49.8, $M^+ - CO_2Et$), 203 (84.6, $M^+ - SePh$), 157 (100.0, PhSeH).

GC; (E only, 11.14 min.).

m-CF_3; 402 (15.6, $M^+ + 2$), 400 (71.9, M^+), 398 (36.3, $M^+ - 2$), 355 (5.5, $M^+ - OEt$), 326 (41.0, $M^+ - CO_2Et$), 246 (46.1, $M^+ - SePh$), 157 (100.0, PhSeH).

GC; (Z, 4.82 min., 28.8%), (E, 5.16 min., 100%).

p-CF_3; essentially identical to m-CF_3 pattern

GC; (Z, 5.00 min., 16.9%), (E, 5 [illegible] min., 100%)

p-CN; essentially identical to m-CN pattern

GC; (E only, 7.20 min.).

m-NO_2; 379 (19.6, $M^+ + 2$), 377 (100, M^+), 375 (49.7, $M^+ - 2$), 332 (5.8, $M^+ - NO_2$), 303 (28.6, $M^+ - CO_2Et$), 286 (9.5, $[M^+ - NO_2] - OEt$), 258 (43.9, $[M^+ - CO_2Et] - NO_2$), 157 (89.4, PhSeH).

GC; (E only, 9.08 min.).

p-NO_2; 379 (13.7, $M^+ + 2$), 377 (73.7, M^+), 375 (37.0, $M^+ - 2$), 332 (5.4, $M^+ - OEt$), 331 (6.5, $M^+ - NO_2$), 303 (21.5, $M^+ - CO_2Et$), 258 (37.4, $[M^+ - CO_2Et] - NO_2$), 227 (33.0, $M^+ - SePh$), 157 (100, PhSeH).

GC; (Z, 4.02 min., 100.0%), (E, 4.12 min., 14.8%).

APPENDIX E

Infrared Spectra

Series A

The infrared spectra for the Series A compounds follow.

NOTE: All samples were obtained neat using NaCl cells.

Common diagnostic peaks observed at:

2970 cm^{-1} = CH (aromatic)

1720-1700 cm^{-1} = carbonyl (CO_2R)

1250-1200 cm^{-1}

Specifically:

2230 cm^{-1} = nitrile (m-CN compound)

2220 cm^{-1} = nitrile (p-CN compound)

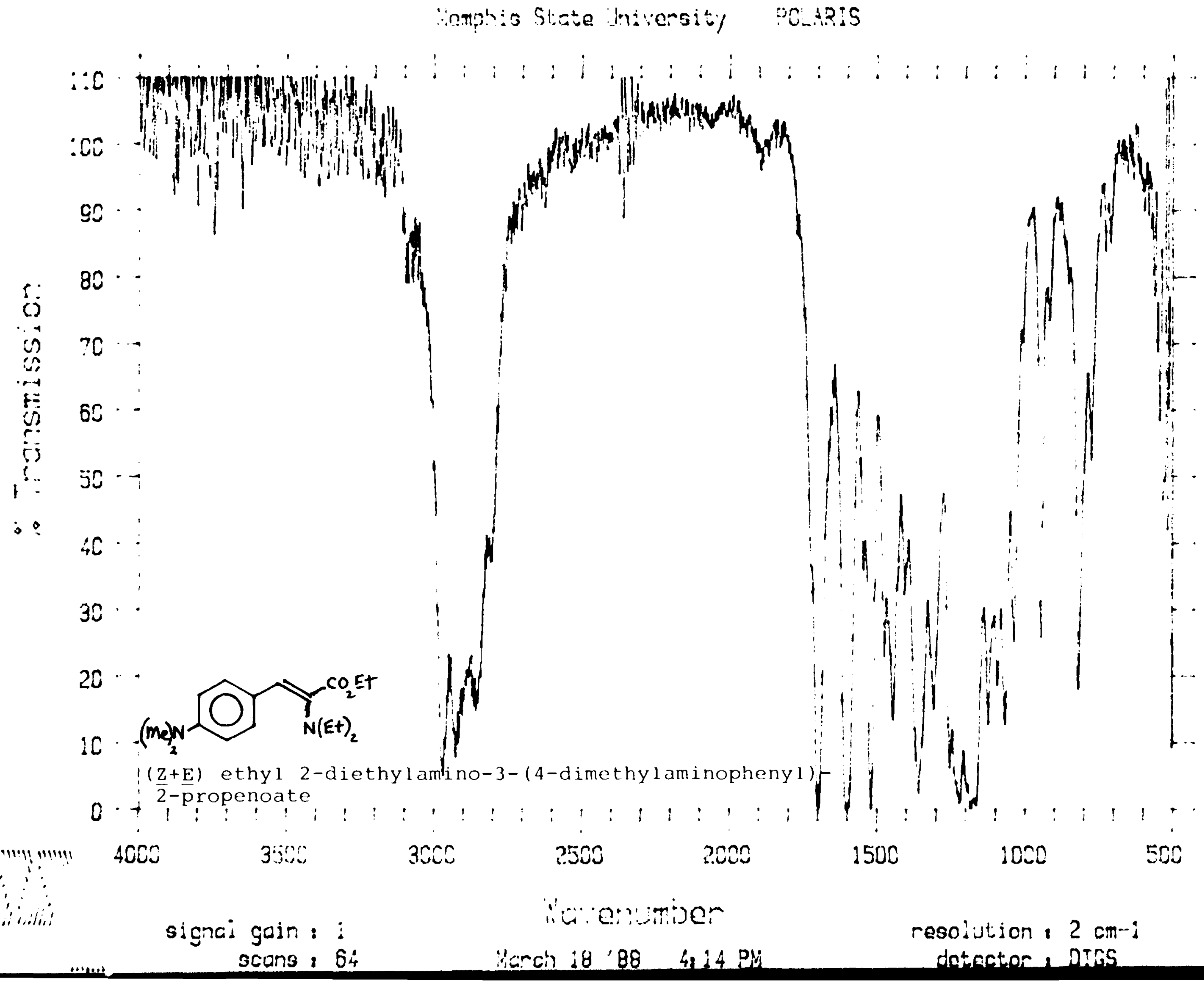
(Z+E) ethyl 2-diethylamino-3-(4-dimethylaminophenyl)-2-propenoate

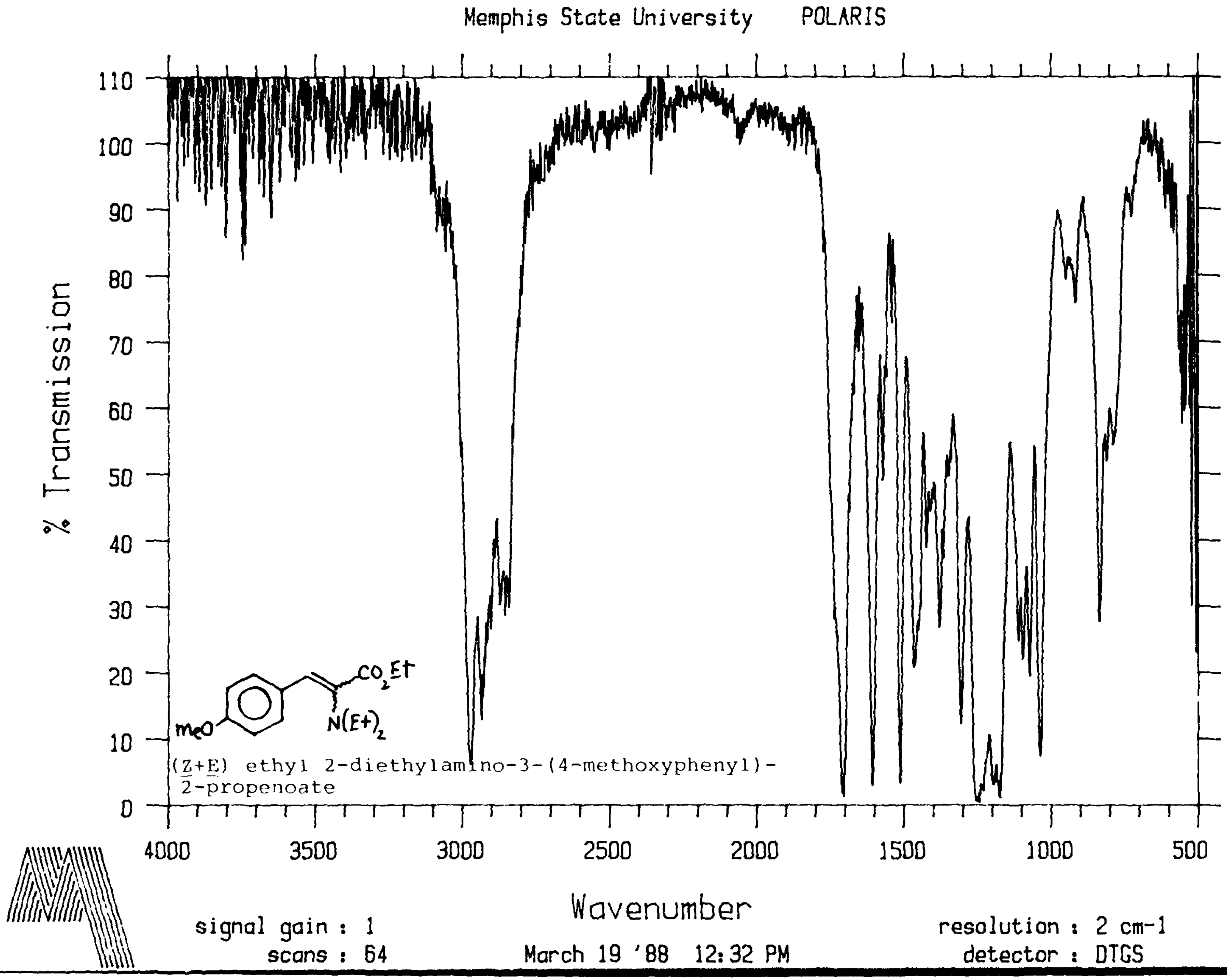
Memphis State University POLARIS
% Transmission
110
100
90
80
70
60
50
40
30
20
10
0
4000
3500
3000
2500
2000
1500
1000
500
Wavenumber
MeO
CO2Et
N(Et)2
(Z+E) ethyl 2-diethylamino-3-(4-methoxyphenyl)-
2-propenoate
signal gain : 1
scans : 64
March 19 '88 12:32 PM
resolution : 2 cm-1
detector : DTGS

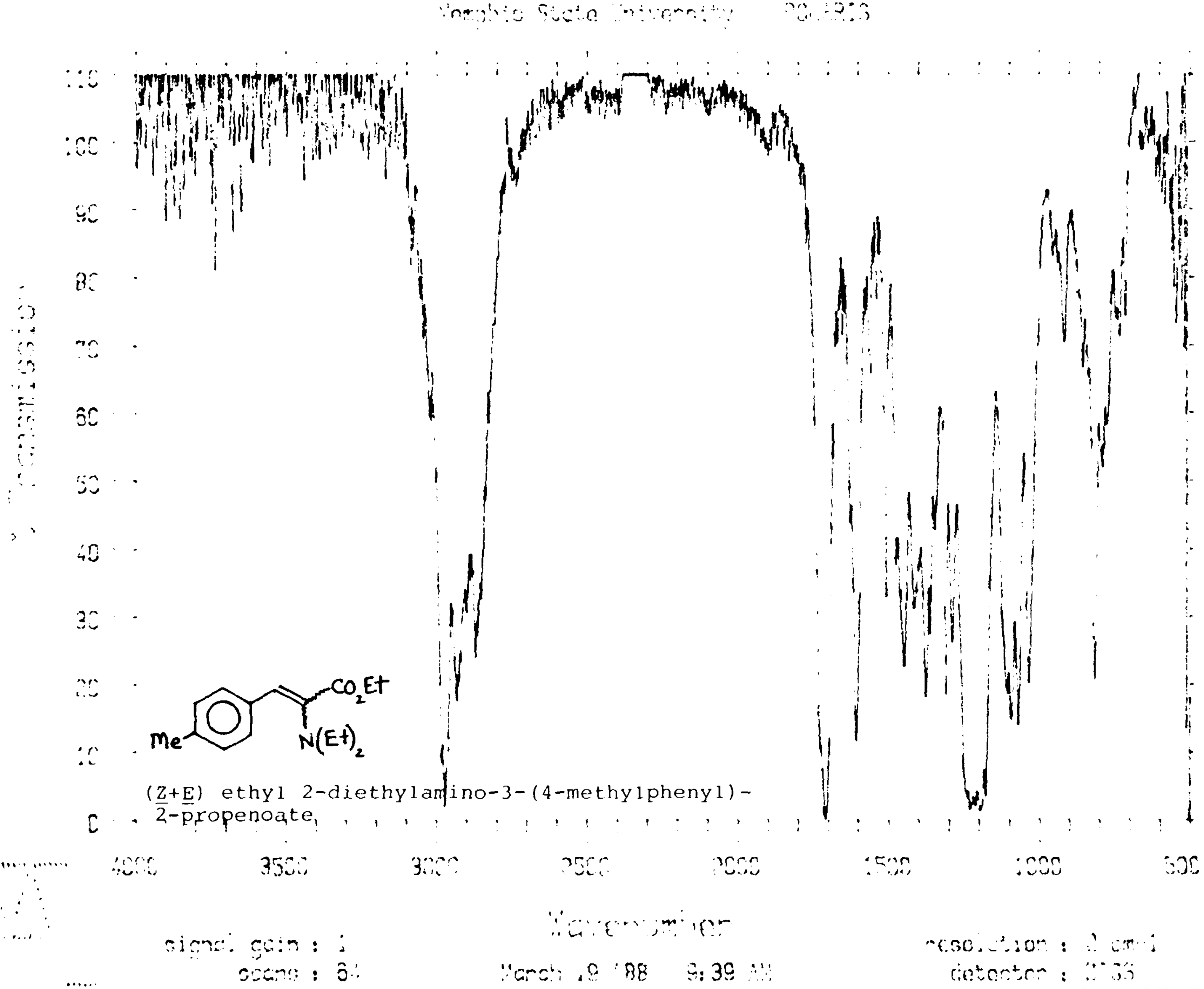

(Z+E) ethyl 2-diethylamino-3-(4-methylphenyl)-2-propenoate

Memphis State University POLARIS

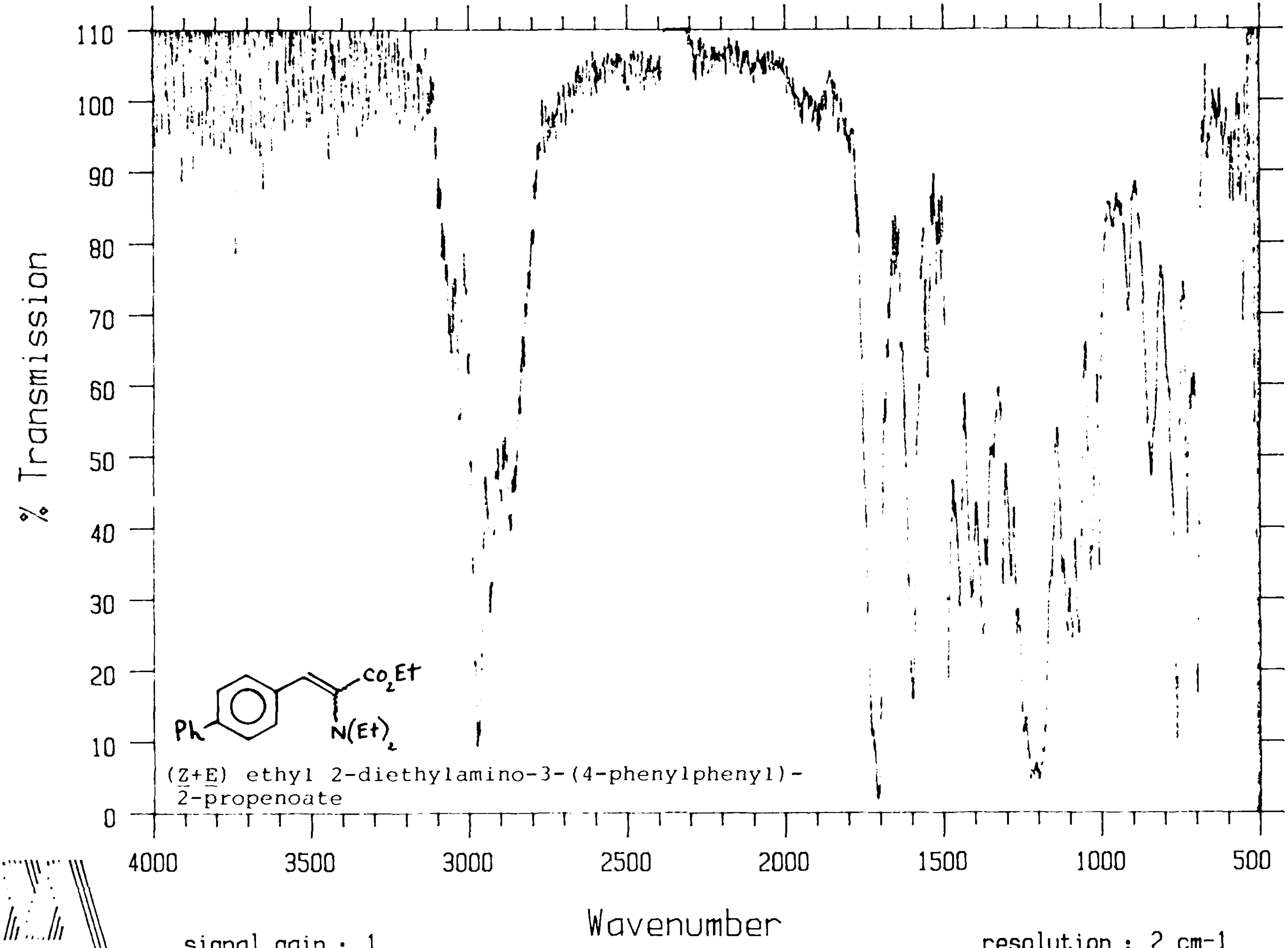

(Z+E) ethyl 2-diethylamino-3-(4-phenylphenyl)-2-propenoate

signal gain : 1
scans : 64

March 19 '88 10:04 AM

resolution : 2 cm-1
detector : DTGS

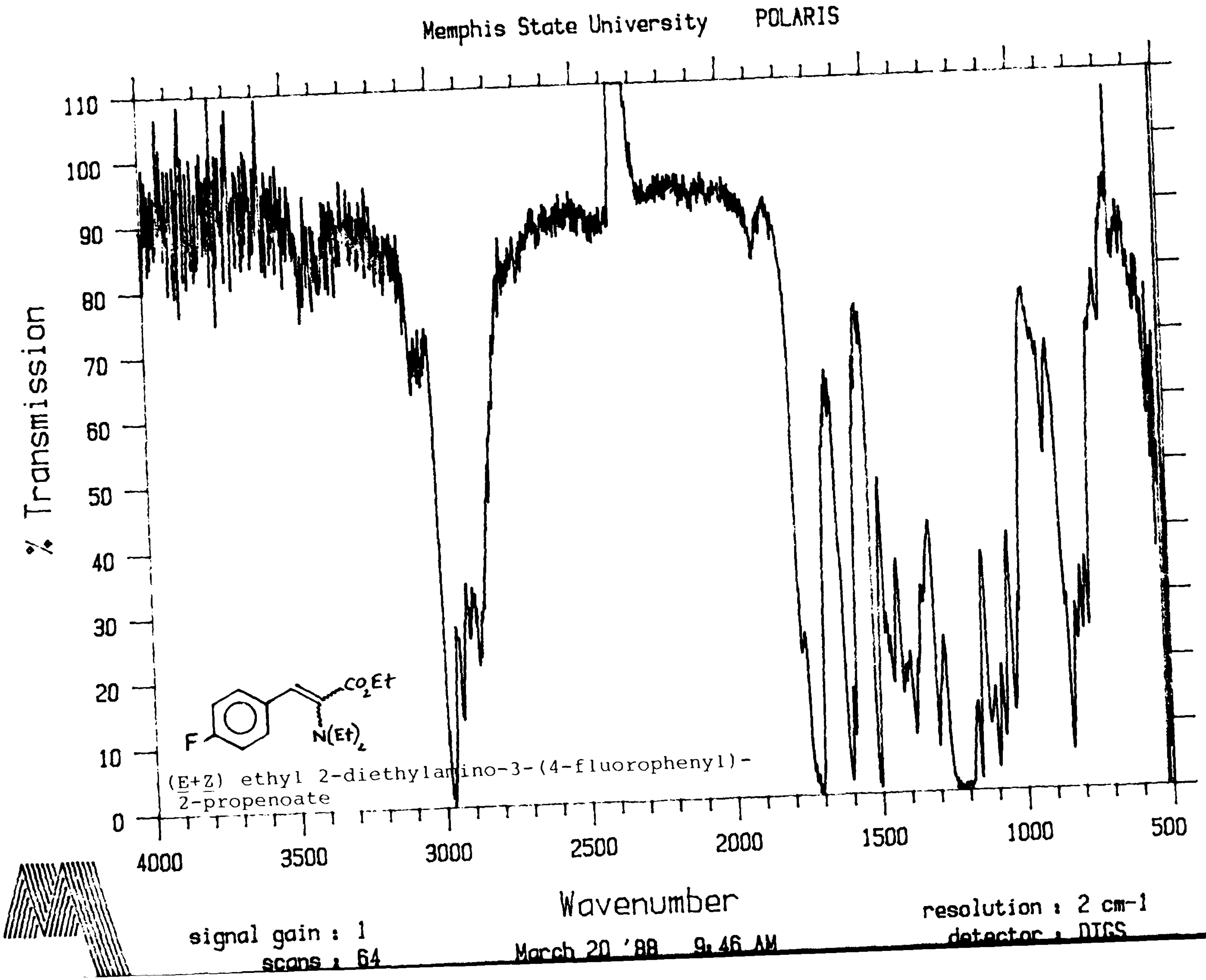
Memphis State University POLARIS
% Transmission
110
100
90
80
70
60
50
40
30
20
10
0
4000
3500
3000
2500
2000
1500
1000
500
Wavenumber
CO2Et
F
N(Et)2
(E+Z) ethyl 2-diethylamino-3-(4-fluorophenyl)-2-propenoate
signal gain : 1
scans : 64
March 20 '88 9:46 AM
resolution : 2 cm-1
detector : DTGS

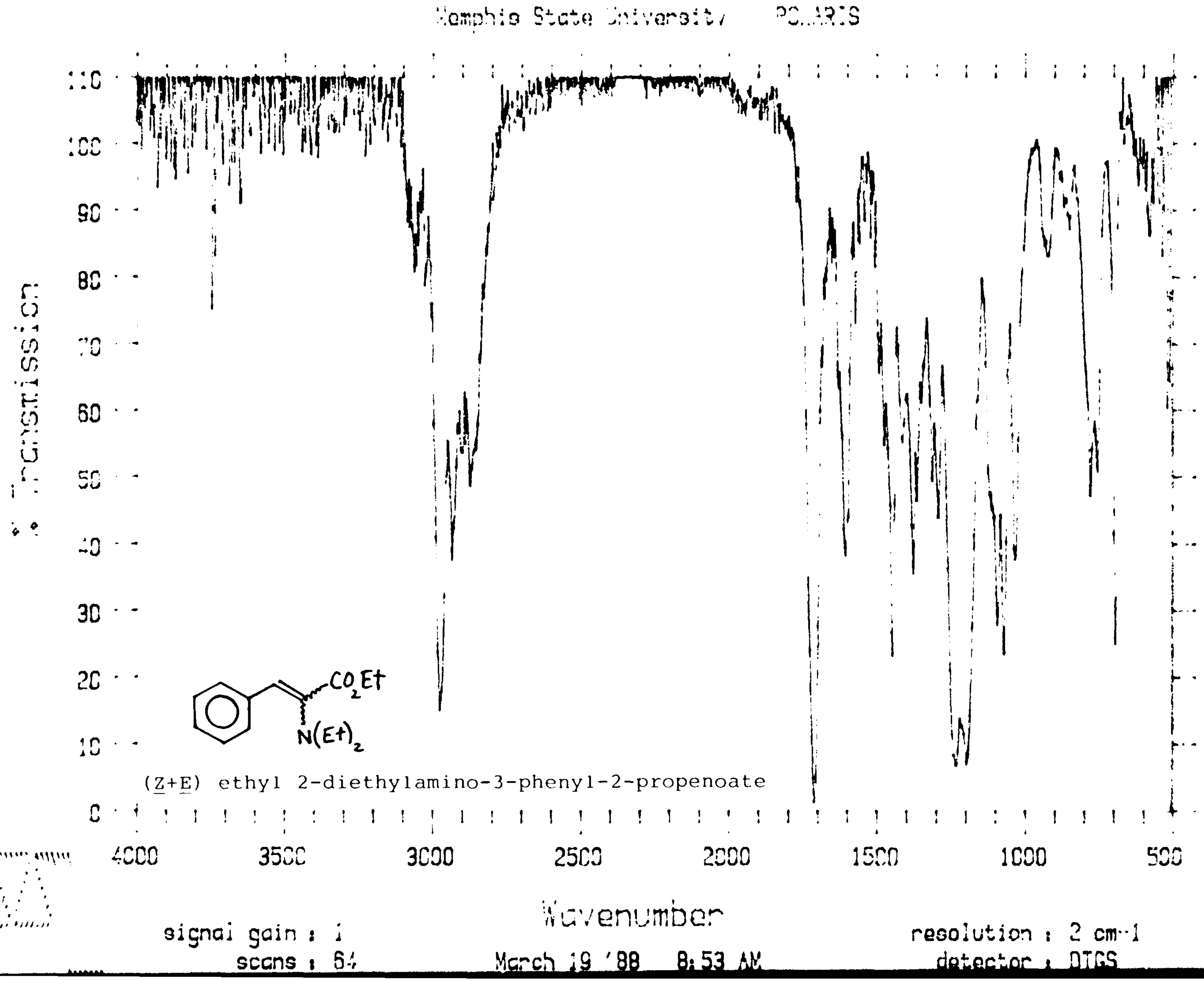

(Z+E) ethyl 2-diethylamino-3-phenyl-2-propenoate

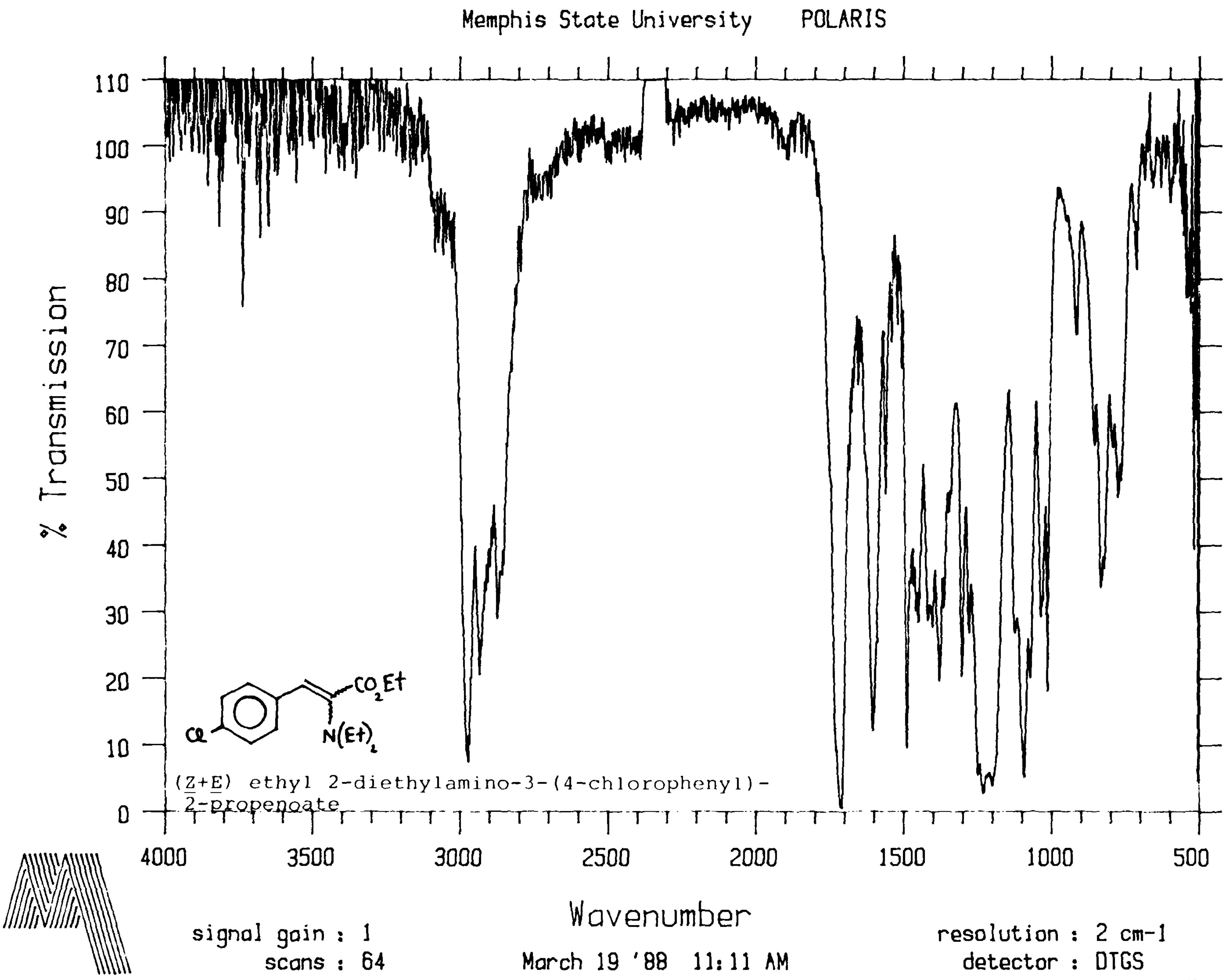
Memphis State University POLARIS
% Transmission
110
100
90
80
70
60
50
40
30
20
10
0
4000
3500
3000
2500
2000
1500
1000
500
Wavenumber
CO2Et
Cl
N(Et)2
(Z+E) ethyl 2-diethylamino-3-(4-chlorophenyl)-2-propenoate
signal gain : 1
scans : 64
March 19 '88 11:11 AM
resolution : 2 cm-1
detector : DTGS

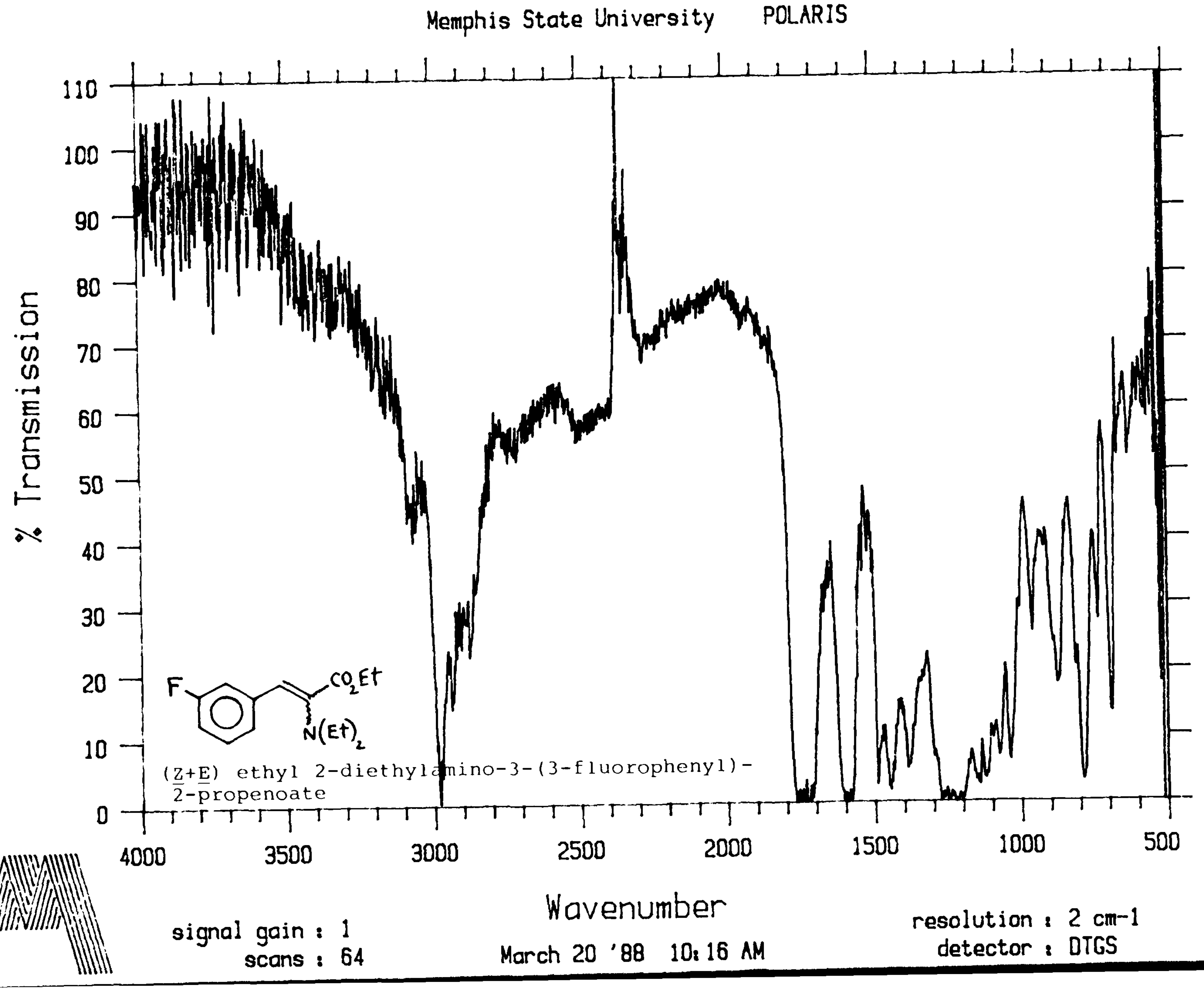
Memphis State University POLARIS
% Transmission
110
100
90
80
70
60
50
40
30
20
10
0
4000
3500
3000
2500
2000
1500
1000
500
Wavenumber
F
CO2Et
N(Et)2
(Z+E) ethyl 2-diethylamino-3-(3-fluorophenyl)-2-propenoate
signal gain : 1
scans : 64
March 20 '88 10:16 AM
resolution : 2 cm-1
detector : DTGS

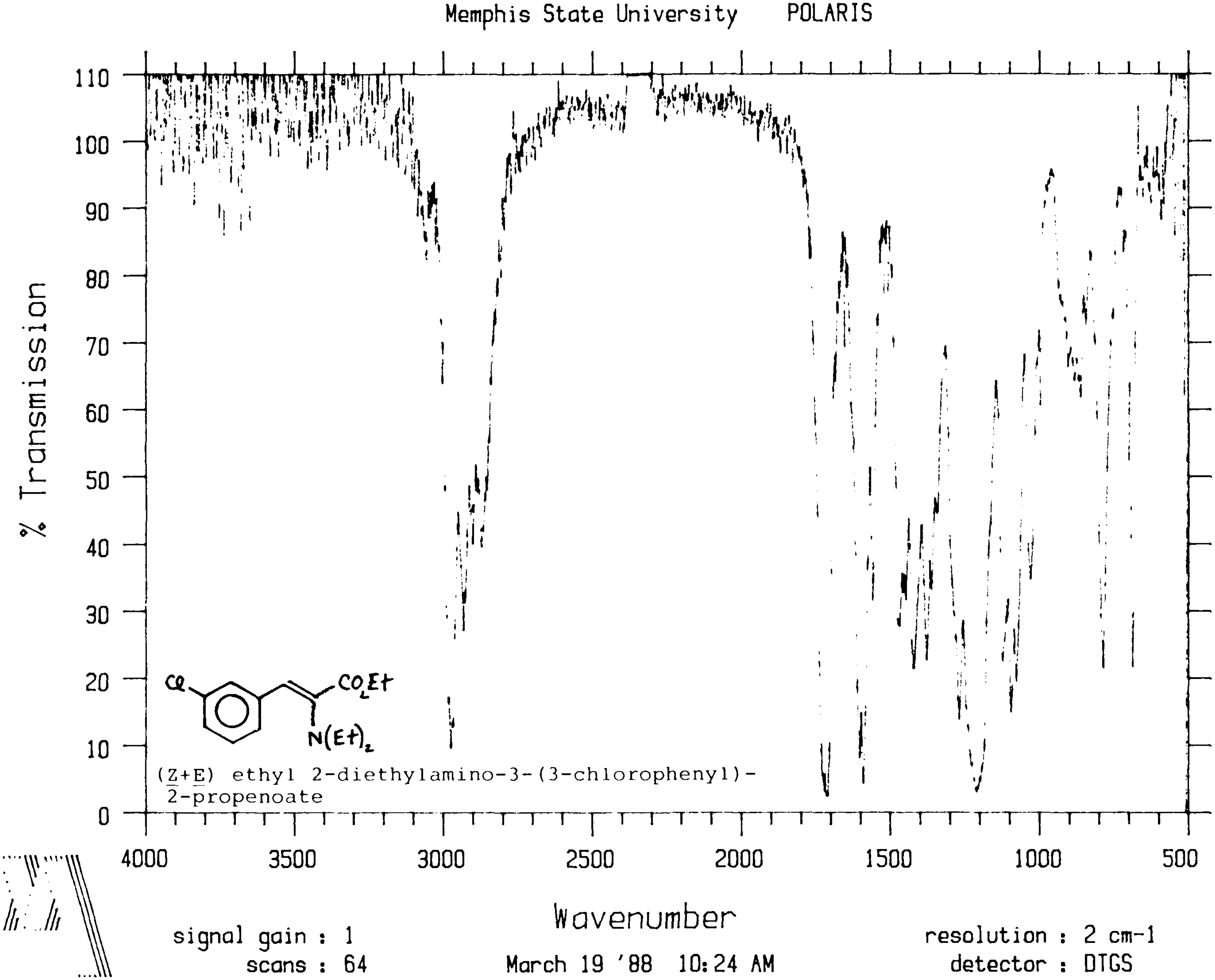
Memphis State University POLARIS
% Transmission
110
100
90
80
70
60
50
40
30
20
10
0
4000
3500
3000
2500
2000
1500
1000
500
Wavenumber
Cl
CO2Et
N(Et)2
(Z+E) ethyl 2-diethylamino-3-(3-chlorophenyl)-2-propenoate
signal gain : 1
scans : 64
March 19 '88 10:24 AM
resolution : 2 cm-1
detector : DTGS

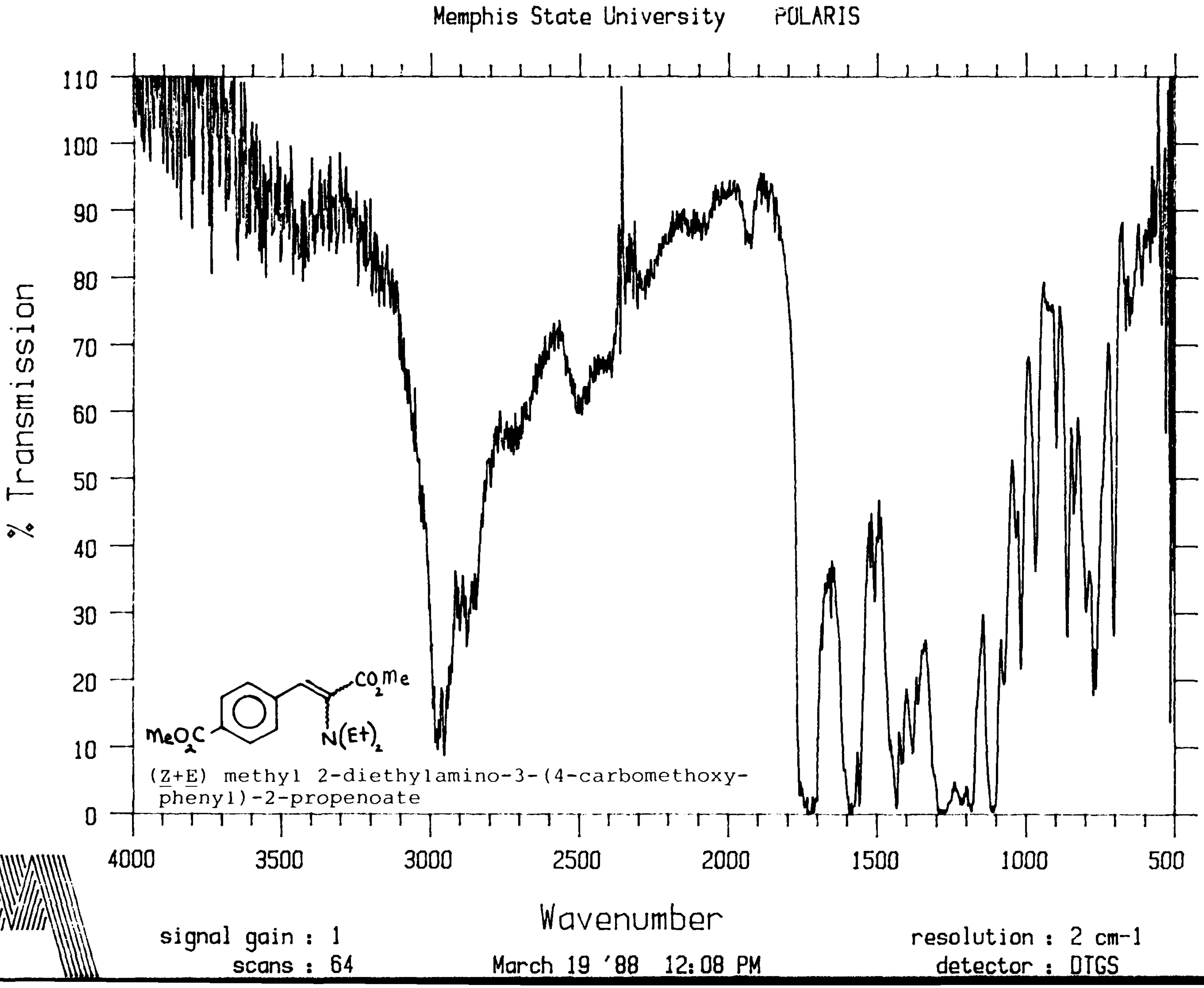
Memphis State University POLARIS
% Transmission
110
100
90
80
70
60
50
40
30
20
10
0
4000
3500
3000
2500
2000
1500
1000
500
Wavenumber
MeO$_2$C
CO$_2$Me
N(Et)$_2$
(Z+E) methyl 2-diethylamino-3-(4-carbomethoxy-phenyl)-2-propenoate
signal gain : 1
scans : 64
March 19 '88 12:08 PM
resolution : 2 cm-1
detector : DTGS

Memphis State University POLARIS

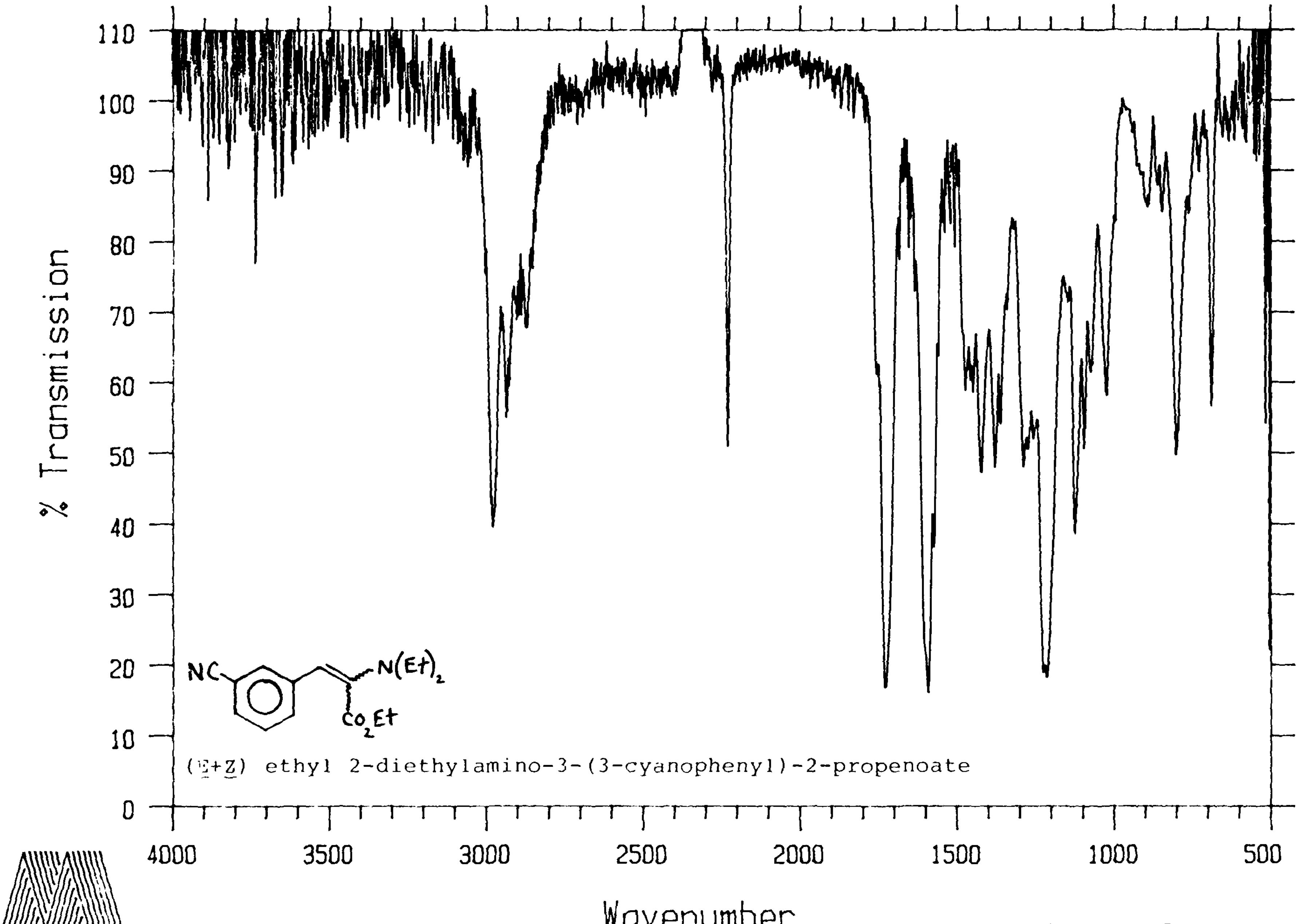

(E+Z) ethyl 2-diethylamino-3-(3-cyanophenyl)-2-propenoate

signal gain : 1
scans : 64

March 19 '88 11:39 AM

resolution : 2 cm-1
detector : DTGS

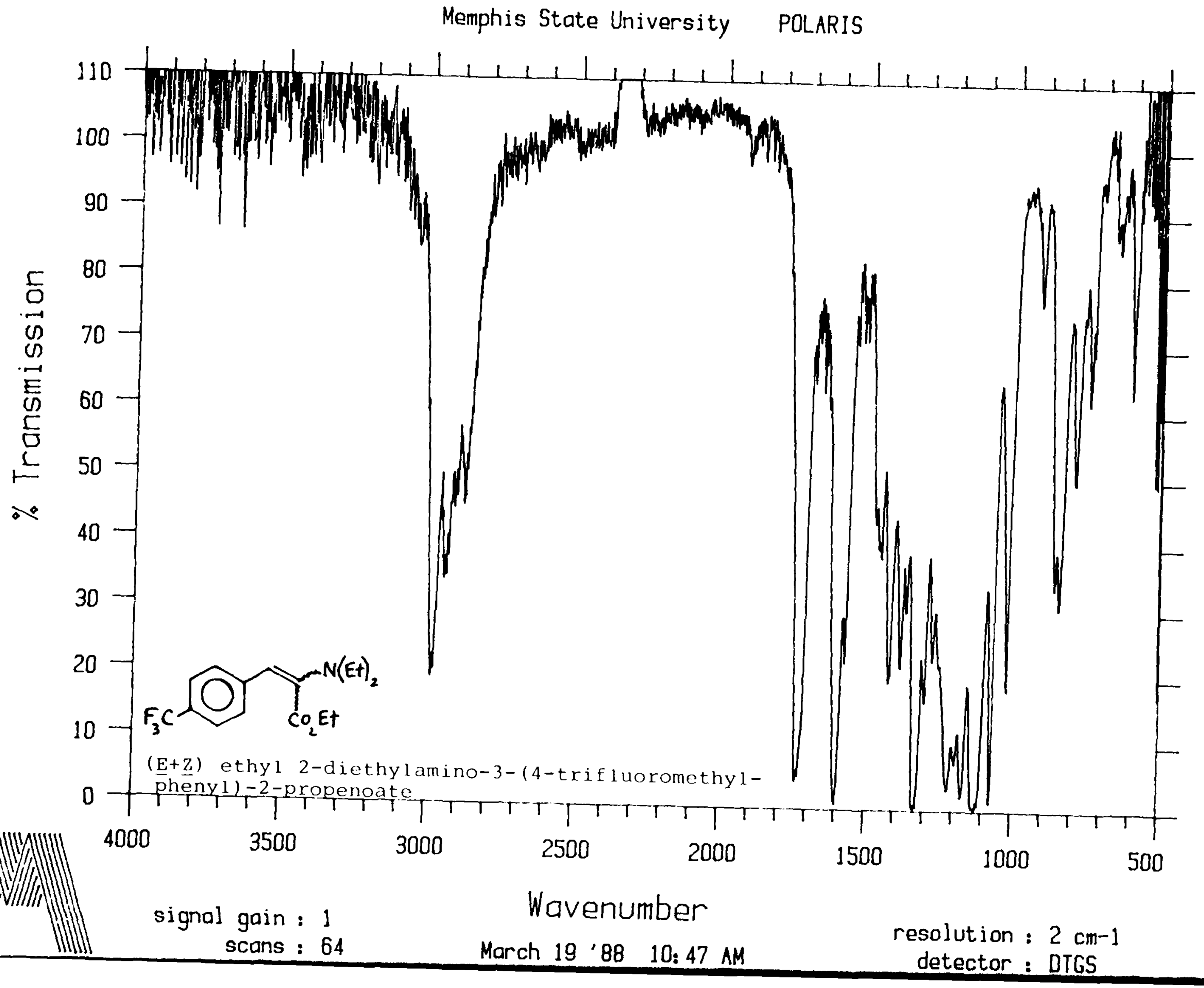

(E+Z) ethyl 2-diethylamino-3-(4-trifluoromethylphenyl)-2-propenoate

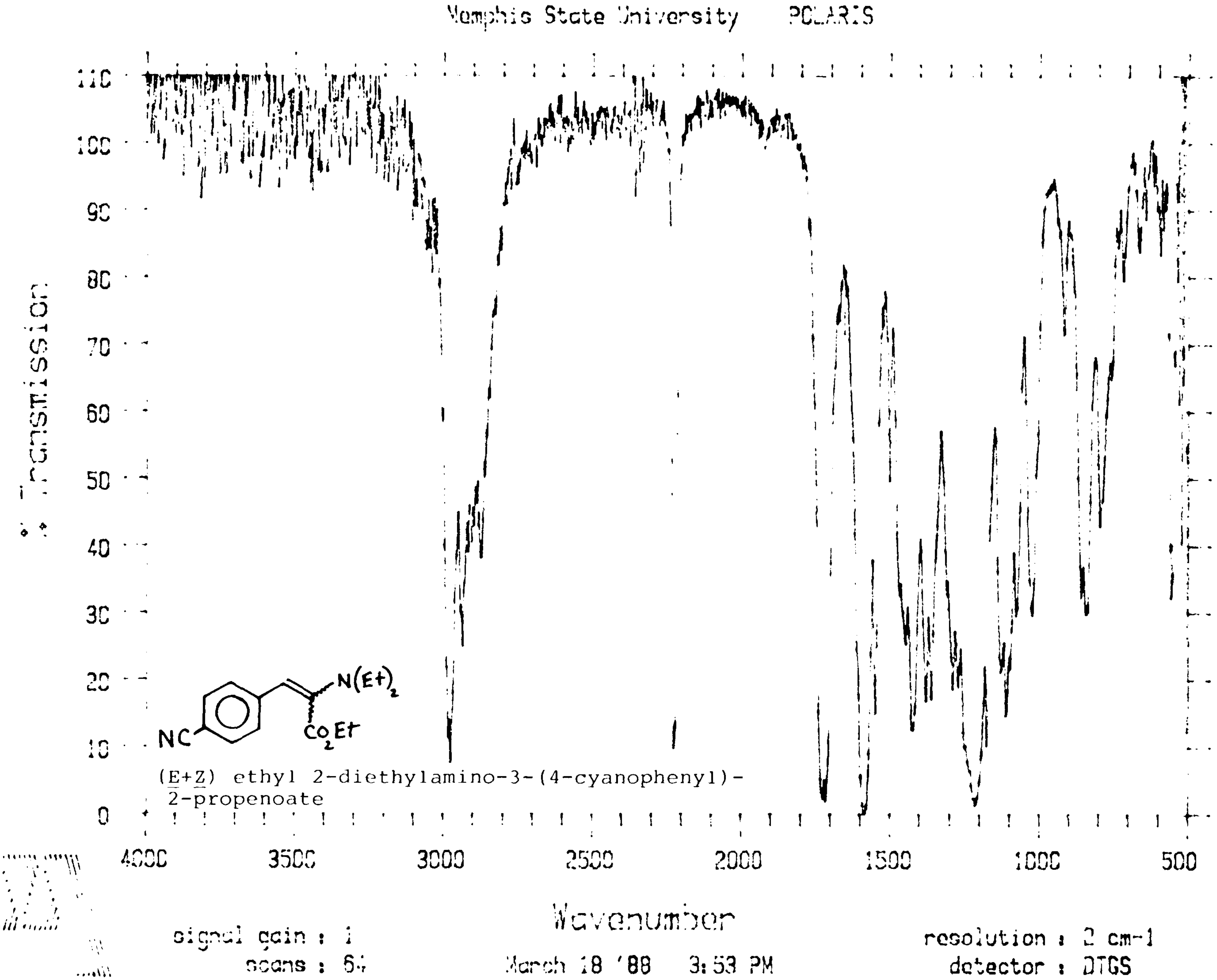

(E+Z) ethyl 2-diethylamino-3-(4-cyanophenyl)-2-propenoate

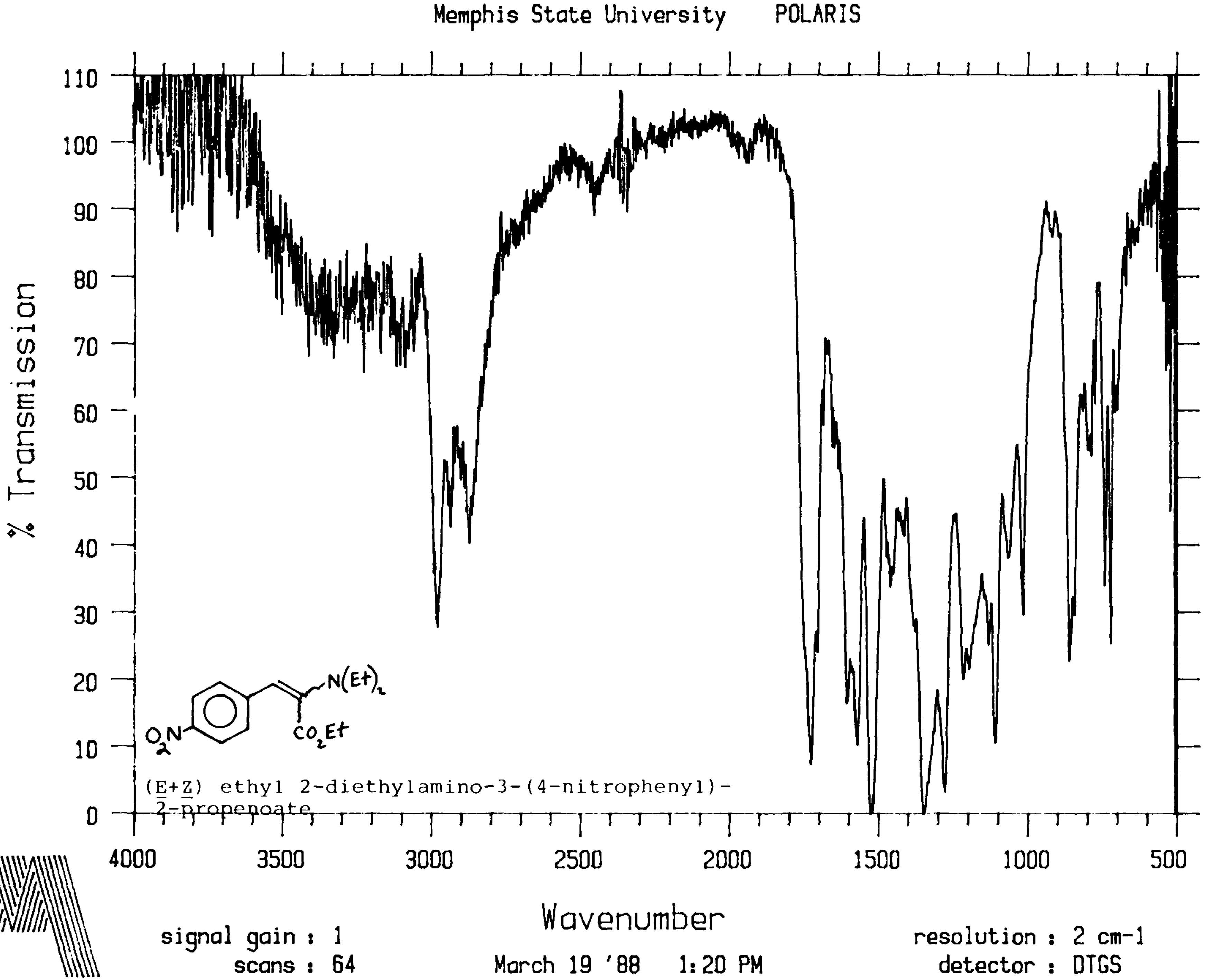

(E+Z) ethyl 2-diethylamino-3-(4-nitrophenyl)-2-propenoate

Series D

The infrared spectra for the Series D compounds follow:

NOTE: All samples were obtained neat using NaCl cells. (Solids were obtained as melts.)

Common diagnostic peaks observed at:

2970 cm^{-1} = CH (aromatic)
1720-1700 cm^{-1} =
1300-1200 cm^{-1} = carbonyl (CO_2R)

Specifically:

2230 cm^{-1} = nitrile (m-CN compound)
2220 cm^{-1} = nitrile (p-CN compound)

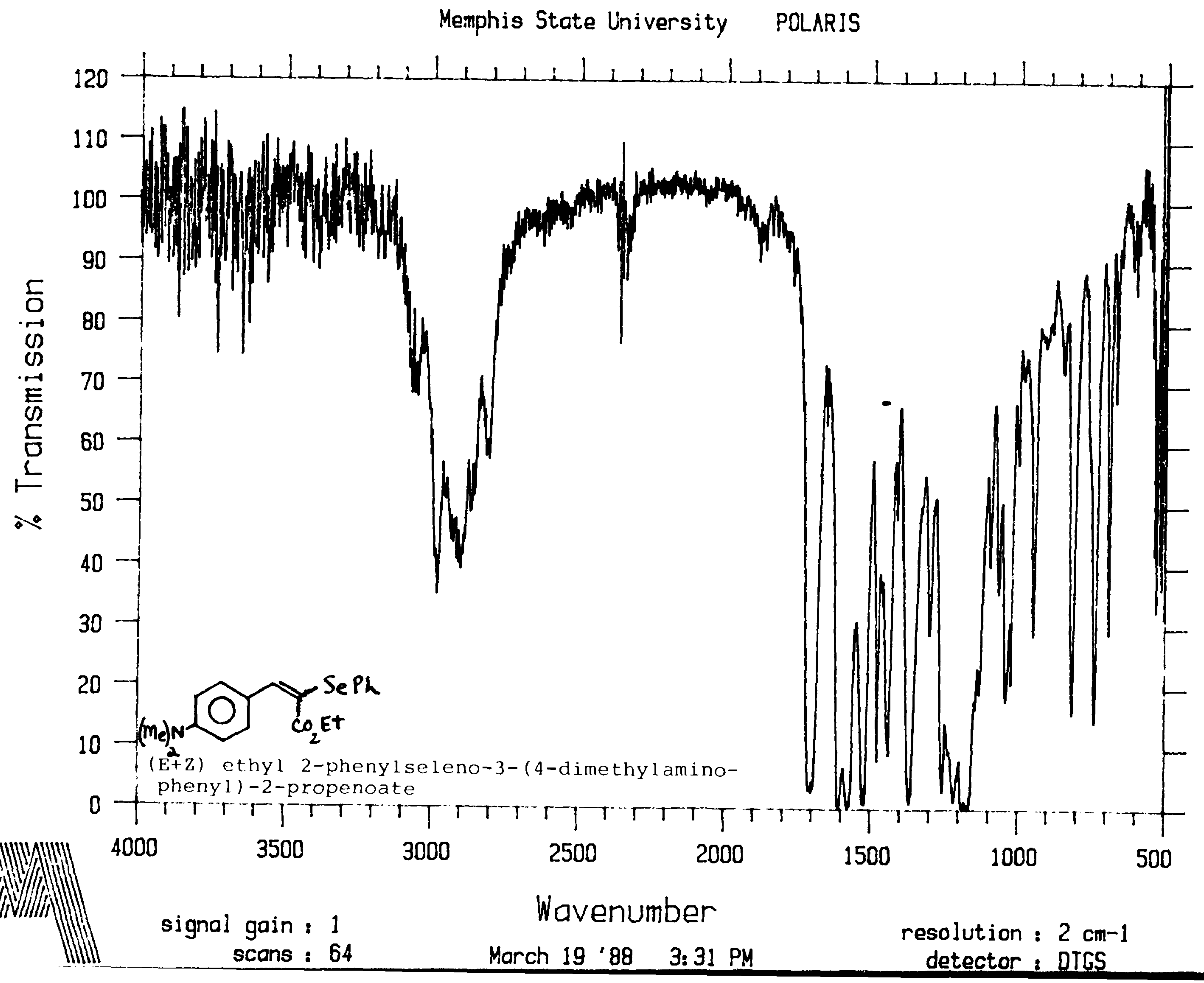
Memphis State University POLARIS
% Transmission
120
110
100
90
80
70
60
50
40
30
20
10
0
SePh
CO2Et
(Me)2N
(E+Z) ethyl 2-phenylseleno-3-(4-dimethylamino-
phenyl)-2-propenoate
4000
3500
3000
2500
2000
1500
1000
500
Wavenumber
signal gain : 1
scans : 64
March 19 '88 3:31 PM
resolution : 2 cm-1
detector : DTGS

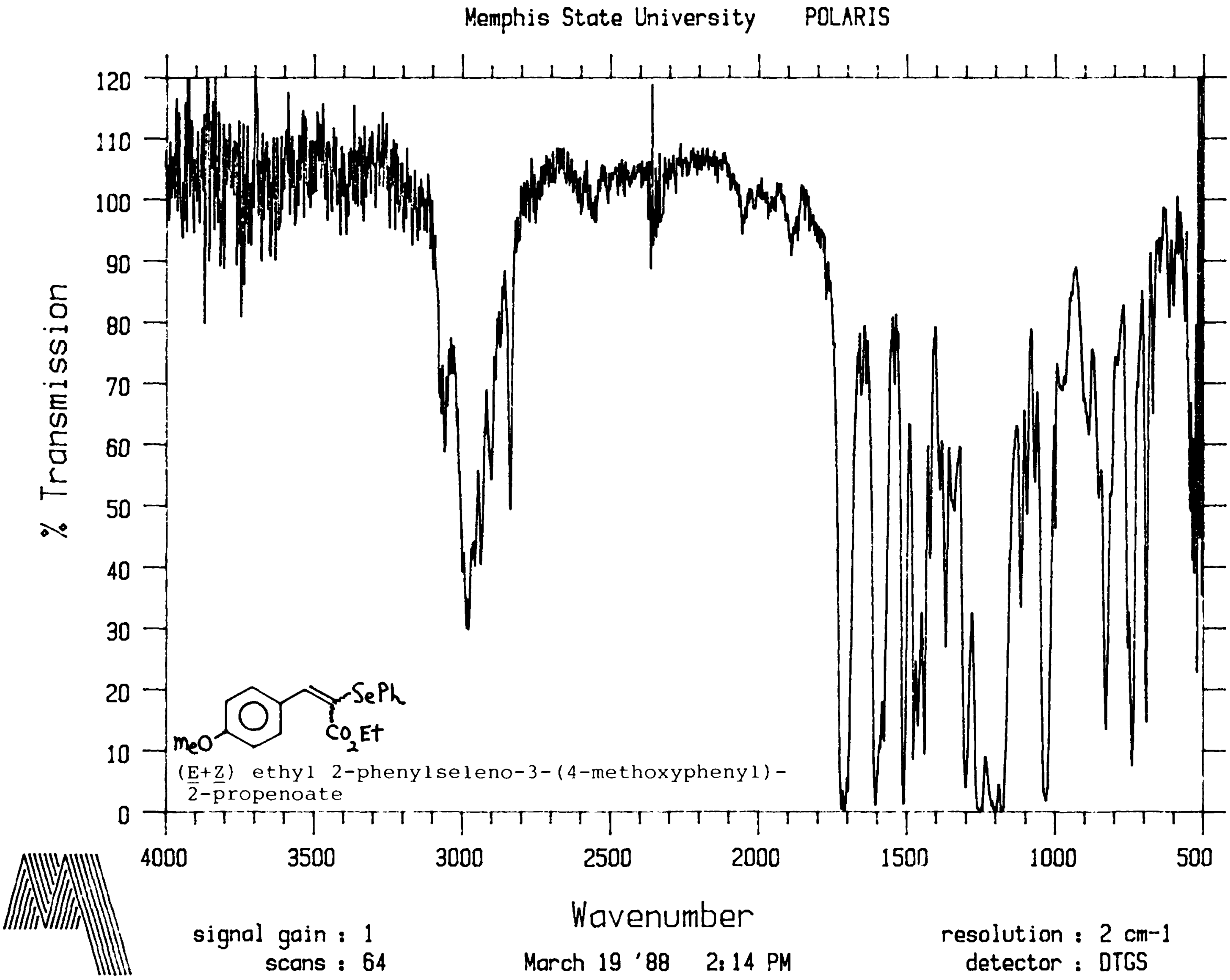
Memphis State University POLARIS
% Transmission
120
110
100
90
80
70
60
50
40
30
20
10
0
4000
3500
3000
2500
2000
1500
1000
500
Wavenumber
MeO
SePh
CO2Et
(E+Z) ethyl 2-phenylseleno-3-(4-methoxyphenyl)-2-propenoate
signal gain : 1
scans : 64
March 19 '88 2:14 PM
resolution : 2 cm-1
detector : DTGS

Memphis State University POLARIS

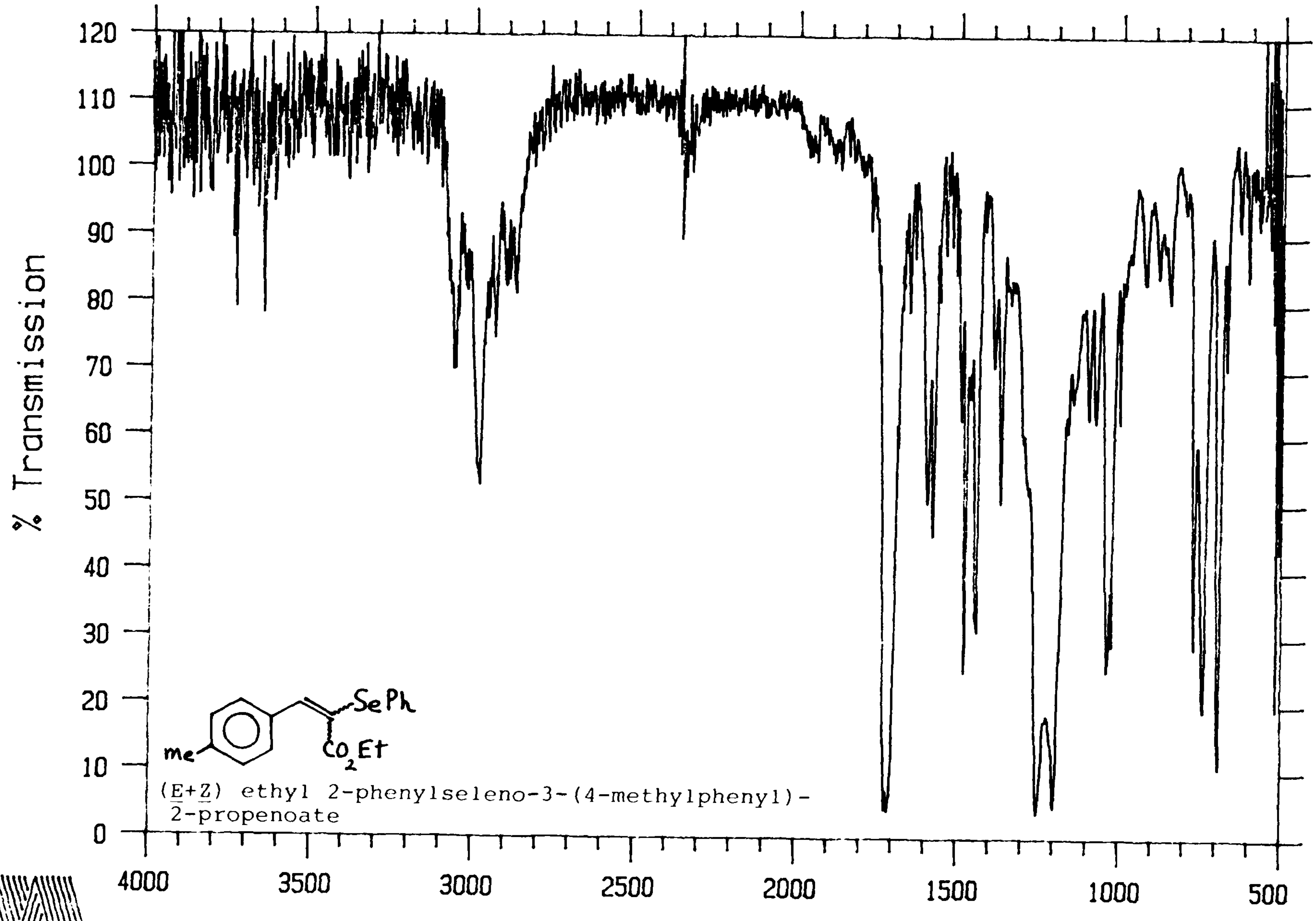

signal gain : 1
scans : 64

March 19 '88 1:46 PM

resolution : 2 cm-1
detector : DTGS

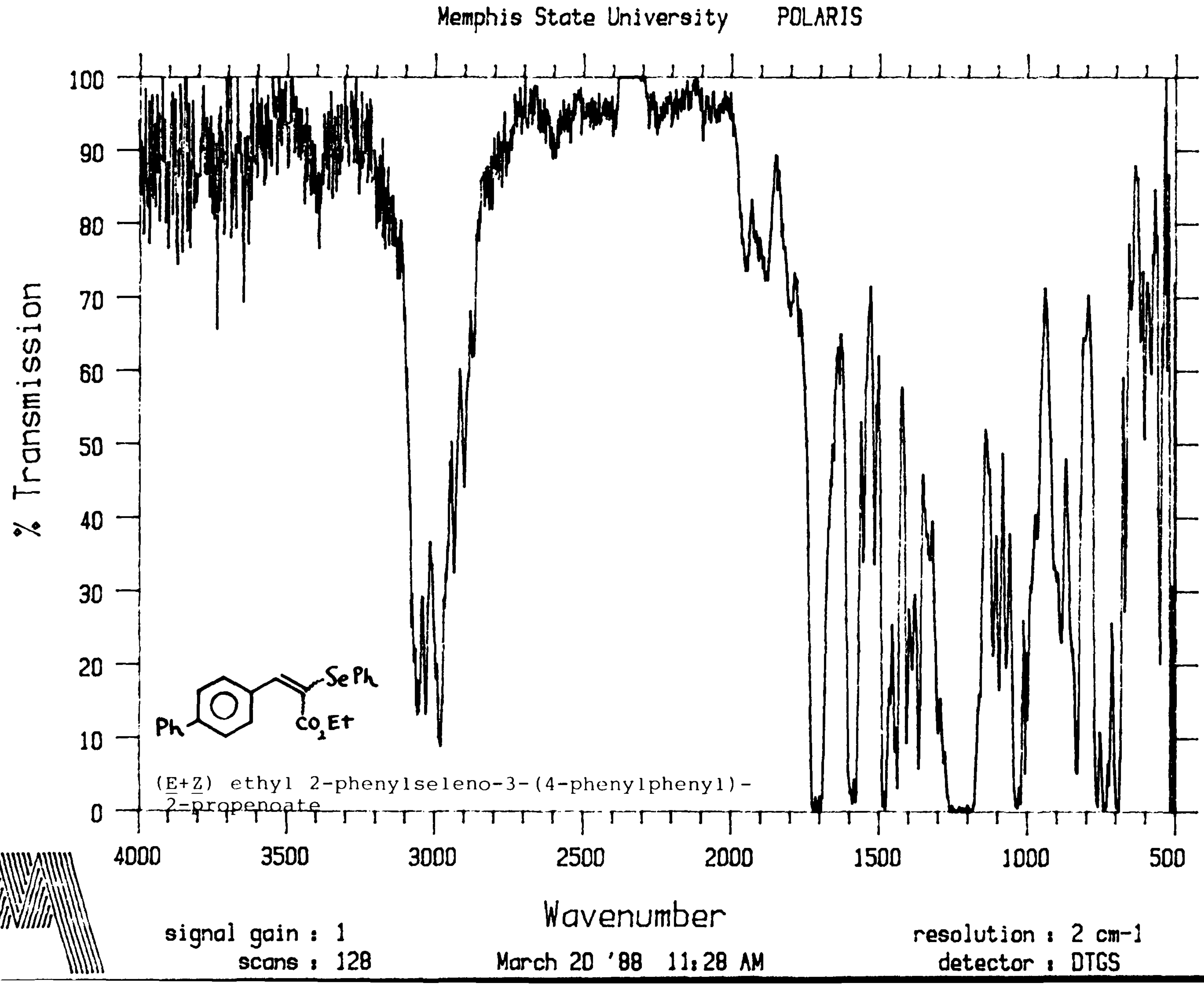

(E+Z) ethyl 2-phenylseleno-3-(4-phenylphenyl)-2-propenoate

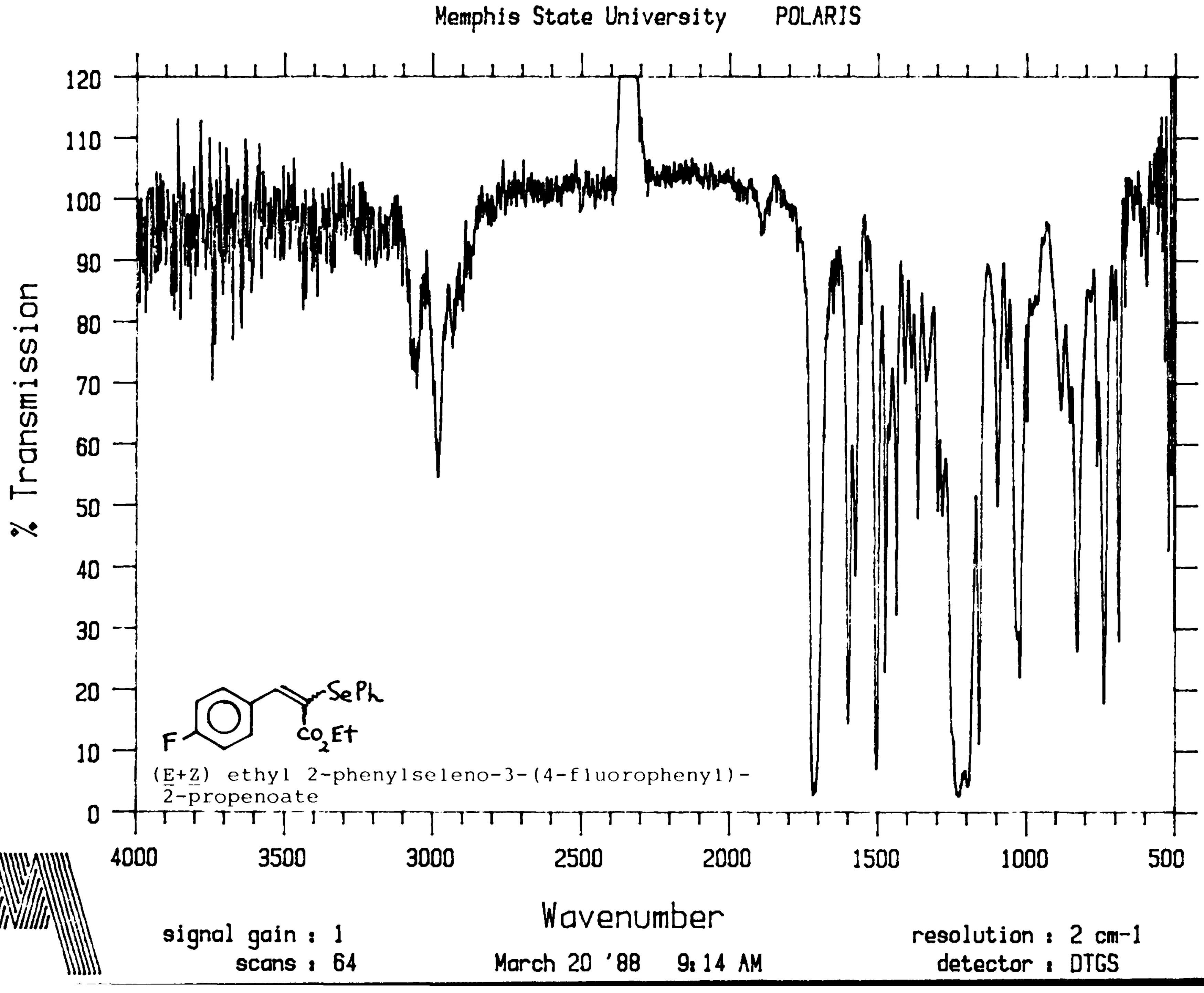
Memphis State University POLARIS
% Transmission
120
110
100
90
80
70
60
50
40
30
20
10
0
4000
3500
3000
2500
2000
1500
1000
500
Wavenumber
F
SePh
CO$_2$Et
(E+Z) ethyl 2-phenylseleno-3-(4-fluorophenyl)-2-propenoate
signal gain : 1
scans : 64
March 20 '88 9:14 AM
resolution : 2 cm-1
detector : DTGS

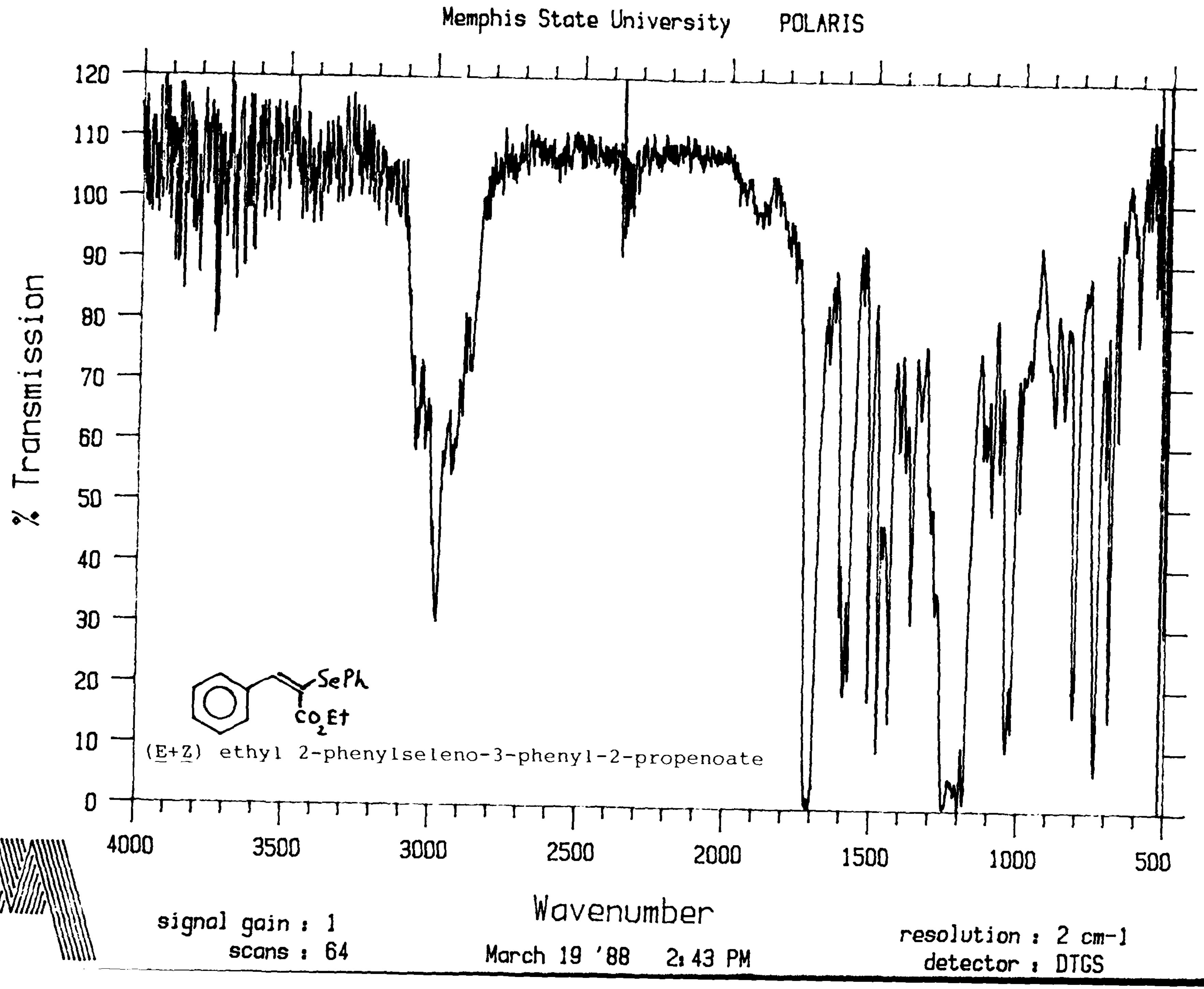
Memphis State University POLARIS
% Transmission
120
110
100
90
80
70
60
50
40
30
20
10
0
4000
3500
3000
2500
2000
1500
1000
500
Wavenumber
SePh
CO2Et
(E+Z) ethyl 2-phenylseleno-3-phenyl-2-propenoate
signal gain : 1
scans : 64
March 19 '88 2:43 PM
resolution : 2 cm-1
detector : DTGS

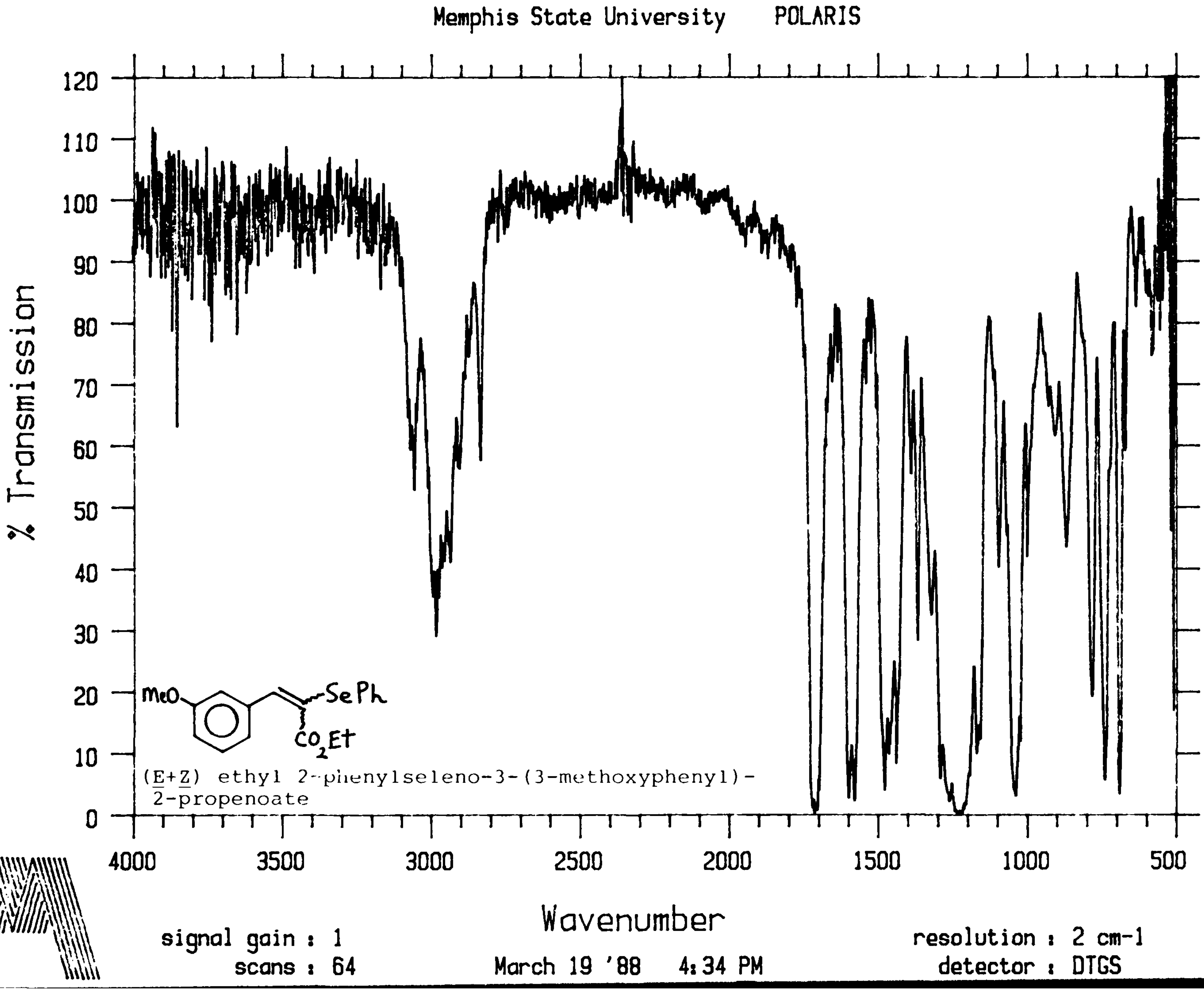
Memphis State University POLARIS
% Transmission
120
110
100
90
80
70
60
50
40
30
20
10
0
4000
3500
3000
2500
2000
1500
1000
500
Wavenumber
MeO
SePh
CO_2Et
(E+Z) ethyl 2-phenylseleno-3-(3-methoxyphenyl)-2-propenoate
signal gain : 1
scans : 64
March 19 '88 4:34 PM
resolution : 2 cm-1
detector : DTGS

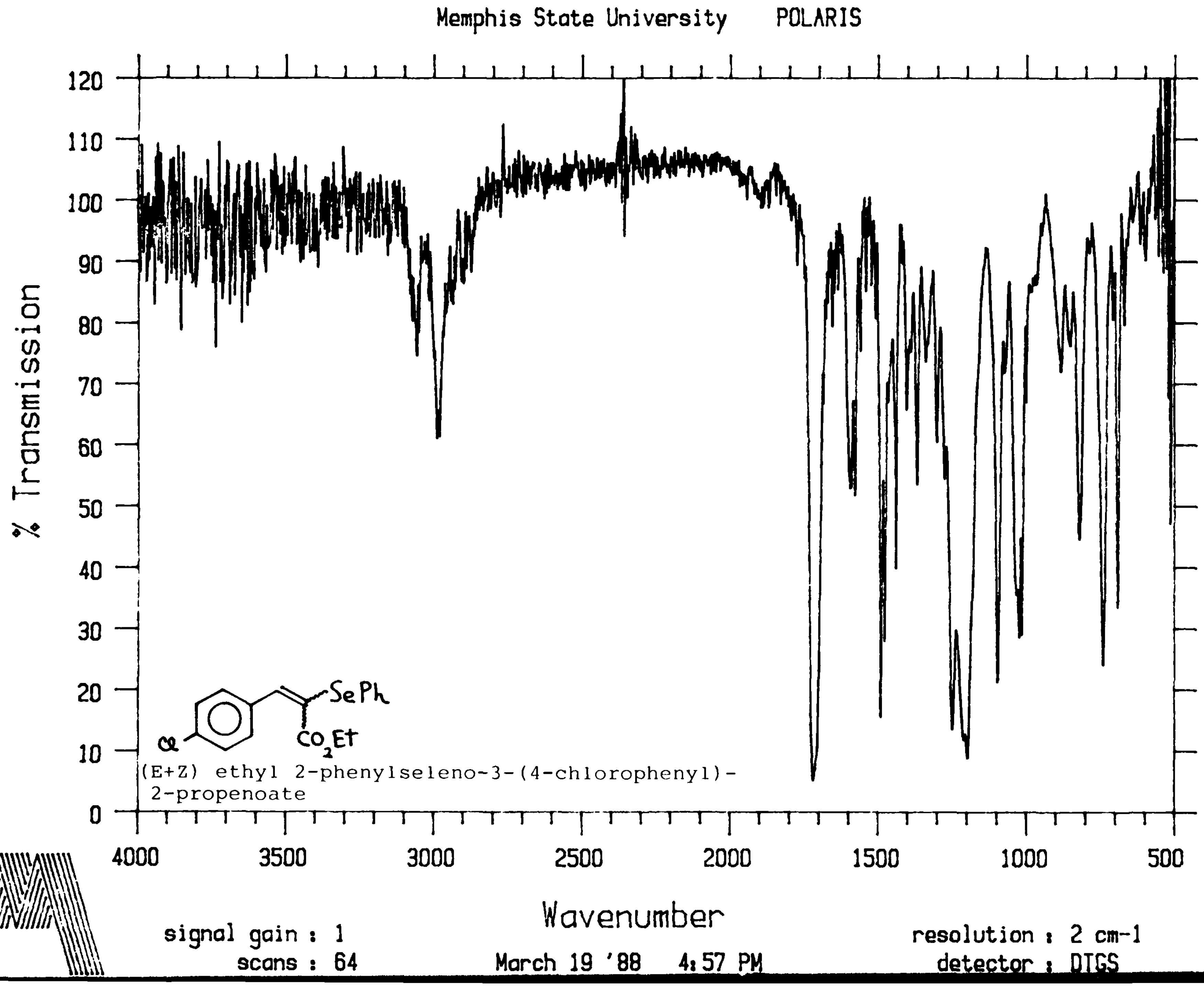
Memphis State University POLARIS
120
110
100
90
80
70
60
50
40
30
20
10
0
% Transmission
SePh
Cl
CO2Et
(E+Z) ethyl 2-phenylseleno-3-(4-chlorophenyl)-
2-propenoate
4000
3500
3000
2500
2000
1500
1000
500
Wavenumber
signal gain : 1
scans : 64
March 19 '88 4:57 PM
resolution : 2 cm-1
detector : DTGS

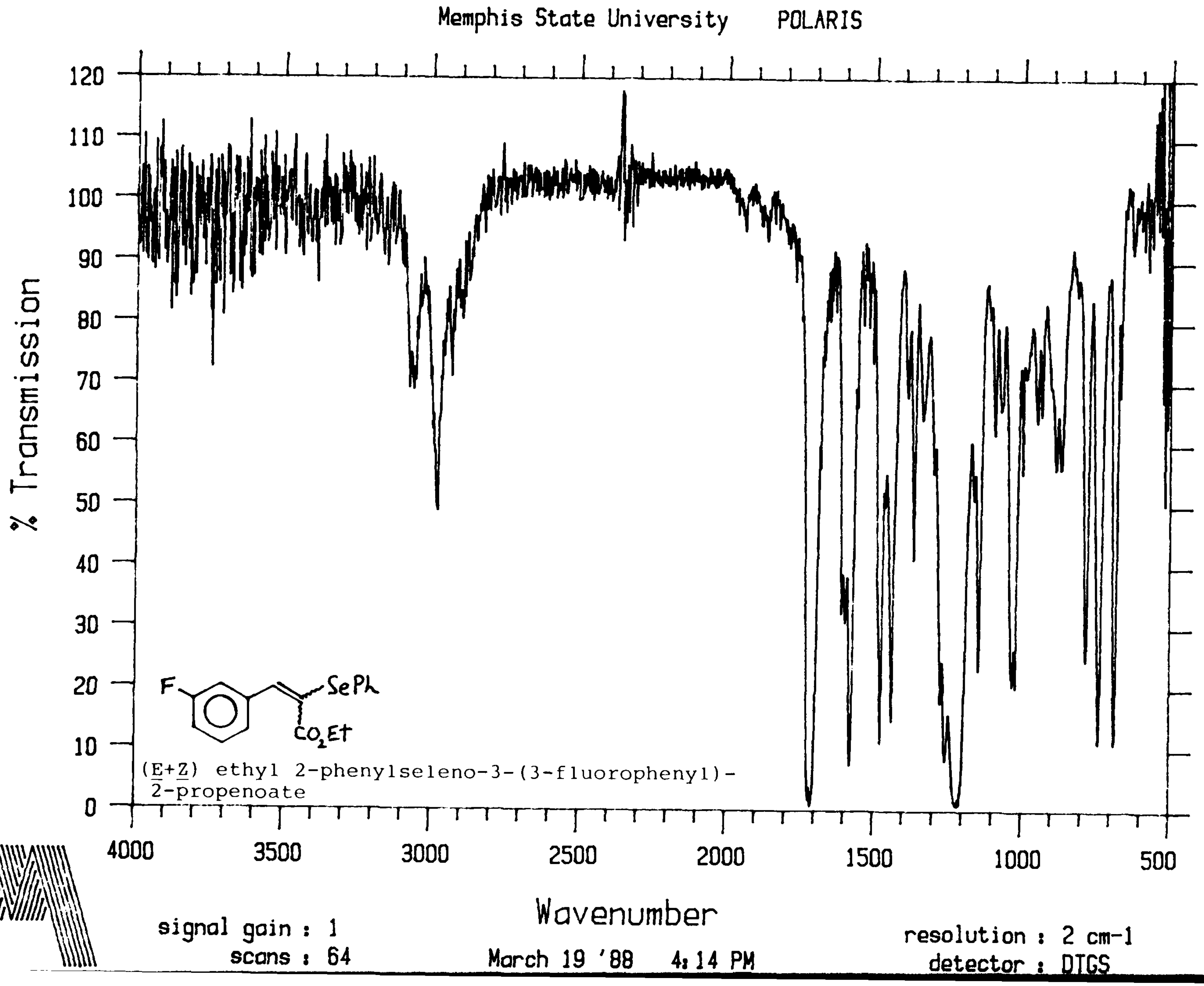
Memphis State University POLARIS
% Transmission
120
110
100
90
80
70
60
50
40
30
20
10
0
F
SePh
CO_2Et
(E+Z) ethyl 2-phenylseleno-3-(3-fluorophenyl)-2-propenoate
4000
3500
3000
2500
2000
1500
1000
500
Wavenumber
signal gain : 1
scans : 64
March 19 '88 4:14 PM
resolution : 2 cm-1
detector : DTGS

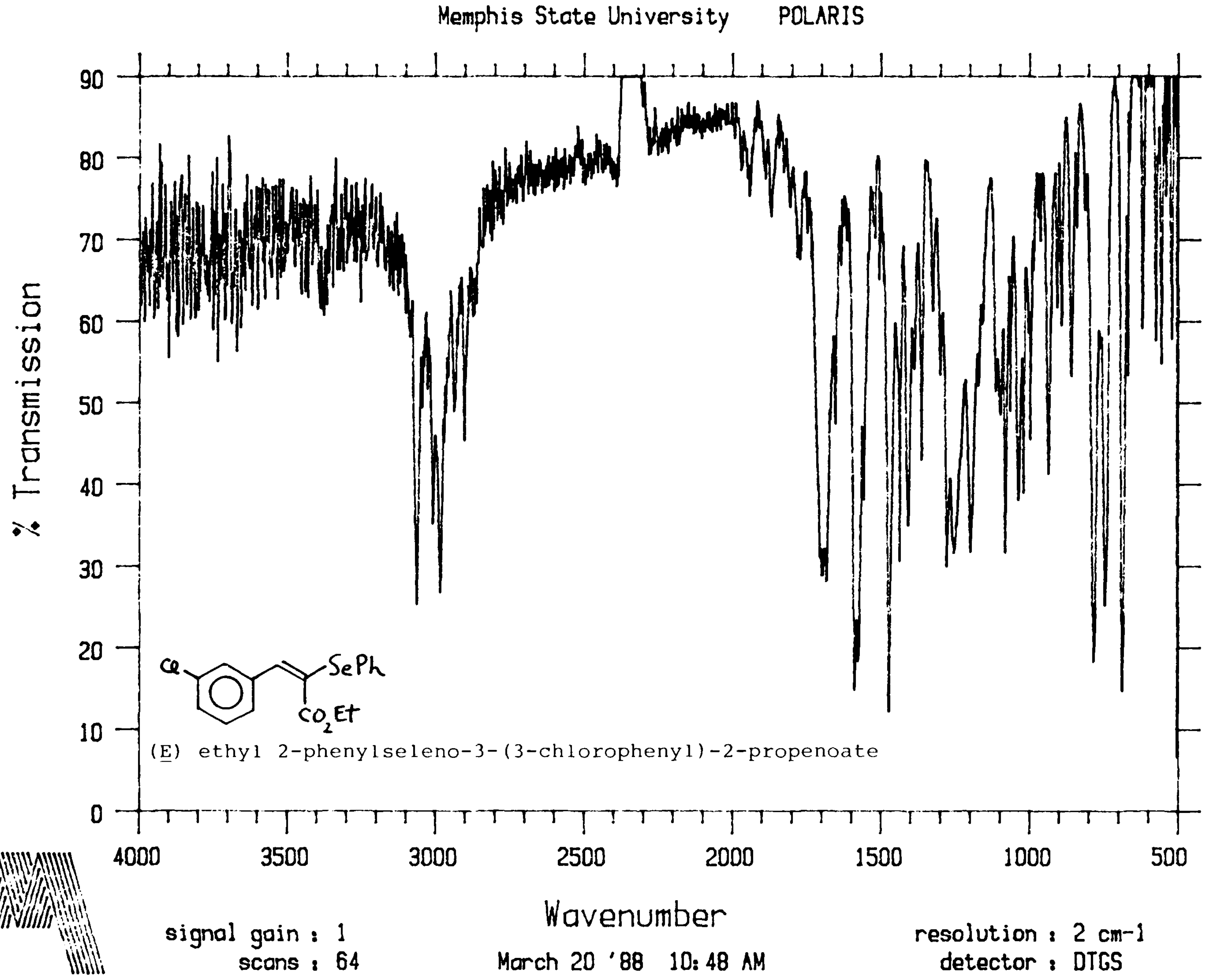
Memphis State University POLARIS
% Transmission
90
80
70
60
50
40
30
20
10
0
4000
3500
3000
2500
2000
1500
1000
500
Wavenumber
Cl
SePh
CO2Et
(E) ethyl 2-phenylseleno-3-(3-chlorophenyl)-2-propenoate
signal gain : 1
scans : 64
March 20 '88 10:48 AM
resolution : 2 cm-1
detector : DTGS

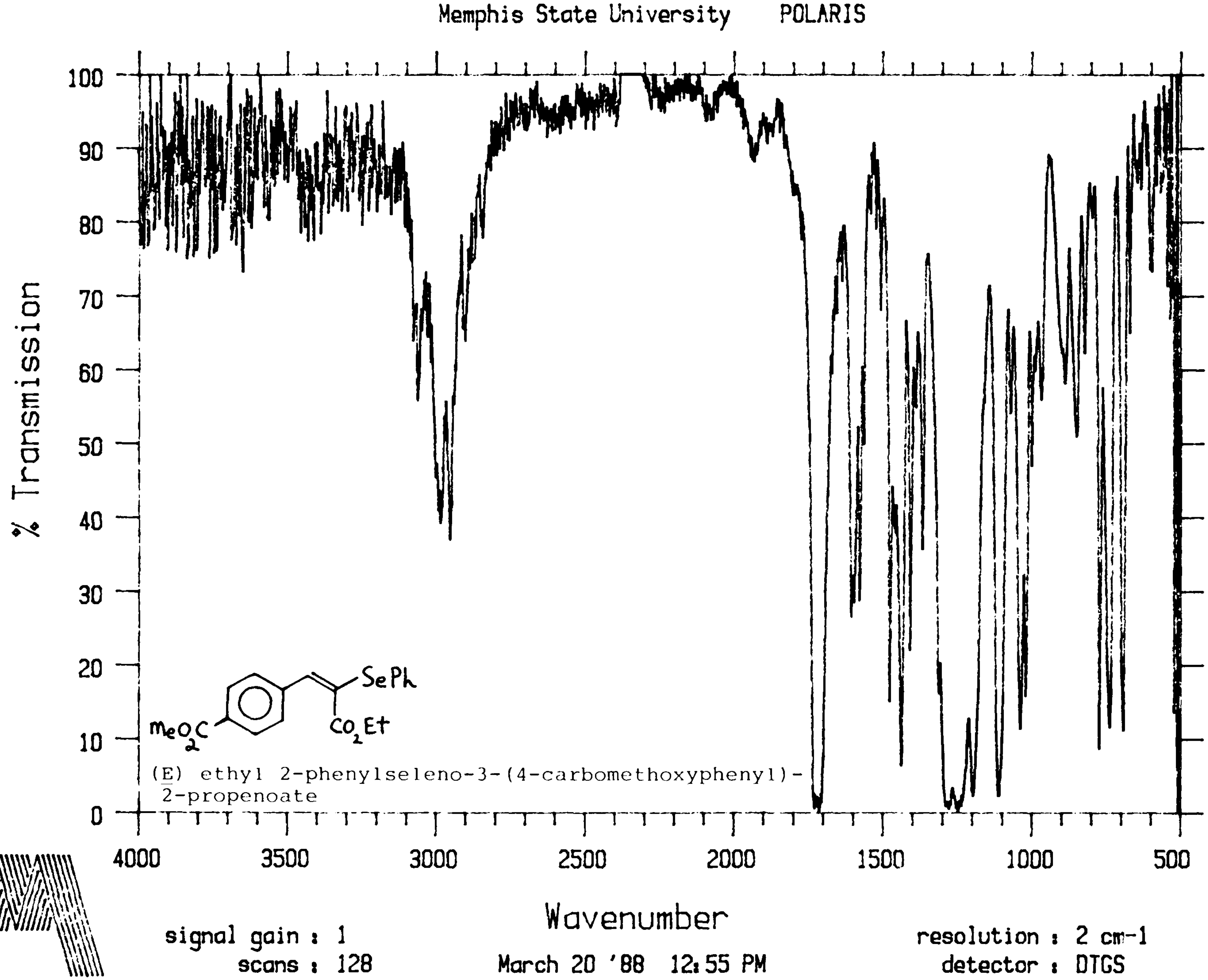
Memphis State University POLARIS
% Transmission
100
90
80
70
60
50
40
30
20
10
0
4000
3500
3000
2500
2000
1500
1000
500
Wavenumber
MeO2C
SePh
CO2Et
(E) ethyl 2-phenylseleno-3-(4-carbomethoxyphenyl)-2-propenoate
signal gain : 1
scans : 128
March 20 '88 12:55 PM
resolution : 2 cm-1
detector : DTGS

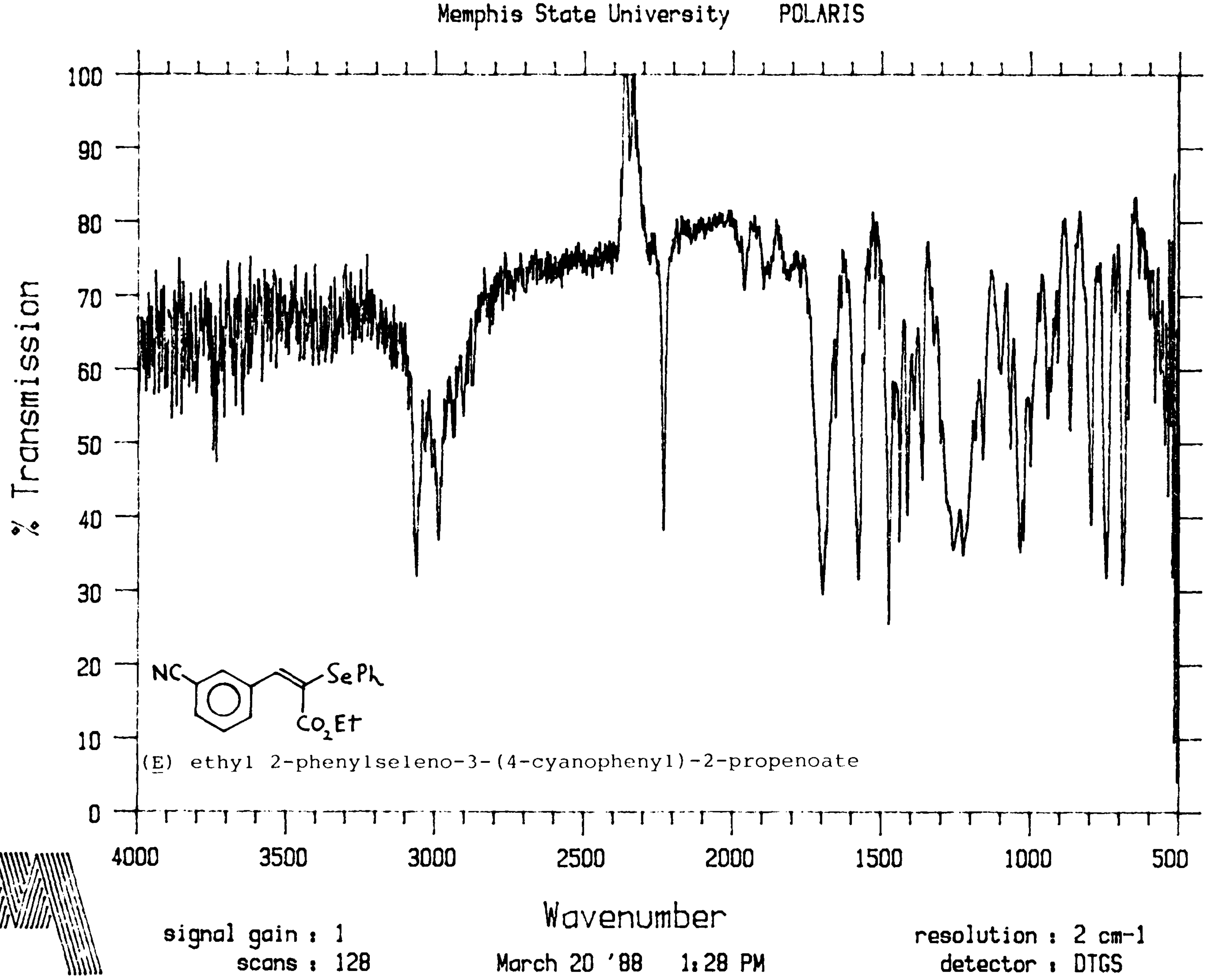
Memphis State University POLARIS
% Transmission
100
90
80
70
60
50
40
30
20
10
0
4000
3500
3000
2500
2000
1500
1000
500
Wavenumber
NC
SePh
CO2Et
(E) ethyl 2-phenylseleno-3-(4-cyanophenyl)-2-propenoate
signal gain : 1
scans : 128
March 20 '88 1:28 PM
resolution : 2 cm-1
detector : DTGS

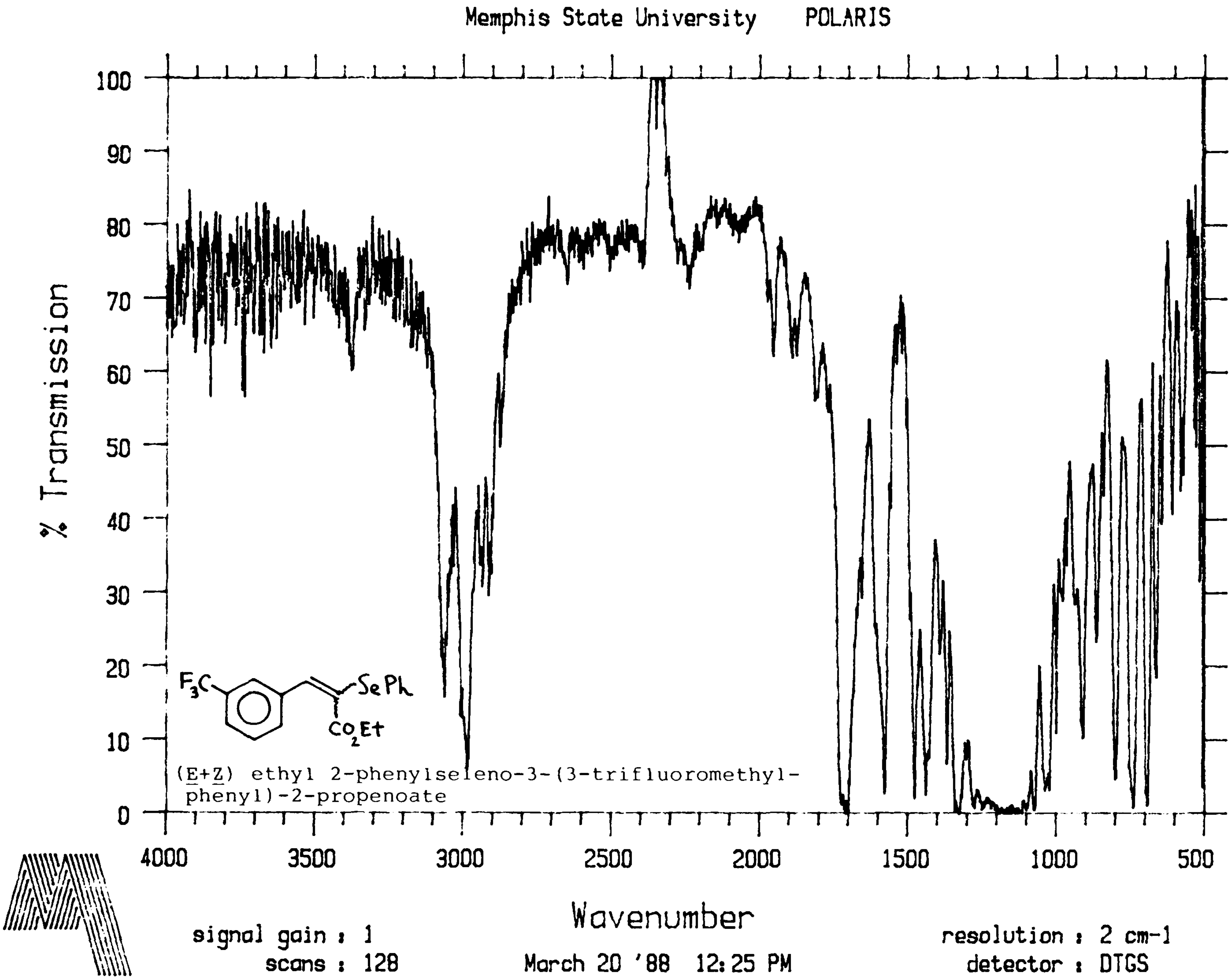

(E+Z) ethyl 2-phenylseleno-3-(3-trifluoromethylphenyl)-2-propenoate

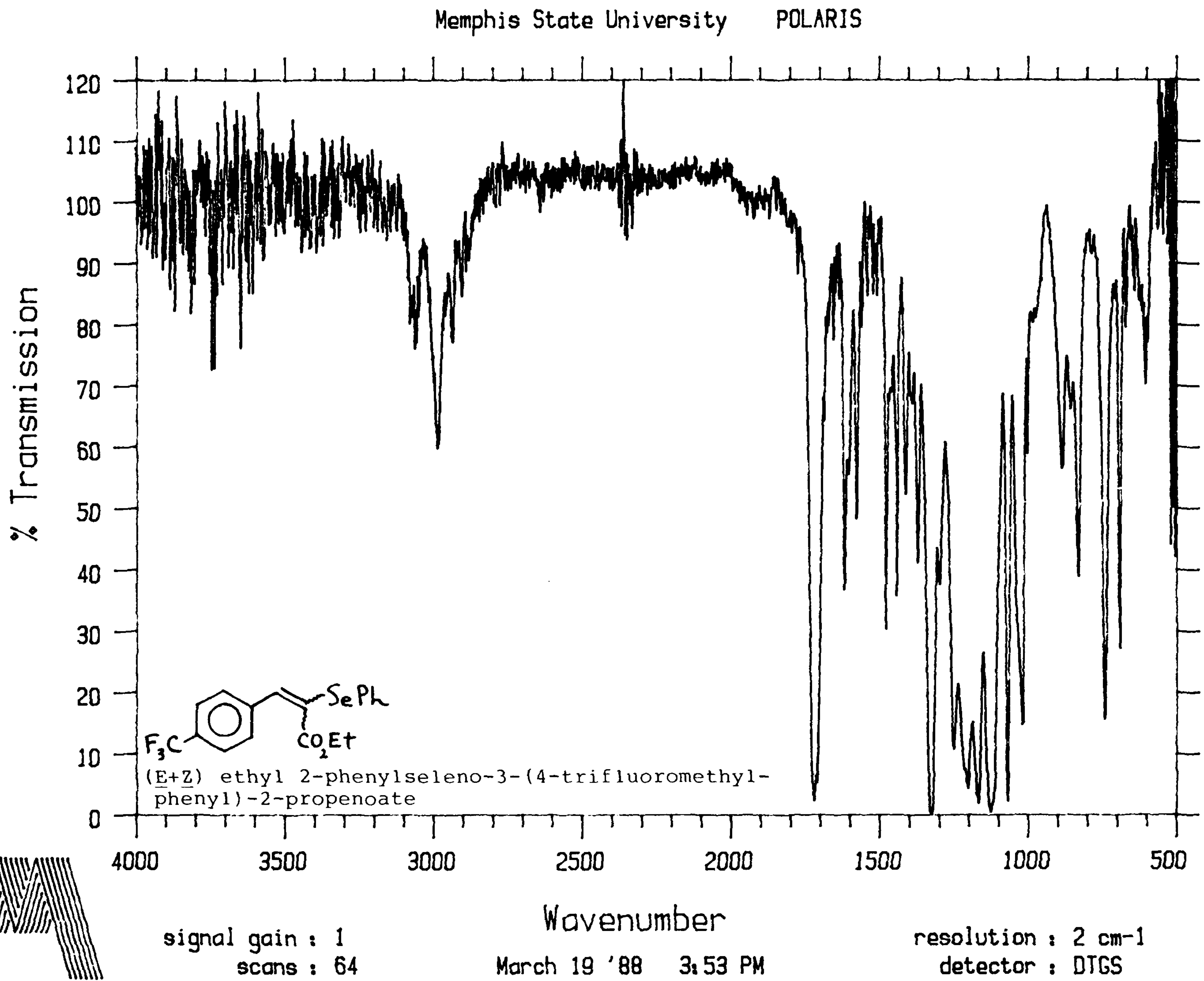
Memphis State University POLARIS
120
110
100
90
80
70
60
50
40
30
20
10
0
% Transmission
SePh
F₃C
CO₂Et
(E+Z) ethyl 2-phenylseleno-3-(4-trifluoromethyl-
phenyl)-2-propenoate
4000
3500
3000
2500
2000
1500
1000
500
Wavenumber
signal gain : 1
scans : 64
March 19 '88 3:53 PM
resolution : 2 cm-1
detector : DTGS

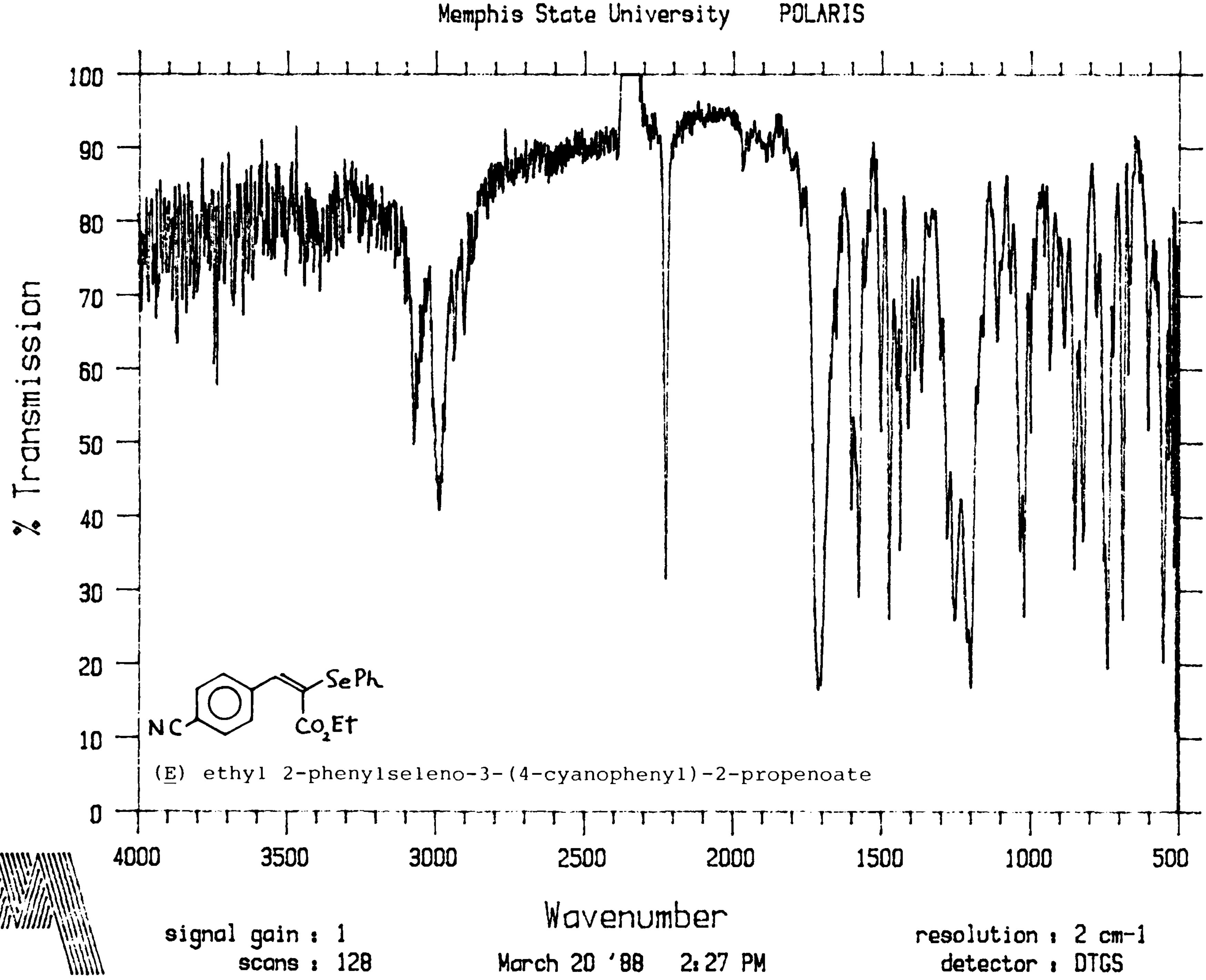
Memphis State University POLARIS
% Transmission
100
90
80
70
60
50
40
30
20
10
0
4000
3500
3000
2500
2000
1500
1000
500
Wavenumber
NC
SePh
CO_2Et
(E) ethyl 2-phenylseleno-3-(4-cyanophenyl)-2-propenoate
signal gain : 1
scans : 128
March 20 '88 2:27 PM
resolution : 2 cm-1
detector : DTGS

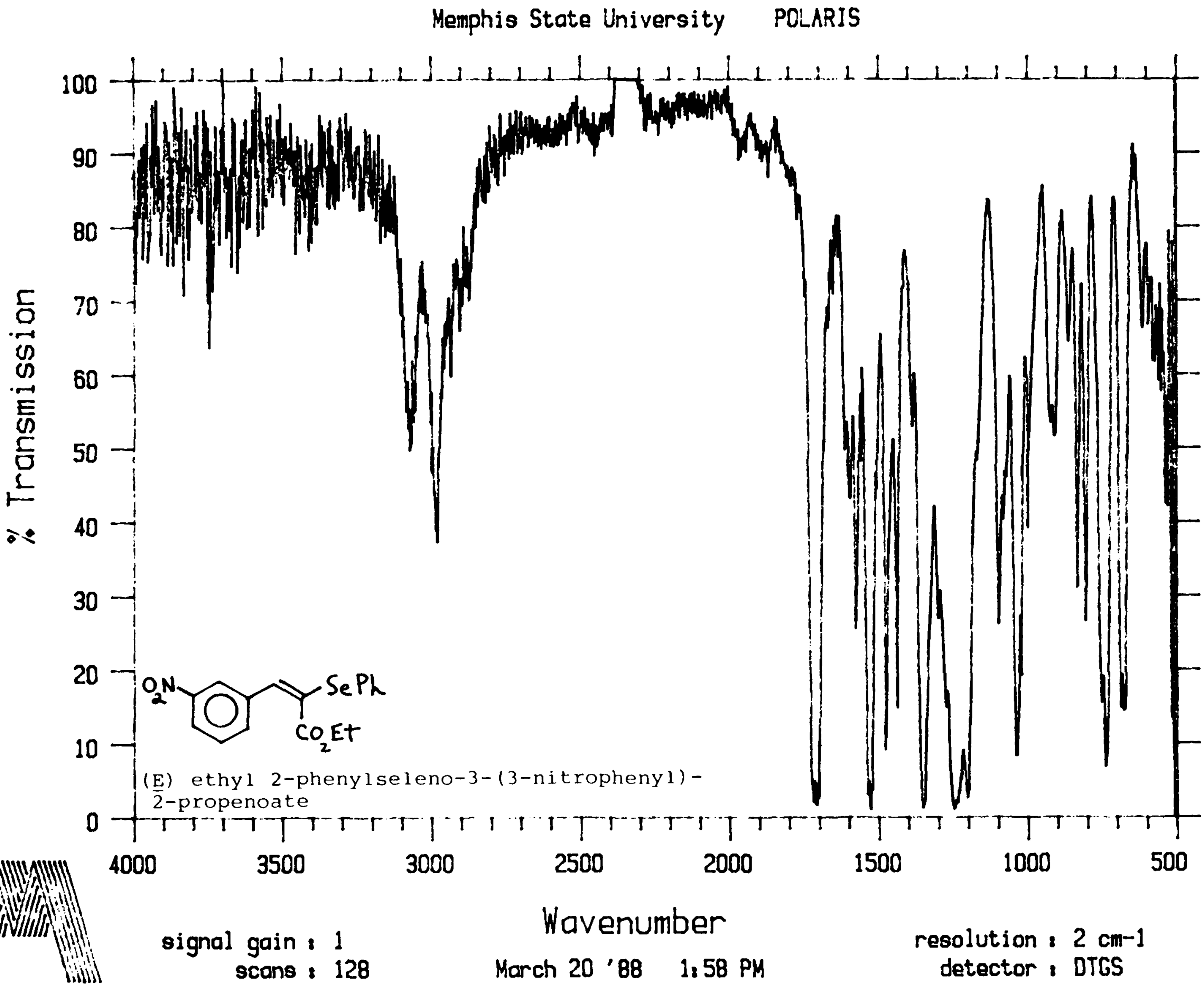

(*E*) ethyl 2-phenylseleno-3-(3-nitrophenyl)-2-propenoate

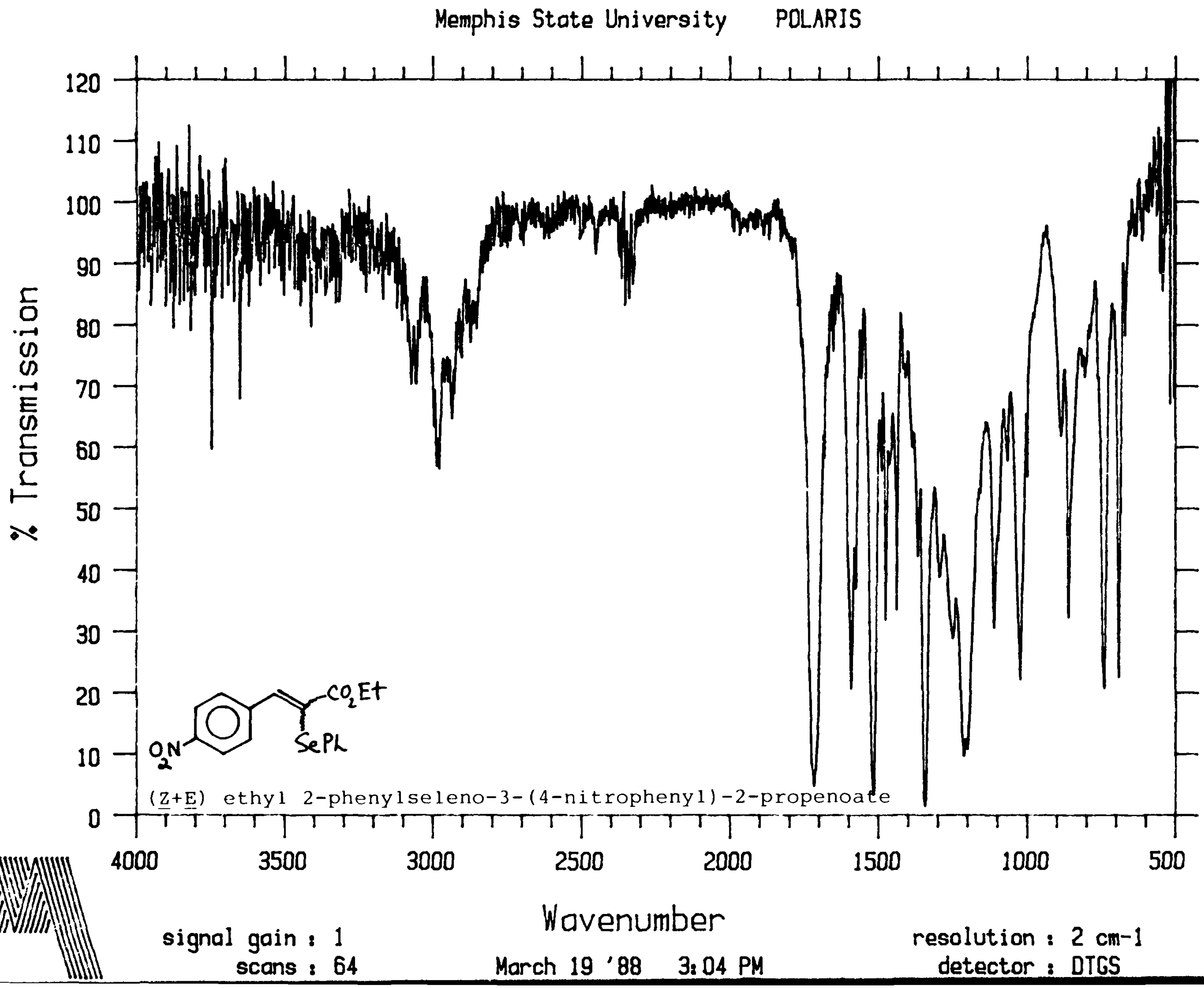
Memphis State University POLARIS
120
110
100
90
80
70
60
50
40
30
20
10
0
% Transmission
4000
3500
3000
2500
2000
1500
1000
500
Wavenumber
O_2N
CO_2Et
SePh
(Z+E) ethyl 2-phenylseleno-3-(4-nitrophenyl)-2-propenoate
signal gain : 1
scans : 64
March 19 '88 3:04 PM
resolution : 2 cm-1
detector : DTGS

VITA

Alan A. Shaffer [redacted] As the youngest son of an Air Force Chaplain, he enjoyed the experience of living in various locales during his childhood, including 3 years (1957-1960) in Great Britain. Perhaps to an extent from this childhood influence, he was commissioned as a 2nd Lt. in the United States Air Force upon his 1973 graduation from Otterbein College.

While on educational deferment, he obtained his M.S. from Miami University in 1975. The following year he entered active duty serving as a research chemist at the Materials Laboratory, Wright-Patterson AFB, Ohio. In 1981, he was reassigned to the Air Force Academy as an instructor in the Department of Chemistry. During the 1983-84 academic year, he had the good fortune to meet Dr. Charles Robinson of Memphis State University, who was then serving at the academy as a Distinguished Visiting Professor. Upon graduation, Major Shaffer will be assigned to the Frank J. Seiler Research Laboratory at the United States Air Force Academy, Colorado Springs, CO.